Palaeomagnetic and magnetic records for the last 300,000 years from Lac du Bouchet, France: applications to geomagnetism and the environment.

by

Trevor Williams

A thesis submitted for the degree of
Doctor of Philosophy.

University of Edinburgh

January 1994

Declaration

The work presented in this thesis is my own, except where otherwise stated. It has not previously been presented for a degree at this or any other university.

Abstract

In 1990, four 50m-long sediment cores were recovered from Lac du Bouchet, a small maar crater lake in the Massif Central of France. The sediment was deposited continuously over the last 300,000 years (3 full glacial-interglacial cycles), and forms a high resolution sequence which is the subject of multi-disciplinary examination at laboratories in Edinburgh, Marseille and Louvain. This thesis is concerned with the use of palaeomagnetic measurements to reconstruct the past geomagnetic field, and the use of rock-magnetic measurements to complement the other disciplines in reconstructing past environmental conditions at Lac du Bouchet. The study is an extension of previous studies of 20m-long cores from Lac du Bouchet, which covered the last 120,000 years.

The cores were sampled at 2·5cm spacing, giving a total of around 2500 samples. The natural remanent magnetisation (NRM), and laboratory implanted magnetisations (susceptibility, IRM and ARM) of each sample were measured.

The top 20m of the sequence had already been dated by ^{14}C to 45 ka, and by correlation to the marine $\delta^{18}O$ stratigraphy back to $\delta^{18}O$ stage 5e. The organic-rich sediments between 32 and 37m depth have been correlated to $\delta^{18}O$ stage 7 by palynology, and the base of the core is thought to be of $\delta^{18}O$ stage 9 age.

The magnetic measurements of susceptibility, IRM and ARM principally reflect the concentration of the magnetic mineral (a low-Ti titano-magnetite) which is derived from the maar crater walls. Susceptibility is low in organic sediments deposited in warm climates, and the record has a very close inverse correlation to the arboreal / non-arboreal pollen ratio. It therefore provides a record of the palaeoenvironment at Lac du Bouchet. The $\delta^{18}O$ sub-stages 5a-e and 7a-e are well defined; substantial changes in susceptibility occur within the last two interglacials; and short duration susceptibility lows punctuate the last glacial.

Palaeomagnetic records of declination, inclination and intensity have been recovered from the sediment sequence. Room temperature magnetic experiments reveal a homogenous magnetic mineralogy in the glacial sediments; thus the geomagnetic recording is likely to be reliable, and any of susceptibility, IRM or ARM can be used to normalise the NRM intensity to recover a record of relative geomagnetic palaeointensity. The relative palaeointensity shows large amplitude, long period variations that are different from the palaeoenvironmental variations. Low palaeointensities correspond to times of reported excursions, although no clearly excursional directions are recorded at Lac du Bouchet. In comparison with other records of palaeointensity, there is agreement over trends, but differences in the details. No firm conclusions can be drawn on possible influences of the Earth's orbital variations over the geodynamo.

Acknowledgements

I would like to thank the following people; they made this thesis possible and the last three years enjoyable:-

Ken Creer and Nicolas Thouveny for initiating the project and for their help throughout; Piotr Tucholka for making me welcome at Orsay, Paris, when I was on Erasmus exchange; Wyn Williams, Randy Enkin and Lisa Tauxe for useful discussions and advice; Lydie Chevalier and Elizabeth Kroll for helping with sampling and measuring the many samples (an onerous task); Christian Robinson, Ian Turton, Karen Dobbie, Norman Dalgleish, Clare Peters, Pierre Francus, Jerry Lloyd, Karen Mair, Jon Kirby, Tom Wright and Ned Pegler for useful discussions and/or reading through the raw chapters; Alan Pike, Gordon Waugh, Colin Grandison and Shane Voss for keeping the cryogenic magnetometer and departmental computers up and running; the fieldwork teams who made the corings at Lac du Bouchet, Lac St. Front and Praclaux, and who helped my colloquial French along no end; J-L de Beaulieu and Maurice Reille for the palynological work on the Lac du Bouchet cores; and the staff and students of the Laboratory of Quaternary Geology, Marseille, who made me welcome on my visits there, particularly Eugene Bonifay, David Williamson, Brahim Damnati and Maurice Taieb.

Finally I'd like to thank my family, friends, and the staff of the Department of Geology and Geophysics at Edinburgh.

This Ph.D. was funded by NERC, and forms a part of the EC-funded Euromaars project.

Contents

Figures

Tables

Abbreviations

BP	before present
ka	1000 years BP / 1000 years ago (an age)
kyr	1000 years (a duration)
NRM	natural remanent magnetisation
NRM_{10mT}	NRM, partially demagnetised in a 10mT alternating field.
MDF	median destructive field
DRM	depositional remanent magnetisation
ARM	anhysteretic remanent magnetisation
IRM	isothermal remanent magnetisation
SIRM	saturation isothermal remanent magnetisation
TRM	thermal remanent magnetisation
VRM	viscous remanent magnetisation
susc	magnetic susceptibility
M_{rs}	saturation remanence (=SIRM)
M_s	saturation magentisation
$(B_0)_{cr}$	remanence coercivity
$(B_0)_c$	coercivity
SD	single domain
PSD	psuedo-single domain
MD	multi domain
SPM	super-paramagnetic
PVC	poly-vinyl-chloride
AF	alternating field
FFT	fast fourier transform
mT	milli-Tesla

Prologue

From "De Magnete", William Gilbert [1600]

"This natural philosophy (*physiologia*) is almost a new thing, un-heard of before; a very few writers have simply published some meagre accounts of certain magnetic forces [...] Nor have we brought into this work any graces of rhetoric, any verbal ornateness, but have aimed simply at treating knotty questions about which little is known in such a style and in such terms as are needed to make what is said clearly intelligible. Therefore we sometimes employ words new and unheard-of, not (as alchemists are wont to do) in order to veil things with a pedantic terminology and to make them dark and obscure, but in order that hidden things which have no name and that have never come into notice, may be plainly and fully published..."

From "A theory of the magnetical compass", Edmund Halley [~1702]

"Now altho the great utility that a perfect knowledge of the Theory of the Magnetical direction would afford to mankind in general, and especially to those concerned in Sea affairs, seem a sufficient incitement to all Philosophical and Mathematical heads, to take under serious consideration the several *Phenomena*, and to endeavour to reconcile them by some general rule: yet so it is; that almost all the Authors, from whome a discourse of this kind ought to have been expected, pass by in silence the difficulties they here encounter. And those that mention this Variation: by affirming it to proceed from causes altogether uncertain (as are the casual lying of Iron mines and Loadstones in the Earth) put a stop to all further contemplation; and give discouragement to those that would otherwise undertake this Enquiry [...]

Now altho (through want of sufficient observations and some other difficulties which I shall anon shew) I cannot pretend perfectly to establish the numbers and rules of a *Calculus* which shall precisely answer to the Variations of all parts of the World: yet I suppose it will not be unacceptable to the curious to propose something of a light into this abstruse mystery; which, if no other, may have this good effect, to stir up the Philosophical *Genii* of the age to apply themselves more attentively to this useful speculation."

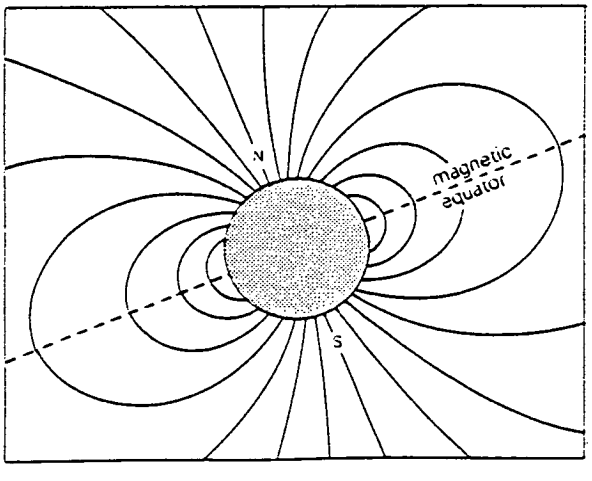

Chapter 1

Introduction

1.1 Introduction

The Lac du Bouchet sediment sequence was cored in 1990 to a depth of 50 m. This sequence contains records of the geomagnetic field and the environment over the last 300 kyr.

The behaviour of the Earth's magnetic field over the last 300 kyr is not well known, and the processes in the outer core which generate the field are poorly understood. Thus the study of geomagnetic variations on this time-scale is still in the descriptive phase, and the world data-set of palaeomagnetic changes is being built up. The records from Lac du Bouchet significantly contribute to this data-set, as they are perhaps the best so far obtained in terms of detail and age control.

By contrast, there is a greater understanding of the climatic changes which have occured in the Quaternary period - the global sequence of warm and cold climates and the broad mechanism which governs them are fairly well established. Studies of environments and climates in the past lead to an understanding of how the climate system works, hence enabling predictions of how it might change in the future, for example in response to man's influence.

1.2 Scientific background

The form of the geomagnetic field at the Earth's surface is very similar to that around a uniformly magnetised sphere (Gilbert [1600]). The field around a uniformly magnetised sphere is the same as the field around a magnetic dipole. The Earth's field is still described in terms of a dipole at the centre of the Earth, for the practical reason that the field recorded at a single site can only give enough information to be interpreted in terms of a dipole. The part of the field that is not described by a dipole is called the non-dipole field: this division is principally a practical and mathematical one.

The field originates in the liquid outer core of the Earth. The magneto-hydrodynamics that generate the field are difficult to model mathematically, so the problem is often split into kinematic and hydromagnetic parts. The thermal regime is thought to take the form of convection rolls parallel to the spin axis, around the inner core. Studies of the historical field at the core-mantle boundary show that non-dipole features, such as flux concentrations and reversed flux patches, are more important there than at the surface (Bloxham and Gubbins [1985]).

The past behaviour of the field is recorded in sediments and volcanic rocks (palaeomagnetism), or by historical observation. On a scale of millions of years, the sequence of geomagnetic reversals is well known. On a scale of tens and hundreds of years, the secular variation of the field is well known. In between these two scales, the field behaviour is less well known: the form of reversals, excursions, palaeosecular variation and palaeointensity variation are all currently under investigation. Observations of these types of behaviour lead to ideas about underlying mechanisms and help to confine theories of field generation in the core (see, for example, Valet and Meynadier [1993]). In particular, the changes in geomagnetic palaeointensity are of current interest, as it is becoming apparent that, with care, relative palaeointensities can be recovered from sedimentary sequences (Tauxe [1993]). Geomagnetic intensity controls the production of the ^{14}C isotope (used in dating) and nitric oxide (which destroys ozone) in the stratosphere.

Palaeomagnetic results from previous work on the top 20m (120 kyr) of the Lac du Bouchet sequence show large palaeointensity variations, and no excursional directions were recorded (Thouveny [1993], Creer et al., [1990] and Thouveny et al. [1990]).

During the Quaternary Period (2.4 to 0 ma), the Earth has been in an ice-age, characterised by a cyclic expansion and contraction of the ice sheets, repeating about every 100 kyr since 800 ka. Times of expanded ice sheets (cold, dry global climate) are called glacials, or stadials if they are short; times of contracted ice sheets (warm, wet global climate) are called interglacials, or interstadials if they are short. The cyclicity is thought to be due to variations in insolation (sunlight), which are due in turn to variations in the Earth's orbit ("Milankovitch theory and Climate", Berger [1988]). The waxing and waning of the global ice volume is recorded by changes in the $^{18}O/^{16}O$ ratio in marine sediments. A standard marine $\delta^{18}O$ stratigraphy has been set up, and dated by tuning the periodicities in $\delta^{18}O$ records to the calculated insolation periodicities (Martinson et al. [1987]). Polar ice sheets hold very detailed records of temperature and atmospheric composition over the last glacial cycle, and the ice core records from Summit, Greenland, are of current interest (Dansgaard et al. [1993]).

Some continental sediments, such as those from maar lakes, contain pollen records which can give quantitative reconstructions of temperature and precipitation (Pons et al. [1992]). Additionally, the magnetic mineralogy of sediments can give information on the environment (Thompson and Oldfield [1986]). There is a striking similarity between the susceptibility record and the tree pollen % record from Lac du Bouchet (Creer [1991]).

The first few figures of this chapter give the location of the Lac du Bouchet records in terms of geography (figure 1.1), comparable sources of environmental and geomagnetic records (figure 1.3, table 1.1), and the present magnetic field (figure 1.2).

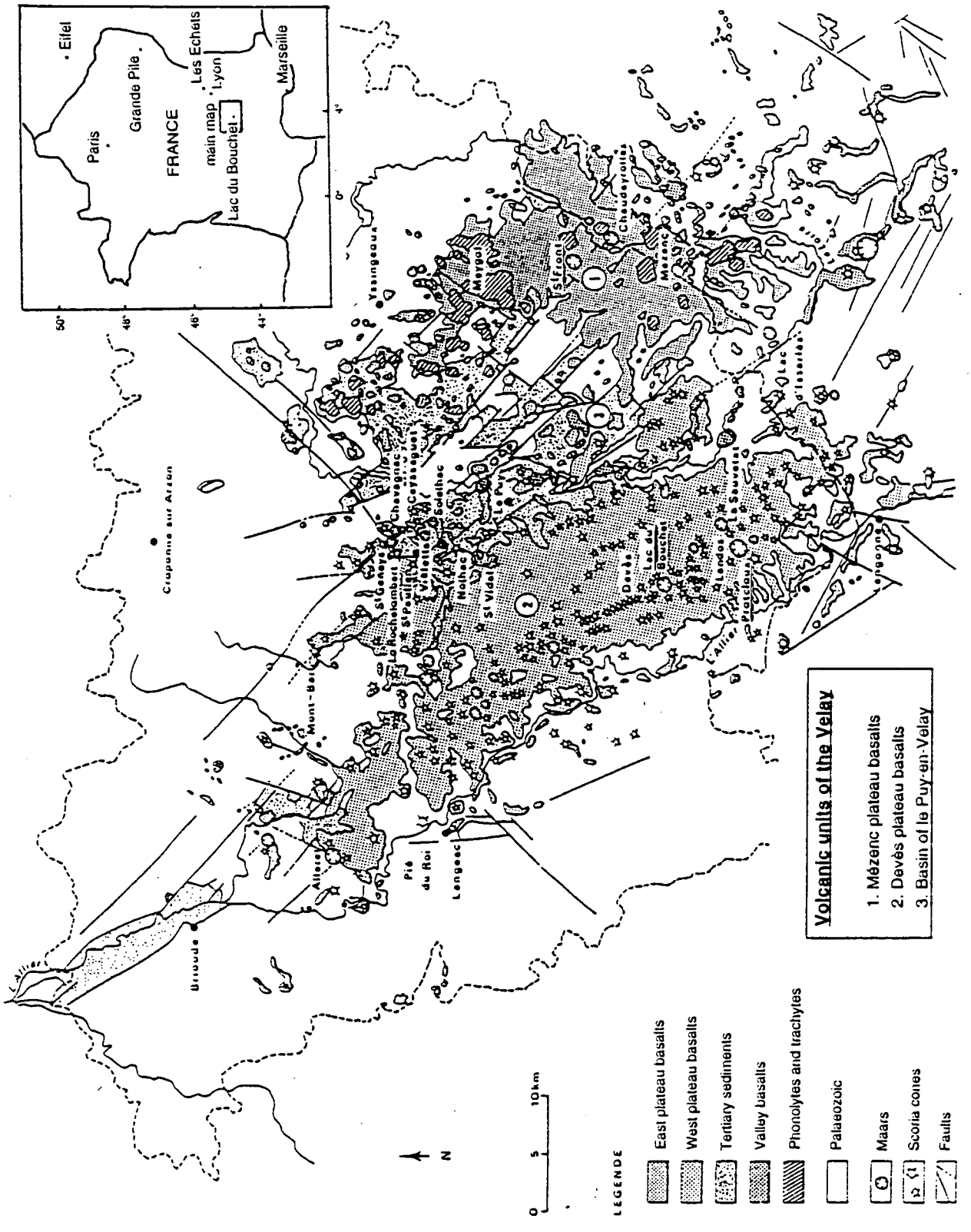

Fig. 1.1 Geological and location map of the region around Lac du Bouchet. The main map is from Truze [1990], and shows the other maars of the area, many of which have been cored (e.g. Lac du Bouchet, Lac de St.Front, Lac d'Issarles, and the dry (fossil) maars of Praclaux and Landos). The inset map gives the wider location, and also the locations of the Eifel volcanic region, and the long-core pollen sites of La Grande Pile and Les Echets.

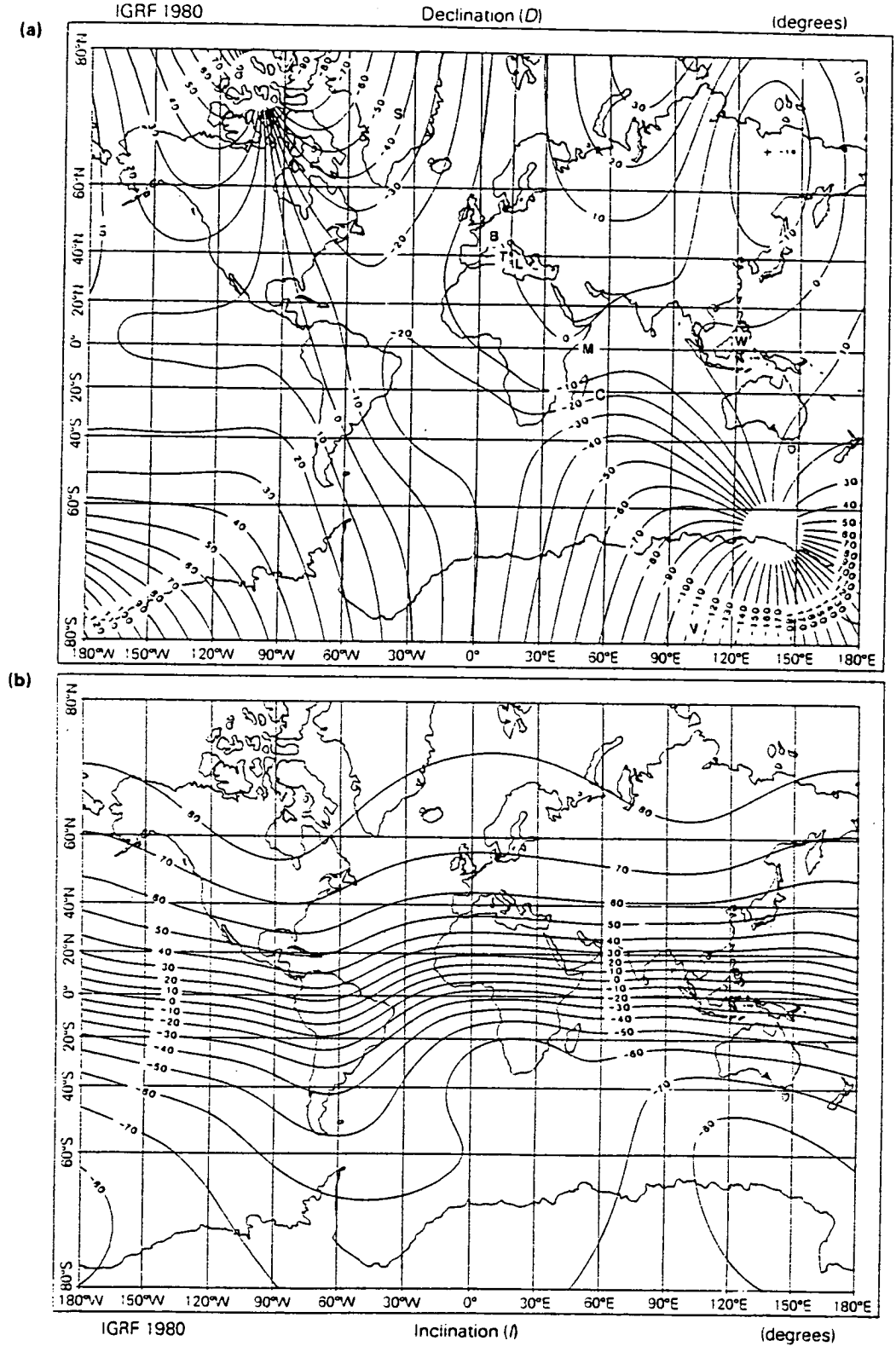

Fig. 1.2 The 1980 magnetic field, at the surface of the Earth: a) declination, measured from the geographical meridian; b) inclination (dip) from the horizontal. (from Fabiano et al. [1983], via Thompson and Oldfield [1986]). The locations of several of the records referred to in chapters 7 and 8 are marked: Lac du Bouchet (B); ice cores from Summit (S) and Vostok (V); the palaeointensity records of Tric et al. [1992] (T), Meynadier et al. [1992] (M), Tauxe and Wu [1990] (W) and Chauvin et al. [1992] (C); and the palaeodirections of Lanza and Zanella [1992] (L).

Table 1.1 Sources of terrestrial palaeoclimatic data. Copied from Negendank and Zolitschka [1993].

Archives	resolution	extent (kyr)	proxy-data on:				
			temp.	precip., humidity	chemical comp. of:	biomass	volcanic eruptions
tree-rings	year/season	10	x	x	air	x	x
lake sediments	year/season	1000	x		water	x	x
maar lake sediments	year/season	300+	x	x	water	x	x
palaeosoils	100 year	100	x	x	soils		x
loess	10 year	1000	x	x	soils		
polar ice cores	year	300	x	x	air		x
mid-latitude glaciers	year	10	x	x	air	x	x
Historical records	year/day	2	x	x		x	x

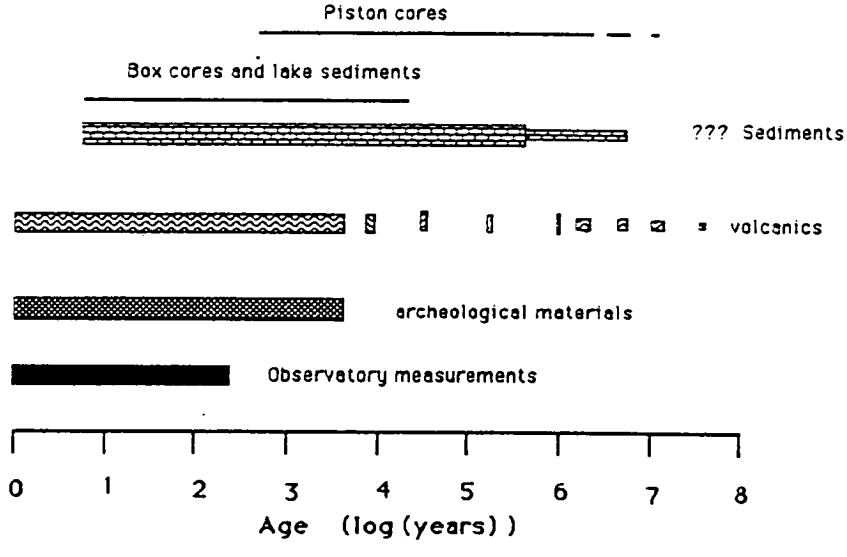

Fig. 1.3 Potential sources of palaeointensity information. From Tauxe [1993].

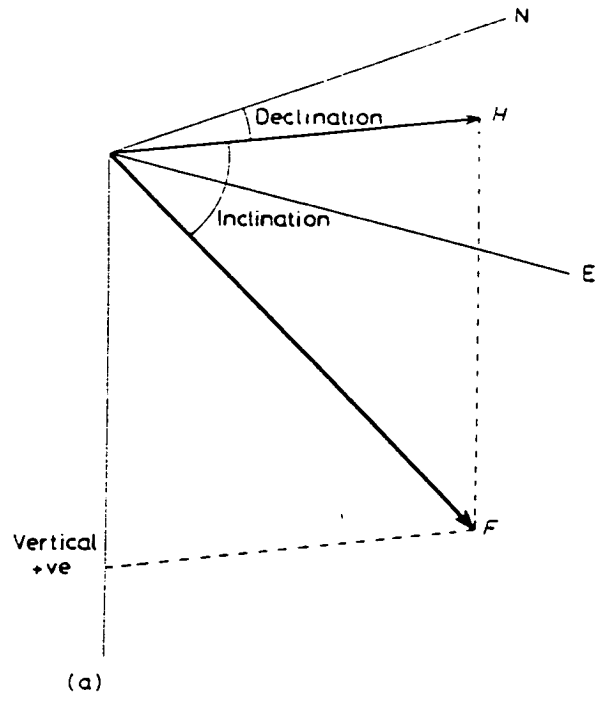

Fig. 1.4 The magnetic vector. The magnetic field at a site can be defined, in polar co-ordinates, in terms of declination (deviation of the horizontal component from geographic North), inclination (dip from the horizontal), and intensity (F).

1.3 Aims of the study

Geomagnetic. The general aim is to add to the knowledge of geomagnetic field behaviour over the last 300 kyr, by palaeomagnetic study of the Lac du Bouchet sediment sequence. Two specific aims are: a) to recover a relative palaeointensity record from the sediments, with a knowledge of its uncertainties, and add it to the world palaeointensity data-set; and b) to assess the influence, if any, of the Earth's orbital variations on the geomagnetic field as recorded at Lac du Bouchet.

Environmental and climatic. The aims of the environmental side of the study are: a) to assess the use of magnetic mineralogy as a recorder of past environmental change at Lac du Bouchet; b) to use the mineral-magnetic records (such as susceptibility) to complement the other palaeoenvironmental studies of the sediments (such as pollen analysis, sedimentology and geochemistry); and c) to see how the climatic changes for the last 300 kyr, recorded in oceans and polar ice, are expressed in the mid-latitude continental environment at Lac du Bouchet.

1.4 A plan of the thesis

The environmental and geomagnetic interpretation of the records is done in chapters 7 and 8; the other chapters are groundwork for these two.

Chapters 2 and 3 concern the coring of Lac du Bouchet in 1990, the sampling of the cores, and the type of measurements done on the samples. Chapter 4 concerns the room temperature magnetic experiments, done in order to characterise the magnetic mineralogy, the stability of the remanent magnetisation, and the sediment's suitability for relative palaeointensity work. Chapter 5 results in stacked, cleaned, records on a common depth scale. The principal method of dating is by matching to the marine $\delta^{18}O$ stratigraphy, and two depth→time models are developed in chapter 6. The necessity of good dating control in general is a running theme in the following chapters.

Susceptibility is used as an indicator of palaeoenvironment in chapter 7, and is compared with the global ice volume record and the Summit ice core temperature record; the Lac du Bouchet record shows variations of similar form to both.

NRM_{10mT} normalised with susceptibility is used as a relative palaeointensity record in chapter 8. The fidelity of the record is assessed, with the conclusion that while most parts record the field well, some parts, for example organic-rich intervals, do not.

Variations in the Earth's orbit are responsible for the insolation variations that are thought to affect the climate. It has also been suggested that orbital variations might affect the generation of the geomagnetic field in the Earth's core, but this is thought doubtful (Tauxe [1993]). Illustrations of the orbital variations ar given in chapters 7 and 8, and their relationship to the Lac du Bouchet records is discussed.

1.5 The physical basis of the method

The sediments from Lac du Bouchet contain between 0.02 and 0.5% (by volume) magnetite (actually a low-Ti titano-magnetite). This magnetic fraction contains information on both the environment and the geomagnetic field around the time of sediment deposition.

The magnetic mineralogy of the sediment, in particular the concentration of magnetite, changes with palaeoenvironment. Low susceptibility reveals low magnetite concentrations in sediments deposited in a warm environment, and vice-versa for high susceptibilities. This is seen to be true by the detailed inverse correlation between susceptibility and the tree pollen % down the cores. A probable basis for this is that during warm conditions, increased vegetation leads to decreased erosion of the magnetite-rich crater walls, and the combination of decreased detrital input with increased organic input decreases the magnetite concentration.

For the recording of the geomagnetic field, the situation is more complex, and there is no internal comparison test to check that the geomagnetic field is being recorded faithfully. Magnetic grains are acted on by a torque due to the geomagnetic field, and are free to align along it in the water and the top of the sediment column. On burial they are "locked in" (no longer free to rotate), thereby recording the ancient field direction (figure 1.5, 1.6a). The intensity of this depositional remanent magnetisation (DRM) depends on both the magnetite concentration and how well the grains are aligned, which itself depends on the palaeointensity of the geomagnetic field (figure 1.6b). The two main assumptions behind the recording and recovery of palaeointensities from sediments are that the magnetic mineralogical effects can be normalised out, and the quality of alignment of the moments is directly proportional to the palaeointensity. Only *relative* palaeointensities can be recovered, because the time-scale and conditions of DRM acquisition cannot be reproduced in the laboratory; exact normalisation is not possible.

A body of theoretical and experimental work has built up on DRM, and is reviewed by Tauxe [1993]. The remanence can be acquired at two stages - at the sediment/water interface (DRM), and below the interface (post-depositional remanent magnetisation, PDRM). In this thesis I will follow the approach of Tauxe [1993], and call the resultant of the two DRM. Near the interface, gravitational and hydrodynamic forces are important; grains will tend to fall into small hollows in the surface, and their long axes (the long axis is also the easy axis for magnetisation) will tend to be more horizontal. Below the surface, grain mobility is enabled by >75% water content with stirring (by bioturbation, for instance) (Tucker [1980]), and the grains can re-align. The time taken for a small grain (<15μm) in water to align along a typical geomagnetic field is of the order of a second (Stacey [1972]); the time taken for a sediment (75% water, stirred) to acquire its maximum DRM in a typical geomagnetic field is around 15 minutes (Tucker [1980]).

There is a smoothing of the changes in the field on recording, because the remanence is acquired over a certain depth range above the locking-in depth, corresponding to about a 100 year interval (Creer et al. [1990]). Smith [1985] concluded that the Lac du Bouchet sediments recorded the geomagnetic field over a short period of time. The measured geomagnetic variations are also smoothed, because the 2cm thick samples represent a time interval of 200 years in typical glacial sediments, and 400 years for the more organic-rich sediments.

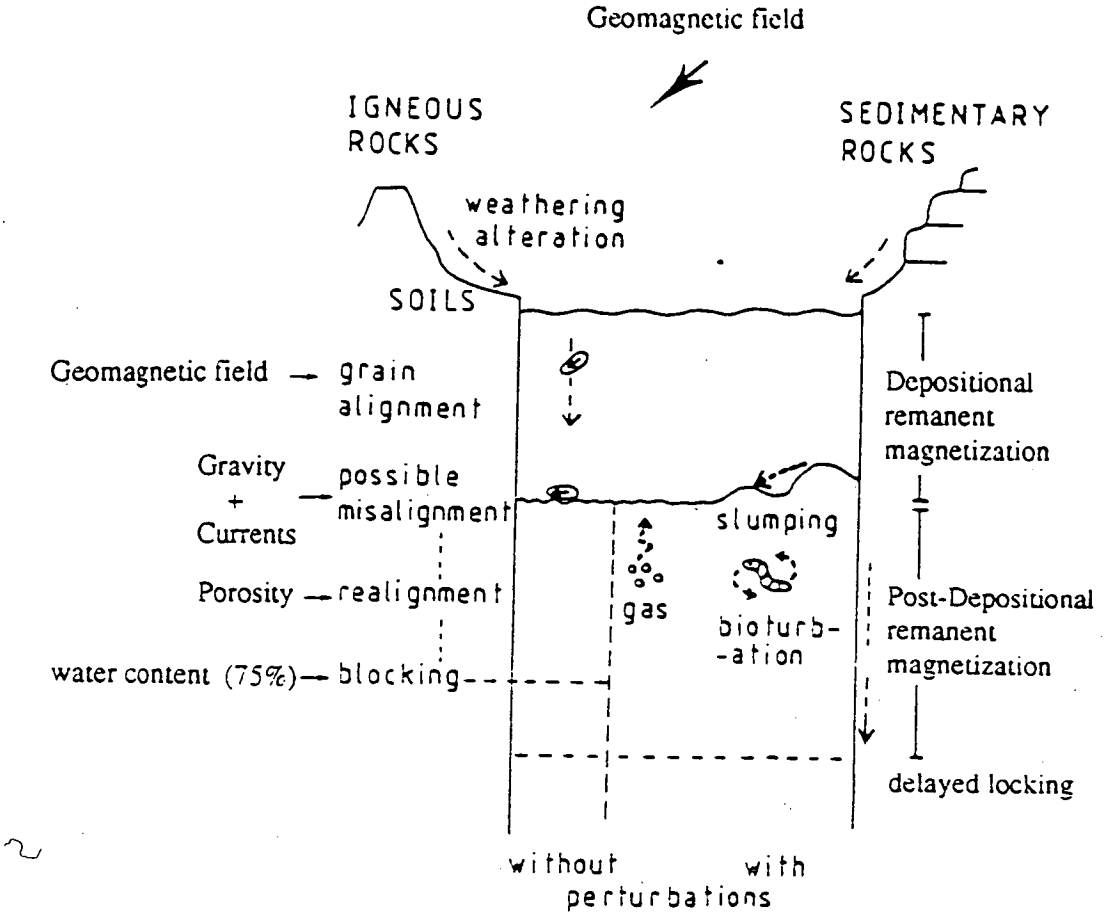

Fig. 1.5 The acquisition of depositional remanent magnetisation (DRM): a) From Thouveny and Williamson [1991], after Tucker [1983].

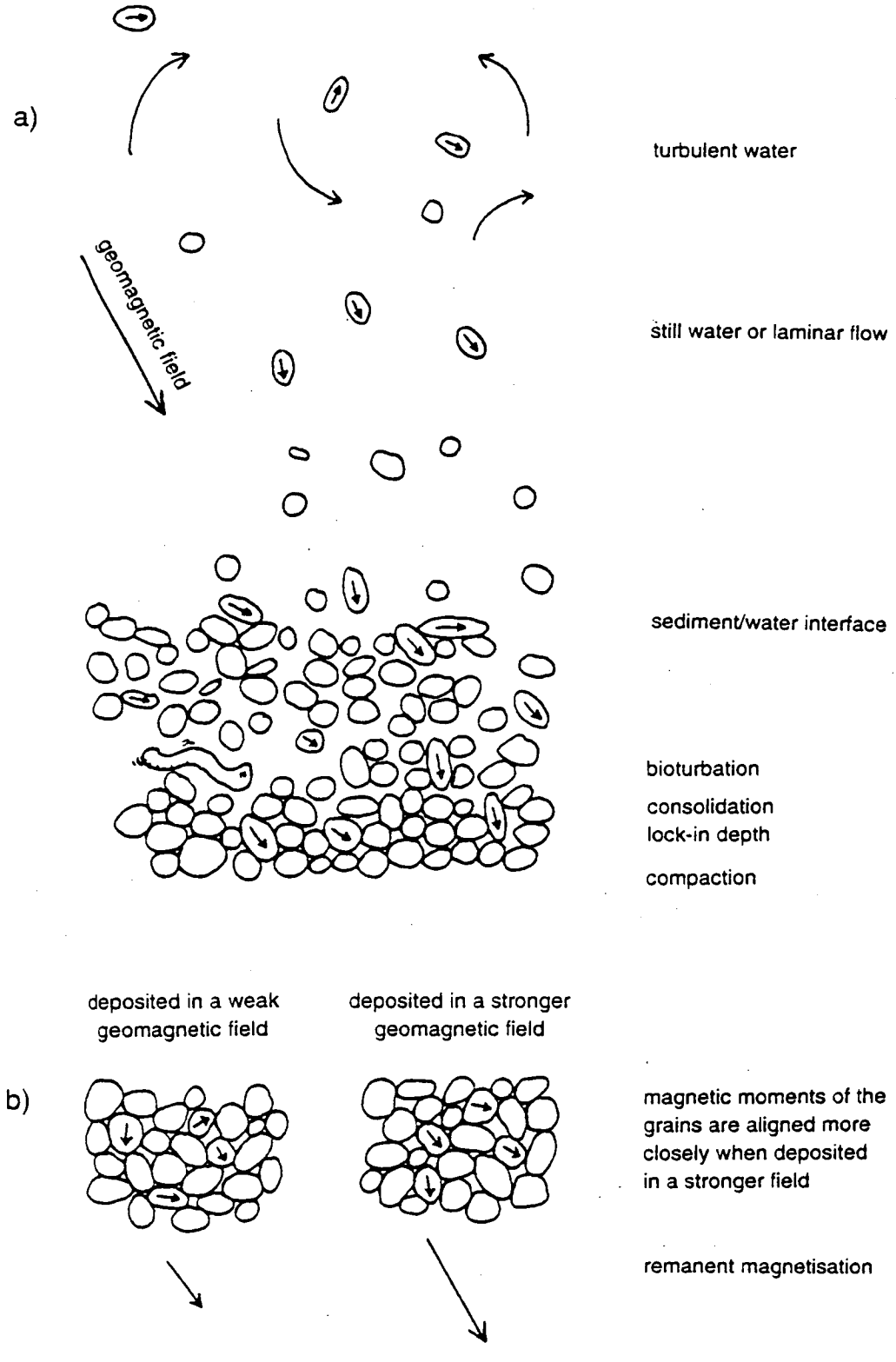

Fig. 1.6 The acquisition of depositional remanent magnetisation (DRM): a) after Tauxe [1993], a schematic illustration of the deposition of individual grains; b) a schematic illustration of the degree of alignment of the magnetic grains (and therefore the overall remanence of the sediment) deposited in weak and strong fields.

1.6 Lac du Bouchet

Lac du Bouchet is a maar crater lake, situated at 44°55'N, 3°47'E in the Haute-Loire region of France, at an altitude of 1205m (figure 1.1). The lake is small and almost circular, with a diameter of about 800m; the lake floor slopes down steeply at 50m away from the shore down to a flat central area with a water depth of about 27m (figure 2.1). There is a 50m accumulation of fine sediments under the lake, underlain by at least 15m of coarse sands and gravels. Much of the information in this section is detailed in Bonifay et al. [1987] and Truze [1990].

Geologically, the Bouchet maar is part of the Pleistocene Deves volcanic complex in the SE of the Massif Central. Effusive volcanic activity (represented by scoria cones, basalt flows, and maar craters) marks the Deves basalt plateau (figure 1.1). The maar craters result from phraeto-magmatic explosions, in which ground water meets magma causing a steam-magma explosion. Lac du Bouchet occupies one of these maar craters.

Potassium-Argon dating of basanitic flows around the crater gave ages of around 800 ka, and palaeomagnetic directions of similar rocks yield scattered normal and reversed directions, so prior to the 1990 coring it was not possible to choose between Brunhes or Matuyama chrons. However, assuming that the 15m of gravels and coarse sediments at the base of the cores represent the high-energy sedimentation in the very young crater (which seems likely), the age of formation would be a little younger than the age of the lowest fine sedimentation, i.e. roughly 340 ka.

After a relatively short phase of high energy, coarse sedimentation, by alluvial fans and mass movement, the crater walls became stabilised (with vegetation), and slow and steady fine sedimentation began. In the future, the remaining ~28m of water will become infilled and the maar will be dry.

Lac du Bouchet is remarkable for its tiny catchment area (figure 2.1), and the long period of time over which its sediments accumulated. No streams enter or leave the lake; its waters are meteoric in origin (Truze [1990]). There have been some changes in lake level in the past - there is a pre-glacial raised beach at 12m above the present lake level, and the lake was lower by 1.5m at the end of the last glacial; it is thought never to have been dry. Vegetation around the lake was dominated by steppe grasses in cold (glacial) times, and by trees in warmer times; there has been no ice sheet on the Deves plateau. Clastic (detrital) material enters the lake mainly by surface run-off. Organic matter is both produced in the lake itself (algae etc.), and brought in from the catchment area. The lake waters are meteoric in origin, and water leaves the system via ground-water and evaporation. There is little weathering of the basalt parent rocks, and the only authigenic minerals are vivianite and

siderite. It is thought that this lacustrine system changes in relation to the physical and biological conditions controlled by climate.

The present day climate at Bouchet has a precipitation with an annual mean of 870mm, concentrated in May and October, and a mean annual temperature of 6°C, ranging from -10°C to 25°C. The climate has oceanic (maritime) influences from both the Atlantic (400km away), and the Mediterranean (165km away). In the past, the palaeoclimate has been influenced by both the ocean (low seasonal temperature contrast, high precipitation) and the continent (high seasonal temperature contrast, low precipitation). During the early Eemian interglacial ($\delta^{18}O$ stage 5e), the climate was strongly oceanic, and the continentality increased through time until the the late glacial when the climate reverted to an oceanic type (Pons et al. [1992]).

From the palaeomagnetic point of view, the low-energy depositional conditions are very good for the recording of the field, because the acquisition process is less likely to be disturbed by currents, slumps, micro-turbidites, and so on. The basalt of the crater forms a rich source of magnetite, so the susceptibility (mean 5.53×10^{-6} m^3/kg) and remanent intensity (mean ~150 mAm^2/kg) are very strong for a sediment. Changes in grain-size down the cores are modest: medians from 3 to 8μm for bulk glacial sediment (Francus, pers. comm.), and 4 to 8 μm for the magnetite fraction (chapter 4).

Coring work at Lac du Bouchet began in 1982, with many coring expeditions recovering longer cores since then (table 1.2). The present work is part of the "Euromaars" programme, and has built on the past work of the "continental palaeoclimatology" and "Geomaars" programmes, all of which were funded by the EC.

Previous work on the palaeomagnetism of the Lac du Bouchet sediments comprises the following: studies of the 20m core set in Creer et al. [1990] and Thouveny et al. [1990]; palaeointensity and cosmogenic isotopes in Thouveny et al. [1993]; excursions (particularly the Laschamp/Olby excursion) in Thouveny and Creer [1992a, b]; anisotropy of susceptibility and deformation in Blunk [1989]; studies of the upper sediments in Thouveny [1987] (including palaeointensity work with normalisation by stirred remanence) and Smith and Creer [1986]; and detailed magnetic and palaeomagnetic studies in Thouveny [1991] and Smith [1985].

Table 1.2 Coring campaigns at Lac du Bouchet

dates	corer	max. depth of sediment recovered	cores recovered	cores sampled	programme
April '82	6m Mackereth	5.5m	5 cores	B1,3, 5, 7,12, 15, 16, 23, 24, 25, 26.	
Sept '82	12m joined Mackereth	5.7m	a few	-	
Nov '82	Mackereth minicorer	1m	many	-	
August '83	9m Mackereth	6.9m	not many	B42	
Nov '83	9m Mackereth	8.2m	successful	B46, 47, 49, 52	
April '85	12m Mackereth	11.2m	successful	B61, 63, 64	
1988	Livingston piston corer	20m	5 cores	A, B, C, D, F	Geomaars
Sept '90	Sedidrill: piston and Mazier	50m	4 cores	G, H, I, K	Euromaars

1.7 The Euromaars programme

This study on the palaeomagnetism of the Lac du Bouchet sediments forms part of the "Euromaars" project, entitled: "Reconstruction of the climatic and geomagnetic history of the middle and upper Pleistocene by the study of the sedimentary sequences of maar lakes in western Europe." The programme is funded by the E.C.

The maar lakes under study are located in four volcanic regions: the Massif Central of France; the Eifel of Germany; Monte Vulture in southern Italy; and the Latium around Rome. The research is being carried out by laboratories in six countries: at Edinburgh; Marseille; Trier (Germany); Louvain-la-Neuve (Belgium); Rome; Dublin; and Durham. Some of the early results of this programme are presented in "the Palaeolimnology of European Maar Lakes," [1993].

The aim is to establish long, continuous, continental records of palaeoenvironmental, palaeoclimatic and geomagnetic changes. These are then to be integrated with the wealth of data from the ocean, ice caps, and other continental sources.

On the palaeoclimatic side, two or three full climatic cycles are being compared and the previous interglacials are being studied in detail; this information can be used to gauge the likely development and termination of the current interglacial. The distribution of the sites on a north-south transect of Europe enables investigation of the spatial as well as temporal variability of climate, under different conditions of latitude, altitude, location, and insolation. Quantitative climate reconstructions are being made from the pollen analyses.

For palaeomagnetism, the aims were to investigate short and medium term geomagnetic phenomena, such as the palaeosecular variation, excursions and possible astronomical influences, and also to gauge the usefulness of the records for stratigraphy.

The sediments are also used to study volcanic and magmatic activity through time (particularly relevant for the Italian regions).

For the 50m Lac du Bouchet cores, de Beaulieu and Reille (Marseille) work on the pollen analysis, F. Chalié and J. Guiot (Marseille) on the quantitative climatic reconstruction from pollen, Pierre Francus (Louvain-la-Neuve) on the sedimentological work, Michel Icole (Marseille) on the organic carbon, Bertrand et al. (Orleans) on the geochemistry, and Nicolas Thouveny and his team also work on the palaeomagnetic aspects of the sediments.

Chapter 2

Fieldwork and Sampling

2.1 Introduction

In the light of previous corings (table 1.2) a new campaign was mounted to core the bottom sediments of Lac du Bouchet with new, heavy duty coring equipment, from a larger raft. It was hoped that coring would reach to the lower limit of the fine sediment found in previous corings, and in fact gravels and coarse sands were struck at a sediment depth of about 50m. Four cores were taken so that within-lake correlation, stacking and control could be carried out. Around 2500 samples from the cores were analysed in Edinburgh to form the data-set for the work.

2.2 Logistics

The size of the operation required a large number of people to be involved with the fieldwork - typically 4 or 5 on the raft during coring, and 7 or 8 during the assembly and positioning of the raft.

The raft comprised 2 long metal flotation chambers (each 10×2·5×2m), on top of which sat the platform and working space (10×7m). The "Sedidrill" coring machine was fixed to the centre of this platform. The raft was pulled to the centre of the lake with a strong rope by a "Zodiac" motorboat, and then fixed to the near and far shores by the ropes. Two steel cables were attached to trees and large boulders substantial enough not to move under the force of a taut steel cable attached to a heavy raft, and were pulled into the raft by the ropes and winched tight. Buoys were attached at points on the cables to keep them close under the water surface. Two more steel cables were pulled to the raft with ropes, so that finally the raft was attached by its four corners to secure points at roughly 90° separation on the lake shore, unable to move significantly either laterally or rotationally. Fine adjustment of the position, so that cores were taken at different places, was achieved by playing out cable from one corner of the raft and re-tightening from the opposite corner.

The exact position of the raft was found by taking compass bearings off the hotel and other features on the lake shore. The depth of water was found by measuring the length of weighted rope taken to reach the bottom sediment, roughly 28m.

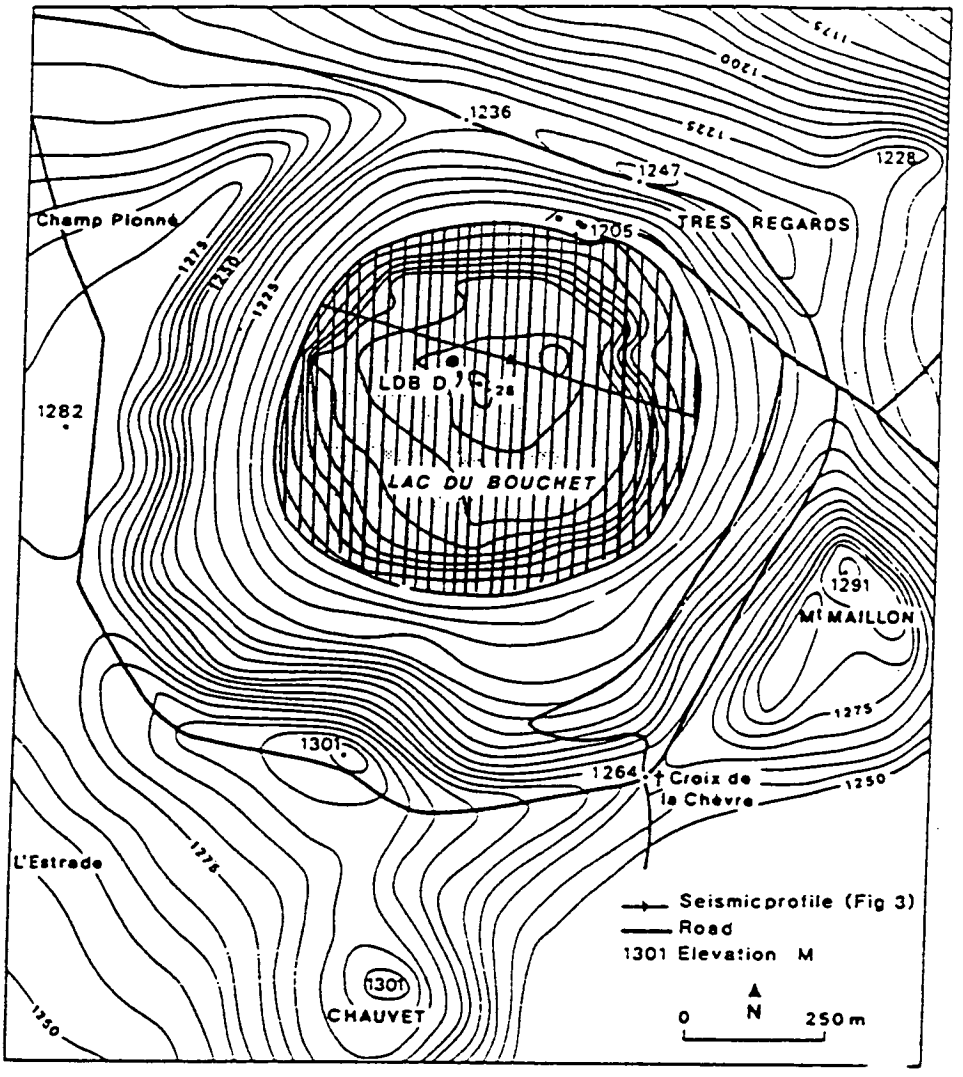

Fig. 2.1 A map of Lac du Bouchet, showing topography, bathymetry and line of seismic section (figure 2.2). From Truze and Kelts [1993], and Truze [1990].

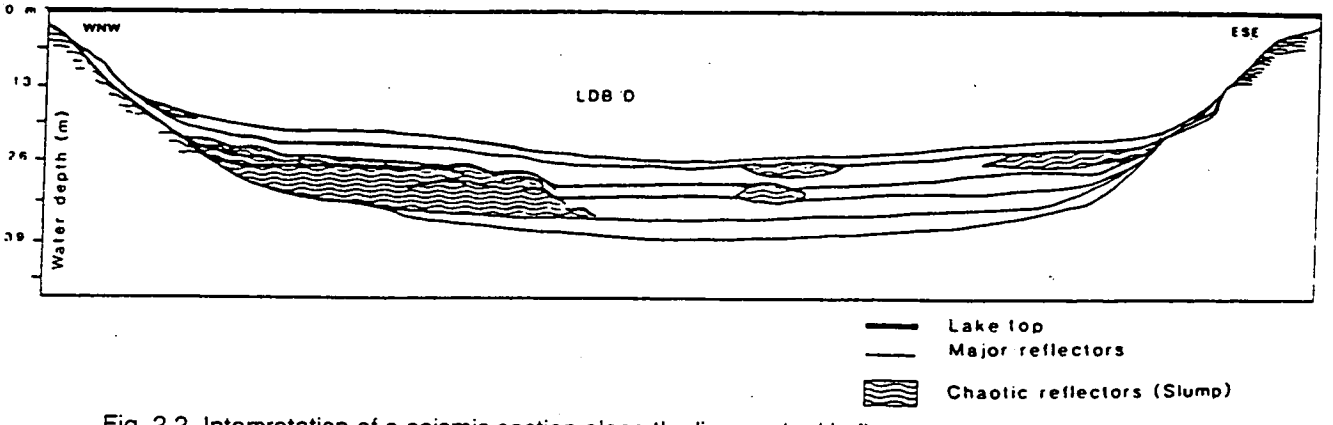

Fig. 2.2 Interpretation of a seismic section along the line marked in figure 2.1 (Truze [1990]).

2.3 Coring procedure

Lining tubes of about 12cm diameter were played down to just below the sediment-water interface. The core lining was pushed down after each section was brought up until it was about 6m down into the sediment, to prevent caving of the core walls in the softer top sediments. At the start of each working day the hole was "cleaned" by running a drill bit down to the bottom and forcing any caved material up out of the hole in the drilling fluid. None of the core sections were azimuthally oriented.

Piston coring

The piston corer was used for the upper half of the sequence. It was lowered down on the end of 1.5m long metal tubes (diameter ~4.5cm), pre-connected in "trains" of three where possible, until the corer was calculated to be at the required depth. The core barrel was pushed hydraulically down from the corer into the sediment, and was known to have reached its lower limit when the hydraulic pressure dropped. It was then brought back to the surface by winch, and by un-screwing all the trains of tubes. The sediment was immediately extruded into a PVC storage tube, marked (with an arrow pointing to the top of the section, the core section name (H12, H13 etc.), and the top and bottom depths), and sealed. Even at this stage, an initial assessment of the sediment can be made from its colour and grain-size - grey and silty sediment indicates glacial conditions (and forms the bulk of the sequence), and dark, organic-rich material indicates warmer conditions.

The piston corer was reliable and obtained clean cores with little wastage down to a limit of 22 - 28m, where the sediment was too hard for the core barrel to be pushed in. Some problems were encountered with the coarser sediment at around 9m depth, as had also been found with the Mackereth and Livingston corers.

Mazier coring

The Mazier corer was used after piston coring failed, having the opposite characteristic of working better with compact, more brittle sediment. Down to about 22m the sediments are a little too soft to be recovered, causing a narrow depth window where neither corer is ideal - this was overcome during the course of the fieldwork by pushing the piston corer deeper and deeper, but still 5m was lost from the first core (G) due to this problem.

The Mazier system comprised an outer tube (~7cm diameter) running down from the raft to the bottom of the hole, with a coring head attached at the lower end. The core barrel unit (~2m long) was dropped to free-fall down the outer tube, through the viscous coring fluid, clicking into place at the end of the outer tube with its tip projecting ~1cm beyond the outer tube. The outer tube was rotated and pushed down while drilling fluid was pumped

down through the tube, round the core barrel unit and through the head. The inner barrel was acted on by the friction of the sediment and should therefore remain un-rotating while it penetrated the sediment. The core barrel unit was recovered by lowering a "catcher" on a cable, which locked onto the top of the barrel unit and released its catch when upward tension was applied. Since only the next piece of outer tubing needs to be added to the column after each section, rather than un-doing and re-doing all 50m of them, this method is much quicker than using the piston corer.

The sections were taken out of the core barrel, already in their PVC tube, and marked in the same fashion as the piston core sections. Some sediment was lost when the core barrel head was unscrewed and removed.

In practice, it was found impossible to prevent rotation of the core barrel absolutely, as the evidence of the section twists in the declination results testifies (section 2.6). There may be a greater risk of disturbance to the magnetic fabric of the sediment when using the Mazier corer, because of the rotation, the high pressure fluid in contact with the sediment, and frictional heating effects.

Gravels and coarse sediments were encountered below 50m, and prevented recovery of whole sections; the only material to be recovered were large (to ~5cm) stones, and, rarely, some coarse sediments. The Mazier corer was used in conjunction with the drill at these depths, and a maximum of 65m was reached, confirming that 50m really was the base of the fine sediments, and the gravels represented the initial infill of the crater.

Table 2.1 Corer comparison

	Piston	Mazier
core diameter	8cm	5cm
section length	105cm	0-150cm
typical loss of sediment per section	3cm	15cm
disturbance of sediment	not much	a little
speed of coring	up to 6m per day	up to 15m per day
depth range at Lac du Bouchet	<~24-28m	>25m
high pressure drilling fluid in contact with sediment?	no	yes
twisting of sections?	no	in some sections

2.4 The cores

Between August 31st and September 29th 1990, four cores were taken. Cores I and K had much of the upper 19m drilled rather than cored, to save time, as this part of the sequence had already been studied in detail from the 1988 20m core set. Core H was chosen as the reference ("master") core, as it was the most complete.

The relative positions of the core sections, missing sediment, and so on, can be seen in the matching of susceptibility records diagram (figure 5.1)

Table 2.2 Coring timetable

core	dates	maximum depth	total length recovered (approx.)	piston-Mazier transition
G	31 Aug - 6 Sept	53.5m	38m	20.2m
H	7 - 15 Sept	53m (65m drilling)	45.5m	25m
I	16 - 20 Sept	64m	37.5m	28.7m
K	26 - 29 Sept	54m	24m	22m

2.5 Storage and sampling

The sealed core sections were transported by car to the Laboratory of Quaternary Geology at Luminy, Marseille, and put into storage in a cold store for the benefit of the geochemists, so that decay of organic matter, or other chemical reactions, would be inhibited. There was no magnetic shielding around the store.

The core sections were opened and sampled during three visits by members of the Department of Geology and Geophysics in Edinburgh (table 2.3), together with Nicolas Thouveny of the LGQ.. Some sections (core H) had already been opened and sampled for pollen.

Table 2.3 Sampling timetable.

sections	n°. samples	Dates	Sampled by:
H12-42	926	February 1991	T. Williams
G1-18, H5-11, I11-13	812	July 1991	Prof. K.M.Creer
G24-40, I14-26, K1-2	954	September 1991	T. Williams, L. Chevalier

To open and sample the cores, the sealing was cut off, and the PVC tubing was cut length-ways down both sides by pulling the section down a track, through a pair of fixed rotary buzz-saws. The sediment was then cut in half by pulling a taut wire down the section, guided by the cuts in the PVC. One half was re-sealed in flexible clear plastic and the other used for sampling.

The sample boxes used for palaeomagnetism were near-cubic, of side 2cm and volume 6.8cm^3, made of clear plastic and with a small hole in one corner so that air could escape when the box was being filled. They were pressed into the sediment every 2.5cm down the central axis, omitting broken sediment where it occurred, and marked with the core section name and ascending integers from the top of the section. The total length of sediment, the depth to the centre of each sample, and any obvious sedimentological features were noted in a sampling notebook, an example page of which is presented as figure 2.3.

The full boxes were extracted using a spatula, leaving a 2cm wide empty trench down the centre of the half-core.

Sampling proceeded down to a depth of 46m, and stopped there, because below that depth the sediment was too compact for the sample boxes to be pressed in.

2.6 Visual inspection of cores

Much valuable information can be gained about Lac du Bouchet's palaeoenvironment and lithology, simply by inspection of the core sections.

The most obvious features are the dark, hard horizons sometimes containing fibrous organic matter. These were expected, and seen, as three bands between 16 and 21m depth, as they had been identified in the 20m cores as corresponding to the warm $\delta^{18}O$ isotope stages 5a, 5c and 5e (figure 6.4); further organic horizons appeared at 31m and 42m. Another obvious feature is the white tephra (ash-fall) deposit, over 65cm thick, found at a depth of ~42m enclosed by organic sediment. The sediment becomes harder, dryer and more brittle with depth, due to compaction by the weight of overlying material.

Various sedimentological features were noted in the sampling notebooks: the occurrence of vivianite (an iron-phosphorus early diagenetic mineral), up to 5mm across, of white colour, that quickly turns dark purple-blue on exposure to the air. Sandy layers (micro-turbidites) were noted when they were obvious enough to identify. Pebbles and scorie were also noted.

High angle normal micro-faulting of up to 3cm throw crossed the sections rarely (for instance in sections H18 and H33).

Unfortunately my notes on the above features were not made in a rigorous fashion, and the down-core logs based on them (for example figure 7.1k) only give a rough qualitative idea of their extent. Their main function here is to be compared with magnetic/palaeomagnetic data. Moreover, sedimentological analysis is beyond the scope of this study, and is being studied in detail at Louvain-la-Neuve and LGQ Marseille as another part of the Euromaars project. On the other hand, all four cores were sampled for palaeomagnetism: much useful information could gained from the inter-core comparison of features such as gravel layers, turbidites and vivianites.

Thursday 27th February 1991

LDB H41

(cored 15 sept'90)

mud length : 137 cm
core length : 150 cm
weight of core (- box):

	depth	susc	
1	21	pilot 885	11.02
2	23.5	717	10.27
3	29	795	11.20
4	31.5	777	11.40
5	34	758	10.82
6	39	729	11.12
7	41.5	796	11.08
8	44	759	11.00
9	48.5	772	11.00
10	51.5	831	11.13
11	54	693	10.66
12	57	711	10.60
13	59.5	702	10.52
14	62	699	10.22
15	65	683	9.72
16	69	pilot 753	10.51
17	71.5	654	10.08
18	74	640	10.09
19	79	671	10.05
20	81	700	10.38
21	83.5	768	10.89
22	86.5	729	10.80
23	89	637	10.27
24	91.5	678	10.53
25	95	507	9.32
26	98.5	592	10.25
27	101.5	552	10.17
28	104.5	611	10.03
29	107	607	10.24
30	110	616	10.38
31	113	653	10.35
32	119	pilot 786	10.61
33	122	771	10.72
34	124	770	10.51
35	128.5	767	10.79
36	131.5	728	10.22

(10 May)

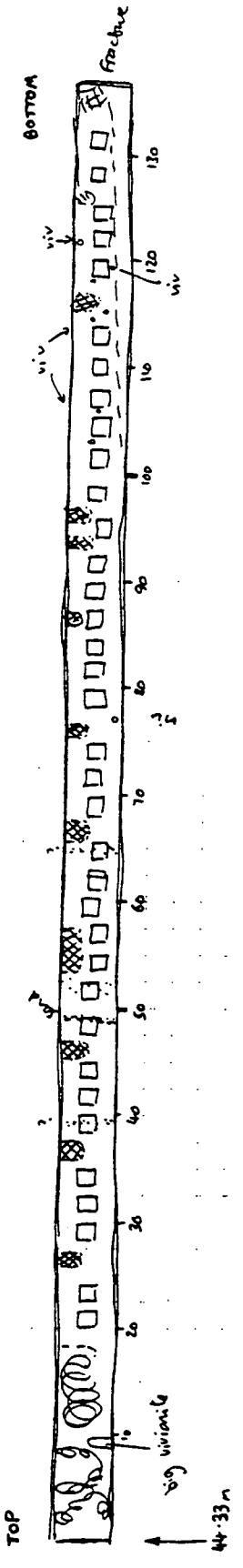

Fig. 2.3 An example page from sampling notebook, core G, section 27.

Chapter 3

Measurements

3.1 Introduction

The data-set on which interpretations of the environment and the geomagnetic field in the past are made is based on the type of measurements described in this chapter. This chapter simply describes what property of the sediment sample is being measured, what it will be used for, which instruments were used to measure it, and the accuracy of the measurements.

The measurements made on the Lac du Bouchet samples can be classified into two major groups: rock-magnetic (or, simply, "magnetic") which are applied to the palaeoenvironment question; and palaeomagnetic, which are used to find the nature of the geomagnetic field in the past.

Table 3.1 Summary of measurements, units and average values for samples from cores G, H and I

parameter	units (SI)	mean	SD	skew	obsevations
susceptibility	$10^{-6} \times m^3kg^{-1}$	5.53	1.47	-1.05	2917
susceptibility	unitless($\times 10^3$)	9.05	2.41	-	2917
IRM	mAm^2kg^{-1}	76.14	23.45	-0.95	2667
ARM	mAm^2kg^{-1}	3.58	1.03	-0.80	2463
NRM	μAm^2kg^{-1}	206.47	158.11	6.45	2890
NRM_{10mT}	μAm^2kg^{-1}	121.05	93.09	3.33	2900
NRM_{20mT}	μAm^2kg^{-1}	74.61	67.37	7.52	2610
MDF	mT	13.10	5.55	-0.37	2588
weight	grams	11.13	0.92	-1.48	2918

(The samples have a volume of $6.8cm^3$ and a weight of about 11 grams.)

3.2 Rock-magnetic measurements

The rock magnetic measurements treat the samples only as assemblages of magnetic grains, with no regard to their magnetic history, and are based on magnetisations implanted in samples by different fields in the laboratory. They reflect the concentration of the magnetic grains, their composition (titanomagnetite, magnetite, haematite, state of oxidation etc.), and domain state (single-, pseudo-single-, or. multi- domain). Grain-size is closely related to domain state. Thus these measurements provide lithological information, which is interpreted in terms of the local environment (erosion, vegetation etc.), itself further related to local, regional and global climate (temperature, rainfall etc.) as discussed in chapter 7.

Three magnetic measurements were performed on all the samples: magnetic susceptibility, anhysteretic remanent magnetisation (ARM) and isothermal remanent magnetisation (IRM). The major difference between them is that susceptibility is a measure

of the reversible magnetisation induced in a sample *during* application of a field, whereas the ARM and IRM are remanences left *after* a field is removed. Also, they each excite slightly different populations of the magnetic grains.

Further rock magnetic measurements were carried out on a selection of 40 samples, representative of the range of susceptibility and NRM_{10mT} intensity variations: demagnetisation of ARM (and IRM), IRM acquisition and back IRM, hysteresis loops, (and decay of viscous remanence).

Susceptibility

Susceptibility is the ratio of the magnetisation induced in a sample to the applied field. Susceptibility is thus the gradient of the initial straight line segment of the hysteresis plot. The greater the concentration of magnetic grains there are (in a sample), the greater the susceptibility will be. Of the natural magnetic minerals commonly found in sediments, magnetite has a susceptibility 75 - 90 times that of haematite.

The susceptibility measurement is very quick to perform, at around 100 samples in half an hour, and since only a small (0.05mT) field is used, the sample reverts back to its previous state on removal. Thus susceptibility is the ideal reconnaissance measurement: quick, easy and leaving the NRM unharmed. In addition, the susceptibility of whole cores can be measured using a pass-through coil. A borehole susceptibility meter has been tested at the dry maar Praclaux in October 1992, but was not used at Lac du Bouchet.

The SI units of susceptibility are m^3. Susceptibility per unit volume (κ) is unitless, and susceptibility per unit mass (χ) has units of m^3/kg. In this thesis I use susceptibility per unit mass most of the time.

Susceptibility was measured using a Bartington Bridge, which was standardised by using a sample of copper sulphate ($CuSO_4 \cdot 5H_2O$), of known susceptibility (7.4×10^{-8} m^3/kg).

Isothermal Remanent Magnetisation (IRM)

An isothermal remanence was implanted in all of the samples by the application of a steady 1 Tesla field at a constant temperature (hence: isothermal), in this case room temperature. At 1T, the samples are very nearly saturated, that is at their maximum stable remanence, and this magnetisation is called the saturation IRM, or *SIRM*. If steadily increasing fields up to 1T are applied and the samples measured after each step, the IRM will increase, and an *IRM acquisition* curve may be plotted; this was done for the 40 selected samples and example curves are shown as figure 4.2. *Back IRM* is the remanence after a steady field is applied in a reverse sense to an already saturated sample, and curves may be built up using increasing back-fields (figure 4.3).

Fixed electromagnets were used for the bulk application of the 1T SIRM, and a Molyneux pulse magnetiser was used for giving IRMs up to 300mT. The fields generated by

these instruments were checked by using field probes. The remanences were measured on a Molspin spinner magnetometer, as were the ARMs. The units are output as mAm^2, and these were subsequently normalised for weight or volume. The Molspin was calibrated using a standard sample of strength 19.6 μA/m, and was run connected to a BBC computer using the program "Molas6".

Anhysteretic Remanent Magnetisation (ARM)

An ARM was implanted in each of the samples by placing them in a small (1mT) steady field, while an alternating field was ramped up to 80 mT and back to zero. The samples are left with a remanence which is proportional to the steady field, for low values. This enables a susceptibility-like (ratio of magnetisation to applied field) parameter, the susceptibility of ARM, to be calculated. The ARM was applied along the vertical axis of a sample using an ancient coil running off a Variac controller, while the voltage across the coil was monitored. AF demagnetisation of ARM was carried out on the selected samples.

Hysteresis properties

Magnetic hysteresis is due to the lagging behind of the magnetisation to the applied field, forming a hysteresis loop when the applied field is stepped down from 1T to -1T and back up again to 1T (figs 4.4, 4.5). The magnetisations in this section are measured in the presence of the applied field, and so are not remanences, except where the field is zero.

Hysteresis loops were made for the selected samples on a vibrating sample magnetometer (VSM).

Useful Ratios

Since susceptibility, SIRM and ARM depend on slightly different sub-sets of the magnetic population (table 4.2), ratios may be exploited to gain information on the relative proportions of grain sizes and domain states. For example the ratio SIRM/susceptibility is indicative of the changing population of super-para-magnetic (SPM) grains (size < 0.03μm). Because only susceptibility responds to these, the ratio will go down when the SPM fraction increases.

3.3 Palaeomagnetic measurements

The palaeomagnetic measurements reflect the magnetisations acquired by the sediment samples at any time from their deposition at the top of the sediment column up until their measurement. These include the depositional and post-depositional remanent magnetisation (DRM), and any overprinting by viscous, thermal or chemical secondary magnetisations, or degradation of the remanence by mechanical disturbance (due to compaction, coring etc.). The aim of this group of measurements is to provide as accurate as possible a picture of the geomagnetic field at, or soon after, the time of deposition.

All of the NRM measurements and demagnetisations were done on the 2G Corporation cryogenic magnetometer held in the Department of Geology and Geophysics at Edinburgh University. The device is controlled by an IBM-compatible PC running the "Datacq" program of Steve Gillette. The samples were demagnetised one at a time, with a measurement after each step. Each sample takes about 10 minutes.

Natural Remanent Magnetisation (NRM)

The NRM is composed of two parts: the DRM, which we want; and any subsequent magnetisations and disturbances to the sediment, which we don't. The process of DRM acquisition is described in section 1.5, but, briefly, the magnetic grains rotate to align along direction of the Earth's field around the time of deposition, and this direction is "locked in" after a few cm of burial, when the grains are no longer free to rotate in the interstices of the sediment. The intensity of the DRM is due to the degree of alignment of the magnetic grains, which is roughly proportional to geomagnetic palaeointensity (Tucker [1981]). Also, the DRM depends, like susceptibility, IRM and ARM, on the concentration, size and composition of the magnetic grains.

Subsequent to the DRM, other factors may influence the NRM, all of which should be checked for importance and taken into account. There may be diagenesis of the sediment, as evidenced by mineral phases such as vivianite and clay minerals. On piston coring, the sediment is largely unshaken and undisturbed, except at the very edges of the 8cm diameter core. However, with the Mazier coring, there is rotation, and drilling fluid is forced at high pressure through the coring head. Therefore there is not only a worry that the 1.5m long sections may be twisted, but also the fine structure of the sediment might be disturbed and some grains re-aligned. Viscous magnetisation (VRM) may be picked up from the present Earth's field, so the samples were stored within large sets of neutralising Helmholz coils to minimise this effect. There is inevitably some drying of the samples between sampling and measurement, and this is a possible opportunity for individual grains to become free and re-align (Tucker [1980]). The NRM was measured after storage in a low field environment, and after the measurement of weight and susceptibility.

Demagnetisation of the NRM

In order to get closer to the original DRM, the samples were progressively AF demagnetised at steps of 2.5, 5, 10, 20, 40 and 60 mT. This demagnetisation, or "cleaning", will remove the "softer" secondary magnetisations (such as VRM) first, leaving the "harder" components intact. This is best illustrated using demagnetisation plots, for example in figure 4.11. The *median destructive field* (MDF) is the field at which the magnetisation falls to half its original value, and this parameter is used to indicate the size of the initial component: the lower the MDF, the higher is the initial component. The other commonly employed type of

demagnetisation is thermal demagnetisation, which needs care when dealing with wet unconsolidated sediments. This was not done at Edinburgh, but some thermal demagnetisations were carried out at Marseille.

Palaeomagnetic ratios: palaeointensity

The aim of dividing the NRM by one of the rock-magnetic parameters is to normalise out, as far as possible, the lithological component from the NRM. These ratios are sometimes called "Q-ratios". Since the NRM and the three rock-magnetic parameters (susceptibility, SIRM and ARM) are all dependant on the concentration of magnetic grains in a sample, NRM divided by one of the others will go a long way to removing the lithological contribution, assuming the similar magnetic grains carry the different magnetisations. The range of grains comprising the different magnetisations is not exactly the same, due to the fundamentally different processes of acquisition, so the normalisation will not be perfect. The matters of which normalising parameter is best, and which NRM demagnetising step is best, are investigated and discussed in sections 4.4 and 4.5.

3.4 Other analyses done on the cores

Magnetic extracts from the sediment, chosen to cover both organic and glacial sediments, were analysed by scanning electron microscopy, by Nicolas Thouveny at Marseille.

Several detailed and lengthy analyses of the non-magnetic aspects of the sediment cores have been carried out at institutions within the Euromaars consortium. Pollen analysis has been carried out on core H and some of core I at St.Jerome in Marseille, by de Beaulieu and Reille. This work is used in chapter 7 for assessing the palaeoenvironmental significance of the rock-magnetic records, and also for relative dating, by correlation with the marine $\delta^{18}O$ stratigraphy. Sedimentological studies have been carried out at Louvain-la-Neuve by Pierre Francus, and geochemical work, including organic carbon, was done at LGQ, Marseille. Bertrand et al. [1992], of Orleans, present an initial combined sedimentological and geochemical study of the 50m Lac du Bouchet cores.

Dating measurements are critical to both the palaeoenvironmental and geomagnetic interpretations, as it is the time variation of the magnetic field and the environment which is under study. Argon-Argon dating on sanidine (K-feldspar) contained in the 65cm tuff layer of core I at 42.5m depth is being carried out by A. Boven in Brussels. ^{14}C datings were done on the Mackereth core series to 8m (45 kyr) (Creer [1991])). There is therefore a lack of direct dating on the Bouchet sediments, and although the Ar-Ar dates are well positioned near the base of the core to constrain the relative dating there, non-unique depth→time models are unavoidable (chapter 6).

The water content of the upper sediments was measured by Smith [1985], and is presented here as figure 3.1.

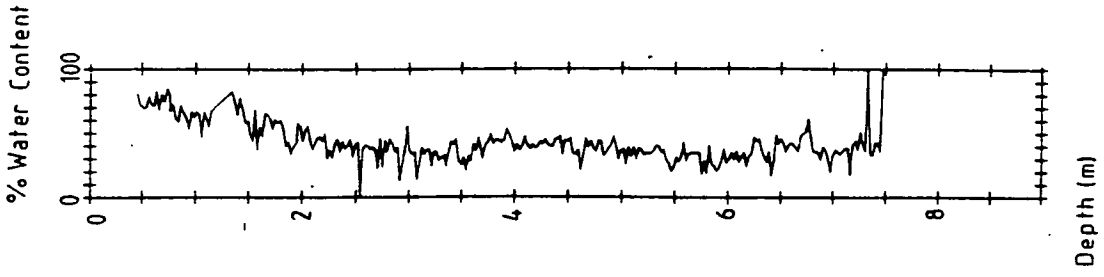

Fig. 3.1 Water content of the upper 8m of the sediment (copied from Smith [1985]).

Chapter 4

The magnetic and palaeomagnetic nature of the sediments

4.1 Introduction and aims

A detailed magnetic study of sediments from Lac du Bouchet was carried out to gain an understanding of the magnetic mineralogy, the stability of the remanent magnetisation, and the suitability of the sediments for palaeointensity work. Previous work on the upper sediments by Thouveny, Smith and Creer has characterised the magnetic mineralogy (the composition is a low Ti titano-magnetite, and concentrations are especially high for a sediment), and has revealed that organic-rich sediment yields unreliable palaeointensities. In this chapter, experiments are described which confirm the previous results for the sediments from the lower parts of the core. Each topic is addressed in turn by appropriate analyses, using measurements and methodology described in the last chapter.

In this thesis I have used the term "magnetic mineralogy" in a wider sense than usual, to cover the composition of the magnetic grains (for example titano-magnetite, haematite), their concentration, their grain-size and domain state. This is because there is often a need to refer to these things as a group. An alternative term is "magnetic activity", used by Tauxe [1993].

The several over-lapping topics investigated in this chapter are introduced below:-

Defining the magnetic mineralogy of the sediments. Susceptibility shows distinctive variations down the cores, and the values are much lower in the organic-rich layers, due to some aspect of the magnetic mineralogy (see figure 7.1). For reliable palaeointensities to be recovered, one of the requirements is that the magnetic mineralogy is fairly uniform down the sediment sequence. Therefore, 40 samples were chosen from the range of susceptibility and NRM intensity variation (figure 4.1) for detailed analysis. These samples come from depths ranging from 18 to 45m, from cores G and I, to cover possible changes in compaction, water content and coring method. Room temperature magnetic experiments were carried out, including the acquisition and demagnetisation of IRM, the demagnetisation of ARM and hysteresis parameters. The results are combined with Curie point information from previous studies to define the range of magnetic mineralogies in the sediment.

Different palaeomagnetic behaviour in the organic-rich samples. The natural magnetisation (NRM) acquired by low susceptibility (organic-rich) sediment is exclusively low compared to that acquired by the bulk of the samples (figure 4.1). The boundary in behaviour occurs at a susceptibility of about 4.2×10^{-6} m^3/kg. The difference in behaviour is

important because it means that relative palaeointensities cannot be recovered from low susceptibility samples. The difference in results of the magnetic experiments between the two sets of samples is carefully examined throughout this chapter, to see if the change in behaviour is due to the magnetic mineralogy. Different physical conditions around the time of deposition is an alternative explanation. It is not likely that the uniformly low NRM of the organic-rich samples is due to low geomagnetic palaeointensities.

Non-organic samples with a low NRM intensity. The interpretation of low palaeointensities (recorded in the Lac du Bouchet sediment) in relation to excursions is discussed in section 8.7. It is important to know that the low palaeointensity of these samples is not due to some aspect of the magnetic mineralogy that has not been properly normalised out. Hence these samples, identified on figure 4.1, have been classified as a group in the magnetic experiments of this chapter.

The secondary component of magnetisation. It is seen from the demagnetisation plots that some samples show a very high secondary component of magnetisation (figure 4.11). The origin of this large secondary component is identified by comparing the average size of the secondary component among different sub-sets of the whole sample set. The AF demagnetisation value best able to remove this component is found by comparing the results of the 10 and 20mT steps (fig 4.17).

Normalisation of the effects of the magnetic mineralogy from the NRM. The NRM intensity depends on the magnetic mineralogy, for example a sample with a high magnetite concentration has a higher NRM intensity than one with a low magnetite concentration, though they might both have been deposited under the same geomagnetic field strength. Susceptibility, ARM and SIRM can be used as uni-variate estimators of the multi-variate magnetic mineralogy. The NRM intensity normalised by each of these three possibilities is compared.

A few samples show anomalously high intensities, and they show up as spikes in the down-core plots. Two or three such samples are included within the "regular" sample group of figure 4.1.

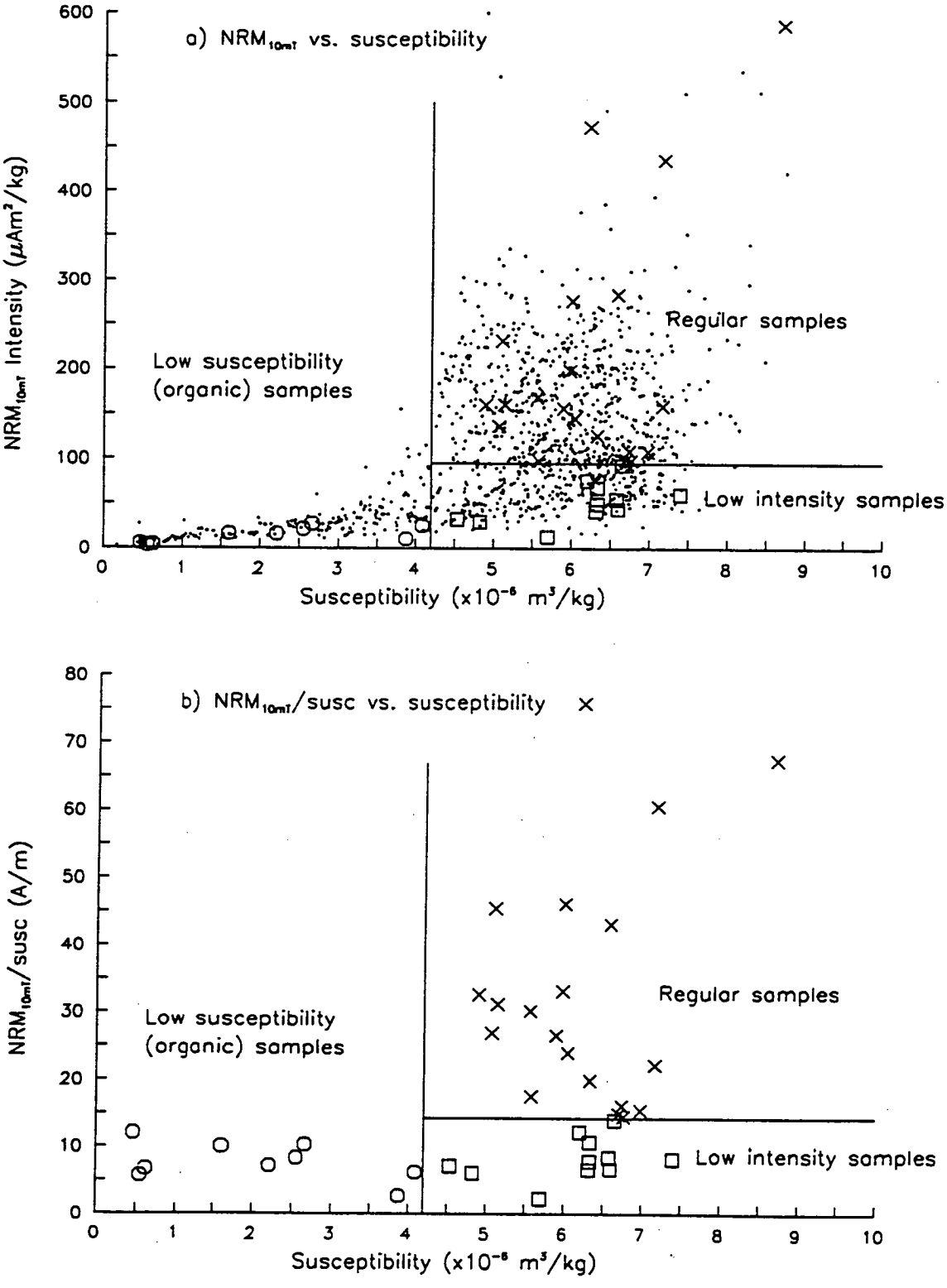

Fig. 4.1 Bi-plots of NRM_{10mT} intensity and NRM_{10mT}/susceptibility vs. susceptibility. All of the samples from core H are plotted as dots on (a). They fall into three regions of interest: samples with a low susceptibility, which only have low intensities for some reason; mid to high susceptibility samples with a low intensity, of interest when considering excursions, amongst other things; and the remainder of the ("regular") samples. The samples with low susceptibility are typically darker sediment rich in organic material, and are thus termed "organic"; I have termed the rest of the samples "non-organic". The 40 samples selected for detailed analysis are shown on (a) and (b), and the region to which they belong is identified by symbol (circle, square and cross) in both this and the following diagrams of this chapter.

4.2 Magnetic mineralogy; criteria for sediment suitable for palaeointensity work

There is an apparent conflict of interests when sediment is used as a recorder of both geomagnetic and environmental changes. For ideal *geomagnetic* recording, the magnetic mineralogy would be constant down the core (the concentration would be high enough to give a strong magnetisation, the composition would be magnetite, and the grain-size would be between 1 and 15 μm). For ideal *palaeoenvironmental* recording, the magnetic mineralogy would vary in a consistent manner with the cycling of warm and cold climatic conditions. For the best compromise solution we would like a sediment sequence (deposited at a constant rate) in which the magnetic grains have a constant size and composition, with only their concentration varying by a modest amount, in tune with local climatic changes.

Susceptibility, IRM and ARM would all be proportional to the concentration in this best compromise situation. The susceptibility, IRM and ARM down-core plots would have exactly the same shape, and any of them would be equally good for normalising the magnetic mineralogical effects from the NRM to give a relative palaeointensity. The Lac du Bouchet glacial sediments come quite close to this ideal situation. There is enough over-sampling to apply rejection criteria so that our remaining samples more closely approach the best compromise situation.

Table 4.1 The criteria for sediment suitable for palaeointensity determination (after King et al. [1983])

	requirement	suggested method
1	the dominant mineral **composition** is magnetite (Fe_3O_4) or a similar composition (e.g. a titanomagnetite with a low Ti content)	Examine IRM acquisition curves. Examine mineralogy, electron diffraction pattern, thermomagnetic properties of magnetic separates.
2	the particle **size range** of the magnetite is about 1-15μm.	Susceptibility vs. susceptibility of ARM plot. (King [1982]) H_{rs}/H_s vs. $(B_0)_{cr}/(B_0)_c$ plot (Day [1977])
3	the maximum (magnetite) **concentration** is less than 20-30 times greater than the minimum.	from range of susceptibility or SIRM values

Guidelines exist for minimum requirements for magnetic mineralogy suitable for geomagnetic palaeointensity determination from sediments (King et al. [1983]) (table 4.1). The composition, concentration and grain-size of the magnetic minerals in the sediment is found by the experiments described below.

Composition of the magnetic minerals

The two magnetic minerals commonly found in sediments are magnetite and haematite. Magnetite has by far the higher magnetisation, and so the high values of susceptibility, SIRM and ARM indicate that there is a high magnetite content.

IRM acquisition. IRM acquisition can be used for distinguishing composition, because of the different coercivities of magnetite (2 - 10mT) and haematite (400mT) (Thompson and Oldfield [1986]). There is also some dependence on the grain-size of magnetite, but this is not as large as the magnetite/haematite effect. The IRM acquisition for the 40 selected samples is shown as figure 4.2. The 31 non-organic samples are averaged together, and their very narrow bunching (small standard deviation) indicates that there is a very constant composition down-core. The samples reach 95% of their maximum by 140mT, and between 300 and 1000mT the curve is at the maximum. Hence the magnetic mineral is magnetite-like, and haematite is not significantly present. The samples with a susceptibility less than 4.2×10^{-6} m^3/kg (organic-rich samples) show generally more scattered acquisition curves, mostly reaching the maximum at higher values, indicating that a small impurity of higher coercivity mineral is present as a trace.

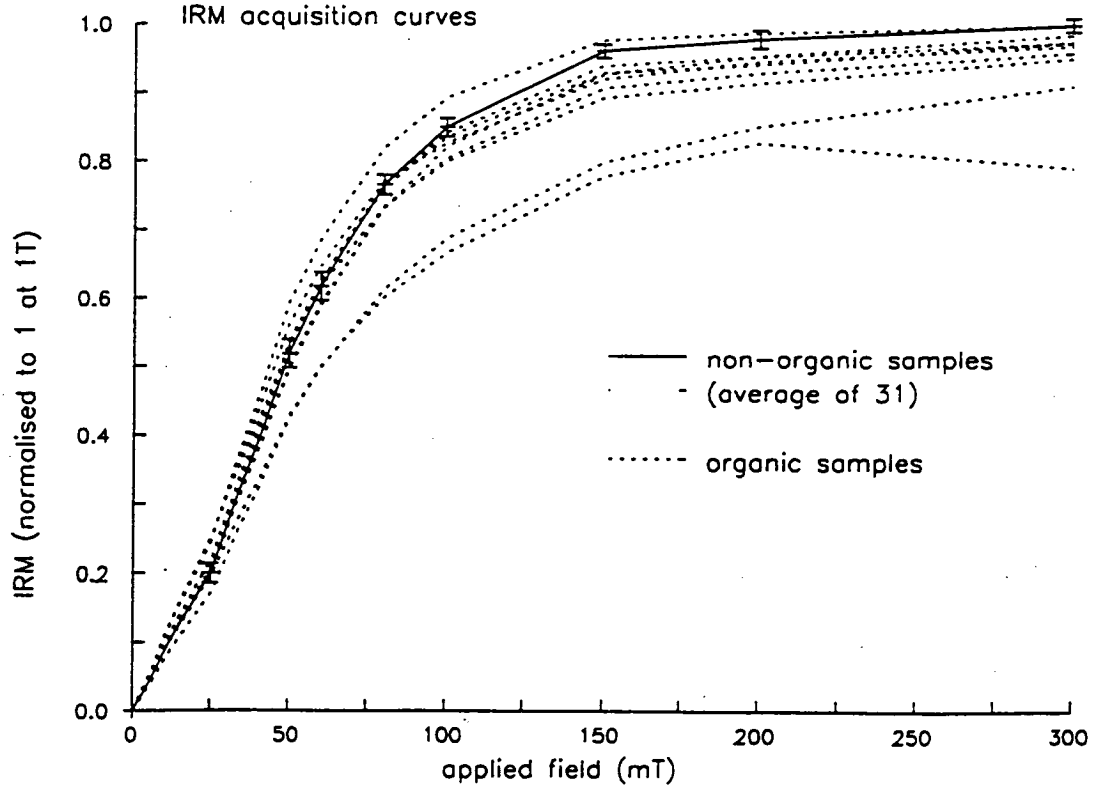

Fig. 4.2 IRM acquisition curves. The 31 non-organic samples are averaged together and have their standard deviation plotted. Organic samples are shown individually with dashed lines.

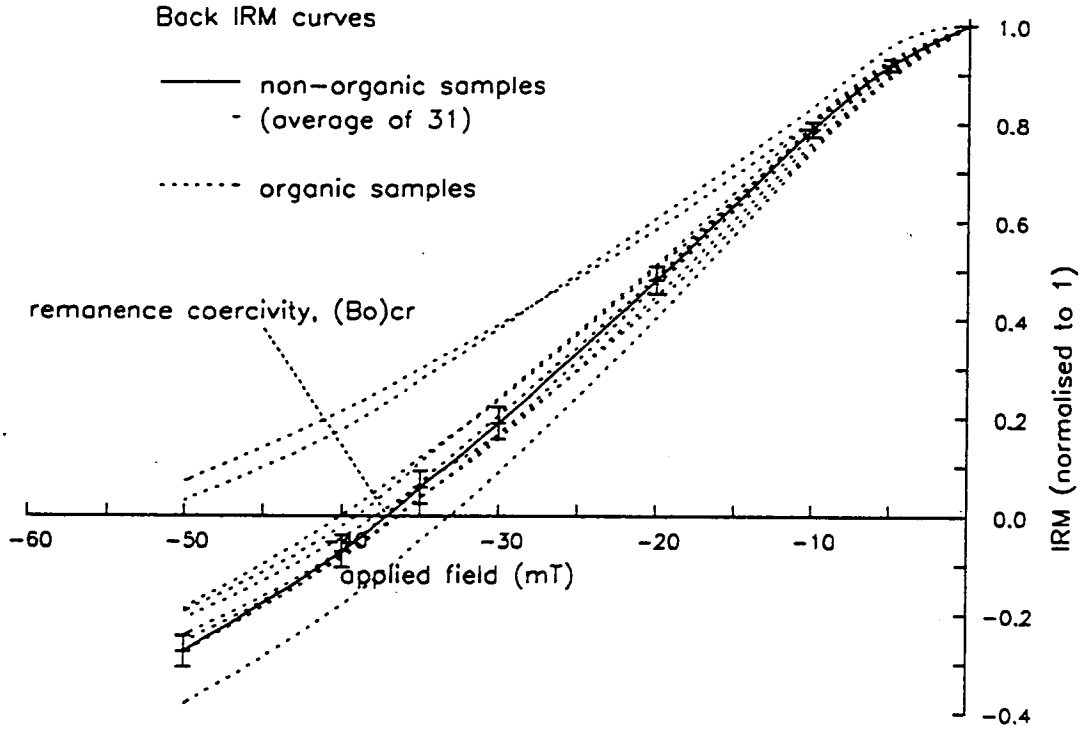

Fig. 4.3 Back IRM curves. The 31 non-organic samples are averaged together and have their standard deviation plotted. Organic samples are shown individually with dashed lines.

Back IRM curves. The stepwise reverse magnetisation of an already saturated sample leads to the back IRM curve, and the field at which the sample achieves zero remanent magnetisation is the coercivity of remanence, $(B_0)_{cr}$. The shape of the curve depends on both the composition and the magnetic grain-size. Smaller magnetite grain sizes have a larger coercivity of remanence, and the non-organic Bouchet samples have curves (figure 4.3) corresponding to grain-sizes of between 0.3 and 1μm (assuming pure magnetite) (figure 4.14 of Thompson and Oldfield [1986]). Two of the organic samples have a $(B_0)_{cr}$ greater than 45mT, which is impossible for pure magnetite. The higher $(B_0)_{cr}$ of the organic samples can be explained by oxidation of titanomagnetite, increased % of haematite, or by a smaller grain-size.

S values. An S value was calculated for each of the 40 selected samples, following Meynadier et al. [1992], to gauge the relative proportions of "hard" to "soft" components. The S value is defined as $-IRM_{-300mT}/SIRM$, and this was then converted to the relative percentage (1+S)/2. The non-organic samples have values above 99%, and the organic samples range down to 85%, though most are nearer 98%.

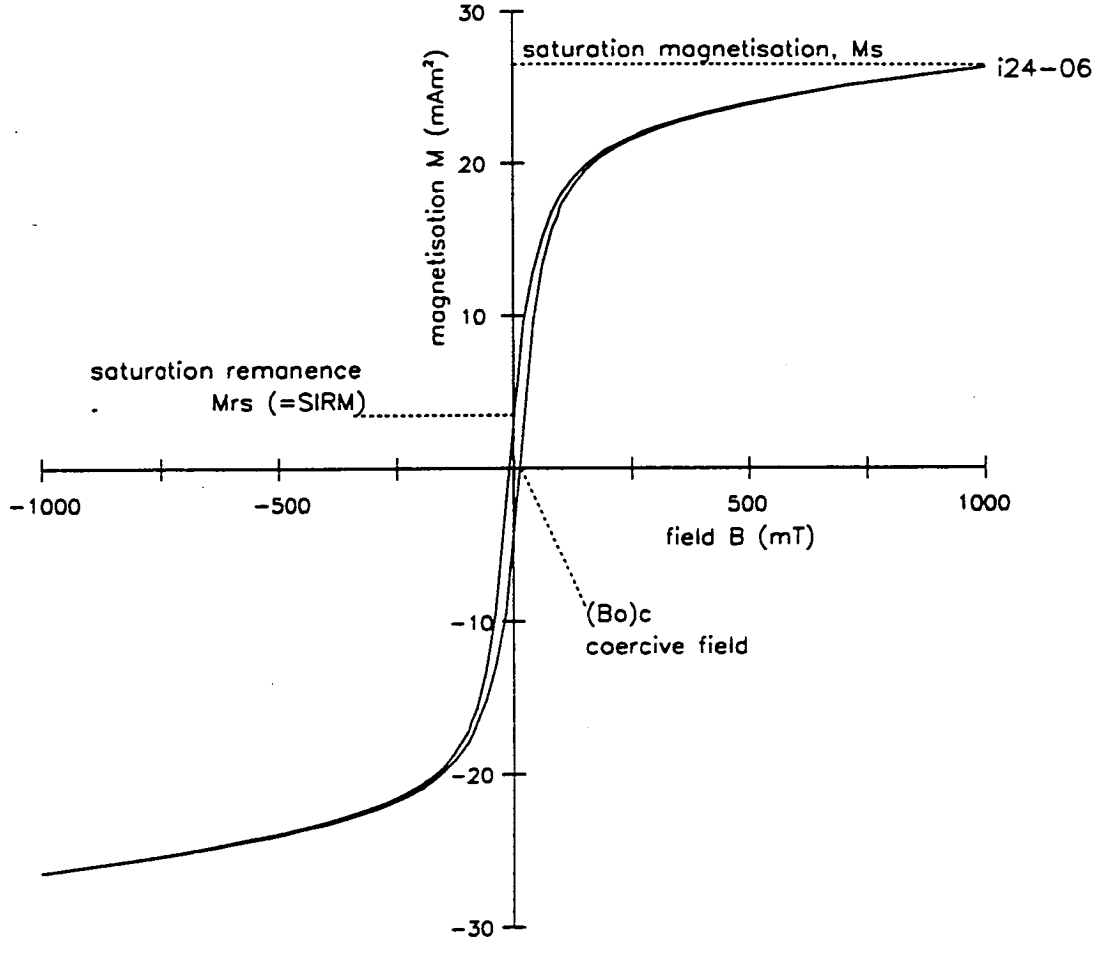

Fig. 4.4 A typical hysteresis loop from core I, section 24, sample 6, showing M_s, M_{rs} and $(B_0)_c$.

Hysteresis loops. Hysteresis loops were made on the 40 selected samples using the vibrating sample magnetometer (figure 4.4, 4.5). All have very similar shaped loops, but with different magnetisations, indicating that concentration is the aspect of the magnetic mineralogy which varies the most. The narrow stem, high M_s, and low coercivity are all typical of a PSD or MD magnetite.

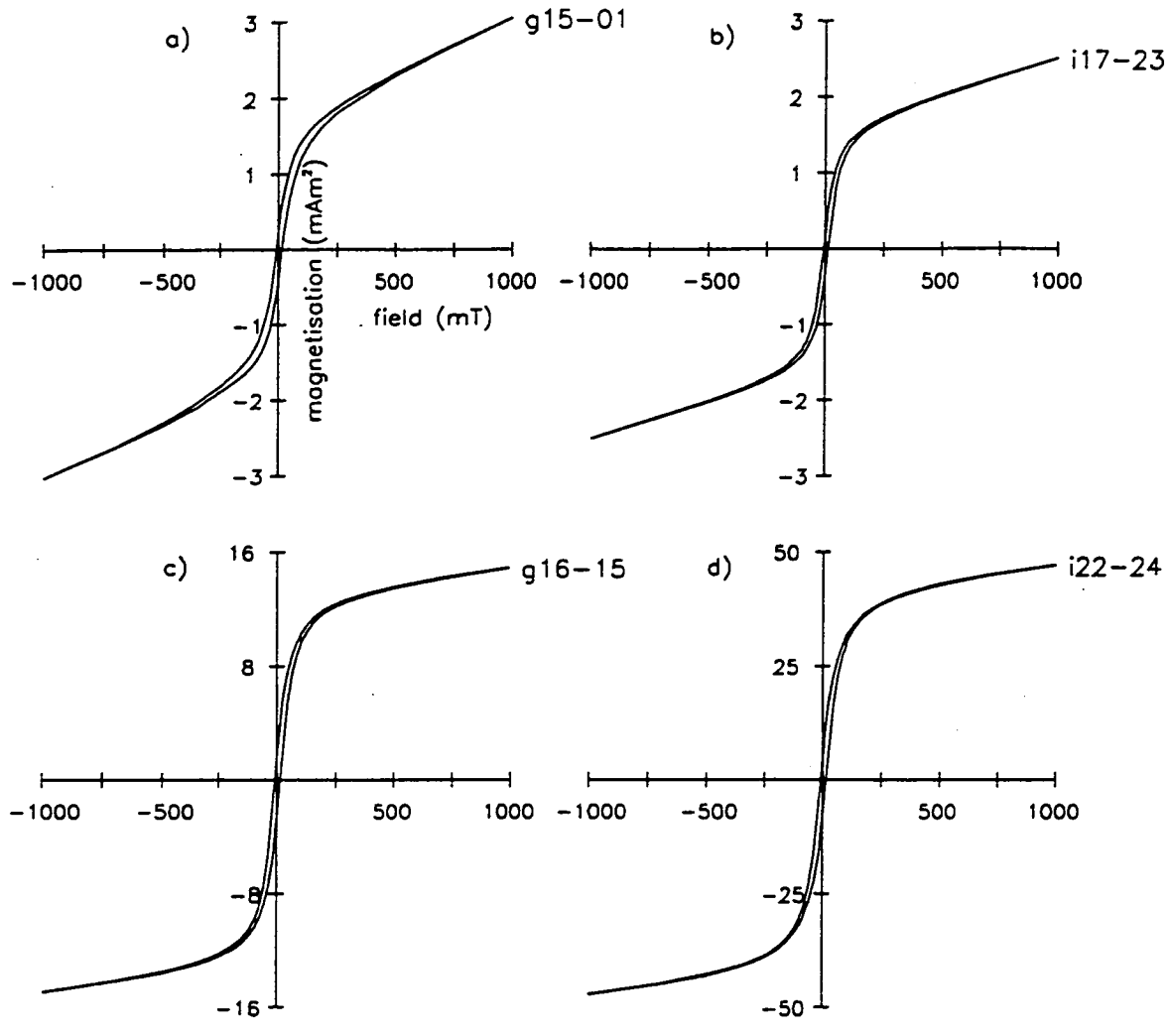

Fig. 4.5 Four example hysteresis loops. (a) and (b) are highly organic samples with susceptibilities < 1×10^{-6} m^3/kg. (c) is a typical sample. (d) is the loop of a sample with anomalously high intensity, showing no difference in shape to (c). (c) and (d) contain less para-magnetic material (relative to ferri-magnetic) than do (a) and (b), as is seen from the gradient of the tails.

Thermal experiments were carried out by Smith [1985] on sediment from the upper 6m of the Bouchet sequence. Both whole sediment and magnetic extracts were heated and cooled to determine the Curie point. For the raw sediment this had a mean of 530°C, and for the magnetic extract a mean of 550°C, both a little less than the Curie point of 580°C for pure magnetite.

Smith [1986] performed EDAX x-ray analysis on three magnetic grains and found that they contained iron with some titanium. If these are typical (as would seem to be reasonable, as they are derived almost exclusively from the basalt of the maar crater walls), it is expected that the magnetic carrier in the sediment is a titanomagnetite ($Fe_{3-x}Ti_xO_4$). If

the difference in Curie points is due to the % of titanium alone, this would suggest a titanomagnetite composition with $x \approx 0.06 - 0.12$ (figure 4.6).

Titanomagnetites have lower values of susceptibility, SIRM and M_s than magnetite, in general proportion to the titanium % for low percentages (figure 4.6). The Lac du Bouchet titanomagnetites will have very similar properties to magnetite, as the titanium % is only small.

Day et al. [1977] say that it is possible to get an idea of the titanomagnetite composition (x) from a M_{rs}/M_s vs. susc./M_s plot, given prior knowledge of the grain size from, for example, a M_{rs}/M_s vs. $(B_0)_{cr}/(B_0)_c$ plot (figure 4.8). However, on attempting such a composition analysis, the plot proves ambiguous, with the samples splaying across the composition bands, suggesting that other factors besides composition are contributing to the susc./M_s.

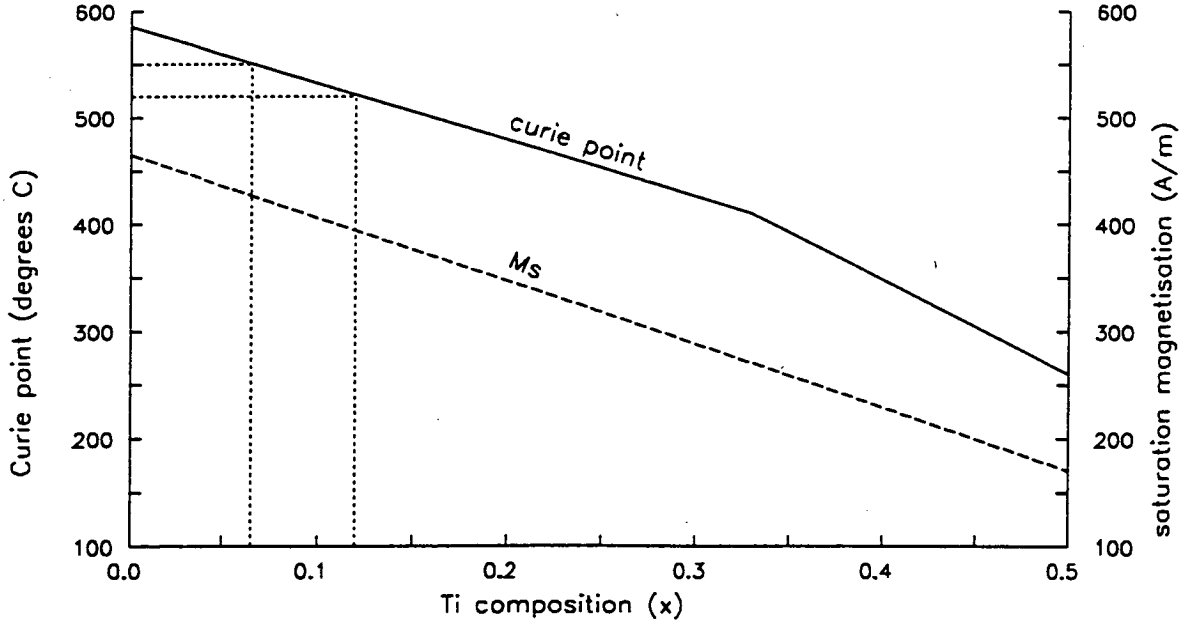

Fig. 4.6 Curie point and M_s vs. Titanium composition ($Fe_{3-x}Ti_xO_4$). Dotted lines represent the curie point determinations, and their equivalent Ti composition, done by Smith [1986].

Concentration of the magnetic minerals

Relative variations in concentration of the magnetite grains are revealed by changes in susceptibility, IRM and ARM. The similarity of the variations down-core of these three measurements (figure 5.9, table 4.7) shows that concentration is the factor having the greatest influence over them. The maximum susceptibility is about 20 times the minimum.

An estimate of the absolute volume concentration can be made. Pure magnetite has a susceptibility of 450 - 530×10^{-6} m^3/kg, and dilution in a para-magnetic matrix will lower this roughly proportionately. The mean susceptibility from all 50m core samples is 5.53 × 10^{-6} m^3/kg, so this gives a little over 1% titanomagnetite, by mass. For the volume %, the mass % is multiplied by the ratio of whole-sample to magnetite density (1.6 ÷ 5.2 g/cm^3). The samples range from 0.03% to 0.5% by volume titanomagnetite.

Grain-size and domain-state of the magnetic minerals

The grain-size of the titanomagnetites is an important parameter to determine because the titanomagnetites change their magnetic properties with size (table 4.2, figure 4.7). More precisely, the balance of the different energies inside the magnetic crystal lattice (exchange energy, internal and external magnetic energies and anisotropy energy) depends on the grain-size, resulting in different domain states. In small grains (<1μm), all the individual spins (magnetic vectors) align roughly in the same direction (single domain (SD) grains), whereas in larger grains (>10μm), regions (domains) within the magnetic crystal have internally consistent directions, and are separated from one another by domain walls (multi-domain (MD) grains). Between these two states, magnetites are observed to have the stability of SD grains, but are too large for just one domain to be theoretically stable; they are termed pseudo-single-domain (PSD) grains and relatively little is known as to why they show the combination of SD and MD properties. However, computational micro-magnetic modelling being done at Edinburgh (Williams and Dunlop [1989]) is beginning to reveal the internal magnetic constitution of the PSD grains. The models predict properties (coercivity and saturation magnetisation) which correspond well with observed bulk magnetic properties.

Table 4.2 Grain-sizes and domain-states.

Domain-state	approx. size range	comments
SPM (super-paramagnetic)	< 0.03 μm	no remanence. ?often bacterial in origin.
SD (single-domain)	>0.03μm, <0.08μm	strong, stable remanence ("hard")
PSD (pseudo-single domain)	>0.08μm, <10μm	stable remanence
MD (multi-domain)	>10μm	relatively weak, unstable overall remanence ("soft")

Grain-size ranges from computational micro-magnetic modelling (Wright [pers. comm.])

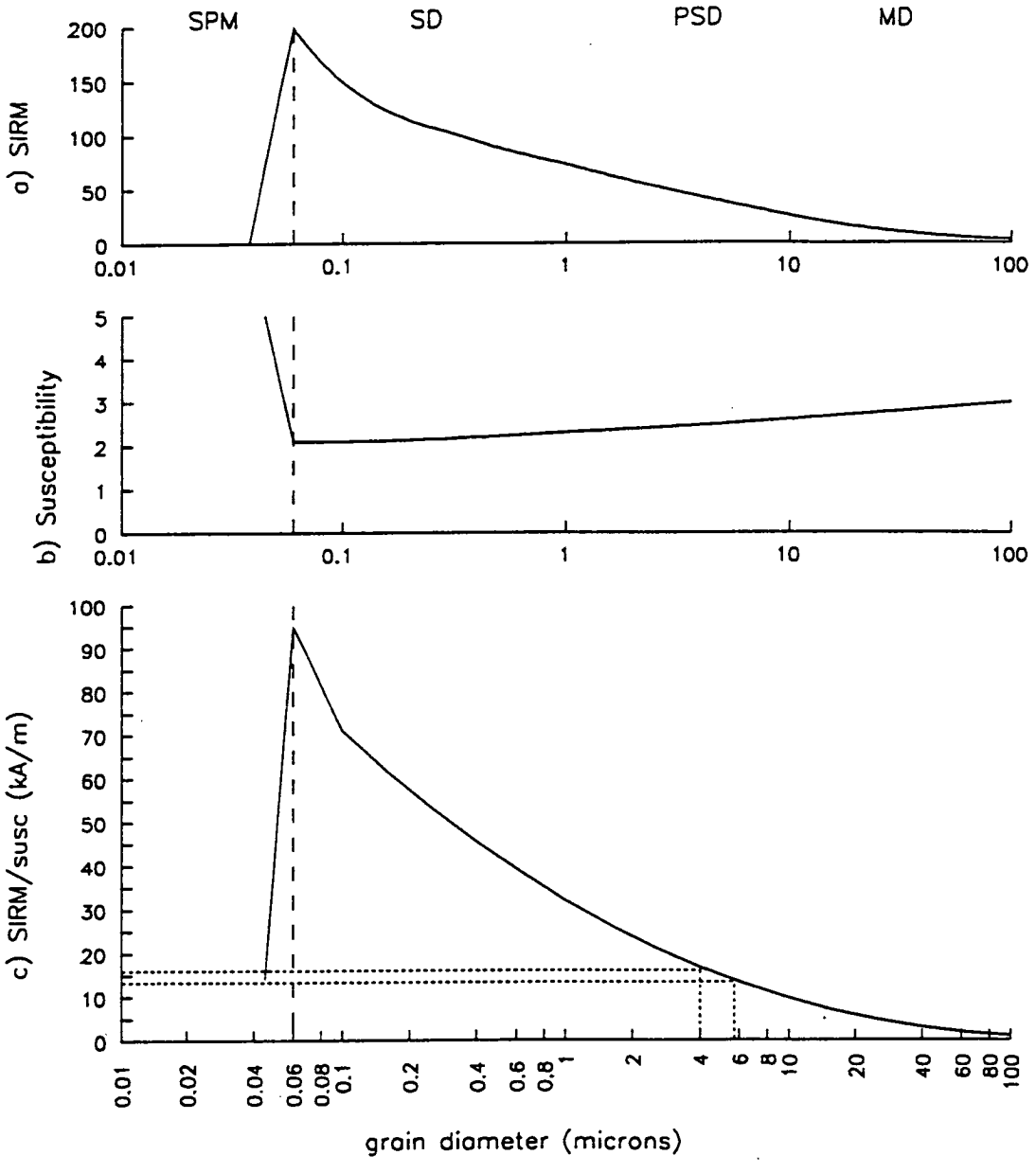

Fig. 4.7 a) SIRM vs. grain-size; b) susceptibility vs. grain-size; c) SIRM/susceptibility vs. grain-size. The dotted lines represent the upper and lower limits of the non-organic range, the dashed lines the transition size from super-paramagnetic to single domain behaviour. Re-drawn from Thompson and Oldfield [1986]).

Several techniques employing room temperature magnetic measurements have been carried out to establish an average magnetic grain-size in the samples. The magnetic grain-size spectrum (i.e. the proportions of SPM, SD, PSD and MD grains) within a sample is more difficult to pin down. However, by using a combination of techniques, comparing the range of samples, and examining hysteresis plots, an impression of the spectrum may be obtained. Many of the techniques have an ambiguity because SPM grains have some similar properties to MD grains.

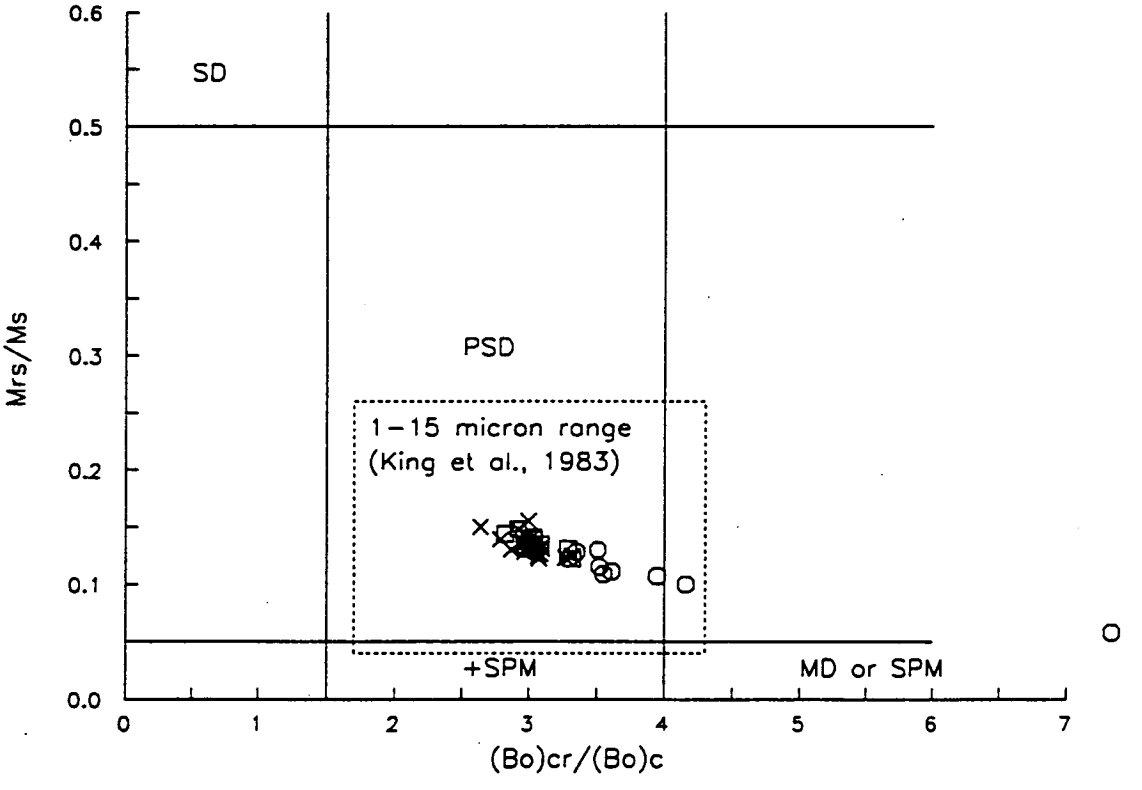

Fig. 4.8 Hysteresis parameters, M_{rs}/M_s vs. $(B_0)_{cr}/(B_0)_c$. (Day et al. [1977]). The 40 selected Bouchet samples (see fig 4.1) are plotted, together with the zone for the size range requirement of King et al. [1983]. Note that the non-organic samples (crosses and squares) are tightly grouped, and that the majority of the organic samples (circles) plot close by.

M_{rs}/M_s vs. $(B_0)_{cr}/(B_0)_c$(hysteresis parameters). Day et al. [1977] prepared artificial samples from sized magnetite, and created a phenomenological model from the results of high field hysteresis measurements in order to find the grain-sizes of magnetites in natural sediments. This has been used by Tauxe and Wu [1990], amongst others. The ratio of remanent saturation magnetisation to saturation magnetisation (M_{rs}/M_s), goes down with

increasing grain-size, and the ratio of coercivity of remanence to the coercive field ($(B_0)_{cr}/(B_0)_c$) goes up with increasing grain-size. M_{rs} (=SIRM), M_s and $(B_0)_c$ were taken from the hysteresis curves (figs 4.4, 4.5), and $(B_0)_{cr}$ was taken from the back IRM curves (figure 4.3).

All of the non-organic samples are tightly grouped in the centre of the range recommended by King et al [1983] (1-15μm) in figure 4.8, and all but the most organic of the organic samples still plot inside the range. A tiny minority splay out to the MD/SPM region.

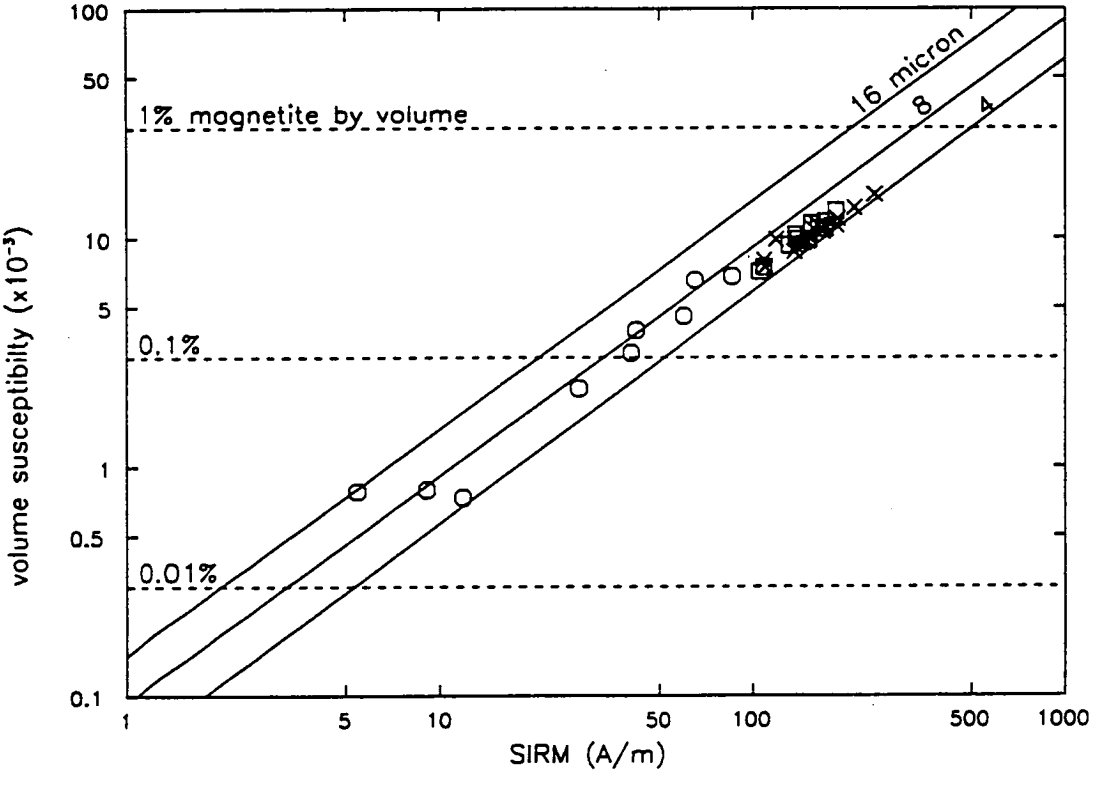

Fig. 4.9 Susceptibility vs. SIRM. Data from the 40 selected Bouchet samples (fig 4.1). Grain-size lines from Thompson and Oldfield [1986]. Circles represent low susceptibility (~organic) samples.

Susceptibility vs. SIRM. This plot exploits the difference in populations of magnetic grains contributing to the SIRM and the susceptibility (figure 4.7). The bi-plot shows, in effect, the SIRM/susc. ratio used in this thesis as the main grain-size indicator down the cores, because almost all of the samples have both parameters measured. The plot also gives concentration information; lines are marked on for volume % magnetite (titanomagnetite has higher %s for the same susceptibility). This plot is deficient because SPM particles show up like MD particles (figure 4.7).

Figure 4.9 shows that all the non-organic samples plot within the 4 to 8μm range, and all samples lie between 4 and 16μm. The concentration clusters around about 0.4% (by volume) titanomagnetite for the non-organic samples, down to about 0.025% for the organic samples.

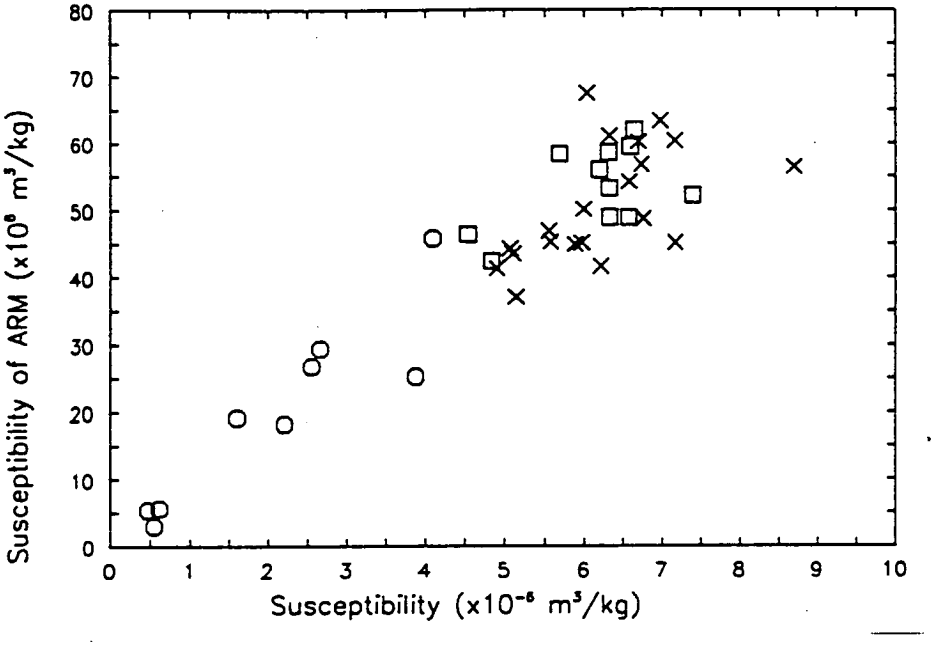

Fig. 4.10 Susceptibility of ARM vs. susceptibility. After King et al. [1983]. The sample type is identified in figure 4.1.

Susceptibility of ARM vs. susceptibility. Another method for deducing grain-size variation is to plot susceptibility of ARM against susceptibility. This was developed by King et al. [1982, 83], and gives similar information to the susceptibility vs. SIRM plot (figure 4.9). King also used the results from sized magnetite to create a phenomenological model. The plot is also unable to tell apart MD and PSD grains. Unfortunately, King's grain-size interpretation of this bi-plot does not transfer well to other data (they suggest typical grain-sizes below the SPM limit, clearly in error) (see Tauxe [1993], pp 336-337).

The susceptibility of ARM is the ARM normalised to the applied direct field; it is called a susceptibility because it is also a ratio of magnetisation to applied field. For small direct fields such as the 0.1mT used here, the magnetisation is proportional to the applied field. The benefit of using this rather than just ARM is so that plots may be compared from laboratory to laboratory when using different direct fields, and in addition, the units are the same on the two axes.

Table 4.3 Ranges of the magnetic mineralogy at Lac du Bouchet in comparison to the King criteria.

criteria	limits of King et al. [1983]	non-organic Bouchet samples (83% of the total)	organic Bouchet samples (17% of the total)
composition	magnetite or low Ti titanomagnetite	titanomagnetite (Ti from x = 0.1 - 0.2)	titanomagnetite, possibly slightly oxidised or with a trace of higher coercivity material
concentration	should not vary to more than 20-30 times the minimum	varies by about 3 times the minimum (figure 4.9)	varies by 10 times the minimum (figure 4.9)
grain-size	between 1 and 15μm	4 - 8μm (figure 4.9)	? between 1 and 10μm. Small amounts of either SPM or MD grains.

In conclusion, the non-organic samples (susceptibility $> 4.2\times10^{-6}$ m^3/kg, 83% of the total samples) have a consistent magnetic mineralogy down-core. The concentration of the magnetic grains (titanomagnetite with x≈0.1) reaches only about 3 times the minimum value, and the mean grain-size varies from 4 to 8 μm. This is far more tightly constrained than the criteria set down by King et al. [1983].

The organic samples show wider variation. They have slightly higher coercivities, and reduced concentrations. All but those with the lowest susceptibility fall within King's limits. It is still unclear whether the organic samples have a smaller average grain size, or are more oxidised than the non-organics (it is probable that reducing conditions existed at the lake bed during the organic sedimentation). The organic samples with susceptibilities above about 1×10^{-6} m^3/kg show very similar characteristics to the non-organic samples in all but concentration of magnetic grains.

There is no discernible difference in any of the above plots between the non-organic samples with low NRM intensity and the ones with average or high intensity. I conclude from this that the observed low intensities in the non-organic samples are not due to the magnetic mineralogy of the sediments.

4.3 The secondary component of NRM

The secondary (initial) component of the NRM is seen from demagnetisation plots (figs 4.12, 4.16) to be often surprisingly large, and present in many samples. The aims of this section are to deduce the source of the secondary magnetisation, and to establish if it causes any reduction of the primary (original) DRM.

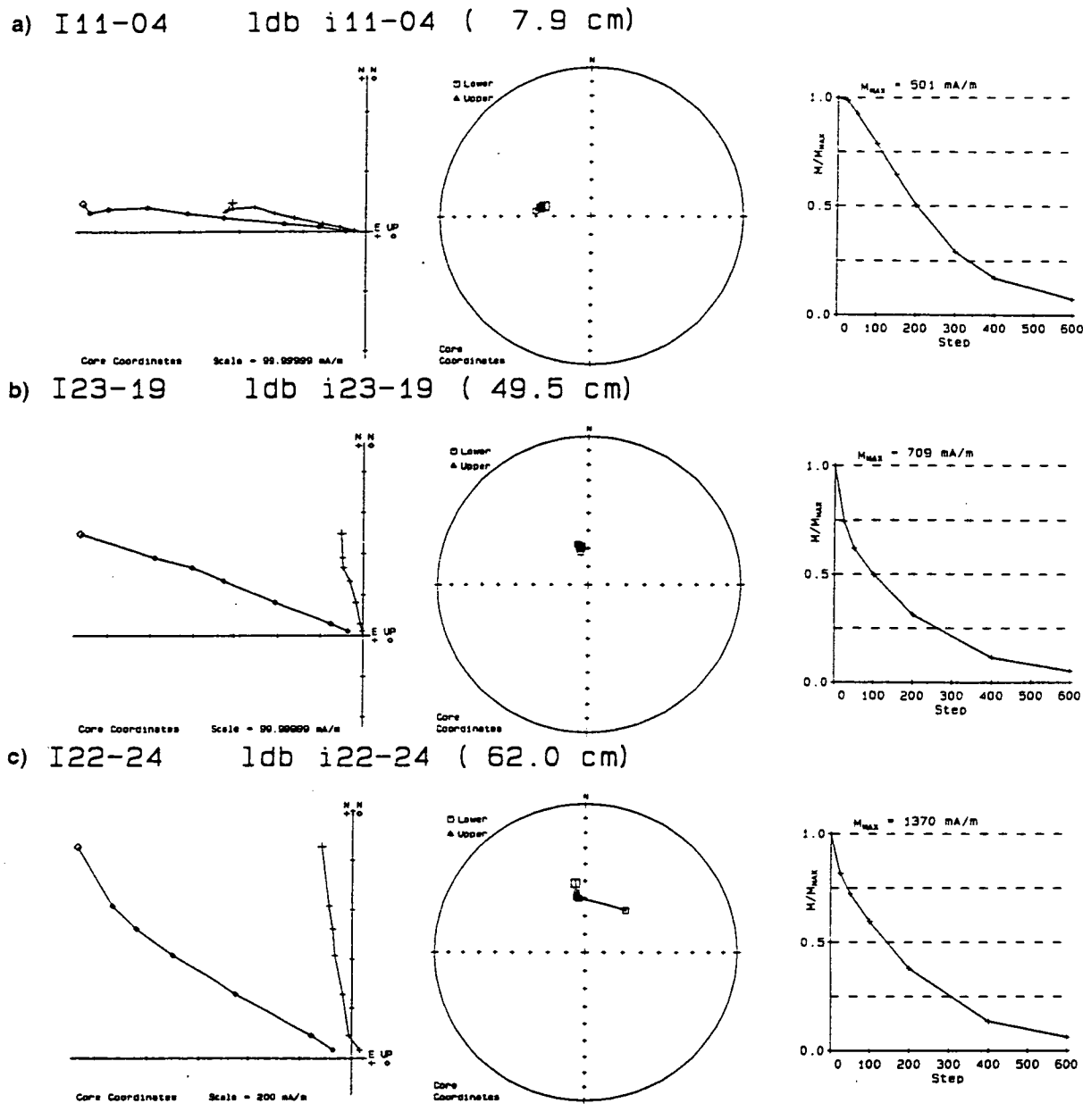

Fig. 4.11 Seven sets of demagnetisation plots, comprising: i) Zijderveld plots; ii) stereographic plots; and iii) linear plots (note the units are Oe, not mT (10Oe = 1mT), illustrating the stable primary component of magnetisation, the unstable secondary component, and the spurious ARM (introduced by the instrument) at higher demagnetisation steps.
(a) stable primary component (on the Zijderveld plot, steps form straight lines leading to the origin; on the stereographic plot, steps overlay each other). (b) Stable primary and small/moderate secondary. (c) stable primary, small/moderate secondary, spurious ARM introduced at 60mT step. Sample has anomalously high NRM intensity. (d) Stable primary at 5,10, 20mT steps, spurious ARM at 40 and 60mT. (e) Very large secondary component, removed by ?10mT, spurious ARM at 60mT and lower, smearing out primary direction. (f) Large secondary component, spurious ARM at 40 and 60 mT. (g) Secondary component removed by 10mT, spurious ARM at 40 and 60mT. Organic, weakly magnetised sample.

d) I19-11 ldb i19-11 (30.0 cm)

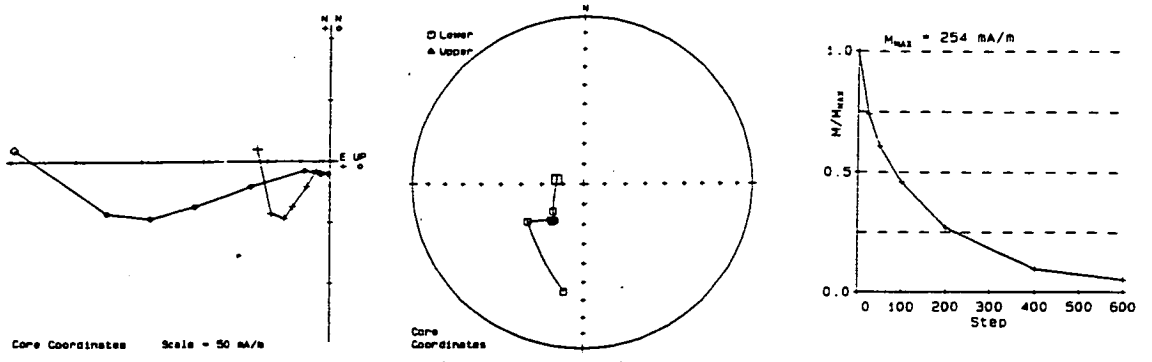

e) I26-25 ldb i26-25 (65.5 cm)

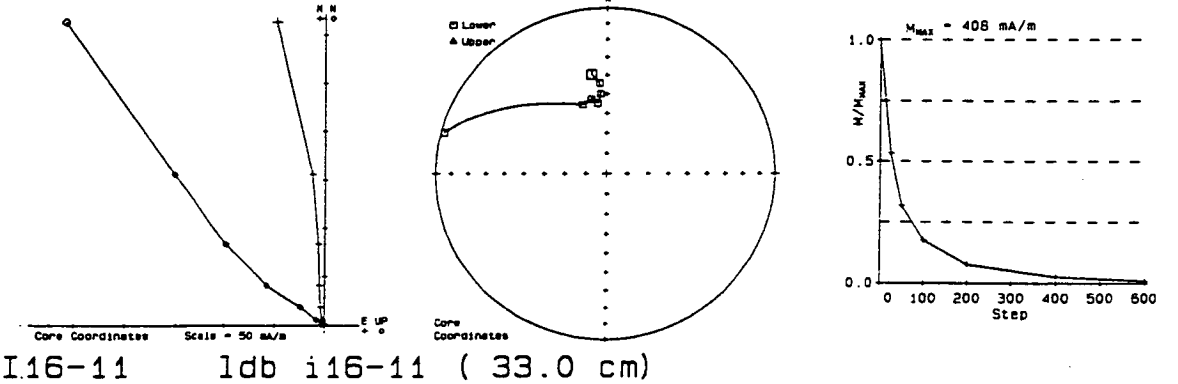

f) I16-11 ldb i16-11 (33.0 cm)

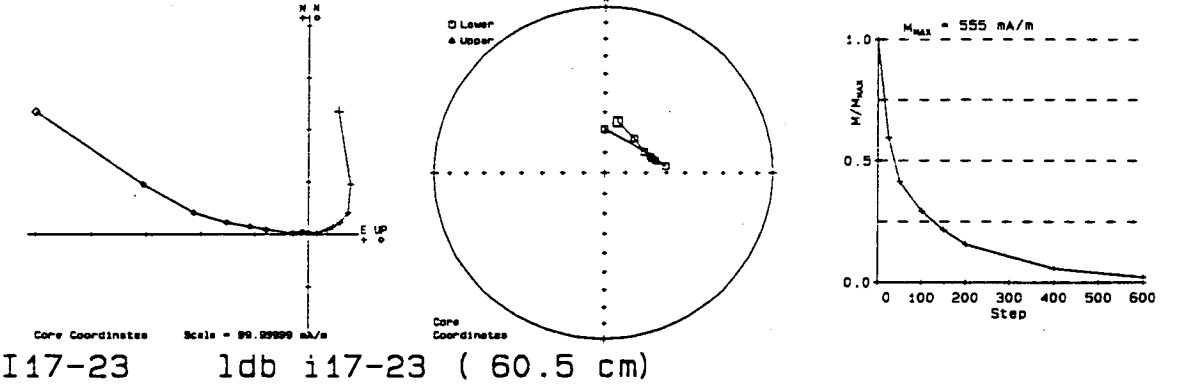

g) I17-23 ldb i17-23 (60.5 cm)

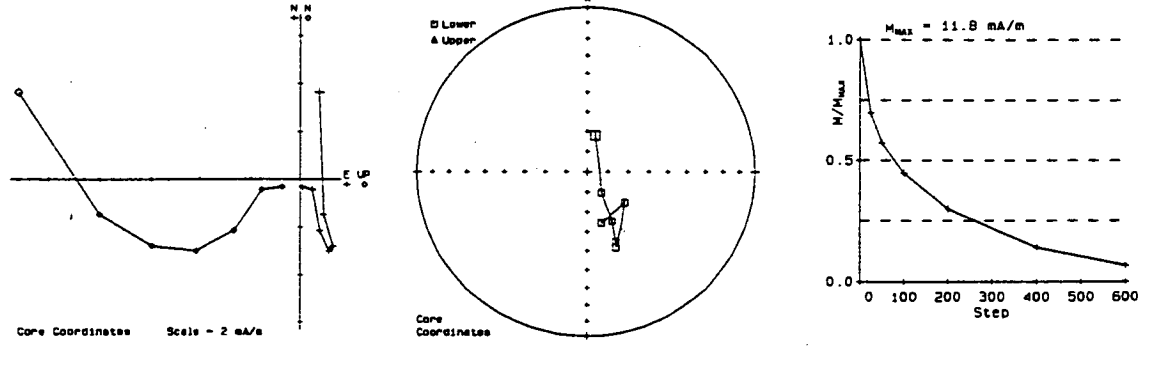

09-14-1993

Fig. 4.11 continued.

There are several factors which I thought could have a part to play in the origin of the secondary magnetisation:

Lithology. In general, organic against non-organic sediment - one type may be more susceptible to VRM than another.

Corer. Two types of corer were used: piston and Mazier. The Mazier system involves fast rotation of a metal outer coring barrel, with possible mechanical disturbance of the magnetic fabric and maybe over-printing of another magnetisation on top of the DRM.

Storage. The sediment was sampled in three phases (table 2.3), transported separately, and stored at different times for different lengths of time. All sets of samples were stored within the same shielding Helmholz storage coils at the laboratory in Edinburgh. It is possible that some aspect of the conditions changed over the 1½ years between first sampling and last NRM measurement.

Core. There is unlikely to be a difference due to the cores themselves, because susceptibility matching (figure 5.2) shows the sediment to be laterally continuous across the region of the lake bed that was cored, and the cores were all treated the same way on the raft and at LGQ, Marseille.

To gauge the size of the secondary component for each sample, two measures were adopted. The median destructive field (MDF) is the demagnetising field which reduces the original NRM by half; the other measure is based on the reduction in magnetisation after the 10mT demagnetisation step. Neither measure takes account of the direction data, even though this can make a difference to both measures if the declination and inclination of the primary and secondary magnetisations differ by much.

The MDF is more commonly used to gauge the relative proportions of "soft" (MD) to "hard" (SD and haematite) magnetic material (i.e. the material's coercivity spectrum), however, in the case of the Lac du Bouchet samples held in Edinburgh, this effect is swamped by the secondary magnetisation. When there is a large secondary component, the MDF will be small, and without secondary magnetisation, MDFs are typically in the range 15 - 25mT. The average MDF from Bouchet cores G, H and I is 13.1mT, with a wide spread of values shown by the standard deviation of 5.5mT, and the average MDF of the ARM is 23mT, with small deviation (figure 4.16). I calculated the MDF by linear interpolation between the steps to the value at which the intensity is reduced by half. Linear interpolation is not ideal when using few steps (typically 7), but is sufficiently accurate for the purposes here.

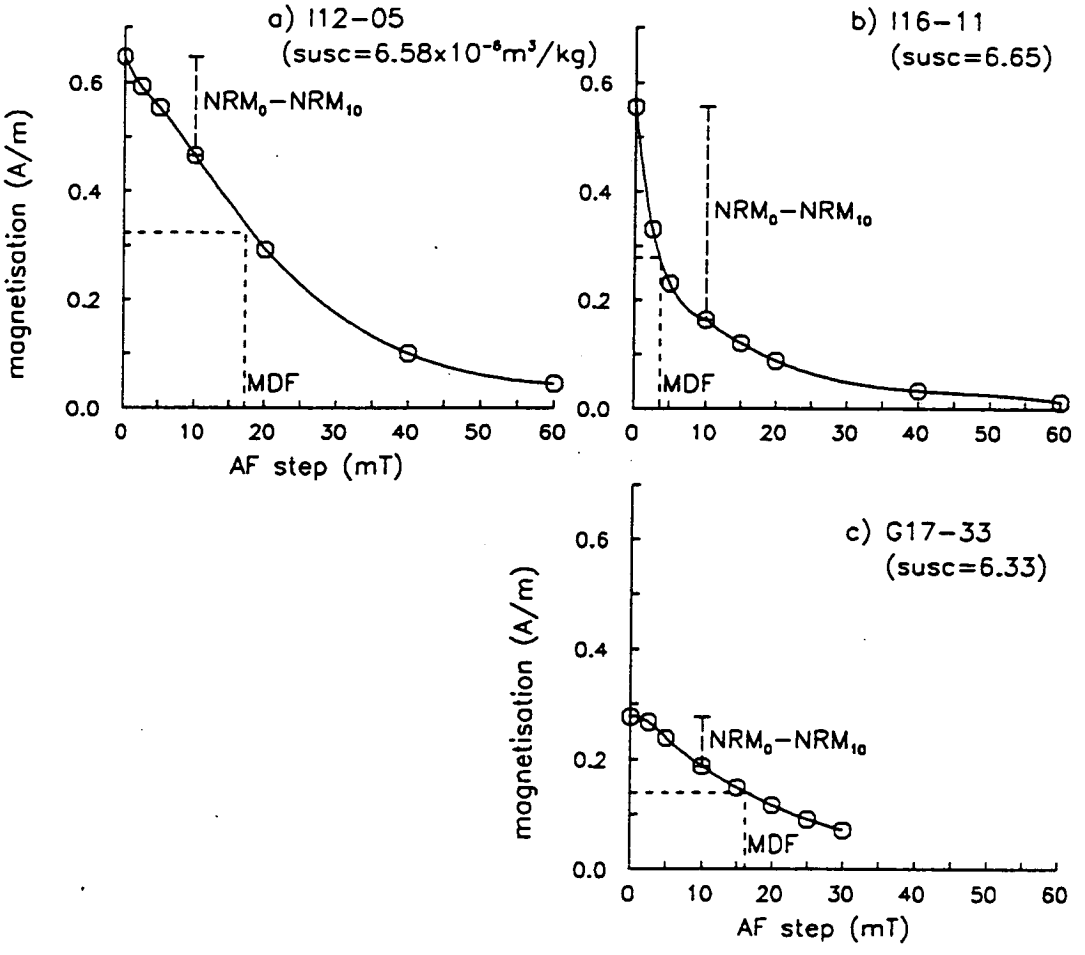

Fig. 4.12 Three demagnetisation examples, showing: a) strong primary and weak secondary components; b) weak primary and strong secondary components; c) weak primary and weak secondary components. All three samples have similar rock magnetic properties. The two measures of secondary component adopted in this study are also marked.

An estimate of the size of the secondary component is also given by subtracting NRM_{10mT} from NRM_{0mT}, and then correcting for magnetic concentration by dividing by susceptibility (figure 4.12). The MDF data are sufficient to make the main point: sometimes large differences in MDF occur between the different cores at the same depth (for example at 32m, or at 29m in core I), but these do not show up in the NRM_{10mT} at the same depth (figure 4.15).

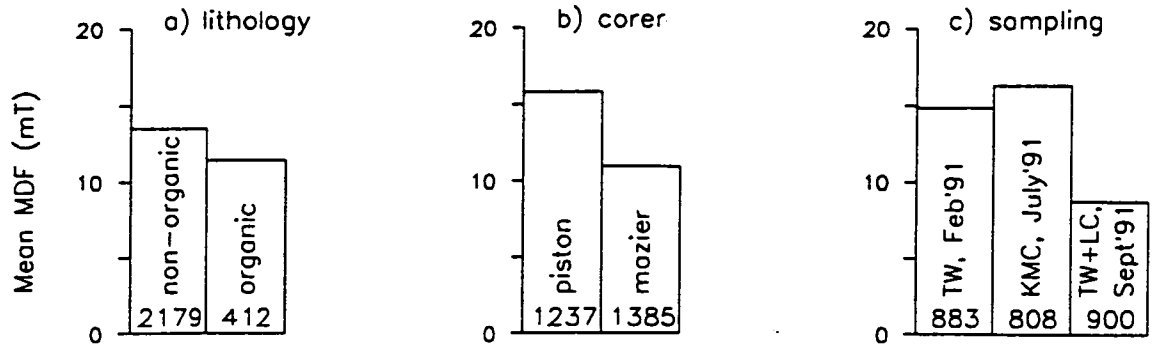

Fig. 4.13 Three histograms comparing the MDFs of all samples, when divided up according to: a) lithology (organic vs. non-organic); b) corer (piston vs. Mazier); c) sampling (by TW, KMC or TW & LC) (see table 2.3). The number of samples in each average are given at the bottom of the bars.

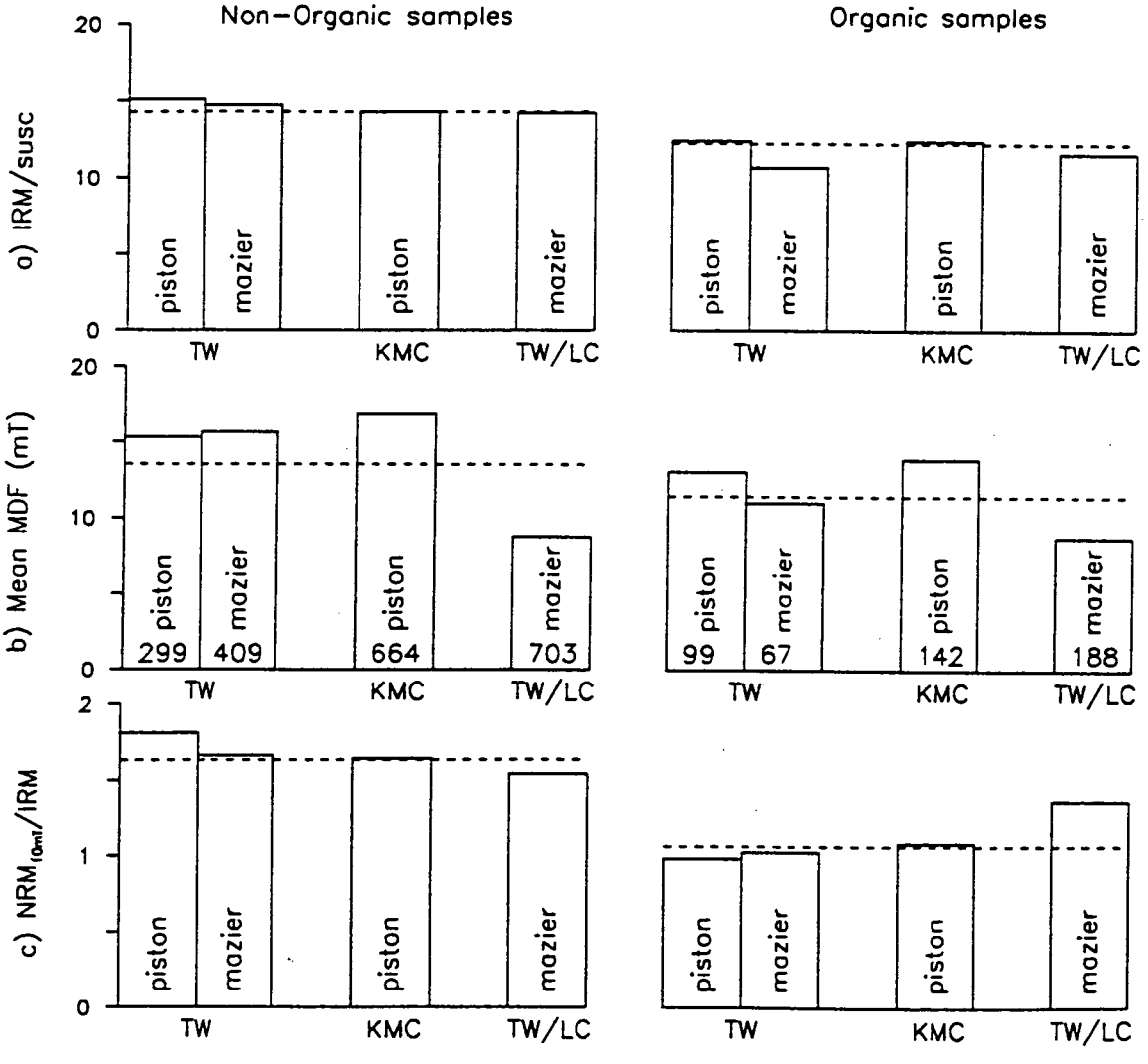

Fig. 4.14 Histograms comparing: (a) NRM_{10mT}/SIRM; (b) MDF; and (c) SIRM/susceptibility, when the samples are divided into different sub-sets based on corer, lithology and sampling alone. The number of samples in each average are given at the bottom of the bars in (b).

In order to establish the factors governing the secondary magnetisation, comparisons are made of average MDFs of different subsets of the whole sample set, based on the above factors, and presented as simple histograms (figure 4.13, figure 4.14).

Figure 4.13 appears to show that all the three divisions (corer, sampling, lithology) affect the MDF value, and therefore the secondary component. However, since the three sub-divisions cross each other, they are split further in figure 4.14, to see which contribute the most. The third sampling (by TW & LC) forms the single group of samples which have acquired the largest secondary component, so it would appear that the storage conditions of this group of samples was not ideal, and did not remove the VRM. Organic samples acquire a larger secondary component than non-organic samples.

Down-core plots of (NRM_{0mT}-NRM_{10mT}) /susc, SIRM/susc (a lithological parameter), and NRM_{10mT}/susc are compared in order to see if a lithological signal is present in the secondary component, and also if the secondary signal is still present in the partially demagnetised, normalised NRM (figure 4.15). The depth range chosen to illustrate this includes the piston to Mazier transition at 29m in core I, and around 32 m where the MDFs for G and I are far lower than for H. Down core values of IRM/susceptibility are included, as any similarity between this and NRM_{10mT}/susc would be deeply suspicious, as would a correlation between the secondary component and the demagnetised intensity.

A summary of the correlations between susceptibility, NRM intensity (normalised and not), IRM/susceptibility and the secondary component, is given in table 4.4. NRM_{10mT} is much more closely related to NRM_{10mT}/susc than it is to susceptibility.

Table 4.4 Correlation coefficients (from about 2500 data-points)

	susceptibility	NRM_{10mT}	NRM_{10mT}/susc	SIRM/susc
NRM_{10mT}	.4022			
NRM_{10mT}/susc	.1627	.9398		
SIRM/susc	.3802	.3530	.3404	
(NRM_{0mT}-NRM_{10mT})/susc	.0776	.1111	.1059	.0015

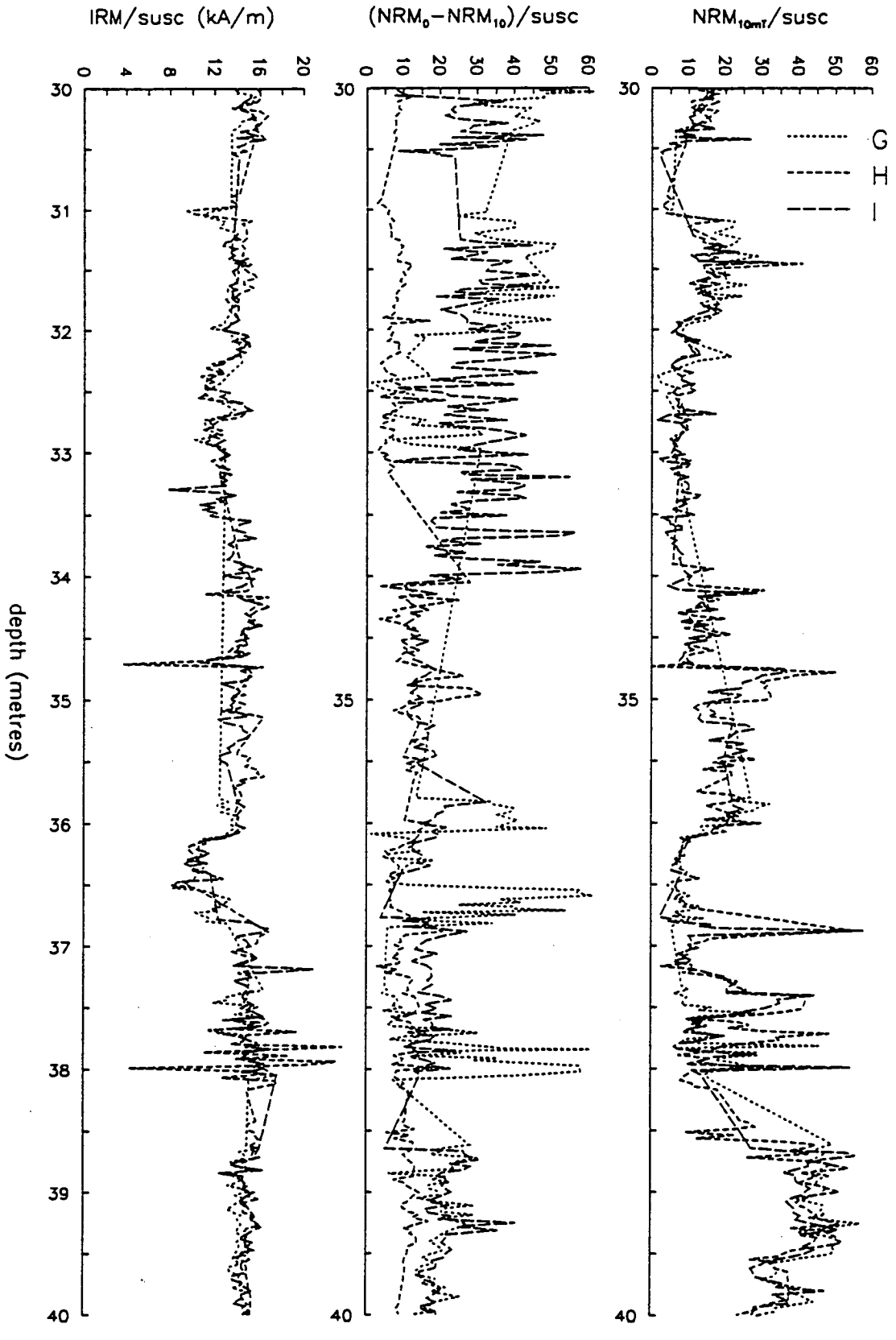

Fig. 4.15 Down-core comparison of SIRM/susceptibility (related to grain-size), (NRM_{0mT}-NRM_{10mT}) /susc (an estimate of the secondary component), and NRM_{10mT}/susc (an estimate of relative geomagnetic palaeointensity), from cores G, H and I. Data on the core H depth scale.

4.4 The best demagnetisation step to use

The question of which is the most suitable demagnetisation step is closely related to the secondary component topic of section 4.3. However, the approach is different: instead of trying to isolate the cause of the secondary component, the question here is what value of demagnetising field is needed to remove it. Thermal demagnetisation was not attempted. The choice is between steps at 10mT and 20mT, as these were the only steps done on all of the samples. Due to the changeover of demagnetisation coils after the measurement of core H, there was a change in the demagnetisation procedure; the sequence of steps was 2.5, 5, 10, 20 and 30mT for core H, and 2.5, 5, 10, 20, 40 and 60mT for cores G and I. For sections I5 to I10, measured in Marseille, I have the raw NRM and the 10mT step on file. For the 20m core set (cores A, B, C, D and F), step demagnetisation was only done on pilot samples, and the bulk of the samples were demagnetised at 15mT only (Creer et al. [1990]). For the Mackereth cores, the bulk of the samples were demagnetised at 10mT only (Smith [1986]).

The two concerns in the choice are that the secondary component should be removed, and the demagnetisation step should not be so high as to introduce a significant additional ARM to the samples.

A spurious ARM is implanted in the samples at high (> 30mT) steps because of an unwanted bias DC field contaminating the demagnetising AC field (see figure 4.11). An partially successful attempt was made to neutralise the spurious DC field, using compensating coils as detailed in Le Goff [1985].

Figure 4.16 shows a comparison of the demagnetisation of NRM and ARM. The curves are normalised so that the values are the same at 10mT and 20mT. Both plots show the curves following common paths after about 10mT, with the NRM curve matched at 20mT perhaps closer to the ARMs. This indicates that the secondary component is substantially removed by 10mT, with a tiny proportion remaining. Interpreting such fine-scale comparisons in terms of the secondary component is difficult and uncertain, because of the different coercivity spectra of NRM and ARM.

Table 4.5 shows that the secondary component is reduced heavily at 10mT, and perhaps a little more by the 20mT step.

Table 4.5 Correlation of NRM intensities at 0, 10, and 20mT steps with the secondary component, showing this to decrease with demagnetisation. (about 2500 data-points).

	NRM_{XmT}/susceptibility, with the NRM demagnetised at:		
	0mT	10mT	20mT
$(NRM_{0mT}-NRM_{10mT})$/susc	0.745	0.106	0.057

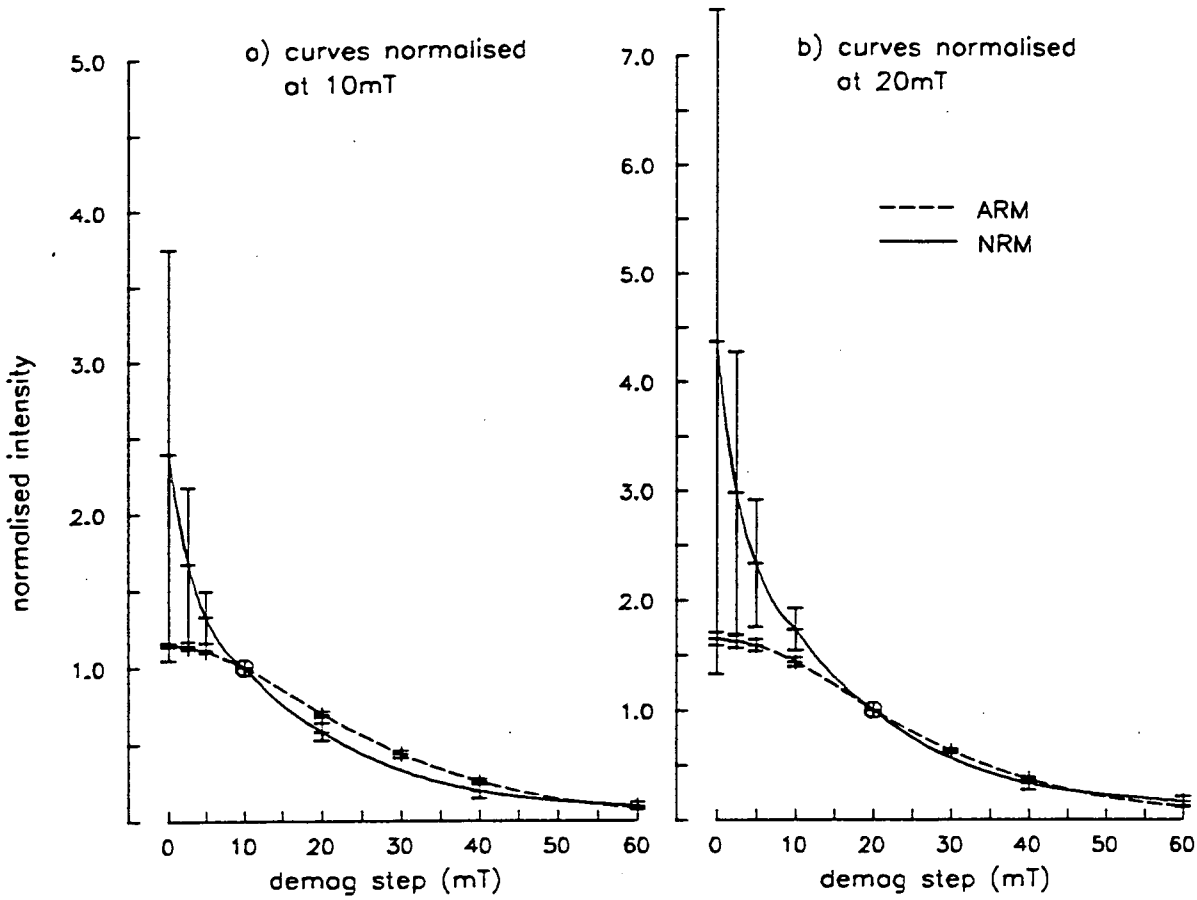

Fig. 4.16 Comparison of demagnetisation of NRM and ARM. Averages and standard deviations from 31 non-organic samples.

Figure 4.17 shows a comparison three cores at the 10 and 20mT step, and it is seen that the two steps give curves which bunch equally well; there is little effective difference in the records.

The dispersion of the NRM directions at the various steps might also indicate how clean the geomagnetic signal is. However, the uncertainty in the declination due to sections not being azimuthally oriented, the twisting of the Mazier sections, and the natural palaeosecular variation, is too great for any cleaning effect to be picked up. To illustrate this, averages and standard deviations are given in table 4.6. They show no improvement with demagnetisation, although the lowest $\alpha 95$s are given by the 10mT step. The processing of the directions is considered in the next chapter (section 5.6).

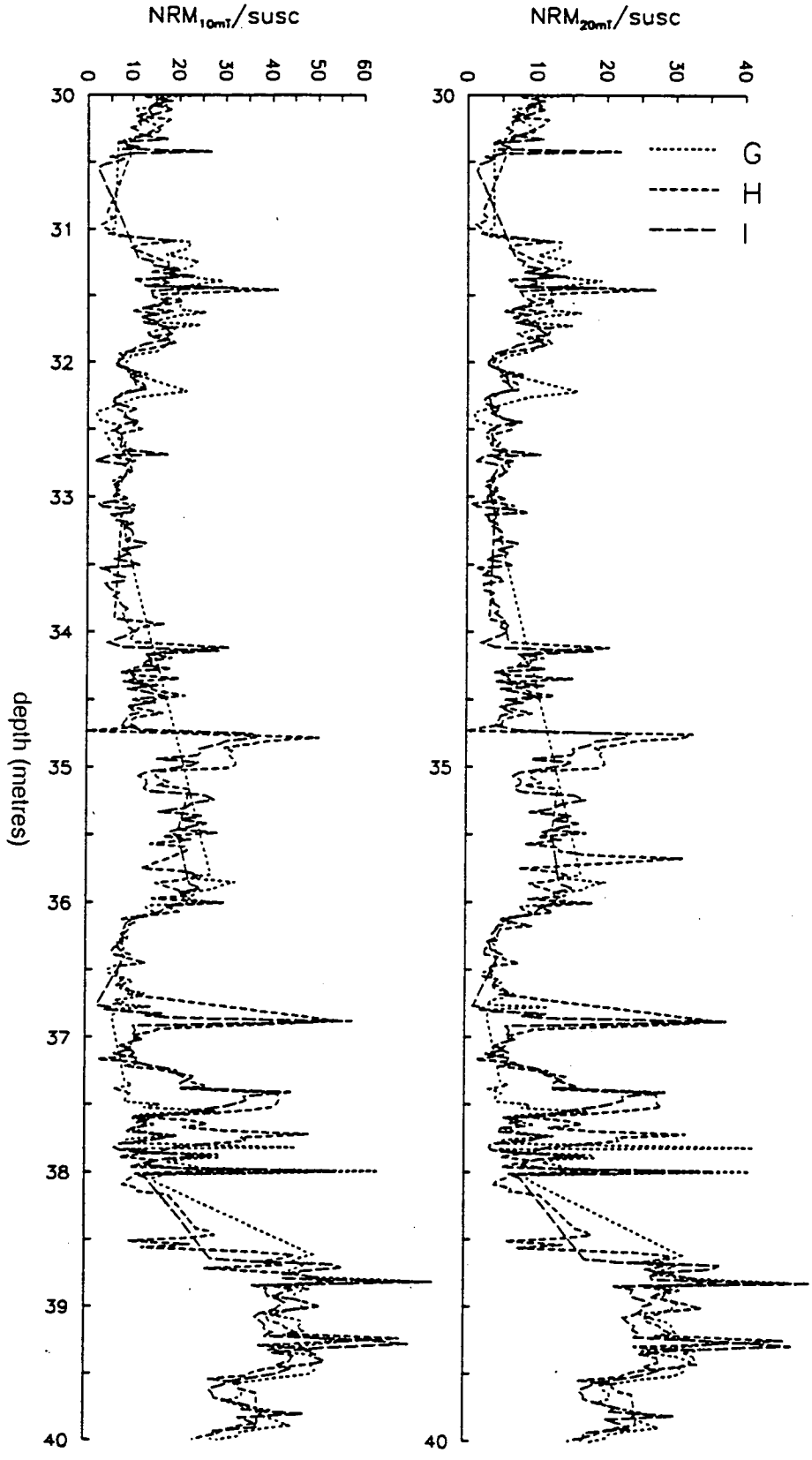

Fig. 4.17 Down-core plots for NRM at the 10 and 20 mT step, comparing cores G, H, and I

Table 4.6 Average directions after AF demagnetisation

core (samples)	standard deviation of **declination** (mean set to zero)			mean **inclination**			Fischerian α95		
	0mT	10mT	20mT	0mT	10mT	20mT	0mT	10mT	20mT
G (951)	43.4	46.5	45.3	58.5	60.3	58.9	1.41	1.24	1.31
H (1048)	47.0	50.0	52.0	59.7	59.5	60.1	1.22	1.19	1.23
I (823)	38.7	42.3	49.3	60.9	61.8	62.4	1.35	1.26	1.65

4.5 The best normalising parameter for the intensity

Contributions from the magnetic mineralogy to the NRM intensity must be removed, to leave a geomagnetic palaeointensity signal due only to the magnetic moments of the magnetic grains. The most important aspect of the magnetic mineralogy affecting the susceptibility, SIRM and ARM was found to be the concentration of magnetic grains (section 4.2). The partially demagnetised NRM intensity is also proportional to this concentration, so if the NRM intensity is divided by either susceptibility, SIRM or ARM, the concentration cancels out and the normalised NRM intensity should represent geomagnetic influence alone. The difficulty is that slightly different families of grains within the sample contribute to the each magnetisation, and so the normalisation will not be perfect. However, the very small grain size range (section 4.2) works in our favour, and makes this worry a small one.

Koenigsberger in 1938 used susceptibility to normalise the NRM, but this is often considered to be bad practice, because of the paramagnetic contribution to susceptibility. Johnson, in 1948, used SIRM as a normalisor. King et al. [1982] preferred to use ARM. Tauxe and Wu [1990] used susceptibility. Tric et al. [1992], found for their marine sediments that any one of the three (susceptibility, SIRM or ARM) was acceptable, and used susceptibility. Meynadier et al. [1992] normalised their intensity with ARM.

Similar demagnetisation plots for NRM, IRM and ARM indicate that similar grains contribute to the magnetisation: after the secondary component is removed, the curves follow similar paths (figure 4.16).

A more direct test is to see whether the intensities normalised by each of the three parameters are similar to each other, by means of correlation coefficients and plotting the down-core records side by side. The correlation coefficients in table 4.7 show the records to be very similar indeed, indicating that, regardless of grain sizes or magnetisation acquisition process, any of the three may be used to normalise the NRM.

Table 4.7 Correlation coefficients of susceptibility, SIRM and ARM with the NRM_{20mT} intensities normalised by susceptibility, SIRM, and ARM

	susceptibility	SIRM	ARM	NRM_{20mT}/susc	NRM_{20mT}/SIRM
SIRM	.9354				
ARM	.8406	.7807			
NRM_{20mT}/susc	.1425	.2276	.0106		
NRM_{20mT}/SIRM	.1143	.1444	-.0155	.9769	
NRM_{20mT}/ARM	.1343	.2130	-.0812	.9562	.9486

4.6 Summary and conclusions

Many attributes of the sediment samples have been measured, and more time consuming measurements were done on a selection of 40 representative samples. The conclusions of this study confirm the results of studies of the shorter cores from Lac du Bouchet (Thouveny [1991], Smith [1985]) for the deeper parts of the sediment studied here. The meaning of the various measurements in terms of the magnetic mineralogy are described below:

Susceptibility, *SIRM* and *ARM* principally show the concentration of magnetic grains;

SIRM/susceptibility and similar ratios indicate magnetic grain size;

MDF and $(NRM_{0mT}-NRM_{10mT})/susc.$ reflect magnetisations acquired after coring.

NRM contains both geomagnetic and magnetic mineralogical information;

NRM_{10mT} *and* NRM_{20mT} contain geomagnetic information, and magnetic mineralogical effects have been normalised out;

The relationships between the measurements are conveniently summarised in a principal component analysis (figure 4.18). The easiest way to read the diagram is to look at which measurements plot together: the closer they are, the greater similarity there is in their variation. Only the first two principal components are plotted, and these account for 57% and 21% of the variance. The plot is intended as a general guide and convenient summary.

Going back to the first figure of the chapter (figure 4.1), it was observed that there is a change in character of the samples with a susceptibility below about 4.2×10^{-6} m^3/kg (termed "organic" samples throughout the chapter): these samples record exclusively low NRM intensities (raw and normalised), and this behaviour is suspicious enough to conclude that these samples are not suitable for palaeointensity determination. From the analyses in this chapter, although there is a slightly wider variation in grain-size and coercivity, the mineral magnetic character of most of the organic samples is still very similar to that of the non-organic samples, and it is only below about 1×10^{-6} m^3/kg that wider variations occur. Therefore there is another factor besides magnetic mineralogy which affects the

geomagnetic recording in these samples. The physical conditions around the time of deposition would be different in a warmer climate environment to those of a colder climate: the sedimentation rate would be slower, there would be a high degree of compaction shortly after deposition due to the organic sedimentology, and diagenesis is more important. These factors could disturb the accurate recording of the geomagnetic field, or degrade the signal. The low inclinations in organic sediment tend to support this possibility.

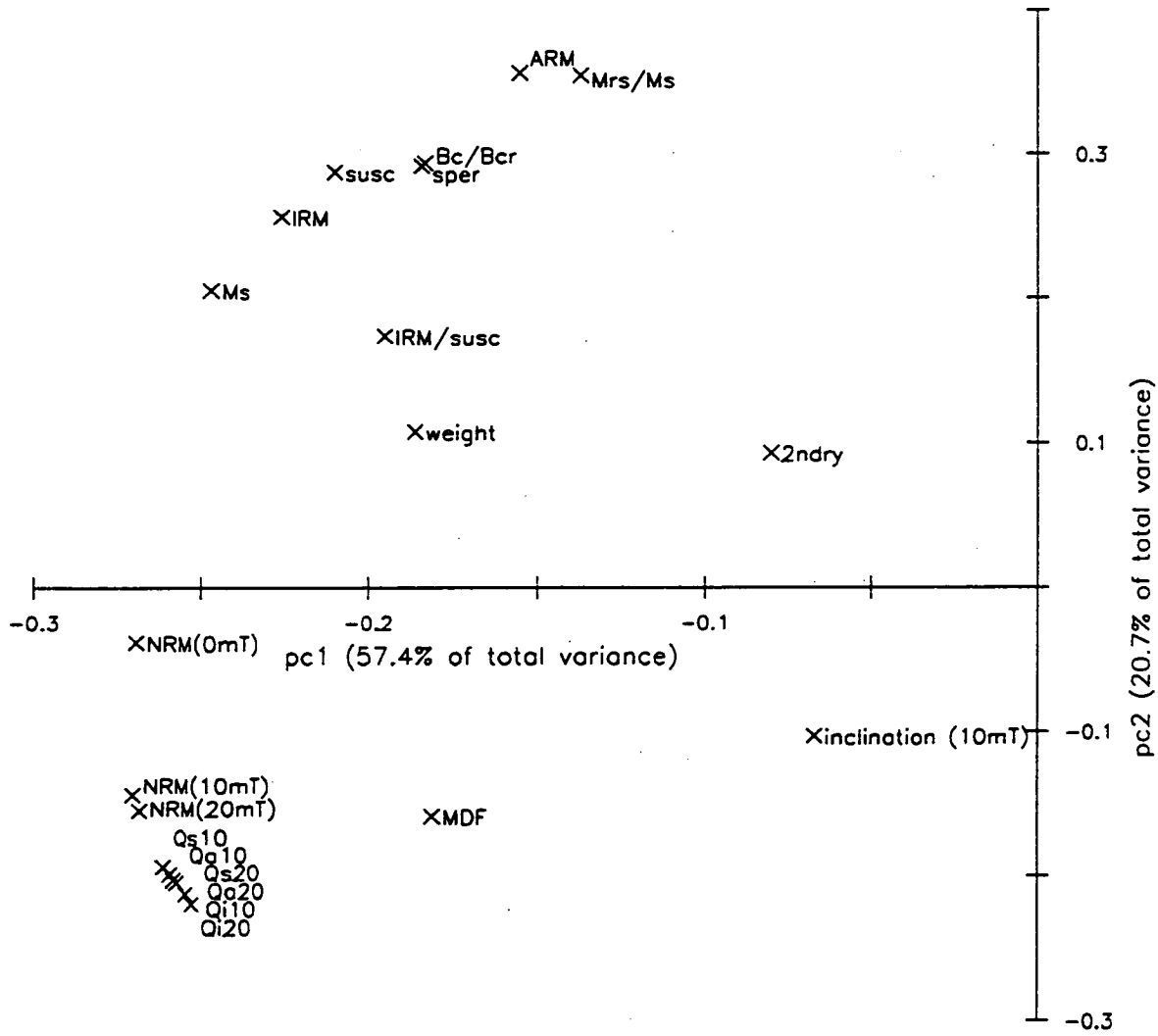

Fig. 4.18 Principal component analysis of the measurements made on 40 selected samples. Note: a) the tight clustering of the different Q-ratios; b) the concentration dependant parameters plot in the same region; c) the NRM intensity values get closer to the Q-ratios on demagnetisation. N.B. Q_{s10} is short-hand for NRM_{10mT}/susceptibility, and similarly for Q_{s20} and so on.

Thus the King criteria for magnetic mineralogies suitable for palaeointensity work are necessary but not sufficient conditions. The ranges of variation of concentration, composition and grain-size of the magnetic fraction in the non-organic samples are far more constrained than the criteria. All but the most organic samples pass the criteria. Sediments whose magnetic mineralogy pass the King criteria are still not guaranteed to be good recorders of the geomagnetic field.

Most samples acquired a secondary component of magnetisation, with the samples taken by Williams and Chevalier in the third sampling showing the largest effect. Therefore this unwanted secondary component was acquired either during transport or storage, when conditions must have differed from the other two samplings. Since any VRM would be removed by storage for a few weeks in zero field, it is probable that the storage conditions were at fault, and the Helmholz storage coils were not negating the present Earth's field properly. The secondary component is almost completely removed by the 10mT demagnetisation step, and therefore no harm has come to the original NRM.

Both the NRM intensity demagnetised at 10mT and at 20mT give very similar records, even though a tiny amount of the secondary component of magnetisation is probably present in some of the samples at 10mT.

The demagnetised NRM can be normalised with either susceptibility, IRM or ARM to give very similar down-core records (figure 8.2). It therefore makes little difference which of these normalisors is used to recover relative palaeointensities from the Lac du Bouchet sediments.

Chapter 5

Data processing; the results on a depth scale

5.1 Introduction

The raw measurements of NRM, susceptibility, ARM and SIRM must undergo some processing to get down-core records best able to indicate the past environment and geomagnetic field.

The records from individual cores need to be stacked into one, in order to increase the signal to noise ratio, and to fill in sections which may be missing from one or more cores. This process requires the same sedimentary layers in each of the cores to be on a common depth scale, so the records of susceptibility from each of the individual cores were plotted side by side, and then common features were matched. Core H had been chosen for detailed pollen and sedimentological analysis, and so was chosen for the common depth scale; equivalent core H depths were calculated for cores G, I, K, and the 20m master core (D).

Stacking the cores was then a simple process that resulted in a data-set that contains about 3000 samples, which is densely sampled in some places, but under-sampled in others. For some analyses, for example FFT spectral analysis, a smaller, evenly spaced data-set is required; the best way to go about this is discussed in section 5.5.

This processing is sufficient to obtain palaeoenvironmental records, but more processing is required for the NRM direction and intensities, because not all samples carry geomagnetic information equally well. There is coring disturbance in some Mazier sections; the organic layers have a slightly different magnetic mineralogy and were deposited under slightly different conditions; and rare samples pick up an anomalously high NRM intensity. Therefore, sample rejection criteria are tested and applied to the data-set.

The records on the core H depth scale which go forward to the following chapters are plotted at the end of the chapter.

Applying a depth→time model, and conversion to the frequency domain (i.e. spectral analysis) may also be considered as data processing, but are held over until later chapters.

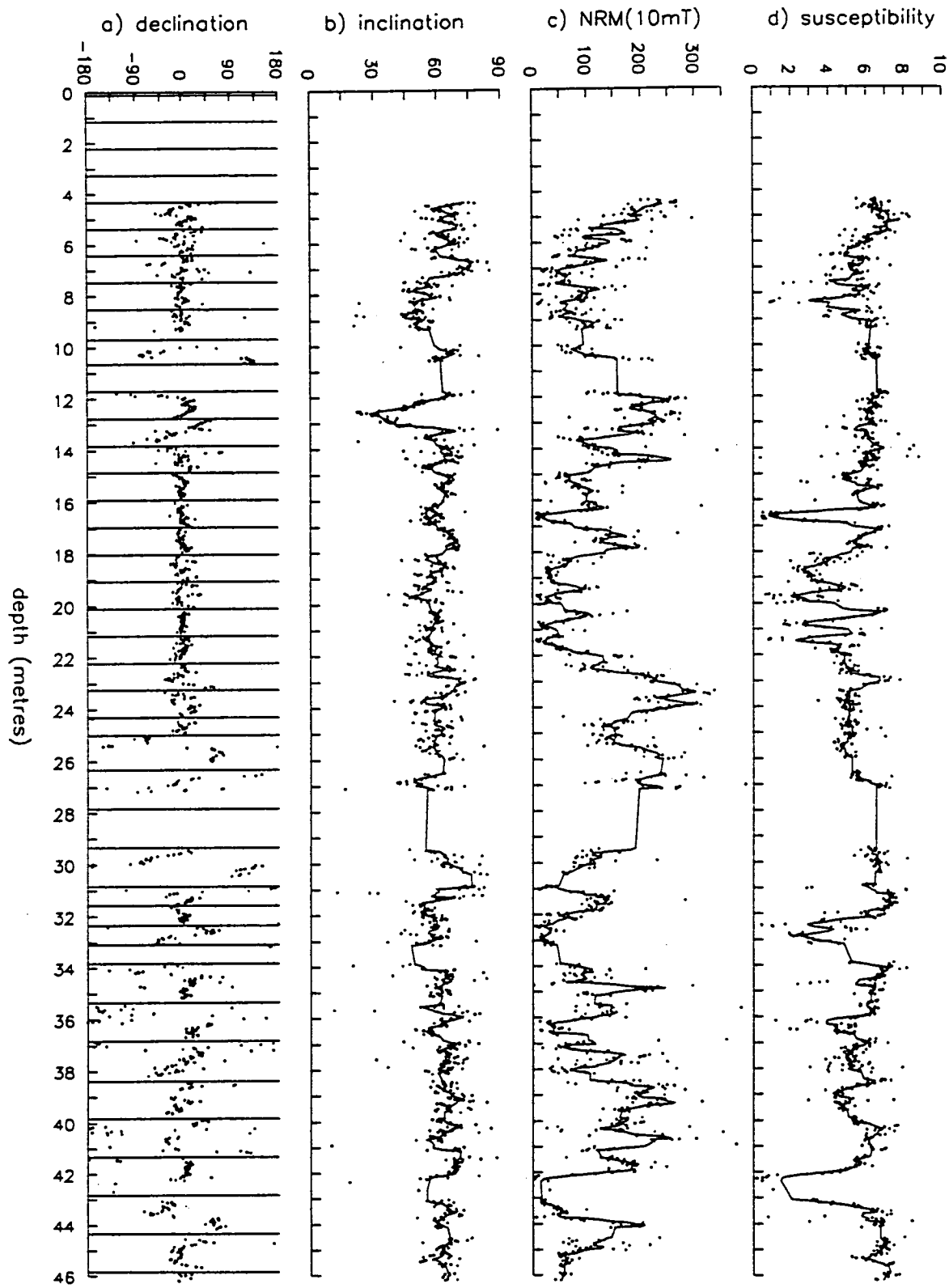

Fig. 5.1 Palaeomagnetic records from core H: (a) declination$_{10mT}$ (°); (b) inclination$_{10mT}$ (°); (c) NRM$_{10mT}$ intensity ($\mu Am^2/kg$); (d) susceptibility ($\times 10^{-6}$ m^3/kg). Bars on the declination plot represent the core H section boundaries; the piston-Mazier corer transition occurs at 25m.

5.2 Single core results: core H

Some core H palaeomagnetic records are displayed in figure 5.1. The records show fine detail. However, there are gaps in the records: the uppermost 4 sections were not sampled because the upper part of the sequence has been analysed in detail in previous coring campaigns and studies; the lowermost part of the core (sections 43 and most of 42) were too hard for sampling; and gaps in the middle of the record are due to the section being either partially recovered or not recovered at all (because of the change-over from piston to Mazier coring (section H27) or coarse sediments (section H11)). The case is the similar for the other cores, and these gaps can be filled with stacking.

The declinations have had their section averages set to zero, and have a greater scatter below 25m, due to the Mazier corer (section 5.6).

5.3 Core matching

Core matching was carried out as a first step in stacking the cores, and also to gauge the lateral continuity of the sedimentary layers under the lake, in a similar fashion to the matching of the shorter cores from Lac du Bouchet (see, for example, Creer et al. [1990]).

The susceptibility records were chosen for the matching because: (a) they represent only lithological changes and so are not complicated by any geomagnetic influence, unlike NRM intensity; (b) susceptibility records are available for all of the 20m core set and most of the Mackereth cores, unlike SIRM and ARM; and (c) the susceptibility meter is very simple, and as such is less prone to instrument drift or pilot error than either the Molspin or cryogenic magnetometers.

Figure 5.2 shows the susceptibility records of cores G, H, I and D (D from the 20m core set) side by side, with tie-lines marked between distinctive features, taken to represent the same sedimentary layers. I started by marking ties between the most obvious features of the records, for example the troughs between 16 and 21m, and around 8m, and then steadily worked out the correspondences in-between. Core section boundaries are shown in the bar to the right of the records.

In general, good matches were found between the cores, but some parts of the sequence proved problematic. Between 11 and 14m, I could not be confident in making any firm ties - this section was identified by as a slump by Truze [1990], and as having a high anisotropy of susceptibility by Blunk [1990]. The difficulty in matching layers from one core to the next tends to support the interpretation of this section as a slump, having important implications for the dating (slumps are deposited instantaneously, geologically speaking), and the palaeomagnetic recording. A full 80cm of the sequence is missing from cores B and D at 18m: this is most probably due some different depth processing of the 20m

core set, rather than a local hiatus or local erosion, because it occurs between sections 11 and 12 of core D, and the missing section is repeated faithfully in cores G and H.

For some sections, the length of recovered sediment was much less than the depth increment penetrated by the corer, for example in sections G27 and G34 (fig 5.2). It was not certain, until the susceptibility matching, where-abouts in the possible 150cm the 86cm section (for instance) came from. The position of some sections was changed on the basis of keeping a roughly similar sedimentation rate in the common layers of the different cores. The initial assumption was that the missing part came from the bottom of the section; only a few sections needed to be changed from this, and they are listed in table 5.1. This cross-checking between cores is one of the advantages of multiple coring.

Table 5.1 Core sections moved from their original depth

core and section	old→new depth	change
H30	31.58→31.68m	+10cm
G28	30.42→31.12m	+70cm
G34	36.22→36.57m	+35cm
I16	30.81→30.91m	+10cm
I20	35.31→35.46m	+15cm
I21	36.81→36.46m	-35cm

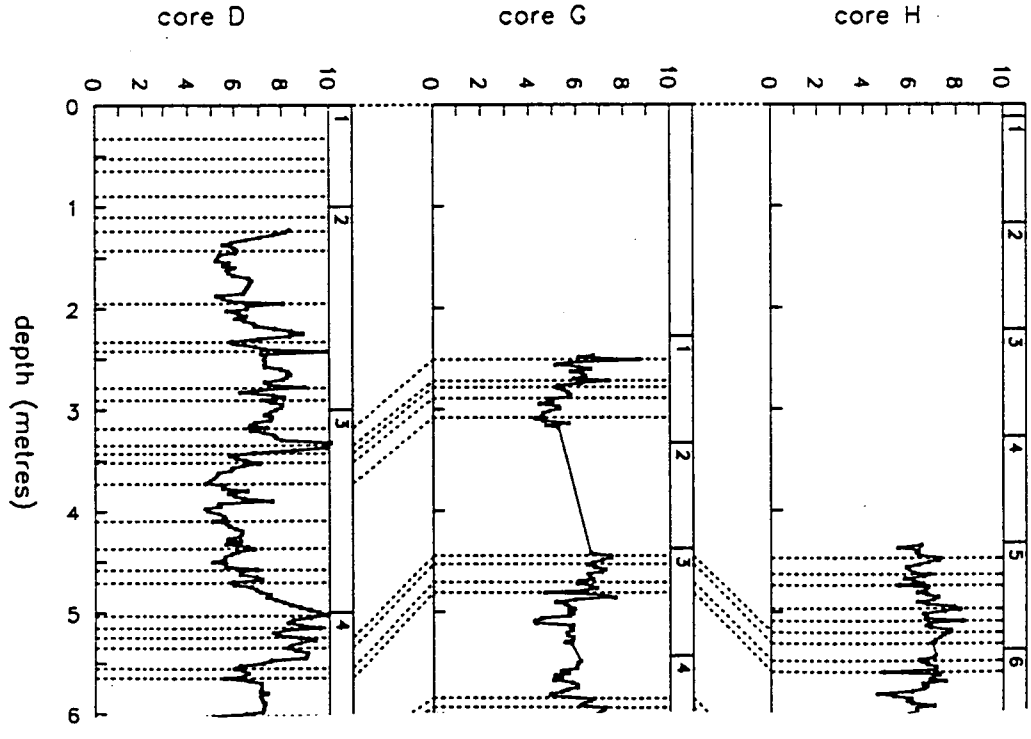

Fig. 5.2a Figure showing tie-lines between the susceptibility records for cores D, G, H and I. From 0 to 6m. Core section boundaries are also marked to the right of the records. The figure continues down the core over the next 3½ pages.

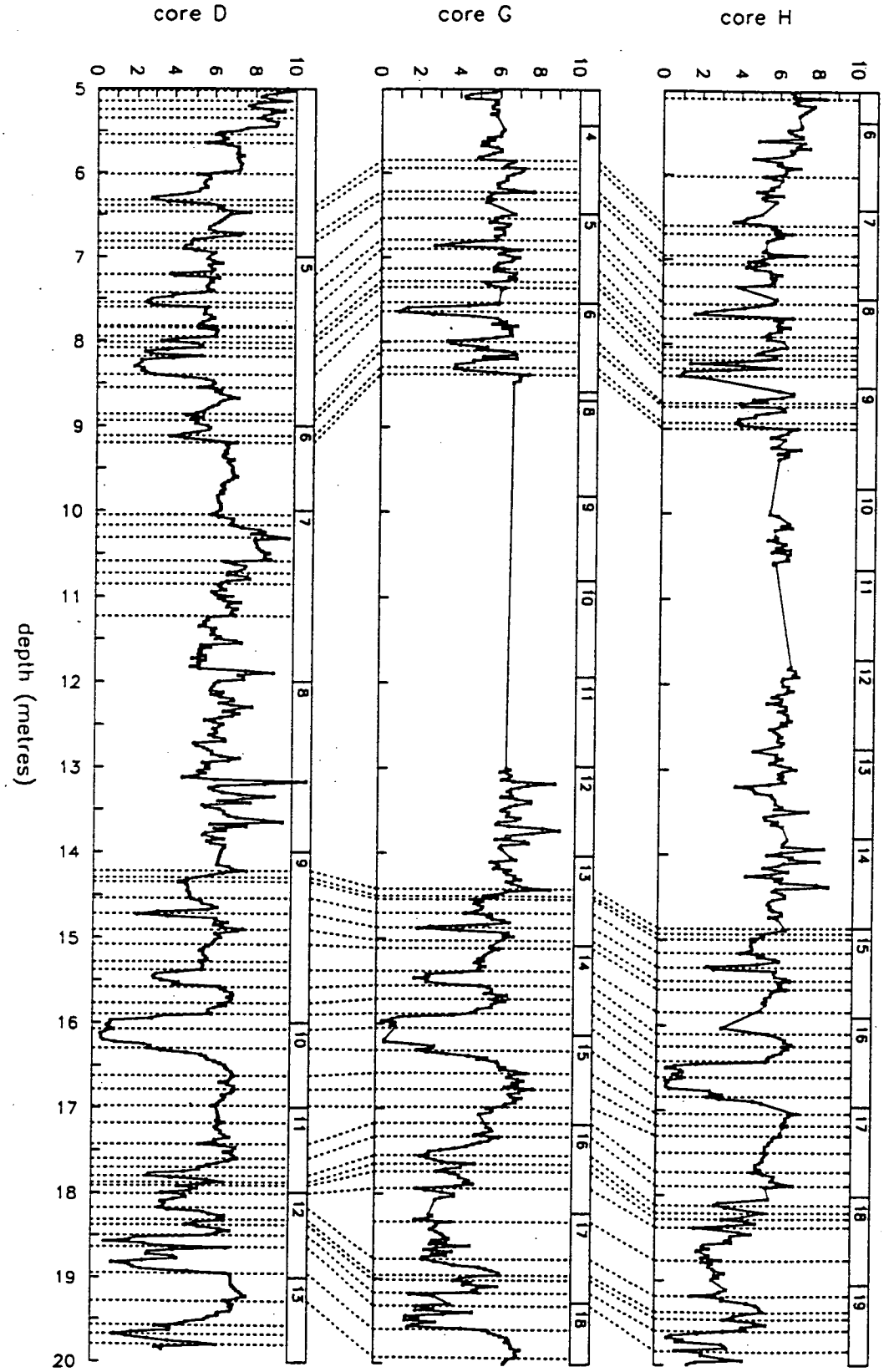

Fig. 5.2b Ties between susceptibility records of cores D, G and H (continued). 5 to 20m.

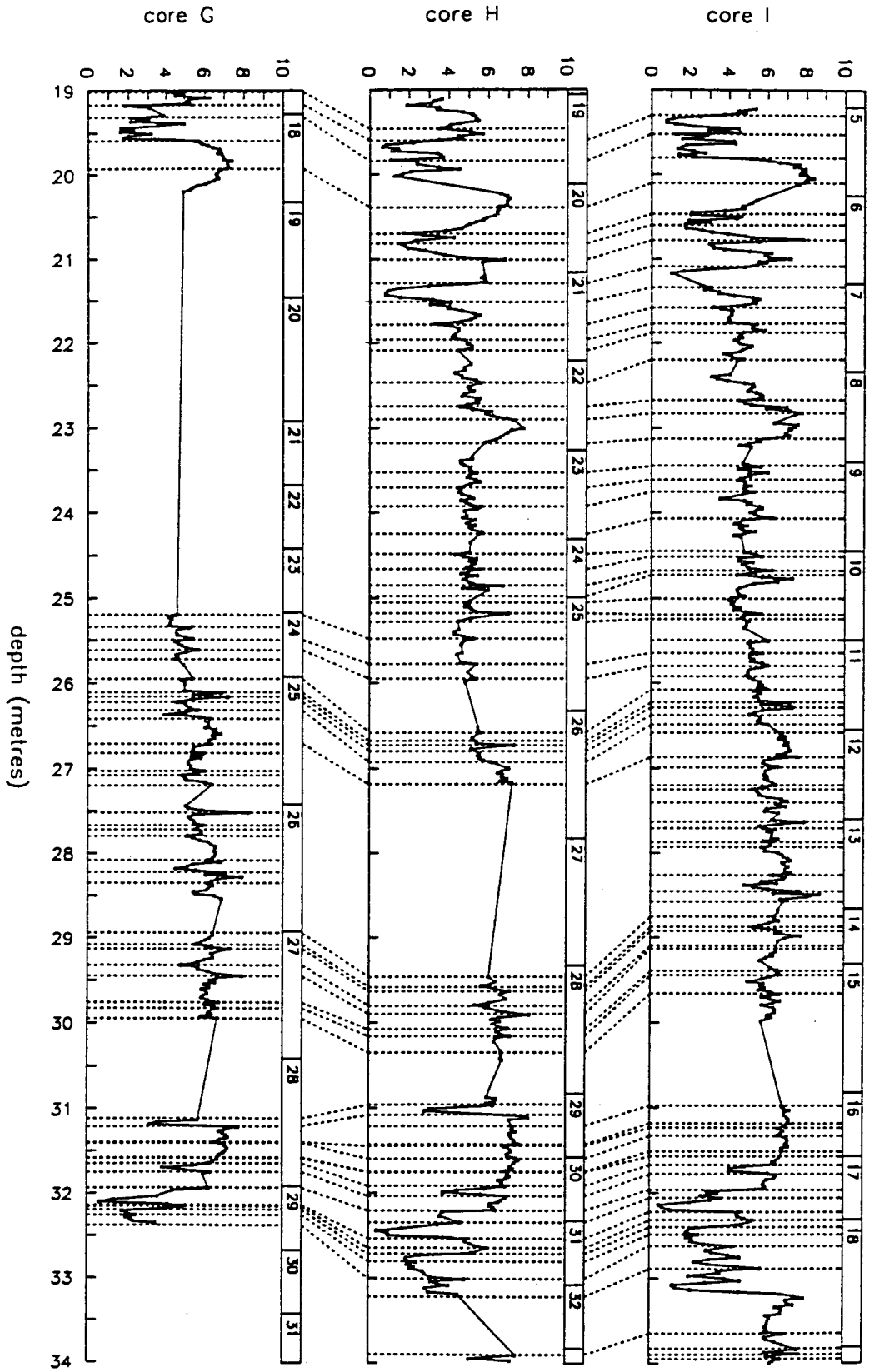

Fig. 5.2c Ties between susceptibility records of cores G, H and I (continued). 19 to 34m.

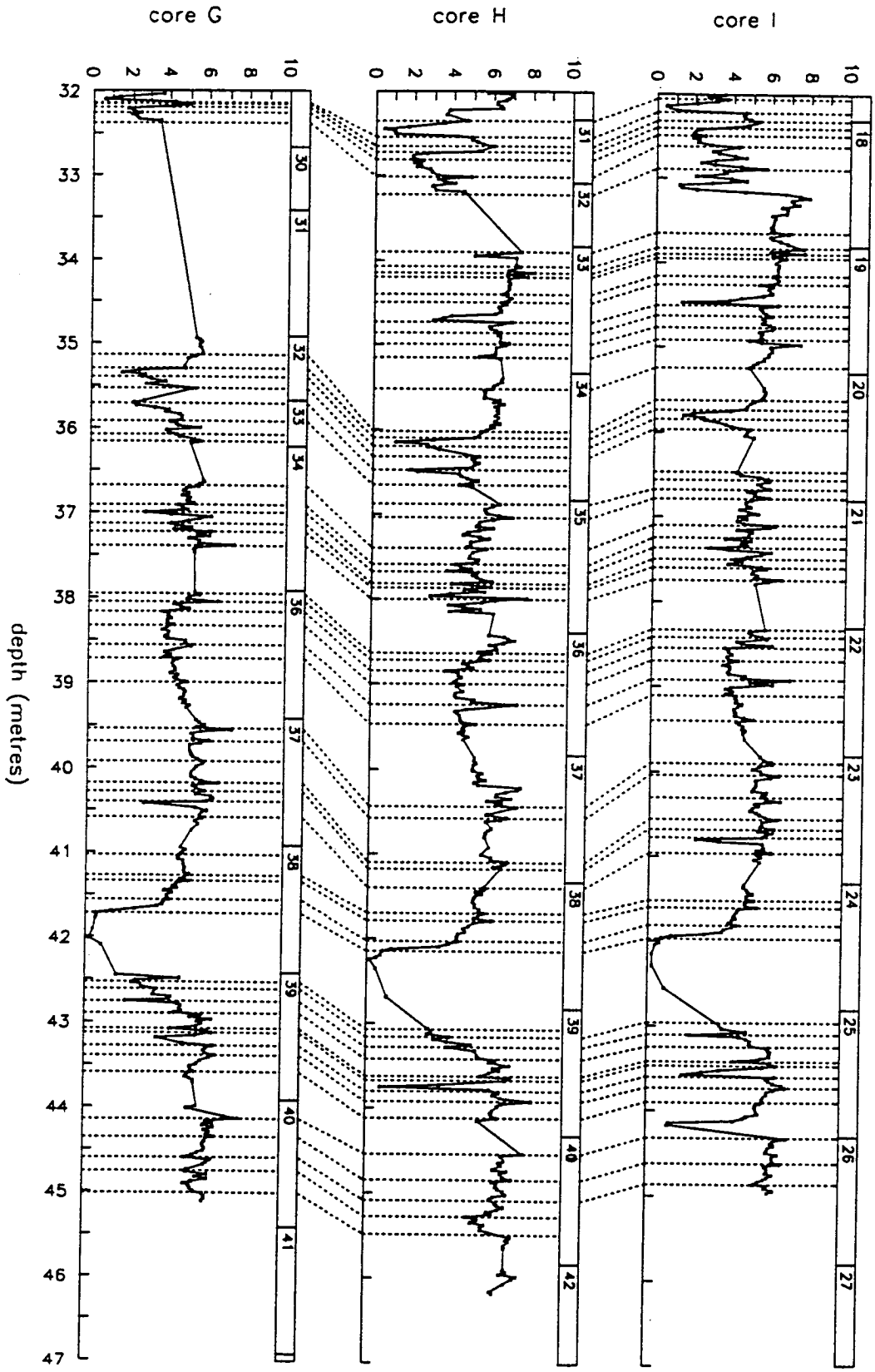

Fig. 5.2d Ties between susceptibility records of cores G, H and I (continued). 32 to 47m.

5.4 Conversion to the core H depth scale

Now that ties between common sedimentary layers had been established, the depths assigned to each sample had to be converted to a common depth scale (core H scale).

The calculation of the new depths was a four step process. Firstly, average thicknesses were calculated for each layer between the tie points (figure 5.2), and these were incrementally added to form a first common scale. This scale was then re-converted to the H scale. These first two steps are necessary because not all ties are present in core H, due to the gaps. Depth→depth transforms, with depths only at the tie points, were created for changing G depths to H depths, D depths to H depths and so on. These depth→depth transforms were then applied to the computer files containing the original depths for all the samples, so that throughout the further processing each sample had both its original depth and equivalent core H depth at hand. New programs were written for stacking 50m cores, as previous programs (Smith [1985]) could not be used due to the new problem of incomplete cores.

Comparisons are shown between the cores for susceptibility (figure 5.3a), NRM_{10mT} intensity (figure 5.3b), declination (figure 5.4a) and inclination (figure 5.4b). It is clear that the matching of susceptibility records has led to a good match in the NRM intensity records.

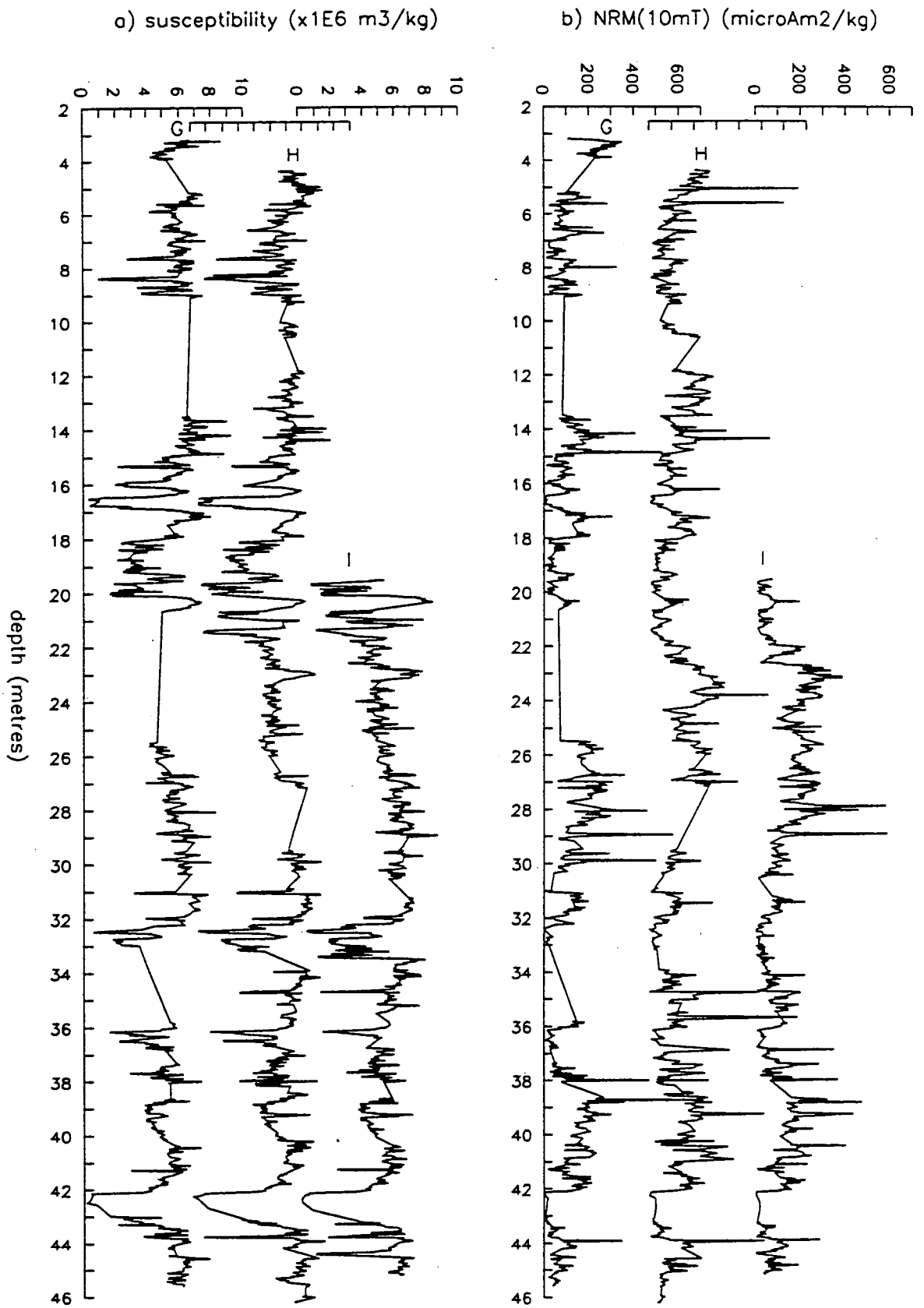

Fig. 5.3 Raw down-core records for (a) susceptibility ($\times 10^{-6}$ m^3/kg), and (b) NRM_{10mT} intensity ($\mu Am^2/kg$): comparison between cores G, H and I.

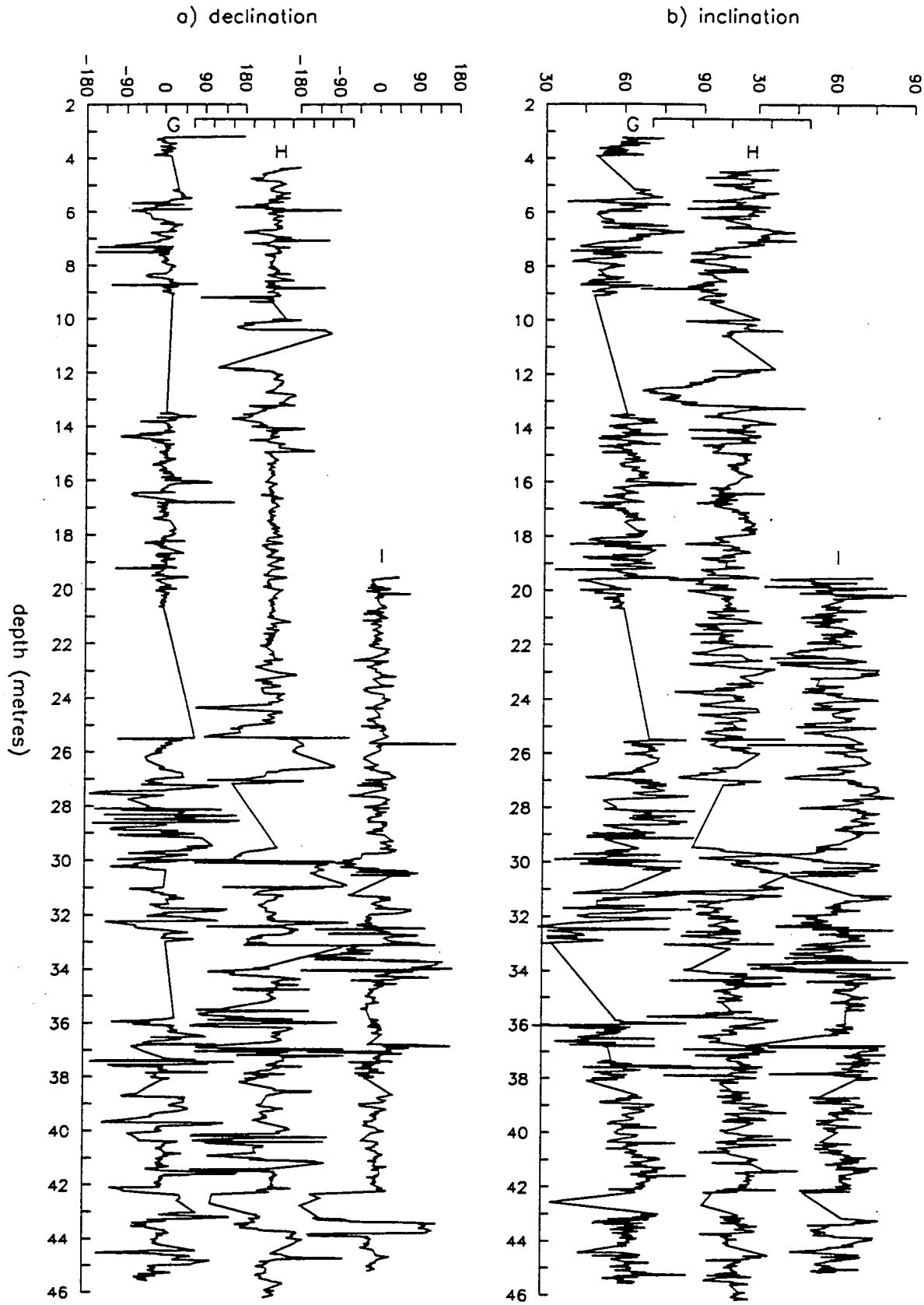

Fig. 5.4 Raw down-core records for (a) declination$_{10mT}$ (°), and (b) inclination$_{10mT}$ (°). The average declination has been subtracted from each section, so that the records vary about zero. Cores G, H and I are shown.

5.5 Stacking the cores and evenly spacing the data

Once all the samples had been assigned a core H equivalent depth, it was a simple matter to stack the individual core records into one computer file, in depth order. The Edinburgh version of the stack of the 20m cores (A, B, C, D, and F) (Creer et al. [1990]) was also merged with the individual 50m cores (G, H, I, and K), for good coverage of the top 20m.

The resulting stack contains ~3700 data-points, and these are unevenly spaced down the sequence: some intervals are over-sampled and some are under-sampled. Two types of re-spacing were done: both to reduce the over-sampling, with the second method leaving an evenly spaced record. The large number of data-points must be reduced to make the manipulation of the data-set more manageable, and the over-sampling was employed to make statistics (standard deviations) to gauge the consistency of the values from core to core (assuming that the core matching is sufficiently accurate).

The first method of re-spacing was to take evenly spaced depth intervals down the core, and calculate the average and standard deviation of the samples within each interval. When only one sample occurred in an interval, its original depth was retained. Where there were gaps remaining (even after merging), they were left alone. The records resulting from this method are shown in the next section. The records are not evenly spaced throughout, but the clumpyness of the original stack has been removed, and the problem of interpolation between points did not need to be addressed (i.e. the over-sampling problem is solved, but the under-sampling is not). These records can be used for spectral analysis by the Lomb-Scargle method.

The second method aimed to produce evenly spaced records, which are needed for FFT spectral analysis. Interpolation into the gaps of the records was the main problem, as it is impossible to make a record which has information at all points from one which has information gaps at some depths. However, the method I chose was to set up an evenly spaced set of depths, and then assign values to these depths from the average of the nearest 10 samples. This is not ideal, and there is inevitably some smoothing, but this smoothing is only pronounced for the under-sampled intervals, because the weighting is done on a per-sample basis rather than a per-depth basis.

5.6 NRM direction correction

Figure 5.4 shows the raw declination and inclination records for cores G, H and I. For the declination, there are scattered outliers in the upper 25m, but it is below 25m (with the Mazier coring) that the records become very noisy. At first sight there seemed no hope of retrieving a match between the 3 cores, but the clean declinations of core I between 37 and 42m indicated that all was not lost. The inclination records are less affected by the piston-Mazier transition, but are also noisy (note the scale ranges only 60°, compared with 360° for the declination). Common patterns in both long term trend and short wavelengths can be made out between 22 - 27m, and 38 - 42m.

The match between the records from individual cores was improved by removal of samples from the record, starting with whole sections. The core records were plotted on the same graph in different colours (not shown), so that both the amplitude and position of the variations could be compared; thus it was obvious where two cores showed a good match and a third did not - the third section was removed. Next, the declination records were trimmed: all samples with a magnitude greater than 55° were discarded. Finally, any remaining outlying samples were identified and removed. Table 5.2 details the sections and samples removed, and the "cleaned" records are shown in figure 5.5.

Table 5.2 Sections and number of samples removed at each stage of the direction correction (number of samples remaining shown in brackets)

	core G (958)		core H (1134)		core I (826)	
	dec.	inc.	dec.	inc.	dec.	inc.
sections removed	G06, 26, 27, 29, 33, 36. (744)	G29, 32, 33, 34. (894)	H13, 25, 26, 28, 31, 37, 42. (939)	H12, 13, 25, 28. (997)	I18, 15. (744)	I15. (798)
declinations >55° removed	(656)	-	(828)	-	(688)	-
outliers	(642)	(882)	(815)	(982)	(684)	(780)

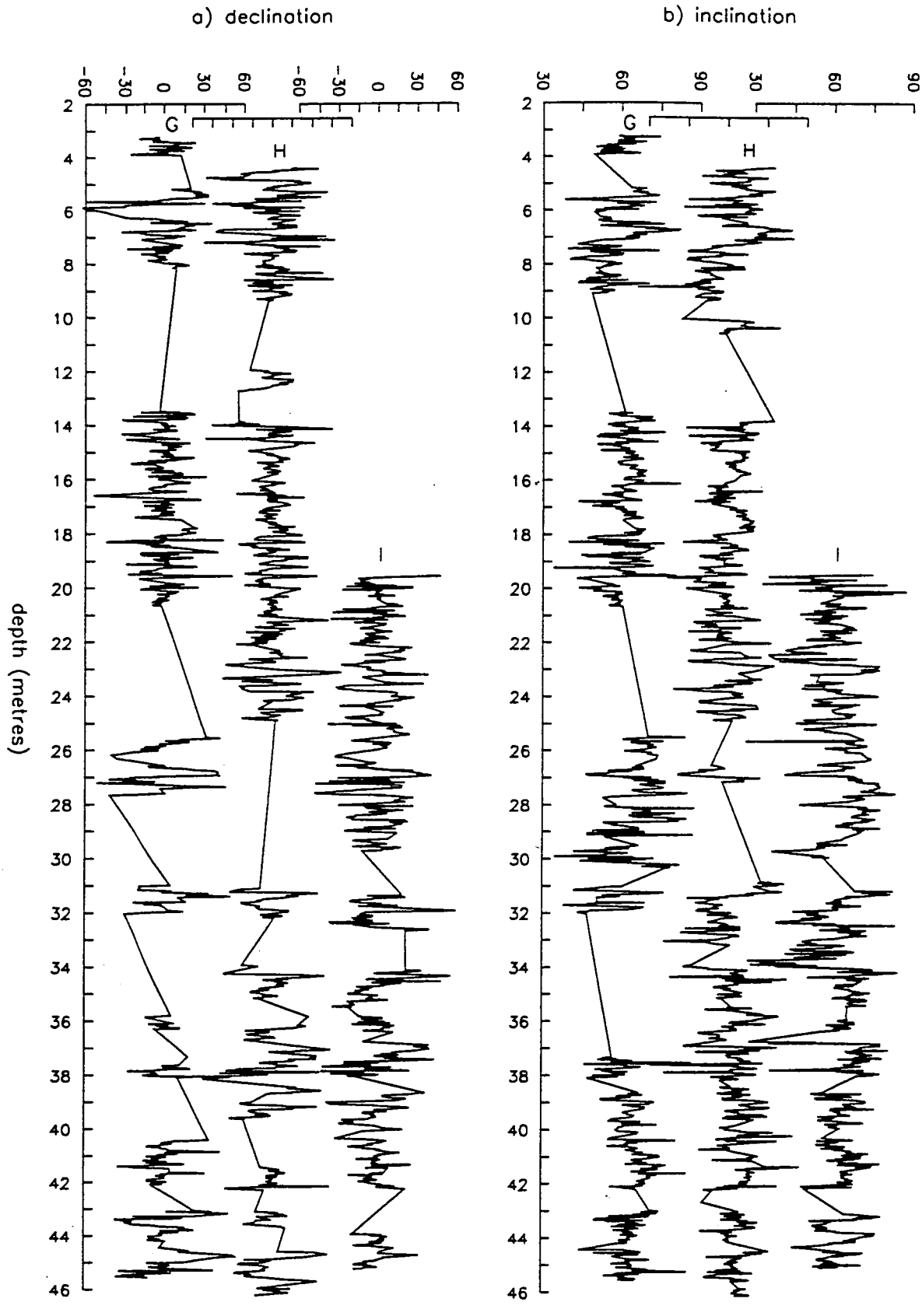

Fig. 5.5 Down-core records for (a) declination$_{10mT}$ (°), and (b) inclination$_{10mT}$ (°), after sample removal detailed in the text and table 5.2. Cores G, H and I are shown.

5.7 Sample rejection criteria for palaeointensity estimates

One of the main aims of the thesis is to recover a reliable record of geomagnetic palaeointensity. Not all samples have a demagnetised and normalised intensity proportional to the field around the time of deposition, and these are identified and removed here. Demagnetisation and normalisation have been dealt with in sections 4.4 and 4.5.

In figure 5.3, isolated spikes are seen in the NRM_{10mT} intensity record. These are a lithological feature, as the spikes are present at the same level in all cores, and are also represented, in a less spectacular way, in the susceptibility record (the 3 spikes at 28, 29 and 30m depth provide good examples). It is unclear to me why these samples should have such an anomalously large response to the field, because magnetic experiments (chapter 4) show these samples to have a very similar magnetic mineralogy to the "regular" samples. On a practical level, they are removed from the record because they give a false impression of the true palaeointensity. Any smoothing with the spikes still there would cause the high to be spread out into the adjacent levels, and spectral analysis would be biased by them. The record remaining after spike removal is shown as figure 5.7b.

In figure 4.1, the samples with a susceptibility below about 4.2×10^{-6} m^3/kg have an anomalously low intensity response, due principally to the different physical and chemical conditions of the organic sediment around the time of deposition (for example the high degree of compaction shortly after burial). The NRM/susceptibility record after removal of the spikes and these organic samples is given as figure 5.7c.

The record of SIRM/susceptibility (an indicator of grain-size) is similar to, but not the same as, the records of susceptibility, SIRM and ARM (which primarily indicate concentration of magnetite grains). The differences can be seen in figure 5.9, and their environmental interpretation is discussed in chapter 7. Here it is sufficient to point out that a narrow grain-size range is preferable for palaeointensity estimates, because lithologically similar samples are more likely to have acquired a DRM with a linear response to variations in the palaeointensity. Therefore the data-set is reduced to exclude values of SIRM/susceptibility greater than 17 or less than 13 kA (figure 5.7d).

The Mazier coring method disturbs the direction records greatly (section 5.6), and it might be thought that the intensity records would be equally disturbed - after all, the palaeomagnetic vector is made up of both direction and intensity. However, the direction records are disturbed mainly because of deformation on the scale of whole sections: this will have only a little effect on the magnetic fabric within a single sample, the disturbance only becoming apparent when a section of samples are plotted as a record. The relatively small standard deviations of the intensity stacks (figure 5.8) give credence to this argument.

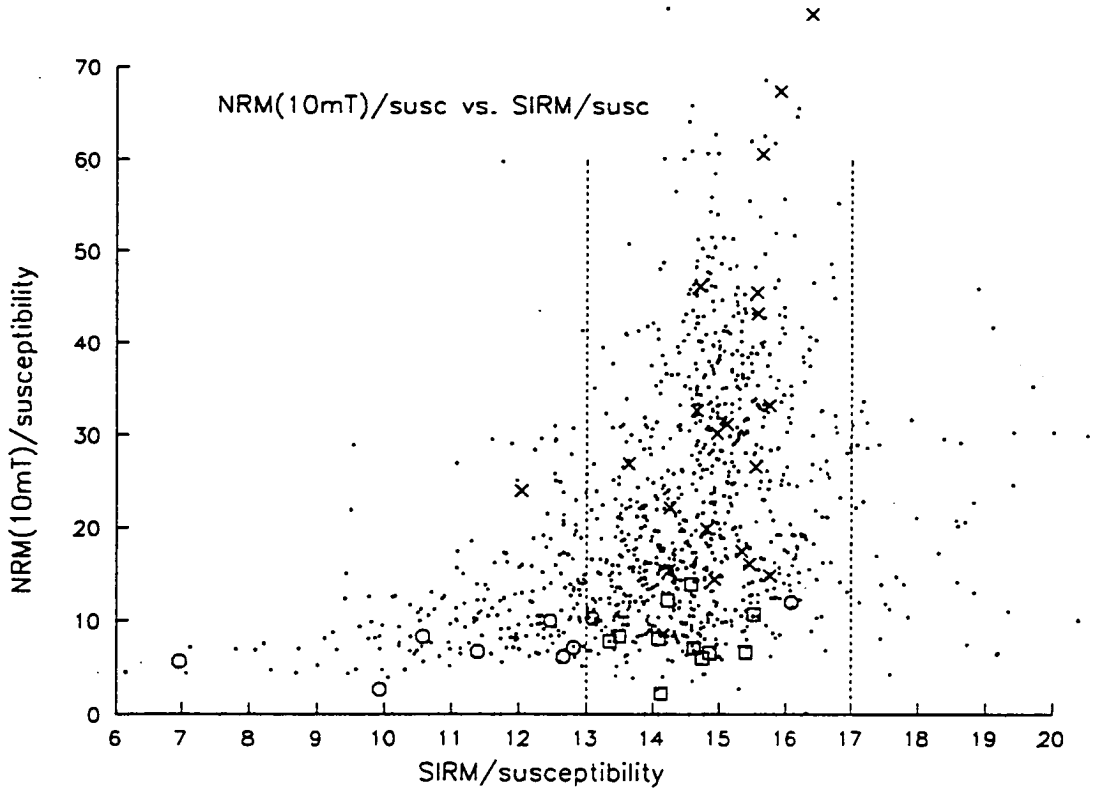

Fig. 5.6 NRM_{10mT}/susceptibility vs. SIRM/susceptibility. Dotted lines mark the limits applied in figure 5.7d.

Figure 5.7 shows the normalised NRM intensity for core H, with samples progressively removed. The discarded samples are mostly low intensity and organic-rich; they tend to be bunched and leave gaps in the record.

5.8 The final down-core records on the core H depth scale

The final records on the core H depth scale are shown below in figures 5.8, 5.9 and 5.10.

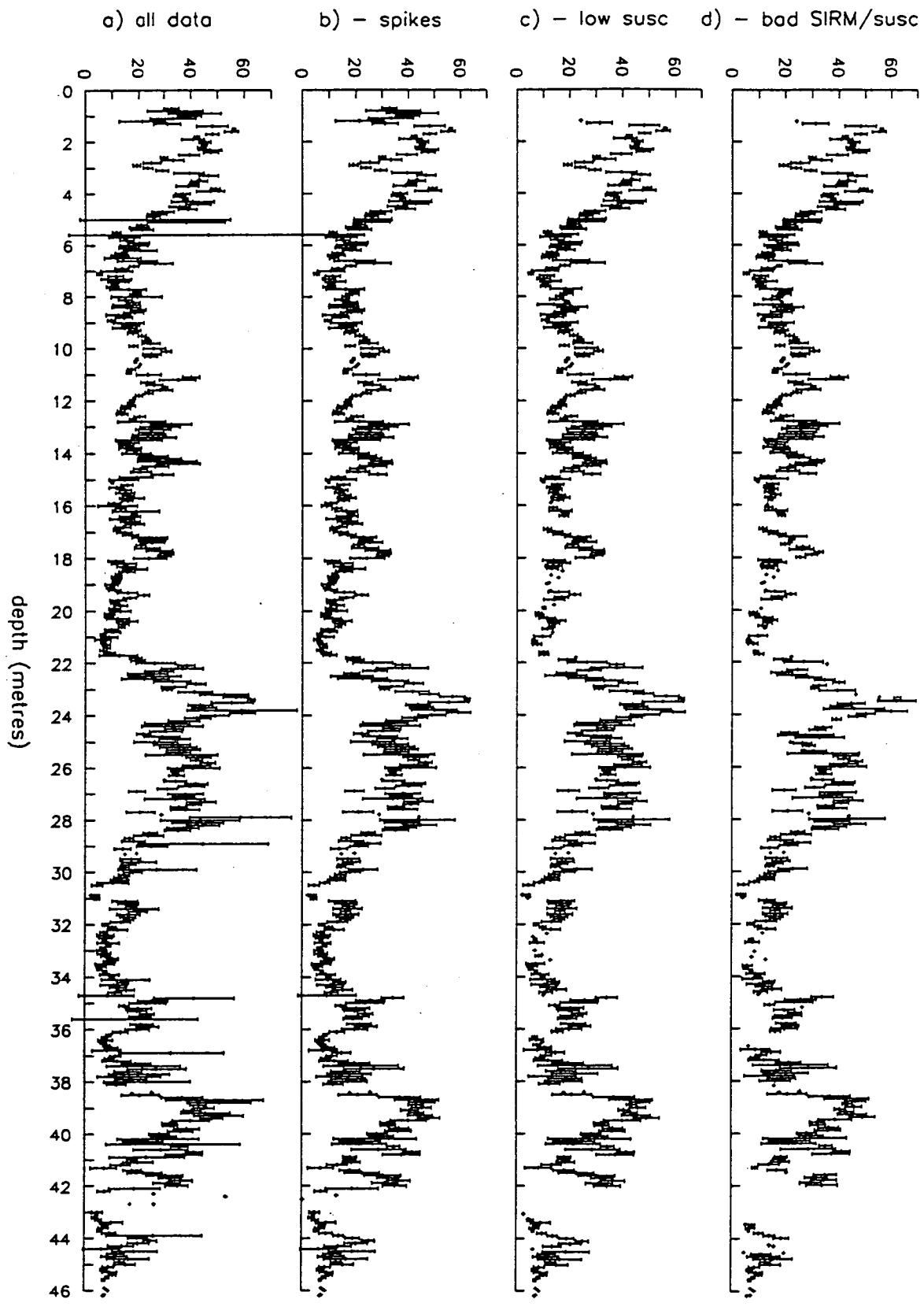

Fig. 5.7 The stacked NRM_{10mT}/susceptibility record after progressive removal of: (b) spikes; (c) samples with susceptibility < 4.2×10^{-6} m^3/kg; (d) samples with SIRM/susceptibility >17 or <13 kA.

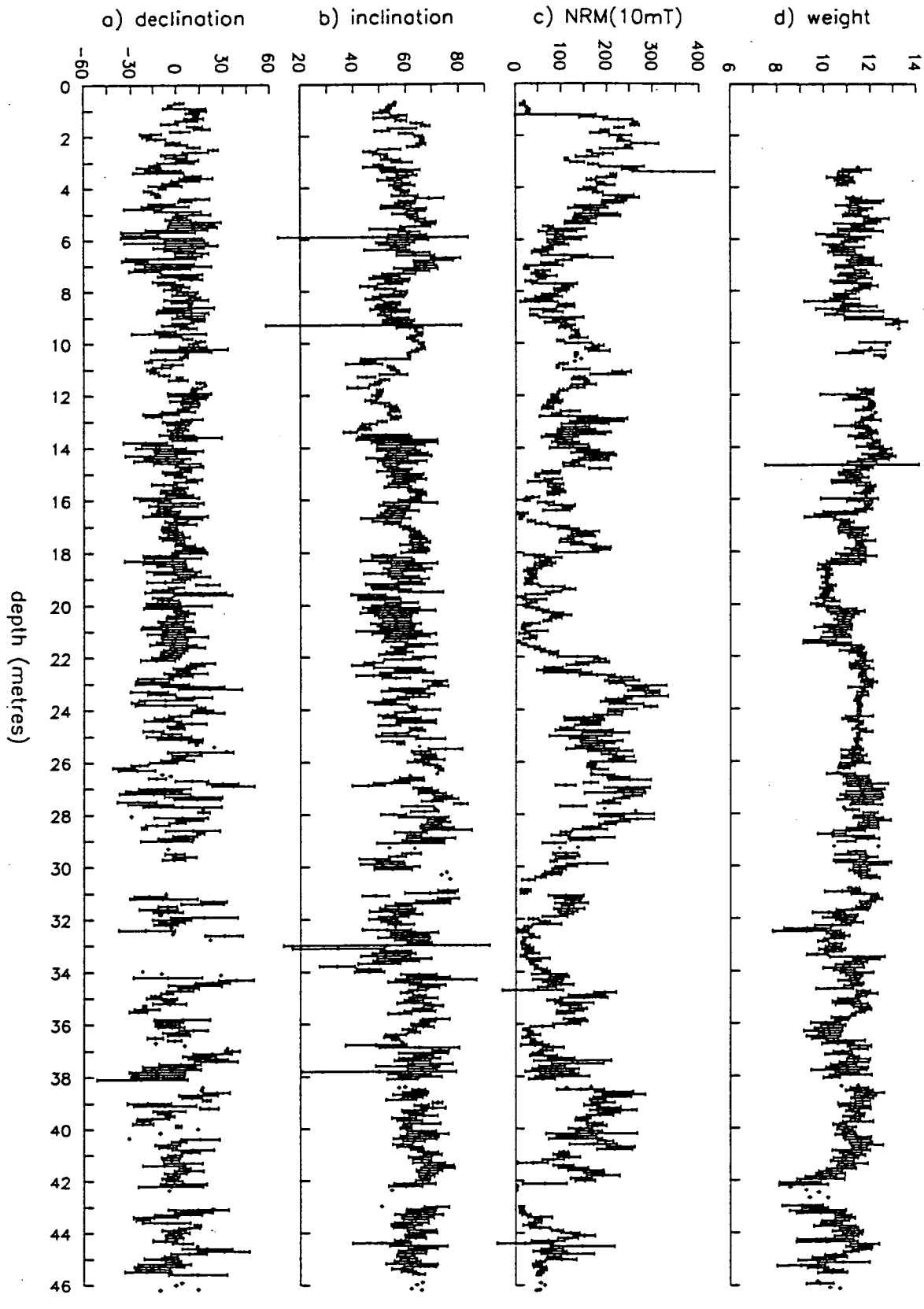

Fig. 5.8 Stacked palaeomagnetic and weight records. (a) declination$_{10mT}$ (°), after processing (section 5.5); (b) inclination$_{10mT}$ (°), after processing (section 5.5); (c) NRM$_{10mT}$ (μAm^2/kg); (d) sample weight (grams)

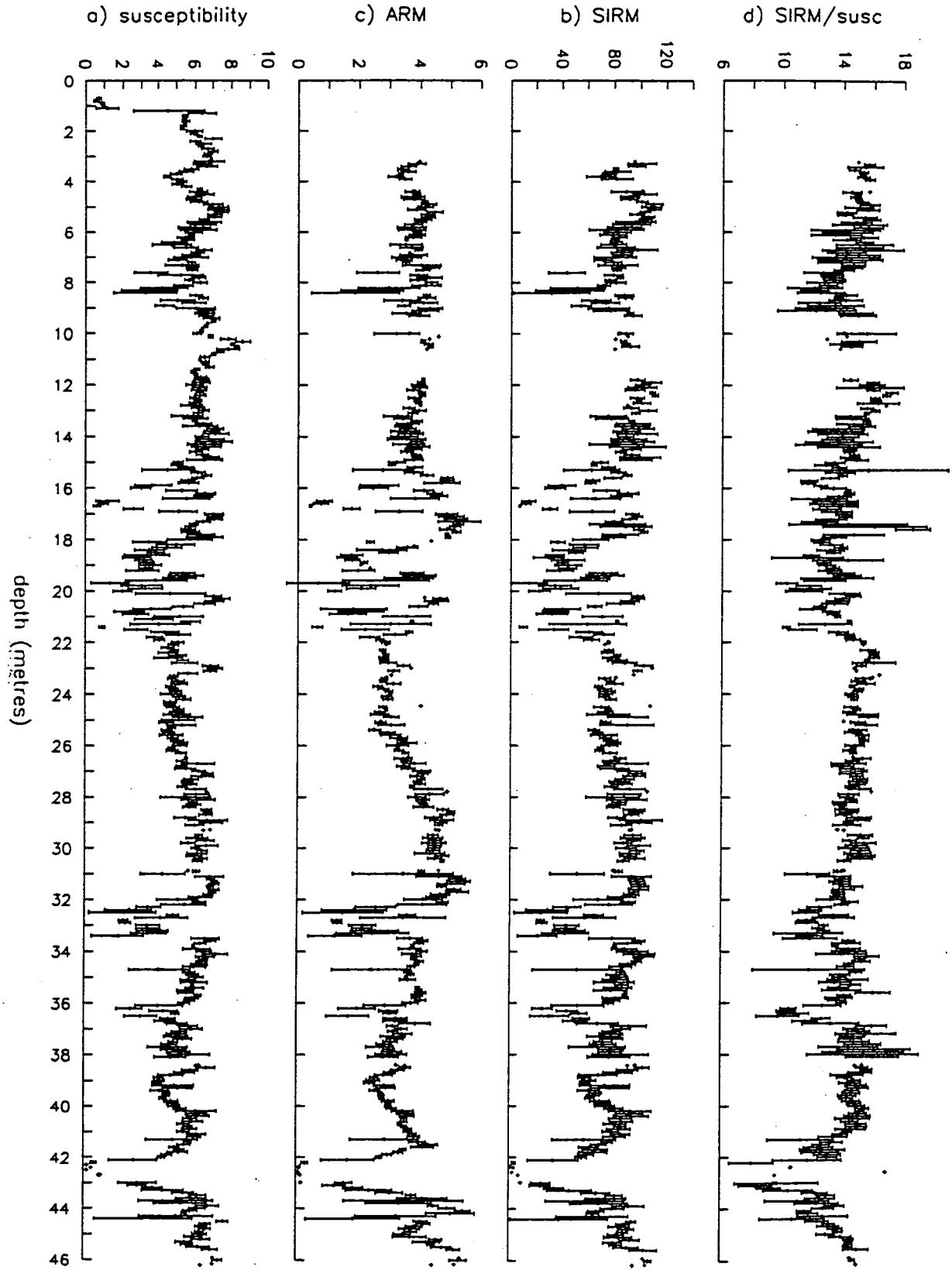

Fig. 5.9 Stacked rock-magnetic records. (a) Susceptibility ($\times 10^{-6}$ m^3/kg); (b) ARM (mAm^2/kg); (c) SIRM (mAm^2/kg); (d) SIRM/susceptibility (kA).

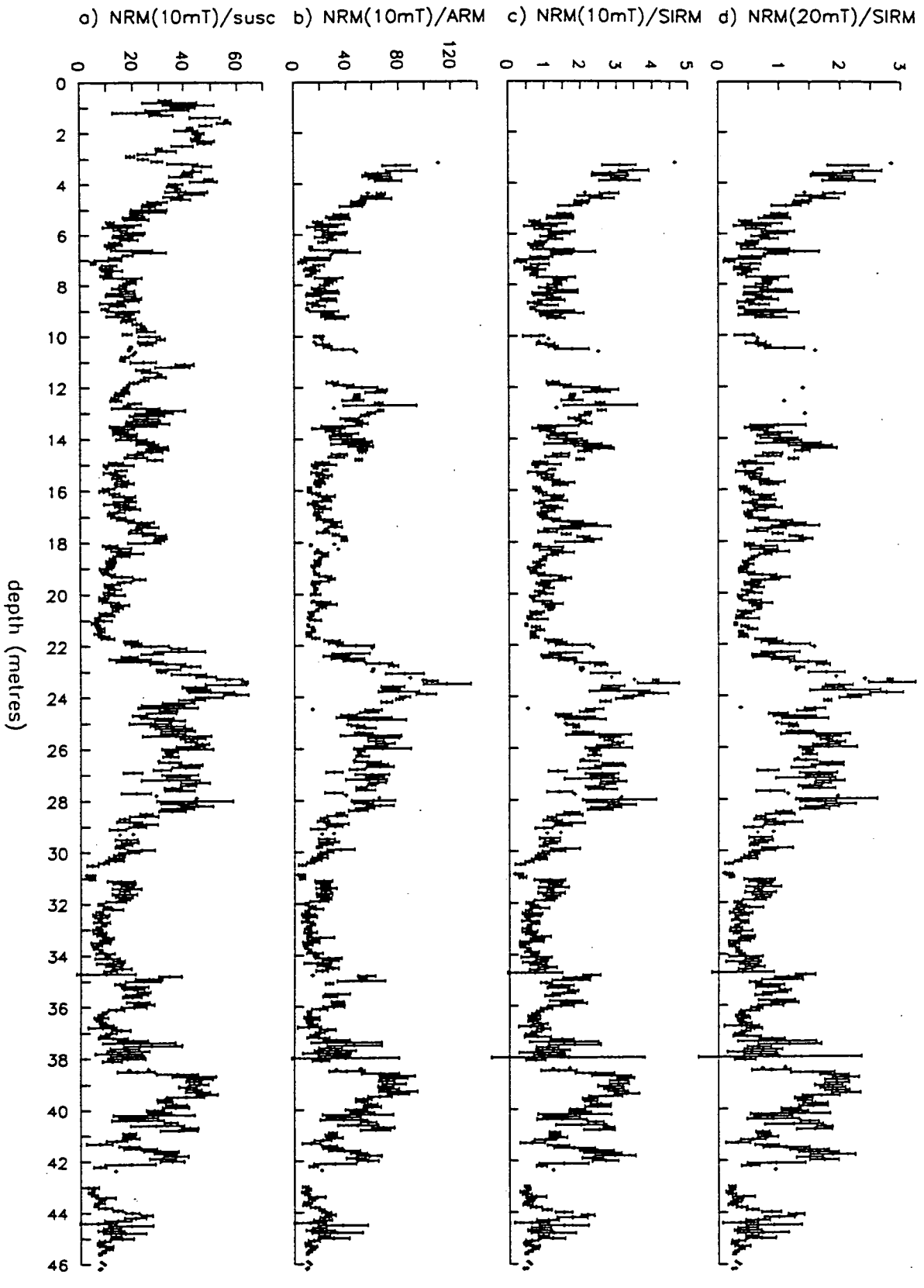

Fig. 5.10 Stacked normalised NRM intensity records. (a) NRM_{10mT}/susceptibility (Q_{s10}) (A/m); (b) NRM_{10mT}/ARM (Q_{a10}) (×1000 unitless); (c) NRM_{10mT}/SIRM (Q_{i10}) (×1000 unitless); (d) NRM_{20mT}/SIRM (Q_{i20}) (×1000 unitless).

Chapter 6

Dating the sediment sequence

6.1 Introduction

The Lac du Bouchet sedimentary sequence needs to be dated so that it can be compared with other palaeoenvironmental and palaeomagnetic records from around the globe. Time spectral analysis also requires dated records. The dating of the core is achieved by constructing a continuous depth→time model from a limited number of dated points down the core.

An advantage of working on sediment cores, rather than on a number of individual geographically separated exposures, is that they are already qualitatively dated: the sediments obey the law of superposition with the oldest sediments at the bottom and the youngest sediments at the top.

Absolute dating of the Lac du Bouchet cores is only possible for the top 10m (45 kyr), by ^{14}C, and on the volcanic ash layer at 42m, by Ar-Ar. These dates provide an approximate depth→time model, a framework for the indirect methods of dating the majority of the sequence.

Indirect dating methods must be used where absolute dating is not possible. They involve matching warm and cold climatic events in our sequence (identified from palynological study) with events in already-dated proxy-climate records, such as the marine $\delta^{18}O$ stratigraphy (Martinson et al. [1987]) and the Devil's Hole calcite vein $\delta^{18}O$ record (Winograd et al. [1993]). There is enough of a consensus (through the large volume of records available), to be confident in the globality, the ordering, and the intensity of the sequence of major warm and cold periods in the past 300 kyr (at least), though the precise timing and duration of some periods (for example, the Eemian, stage 5e) is not yet settled. Thus dating by matching climatic events depends upon the palaeoenvironmental interpretation of the Bouchet sequence, through pollen analysis and also magnetic records such as susceptibility. There is therefore some overlap between this chapter and chapter 7, in which the palaeoenvironmental interpretation is addressed.

This indirect dating compromises the aim of comparing the Lac du Bouchet records with global records. We can compare the intensity of events (for example the relative warmth of different interstadials), and the rate of change of environmental conditions, but the duration or phase cannot be compared because they have already been fitted to one of the global records. Time spectral analysis is also compromised when the marine $\delta^{18}O$ stratigraphy is used, as this is already tuned to the periodicities in insolation (Milankovitch theory); the Lac du Bouchet record is therefore also constrained to show the same

periodicities. However, there are many ways in which the dated records, both palaeoenvironmental and palaeomagnetic, add to the world data-set, and these are discussed in chapters 7 and 8.

There is an extra factor to be considered with the dating of sedimentary palaeomagnetic records, because the acquisition of magnetisation occurs at the lock-in depth, some cm below the sediment/water interface (figs 1.5, 1.6). Therefore the time of magnetisation lags the time of deposition (which is dated) by a few centuries at Lac du Bouchet (Creer [1990]).

Sedimentological information is relevant to dating the core, as slumps represent no geological time. The warm periods at Lac du Bouchet are represented by condensed sequences.

6.2 Direct dating: ^{14}C and Ar-Ar

The radiocarbon method. Twenty-six ^{14}C dates were obtained from the 20m and Mackereth core sets, measured at labs at Gif sur Yvette, Oxford and Tuscon (Creer [1991]). No new dates have been added from the 50m cores, because the method is limited by the half-life of the ^{14}C isotope to dating material younger than about 45 kyr. There is dense coverage of the first 8m of sediment, and the datings are marked with triangles and diamonds in figs 6.1, 6.5 and 6.6.

The method relies on the decay of the ^{14}C in relation to the stable ^{13}C and ^{12}C isotopes, and to a first order approximation the ratio $^{14}C/^{13}C$ will be a constant at the time of formation of the organic matter to be dated. However, the concentration of new ^{14}C in the atmosphere is not exactly constant. It was recognised from the absolute dates given by tree-ring counting that there was a discrepancy between real ("calendar") years, and ^{14}C years (Stuiver [1986]). Bard et al. [1990] dated a coral sequence from Barbados with both ^{14}C and uranium series dating, found a mis-match, and attributed this to changes in atmospheric ^{14}C. Thus they made calibration points to convert from ^{14}C years to calendar years (given by the U series dating), for the last 30 kyr: ^{14}C years are younger by 2 kyr at 20 ka, so the differences are significant. ^{14}C is formed in the stratosphere by a cosmogenic reaction, and the rate of formation depends upon the magnetic field strength at the time. A stronger field gives greater shielding to cosmic rays, so less ^{14}C is produced (Thouveny et al. [1993], Mazaud et al. [1991]). Figure 6.2 is a copy of figure 4 from Mazaud et al. [1991], and shows both Bard's correction, and Mazaud's theoretical correction based on changes in the geomagnetic field, using the relative palaeointensity curve of Tric et al. [1992]. The theoretical correction will be different if based on the Bouchet relative palaeointensity estimates: since these are generally lower than Tric et al.'s, from 50 to 28 ka, this would lead to the an increase in the correction. Previous depth→time models of the Bouchet sequence

have not corrected from ^{14}C to calendar years, because they were made before the calibration curves were published.

The effect of recycled carbon (organic material deposited on land, and subsequently re-worked into the lake) would be to give estimates for the time of sedimentation which are too old. This problem is avoided by analysing different types of organic matter.

The actual uncertainty of the ^{14}C dates is greater than the standard deviation quoted for them, which is based only on instrumental error. For example, the two datings on core D at 7.53m gave ages of 26.81±0.78 and 30.60±1.00 kyr: clearly the uncertainty is at least ~ 4 kyr here.

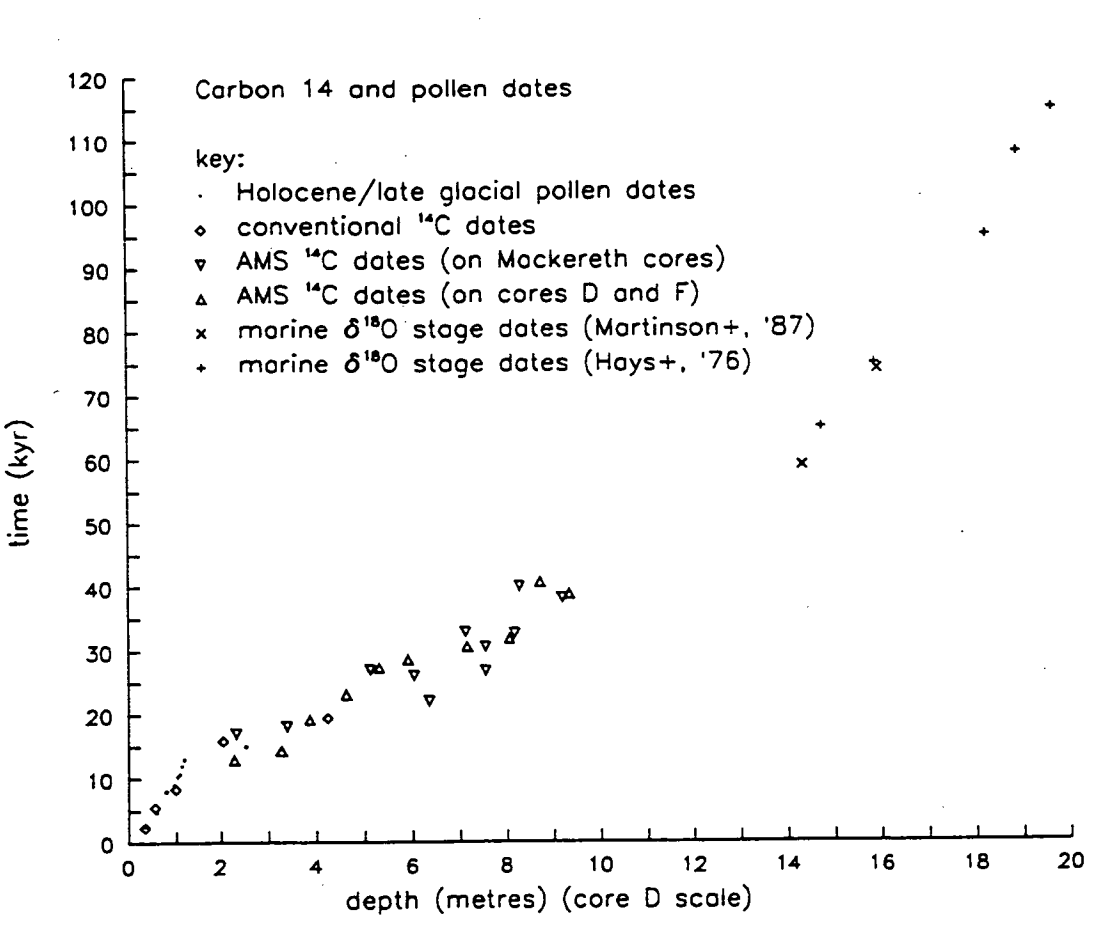

Fig. 6.1 Radiocarbon dates on previous Bouchet cores, detailed in Creer [1992].

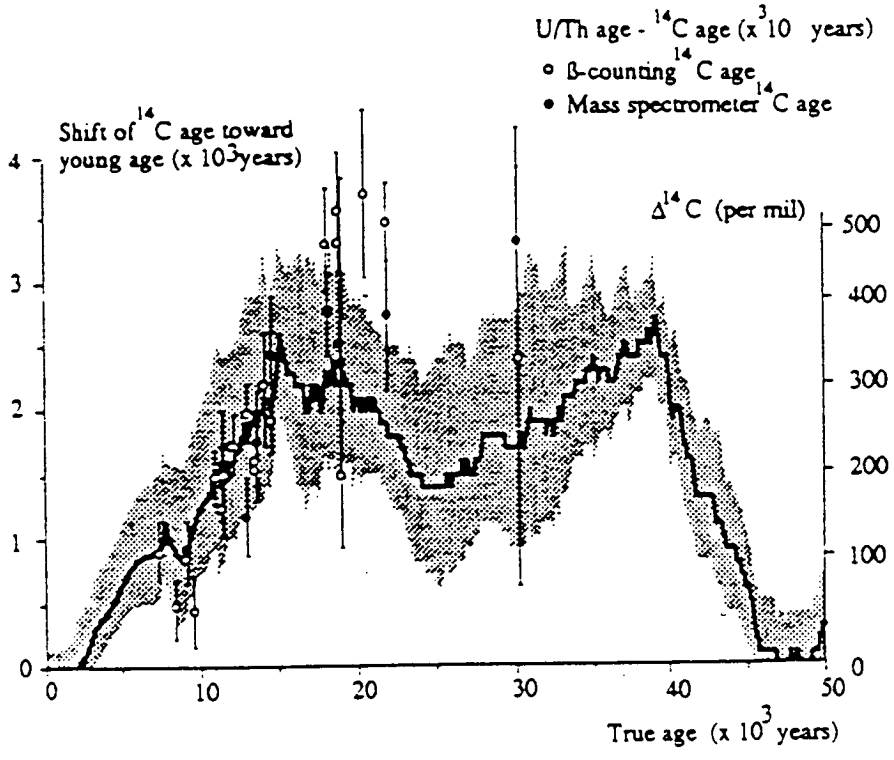

Fig. 6.2 Calibration of the radiocarbon time scale (a copy of figure 4 of Mazaud et al. [1991]). The symbols mark the ^{14}C - U/Th determinations of Bard et al. [1990]. The curve and shaded area marks the theoretical age correction based on changing ^{14}C production due to the geomagnetic field strength, itself based on the palaeointensity curve of Tric et al. [1992].

The argon-argon method. The argon used in Ar-Ar dating is associated with potassium in sanidine (potassium feldspar) crystals. In the Lac du Bouchet sequence, these are only found in sufficient quantity in the thick volcanic ash layer at 42.5m depth. Therefore, only one level of this sequence can be dated using this method. However, this level is located at a near-ideal location near to the base of the sequence, within a correlateable warm climatic episode, and in an ash layer which is almost certainly present in other maar sequences in the Velay region (at the dry maar at Praclaux for example).

Ar-Ar datings are currently being carried out by Ariel Boven in Brussels, but the result of the dating has not yet become available.

6.3 Dating by matching to the $\delta^{18}O$ curves

The global sequence of cold (glacial and stadial) and warm (interglacial and interstadial) periods is now well established for at least the last 300 kyr. A stratigraphy of numbered stages has been created from $\delta^{18}O$ records of marine sediment sequences (see, for example, Hays et al. [1976]), and this is widely used for marine sediments. Woillard and Mook [1982] correlated the French pollen records of la Grande Pile to this marine $\delta^{18}O$ stratigraphy with the aid of ^{14}C dates.

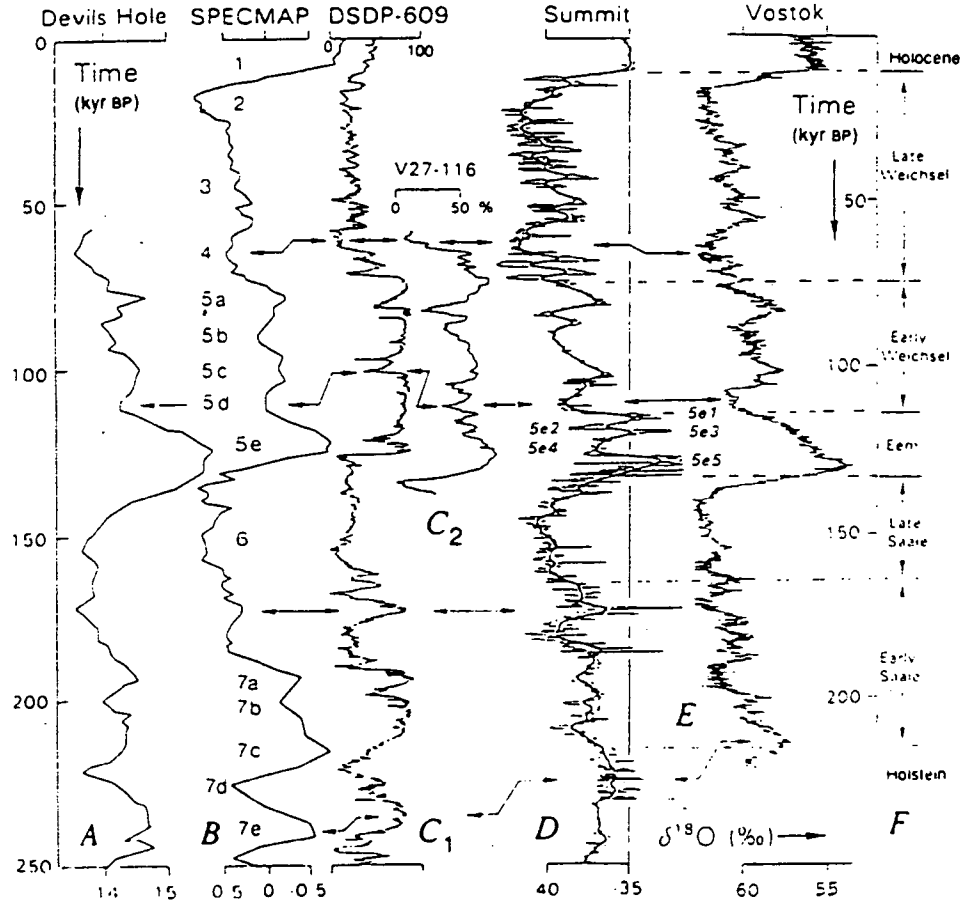

Fig. 6.3 Climate records spanning the few 100 kyr (a copy of figure 2 of Dansgaard et al. [1993]).

In this thesis, the warm and cold intervals at Lac du Bouchet are identified by their interpreted $\delta^{18}O$ stage numbers, together with the names "Holocene", for the present interglacial ($\delta^{18}O$ stage 1), and "Eemian" for the last interglacial ($\delta^{18}O$ stage 5e). The local names for the interglacials and interstadials at Lac du Bouchet, and their $\delta^{18}O$ stage numbers (interpreted by palynology) are given in figure 7.2.

The nub of the dating method is this: the sequence of warm and cold periods seen in ice and marine records will also be seen in the Bouchet sequence. I correlated the Lac du Bouchet tree pollen % and magnetic susceptibility records to three $\delta^{18}O$ records from

widely different areas of the Earth: the Specmap marine $\delta^{18}O$ stratigraphy, the Devils Hole (Nevada) calcite vein, and the Summit (GRIP) ice core from Greenland (figure 6.4). Each is dated independently using different methods and assumptions. Figure 6.3 shows these records, plus the Vostok ice core from Antarctica and two marine cores from the north Atlantic.

$\delta^{18}O$ is used as a palaeoclimatic indicator in all of the records. $^{18}O/^{16}O$ is the ratio of the rarer, heavier, ^{18}O isotope to the more common ^{16}O isotope. "$\delta^{18}O$" is the ratio of the measured $^{18}O/^{16}O$ ratio and the ratio of a standard (usually standard mean ocean water (SMOW) for water or ice, and belemnite shell (PDB) for carbonates), expressed as per mil. The changes in ^{18}O:^{16}O are small; from about 1:495 to 1:515 in the natural environment (Dansgaard [1954]). The $\delta^{18}O$ changes under different global conditions and in different environments, because of differentiation due to the slightly different evaporation and precipitation properties of the two isotopes. For example, when sea water evaporates, the heavier ^{18}O tends to remain in the sea water, and the atmospheric water will be relatively depleted in ^{18}O. In glacial times, when a large % of the world's (^{18}O-depleted) water is in the ice-caps, the ocean will have higher ^{18}O than in warmer times. The ancient $^{18}O/^{16}O$ ratio is fossilised in either the oxygen of H_2O in ice, or of calcite ($CaCO_3$) in marine micro-fossils or underground speleothems.

The three palaeoclimate records that were used to create a depth→time model for the Lac du Bouchet sequence are described below, with a description of the dating method used in each case:

The Specmap marine sediment $\delta\ ^{18}O$ *stratigraphy (figure 6.4a).* The significance of the $^{18}O/^{16}O$ ratio in marine sediments was first realised by Emiliani in 1955, who showed that the ancient $^{18}O/^{16}O$ ratio was incorporated into fossil foraminifera, which make their calcite skeleton by using the surrounding oceanic water. The $\delta^{18}O$ represents principally the global ice volume, and is therefore closely related to global temperature. Benthic (bottom living) forams are usually used in preference to planktic (surface living) forams, as the $^{18}O/^{16}O$ ratio is less prone to more local or regional sea surface effects at depth. The planktic forams are used for sea-surface temperature records. The Specmap (Spectral mapping) project was set up to collect a large number of marine sediment cores, and to use them in conjunction with Milankovitch theory to test the theory and to form a dated, stacked global $\delta^{18}O$ record. The most recent version of the orbitally tuned marine $\delta^{18}O$ stack is given by Martinson et al. [1988], for the last 300 kyr (figure 6.4a). The major assumption of this method of dating is that the climate responds roughly linearly to insolation changes, and, although it is generally agreed that the summer insolation changes at mid-high northern

latitudes form a rough pacemaker of glacial advances and retreats, internal climate dynamics also has a large part to play.

The Devils Hole calcite vein (figure 6.4e). The Devils Hole calcite vein (Nevada, USA) contains a 500 kyr $\delta^{18}O$ record (Winograd et al. [1992]). The calcite was precipitated from ground-water, which had fallen as rain on the ground-water recharge area some thousands of years before. This $\delta^{18}O$ is thought to reflect principally the local winter-spring land surface temperature at the time of raining. The record has the advantage of direct dating (mass spectrometric uranium series dating), itself very accurate (instrumental errors with 2σ of 1 kyr at 130 ka and 3 kyr at 250 ka), but this dates the time of calcite precipitation. The uncertainty of the groundwater residence time in the major disadvantage with the dating of this record: dates of events in the (uncorrected) Devils Hole record are therefore minimum ages.

The Summit (GRIP) ice core (figure 6.4d). The GRIP ice core from Greenland (Dansgaard et al. [1993]) gives a 250 kyr $\delta^{18}O$ record, with the $\delta^{18}O$ thought to represent the temperature at the time of formation of the polar glacier ice. It is indirectly dated below 14.5 kyr, by ice flow modelling, with a $\delta^{18}O$-dependant accumulation rate. This gives a sequence with deeper layers which are thinner than the upper ones, and the lower parts of the sequence (older then 115 ka) are less certain, due to assumptions about the layers close to the bedrock. An earlier 160 kyr ice core from Vostok, Antarctica is illustrated in figure 6.3 (Jouzel et al. [1987]).

Problems arise when trying to match our detailed Bouchet records with the smooth Specmap and Devils Hole records - it is difficult to pick a particular age for the boundary between a warm and cold climate in the smooth records. The smoothness of these two records has different origins - the Devils Hole record comes from a 36cm long calcite core, with detail limited by the thickness of the samples (1.26mm ≈ 1.8 kyr), whereas the marine $\delta^{18}O$ record is a stack of several world-wide cores, the smoothness due to averaging around the globe, bioturbation, and the time taken for large ice volume changes. The Summit (GRIP) record is more detailed because it comes from a 3km deep ice core, and is only a spot reading of temperature.

The Specmap $\delta^{18}O$ record, or similar, has been the generally accepted standard stratigraphy for several years. However, the exact age and duration of the Eemian interglacial are now being questioned: the Vostok, Summit, Devils Hole and Barbados coral records (Bard et al. [1990]) all give older ages for the start of the Eemian than the Specmap $\delta^{18}O$ does. Therefore, I have constructed two depth→time models, based on the possibility of either a long or short Eemian. The overall difference between the two models is small.

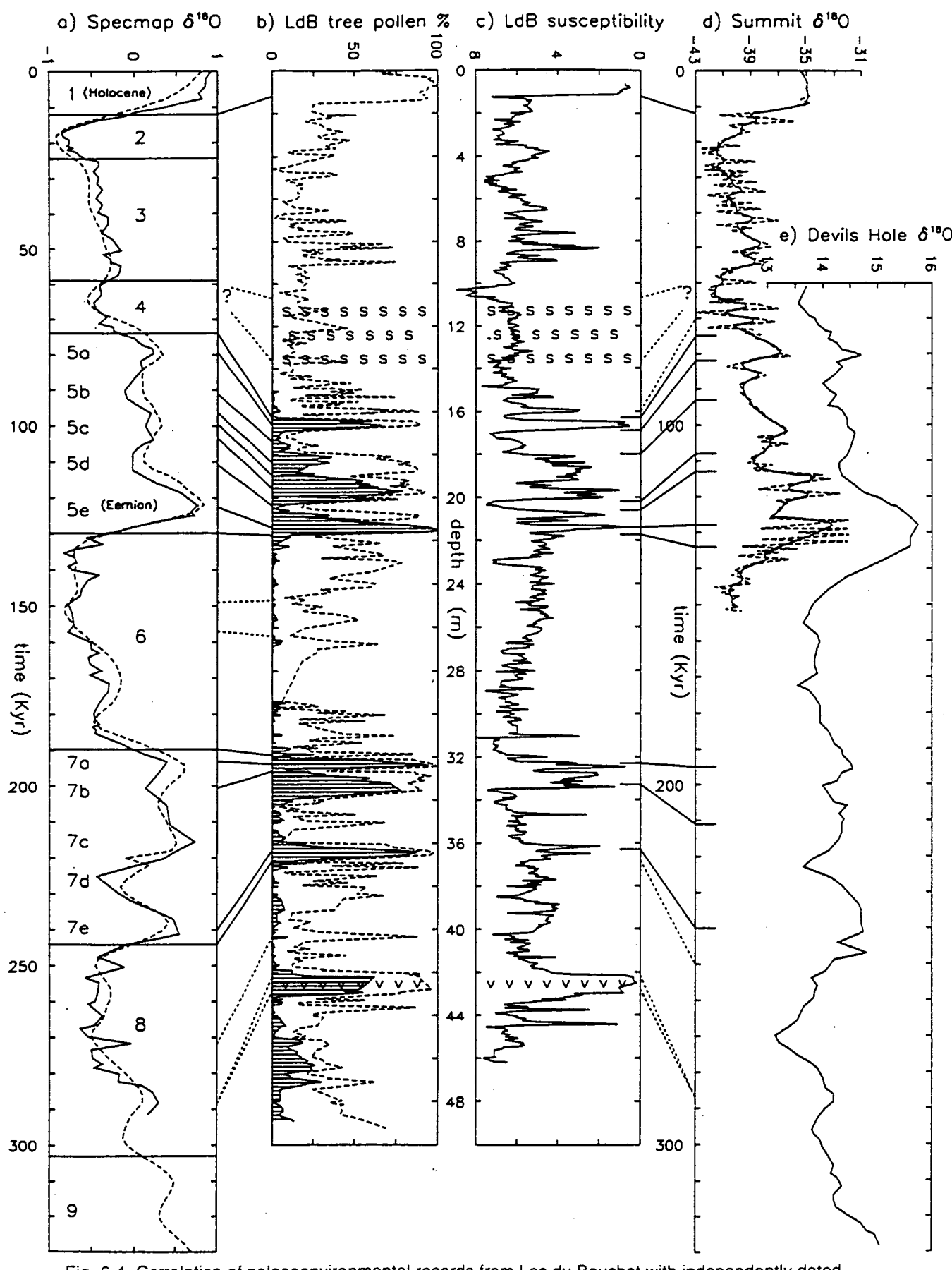

Fig. 6.4 Correlation of palaeoenvironmental records from Lac du Bouchet with independently dated $\delta^{18}O$ records from around the globe. a) Specmap marine $\delta^{18}O$ stacked records of Martinson et al. [1987] (solid line), and Imbrie et al. [1984] (dashed line); b) Lac du Bouchet tree pollen % (dashed line) and tree pollen % (without pine) (shaded curve) (below 15m only) (de Beaulieu and Reille); c) Lac du Bouchet susceptibility ($\times 10^{-6}$ m^3/kg), NB inverted scale; d) the ice $\delta^{18}O$ record (GRIP) from Summit, Greenland (Dansgaard et al. [1993]); e) the calcite $\delta^{18}O$ record from Devils Hole, Nevada (Winograd et al. [1993]). s=slumps, v=volcanic ash. I have digitised the 3 $\delta^{18}O$ records and the pollen record from paper. See text.

The assumptions implicit in dating by matching to other records (figure 6.4) are that the major warm and cold phases (for example stages 5a, 5c and 5e) are *global* features, and they are *contemporaneous*. It is evident from the geographic spread of records showing the same sequence of warm and cold cycles that these features are global. However, it is less certain that the features initiate at the same time, for several reasons: each type of record represents a slightly different aspect of climate; there may be delays between the time of $\delta^{18}O$ fixing and deposition; and there is uncertainty over the mechanisms of these long-term climatic changes (for example whether ice volume lags or leads global temperature).

Past warm periods at Lac du Bouchet are represented by low susceptibilities and tree pollen % counts, with deciduous trees only occurring in the warmest times. For the 20m core set, the Bouchet pollen records had been correlated to previously studied pollen records from La Grande Pile peat bog and Les Echets mire (collated and summarised in Pons et al. [1992]), which had already been correlated with the marine $\delta^{18}O$ stratigraphy (Woillard and Mook [1982]). The three peaks between 16 and 22m (on the core H depth scale) were identified in this way as stages 5a, 5c and 5e. The Holocene / late glacial boundary appears at 1.2m. The organic sediments between 32 and 37m depth have been interpreted as $\delta^{18}O$ stage 7 (de Beaulieu and Reille, Marseille Euromaars meeting [1993]). Figure 6.4 was constructed from these correlations. The more uncertain correlations are indicated by dashed tie-lines in figure 6.4.

The Lac du Bouchet records show much more variation during the warm periods than during the cold periods. $\delta^{18}O$ stages 2, 3 and 4 are difficult to differentiate in our record, although between 6 and 10m, there is evidence of slightly warmer conditions. To 10m depth (and deeper), the Bouchet records have more in common with the Summit record than with the Specmap record. Matching the warm events within stages 2 - 4 at Lac du Bouchet to the Dansgaard-Oeschger events in the Summit record is not attempted here (section 7.6), as wiggle-matching on this scale is ill-advised (if you stare at any two records for long enough, correlations will be found, whether or not they are really justified). Sedimentology (Truze [1990]) and magnetic anisotropy studies (Blunk [1990]) of cores C, D and F show a slump with its base at 13.7m, and ending at about 11m (D depth scale) (table 6.1): this might represent very little time, and this is indicated in figure 6.4. The two small susceptibility peaks at 15.2 and 16m may correlate with the two peaks just younger than the stage 4 / 5 boundary in the Summit record. Stage 6 (22 to 31m) is very difficult to sub-divide, given the sparser pollen points, and the long term susceptibility trend being in the opposite sense to the world records in this interval. For stage 7, I have followed the suggestions of the pollen analysts. This identification of stage 7, though not yet 100% certain, leads to similar sedimentation rates for similar sediments - about 10 kyr/m during the warm stages 5 and 7, and about 16 kyr/m during stages 2 - 4 and 6. I correlated the organic sediment enclosing

the volcanic ash layer (42.5m) with the peak at ~288 kyr in both Specmap and Devils Hole records. The high tree pollen values between 45 and 47m reflect an unusual vegetation assemblage not seen elsewhere in the sequence, and the base at 50m may well reach down into stage 9.

The sediment sequence from the nearby dry maar at Praclaux is contemporaneous with the lower part of the Lac du Bouchet sequence, and extends older, perhaps to $\delta^{18}O$ stage 11 (~400 ka) (figure 7.2).

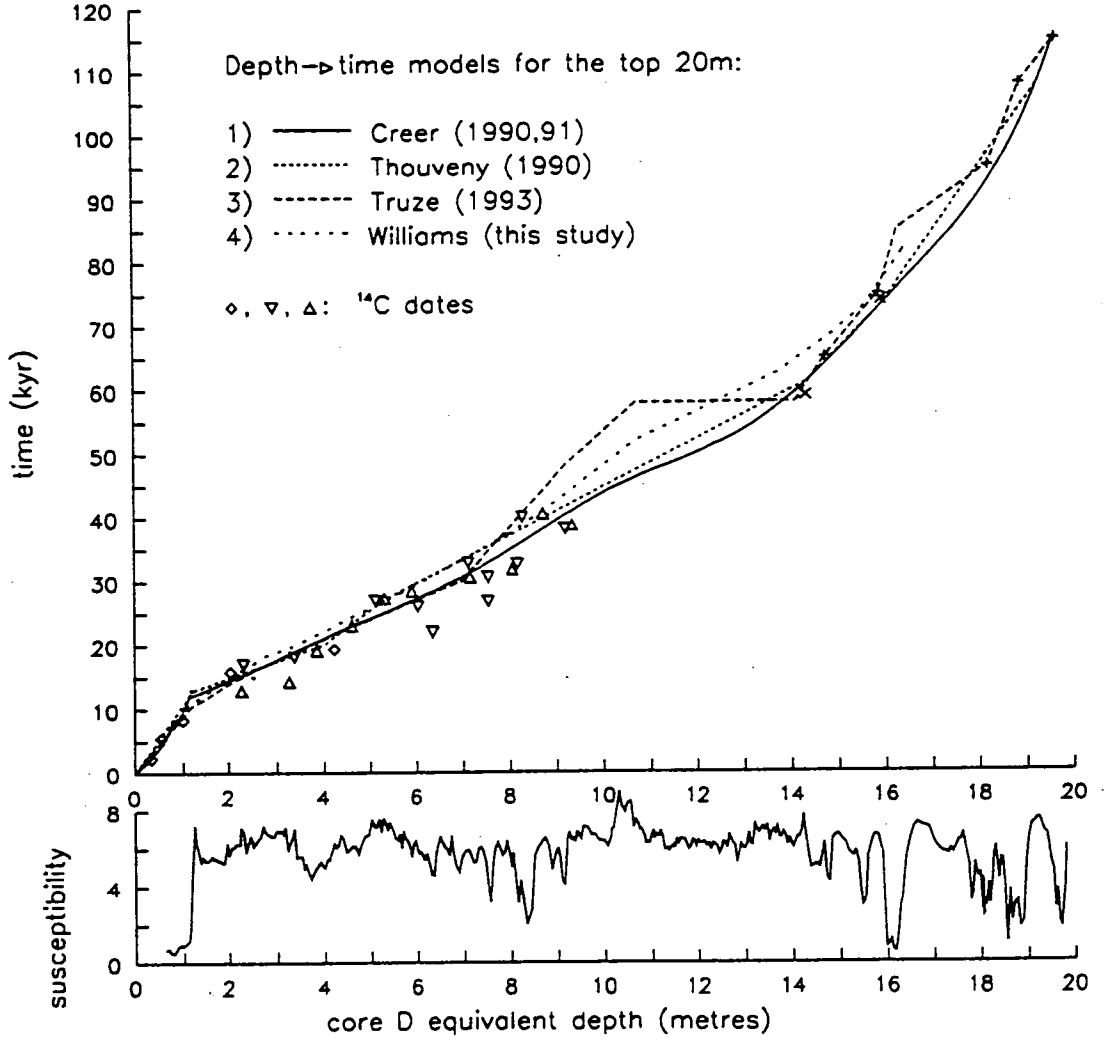

Fig. 6.5 The previous depth→time models for the 20m core-set.

6.4 Previous depth→time models for the top 20m

Three depth→time models have been created for the top 20m of the Lac du Bouchet sediments, by Creer [1990, 1991], Thouveny [1990], and Truze and Kelts [1993]. Their models are shown in figure 6.5, and it is seen they differ slightly. The differences are due to using different subsets of the ^{14}C dates, different methods of fitting a line to them, different approaches to the sedimentology, and the use of slightly different dates or depths for the $\delta^{18}O$ stage 5 boundaries. None of the models corrects from ^{14}C years to calendar years. The common depth scale for the 20m core set was the core D depths. The differences are not too significant except between 8 and 15m (35 - 70 kyr).

All of the ^{14}C and pollen dates are detailed in Creer [1991]. Creer rejected 6 out of 30 ^{14}C dates - the 6 gave comparatively younger ages, and mostly they stand out as being erratic when plotted. The $\delta^{18}O$ stages of Hays et al. [1976] were used. Cubic spline fits to the (remaining) data were tested, and the spline with 6 knots was chosen. Creer noted that his curve showed a flattening in the region of the slump, and attributed the mostly concave shape of the curve to compaction with depth.

The depth→time model of Thouveny is described in Thouveny et al. [1990]. The mass spectrometer ^{14}C dates on cores D and F were not yet available, and 5 out of 15 ^{14}C dates were rejected on the grounds of sample preparation error, outlying results, low organic carbon content in the sample, or very large error bars. Again, the $\delta^{18}O$ dates of Hays et al. [1976] were used. Three straight regression lines were computed between 1.2 and 8.5m depth, weighted according to the quoted σ (instrumental standard deviation). Linear interpolation between the older age control points completed the curve, but it was recognised that the assumption of constant sedimentation rates between the points is not perfectly accurate. No account is taken of the slumped layer.

The model of Truze takes into account 13 mass spectrometer ^{14}C dates, the $\delta^{18}O$ stage dates of Shackleton and Opdyke [1973], and sedimentological information. Truze and Kelts [1993] concerns the sedimentology of the 20m cores, and its subdivision into facies. They identify slumps between 10.7 and 13.7m (table 6.1) which "were emplaced as a unit very quickly, perhaps within a few hours". A problem now arises, because a reasonable model cannot be made which fits both the older ^{14}C dates, the slumps, and the boundary between stages 4 and 5. Truze and Kelts give preference to fitting the slump, while giving their dating points at 7, 9 and 10.7m question marks. They note that ^{14}C dates get less reliable the older they are.

Table 6.1 The slumped layer.

identification method	extent (core D depths)	description
sedimentology	10.7-13.7m	"numerous disturbed layers of dark brown mud and sand layers, marked by micro-faults and folds" (Truze and Kelts [1993])
magnetic anisotropy	11.2-13.7m 9.2-13.7m	α (dip parameter) > 20°, in patches μ (shape parameter) > 20°
(lack of inter-core susceptibility correlation)		different susceptibility signatures between individual cores.

N.B. there is also evidence of a slump between 2.8 and 3.3m from each of the three methods above.

The three models detailed above give an indication of the error bars that should be associated with the depth→time model.

6.5 Creating a depth→time model for the full 50m

In creating a depth→time model, I have taken several constraints into account; they are listed below, roughly in order of importance:

- ♣ direct datings: ^{14}C dates, corrected to calendar years.
- ♣ the position in the core of warm periods equivalent to $\delta^{18}O$ stages 1, 5 and 7.
- ♣ slumps take no geological time to form.
- ♣ sediments of similar lithology will have a similar sedimentation rate.

For the top 8m, a curve has been taken which is in-between the similar models of Creer and Thouveny, and the ^{14}C dates have been corrected to calendar years by using the U-Th calibration of Bard et al. [1990], shown in figure 6.2 and figure 8.5. The core D depth scale was then converted to the core H scale.

For the $\delta^{18}O$ stage dates, there are two broad alternatives for the last 300 kyr: records with a short Eemian (5e) (the Milankovitch-tuned marine $\delta^{18}O$ records of Martinson et al. [1987], Prell et al. [1986], Imbrie et al. [1984], Hays et al. [1976], or Shackleton and Opdyke [1973]), or records with a long Eemian (the Devils Hole $\delta^{18}O$ record, the Summit and Vostok ice $\delta^{18}O$ records). Therefore I made two depth→time models, one based on the Specmap record of Martinson et al. [1987], and the other based on the Devils Hole record (Winograd [1993]) for stage 5 and older. The Devils Hole record is too smoothed to pick out exactly where the stage boundaries occur, but the stages seem roughly co-incident with the more detailed Summit record down to stage 5. The two sets of ties are shown in figure 6.4.

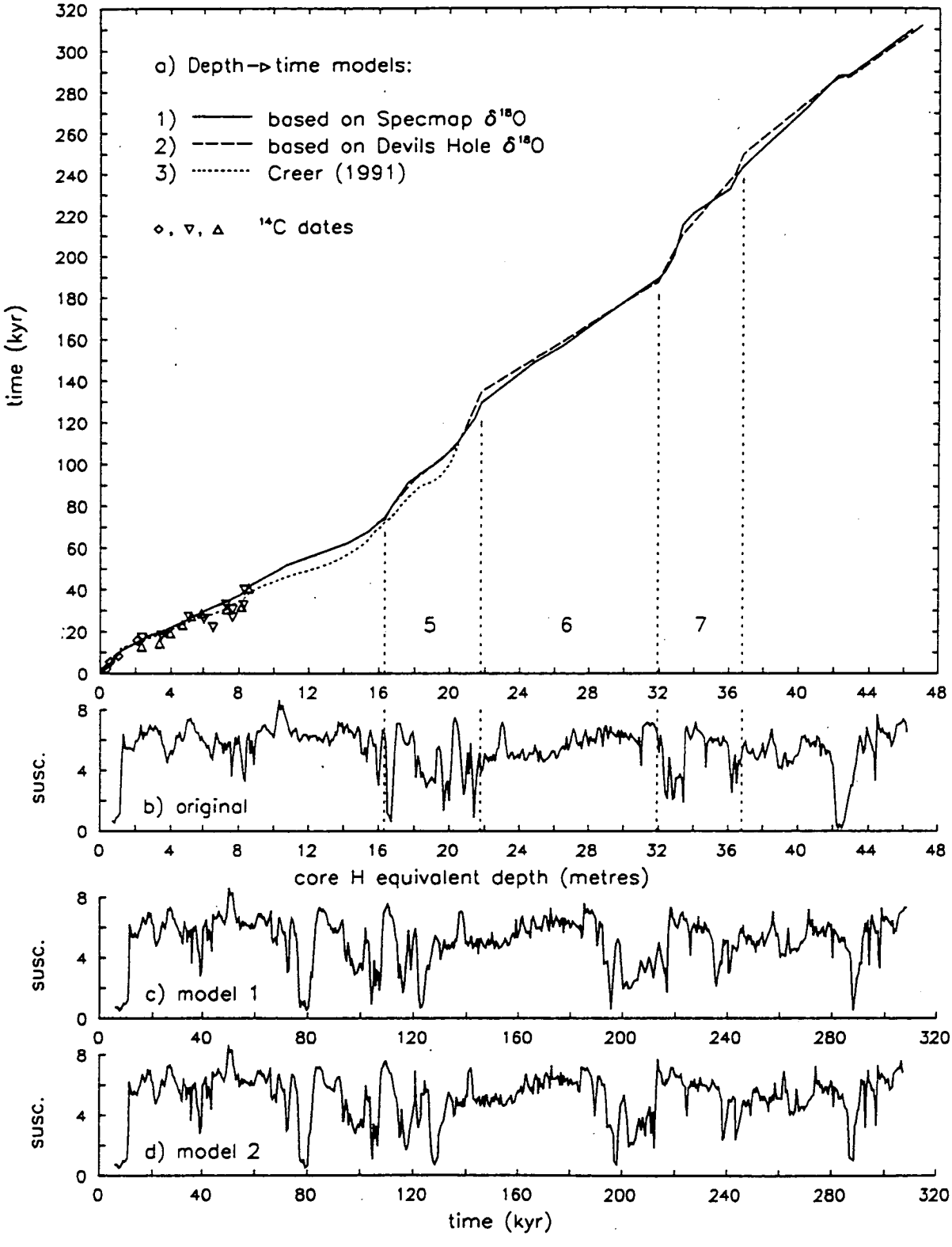

Fig. 6.6 The depth→time models for the 50m core set. ^{14}C dates also shown.

I have had to compromise for the interval of slumps between 10.8 and 14.0m (core H depth scale). This interval most probably formed over a much shorter time than that in the depth→models, but in this way the model still has a reasonable fit to the ^{14}C dates, and a reasonable sedimentation rate between 8.5 and 10.8m. On the other hand, there is a good correlation between the susceptibility records of Lac du Bouchet and Lac St.Front over the last glacial (fig 7.2), including the interval in question, indicating that the slumps at Lac du Bouchet may have been deposited over a longer time than Truze and Kelts [1993] suggest. The model is incorrect, but in this interval I am unable to satisfy all four of the constraints.

The model thus obtained is consistent with similar sediments having similar sedimentation rates.

I do not think that compaction with depth has a great part to play outside of the top few metres, in contrast to Creer [1991]: there is no overall increase in weight with depth, as would be the case if compaction were a serious effect (figure 5.8).

I have made and used two depth→time models: model 1, based on Specmap dating, and model 2, based on Devils Hole dating. These are only two out of a whole range of possibilities, and in particular it is noted that the identification of $\delta^{18}O$ stage 7 and older is not yet confirmed. In fact the working time-scale used in this study before the pollen of core H was fully analysed rested on the organic matter around the tephra layer (42.5m) representing stage 7e. Discrete models out of the range are needed so that comparisons and time-series analysis can be done.

Chapter 7

Palaeoenvironmental aspects

7.1 Introduction

The sediment sequence at Lac du Bouchet contains a continuous record of the environment over the last 300 kyr. Three full glacial-interglacial cycles are recorded, and these are resolved in great detail. The Lac du Bouchet sediment is excellent for studies of the palaeoenvironment, because it was deposited under mostly low energy depositional conditions, and is almost free of turbidites and hiatuses.

The main aims of the chapter are to: a) assess the usefulness of the magnetic measurements (susceptibility for example), as palaeoenvironmental indicators at Lac du Bouchet; b) to use this magnetic environmental record to complement the other palaeoenvironmental studies of the Bouchet records; and c) to compare these records to marine sediment and ice core records of palaeoclimate.

Background Quaternary climate

The cycling of glacial and interglacial climates within the Quaternary ice age (2.4 - 0 ma) was first postulated from distributed glaciological evidence, and subsequently confirmed in continuous marine sediment $\delta^{18}O$ sequences (Emiliani [1955]). The main warm climatic events (interglacials) have occurred about every 100 kyr since 800 ka, and about every 40 kyr before that, and are separated by the cold glacials. The global ice volume is a measure of global climate, and is recorded by $\delta^{18}O$ in marine sediments. It changes in response to insolation variations according to the astronomical theory of climate change (Milankovitch [1941]), and a global $\delta^{18}O$ stratigraphy has been set up and dated by tuning the periodicities in $\delta^{18}O$ records to the calculated insolation periodicities ("spectral mapping", or "Specmap", see Berger [1988]).

The main source of palaeoclimate records are marine sediment sequences, which hold records of sea surface temperature and global ice volume. Ice cores from Antarctica and Greenland give shorter but more detailed records of $\delta^{18}O$, CO_2, CH_4, atmospheric dust and so on (for example, Jouzel et al. [1987]). Coral terraces mark past sea level changes (Bard et al. [1990b]). On the continents, sequences of loess, lake and bog sediment record palaeoenvironmental change, which is interpreted in terms of palaeoclimate. The extension of the long maar lake sediment records from Lac du Bouchet to 300 ka will add much to the knowledge of Quaternary palaeoclimates.

A plan of the chapter

Palaeoenvironmental study of the Lac du Bouchet sediments can be looked at in three stages: a) characterisation of the lithology and constituents of the sediment; b) the interpretation of this lithology in terms of the local palaeoenvironment; and c) the interpretation of this palaeoenvironment in terms of wider palaeoclimatic changes.

Firstly, the sediment is understood in terms of its constituent parts, such as detrital material, organic matter, grain size, pollen content, geochemistry and magnetic mineralogy. The relationships between these parts, and how they vary down the core, can be seen in figure 7.1.

Secondly, the evidence of the constituent parts is interpreted in terms of changes in the local environment, such as the rate of erosion of detrital material (from susceptibility records, for instance), and the vegetation surrounding the lake (from pollen records). The range of variation and speed of change of the environment can be gauged, and comparisons can be made between different glacials and interglacials at Lac du Bouchet. The palaeoenvironment at Lac du Bouchet can be compared with that at nearby lakes, such as at Lac de St.Front (25km to the SE).

Thirdly, these local environmental changes can be used to infer climatic change on a local or regional scale. Local temperature and precipitation changes can be calculated from the vegetation assemblage (Guiot [1990]). The large changes in the Lac du Bouchet palaeoenvironment must be related to the pattern of global climatic change, as non-climatological influences on Lac du Bouchet, such as lake in-fill and volcanism, are not thought to be important.

Many questions present themselves: How closely does the local climate follow the world $\delta^{18}O$ records - do local/regional effects dominate or does Lac du Bouchet follow the global pattern? Does Lac du Bouchet follow an oceanic or continental climate, and does this change with time? Are the size and importance of the various warm episodes similar to each other? Are the short warm Dansgaard-Oeschger events, found in Greenland ice and North Atlantic sediments, also found in southern France? Is Lac du Bouchet responding indirectly, directly, or not at all to the insolation changes governed by the Earth's orbital variation? Are the glacial-interglacial cycles similar, and what are the implications for the present interglacial? Some of these questions have already been answered with the short-core records from Lac du Bouchet, and the magnetic records from the 50m cores can illuminate further answers.

For a proper palaeoenvironmental analysis and reconstruction, all aspects and evidence from the Bouchet core must be collated and combined. I will concentrate on the magnetic measurements, but will also draw information from other sources (palynology,

sedimentology, geochemistry etc.). The rock-magnetic records are less directly related to palaeoclimate than the pollen records, nevertheless they give detailed and valuable information. In certain respects, the magnetic records are superior to the pollen or sedimentological records - measurements have been taken at 2.5cm intervals, on all cores, therefore the resolution is far better, and on a practical level, making magnetic measurements is far quicker.

Glacials and interglacials are given local and regional names in different parts of the world. The local names for the warm and cold episodes at Lac du Bouchet are given in figure 7.2, together with their correlation to the Specmap $\delta^{18}O$ record, as interpreted from the pollen data by de Beaulieu and Reille [unpubl.]. Throughout the chapter I have referred to the various warm and cold episodes mostly by their interpreted Specmap $\delta^{18}O$ stage numbers, because the wealth of local names can be confusing. For example, the Holsteinian interglacial has been associated with $\delta^{18}O$ stages 7, 9 and 11 in different studies.

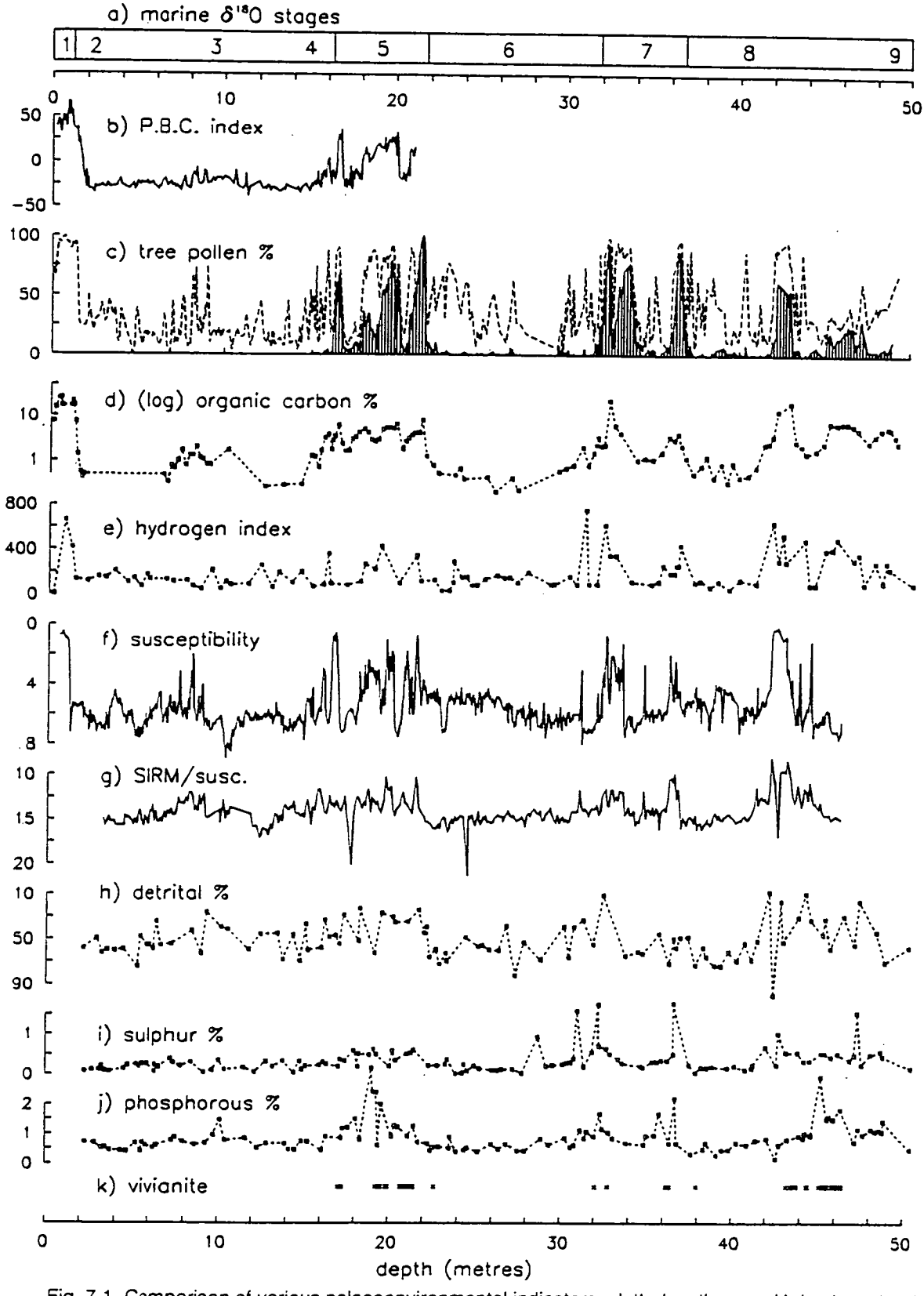

Fig. 7.1 Comparison of various palaeoenvironmental indicators, plotted on the core H depth scale. (a) $\delta^{18}O$ stages (figure 6.4) for time reference. (b) P.B.C. (palaeo-bio-climatic) index, calculated for the 20m cores (Guiot), and put onto the core H depth scale. (c) dashed curve = tree pollen %, shaded curve = tree pollen % (without pine) (below 15m only) (de Beaulieu and Reille). (d) Organic carbon %, on a log scale (Icole). (e) Hydrogen index (IH). (f) magnetic susceptibility ($\times 10^{-6}$ m^3/kg). Principally reflects the concentration of magnetite. Samples averaged at 5cm intervals. (g) SIRM/susceptibility. Indicates grain-size of the magnetite. Samples averaged at 10cm intervals. (h) % of detrital minerals. (i) % sulphur. (j) % phosphorus. (k) occurrences of vivianite noted while sampling. (e),(h),(i),(j) digitised from Bertrand et al. [1993]. All records are single core only, apart from (b), (f), and (g). NB (f), (g), and (h) have inverted scales.

7.2 Magnetic and other records from Lac du Bouchet

The chief palaeoenvironmental indicators at Lac du Bouchet are pollen and organic carbon content. Mineral magnetic measurements, such as susceptibility, are complementary. Figure 7.1 shows these and other down-core records relating to aspects of the palaeoenvironment of Lac du Bouchet.

The wide differences in sampling density are shown in figure 7.1. The sampling for magnetic study has an average separation of about 1.2cm over all the cores, which is a far greater density than for any of the other studies. Core H, and some of core I, were sampled for pollen analysis at close spacing in the organic layers, but less closely in the glacial clays. The other studies had sampling at wide enough spacings for the individual samples to be plotted in figure 7.1. Thus, details that are picked up in the susceptibility record are missed in many of the others.

There may be slight mis-matches in the position of some features, because slightly different schemes may have been used in the different laboratories to construct the depth-scale from the individual core sections. I digitised the pollen records for core H (between 16 and 50m) from a plot with a non-linear scale, and then converted it to a linear scale; however, errors which accumulate through the changes of scales only become a problem when looking at fine detail, for example in figure 7.4.

Pollen analysis

The vegetation around the lake can be reconstructed, species by species, from the pollen grains found in the sediment. Each species grows better under certain climatic and environmental conditions; some species (e.g. grasses) prefer cold conditions, and some (e.g. deciduous trees) prefer warm conditions. Thus the tree pollen % (also called the arboreal / non-arboreal pollen %) is a good general climatic indicator, and is illustrated, together with the tree pollen % (without pine) in figure 7.1c. The tree pollen % (without pine) record forms a clearer indicator of climate: significant counts of non-pine trees are only found when the climate is warm. The full pollen analysis by de Beaulieu and Reille [to be publ.] contains more detail than is required here. The species by species counts are used to reconstruct the vegetation dynamics (for example the progression of juniper, oak, hazel to hornbeam, fir and lime during warm climates), and also to calculate quantitative estimates of precipitation and temperature, even at a seasonal level (Guiot [1990], Huntley [1988]). The PBC (palaeo-bio-climatic) index (figure 7.1b) is a general climatic indicator derived from knowledge of the climatic preferences of indicative species. The PBC index and seasonal precipitation and temperature records are published for the top 20m (Pons et al. [1992]). Similar records will become available for the full 50m (300 kyr).

The organic carbon record (Michel Icole [to be publ.]) reflects the amount of biological activity going on around the lake, with high values indicating warm climatic conditions.

Proxy-palaeoenvironmental records from Lac du Bouchet

Figure 7.1 shows 10 records of various palaeoenvironmental indicators of the Lac du Bouchet sequence (note that (f), (g) and (h) have inverted scales). The glacial layers are distinct from the organic-rich layers in all of the various records; all show peaks corresponding to warm palaeoclimate, equivalent to $\delta^{18}O$ stages 1, 5 and 7. The tree pollen % (without pine) record (shaded figure 7.1c) provides the clearest evidence as to which layers correspond to which $\delta^{18}O$ stage. Low susceptibility results from a warm palaeoclimate.

Susceptibility follows the total tree pollen % record closely; it matches both in general trend, and in the detail of the duration and size of the peaks. Some small differences can be seen between the records, for example in stage 5c (18 - 20m depth), and in the relative amplitude of the stage 5 peaks (5a is the most pronounced in susceptibility, and 5e the most pronounced in the tree pollen %). Susceptibility also mimics the PBC index curve well. These are remarkable results because pollen-derived records relate to the vegetation, which responds directly to climate, whereas susceptibility is simply a measure of the concentration of magnetite in the sample.

Susceptibility has the same general trend as the % of detrital minerals, but as the magnetite is contained in the detrital fraction, the match is not so good in the details as might be expected.

Fast changes in the palaeoenvironment are observed from all records with a close enough sampling to define them. Sharp short peaks indicate warm episodes of short duration, and these occur in glacial stages as well as warm stages. Within warm stages, there are often quick oscillations between warm and cold local climate. The warm stages are more condensed than the glacial stages, because the sedimentation rate goes down. There seems to be a certain stepwise character to the tree pollen % (without pine) record: either there are deciduous trees, or there aren't. The susceptibility record has a similar, but less obvious, step-wise shape. Between 45 and 50m there is an odd combination of species, not seen elsewhere in the core, and this has yet to be fully interpreted by the pollen analysts (de Beaulieu and Reille, Euromaars meeting, March 1993).

Susceptibility and the palaeoenvironment at Lac du Bouchet

It is clear from figure 7.1 that in the case of Lac du Bouchet, susceptibility is an excellent indicator of local palaeoenvironment and palaeoclimate. What is less clear is why this should be so.

The magnetite (its concentration measured by susceptibility) is contained in the detrital fraction, and is derived from erosion of the basaltic crater walls. The magnetite may reside for a short time in the soil before being deposited onto the sediment column in the lake. There may be some diagenesis, perhaps reducing the grain-size (evidence from scanning electron microscopy, and the SIRM/susceptibility grain-size indicator). There may also be some super-paramagnetic (i.e. very fine, $< 0.01\mu m$) magnetite, possibly bacterial in origin. The magnetite in the sediments of La Grande Pile is thought to be almost entirely of aeolian (wind-borne) origin, and has a susceptibility 500 times less than the average from Lac du Bouchet sediments. The two sites are reasonably close, so the aeolian contributions at both should be roughly the same, and therefore the aeolian contribution to the magnetic fraction at Lac du Bouchet is negligible.

A possible controlling mechanism for the magnetite concentration is the following: during warmer climates, erosion of the crater walls is inhibited by the greater binding from the extra vegetation, and the reduction of freeze-thaw weathering. This lowers the rate of magnetite input into the lake. At the same time, the increased organic matter input dilutes the magnetite, lowering the susceptibility. The overall sedimentation rate, a combination of the detrital rate and the organic rate, is lower during warm climates.

The sharp peaks (troughs with the non-inverted axis) in susceptibility are not so pronounced in the detrital % record (fig 7.1h), which is not expected. These peaks cannot be due to increased bacterial magnetite (super-paramagnetic) in the more organic layers, because susceptibility is more sensitive to these very fine grains and they would tend to reduce the susceptibility peaks, not make them more pronounced. Additionally, the modest changes in the SIRM/susceptibility ratio indicate that grain-size changes are not very significant. It could be that some magnetite is removed from the system entirely, either in the soils of a warm climate or by diagenesis after deposition. Two authigenic minerals found in the Bouchet sediments are vivianite ($Fe_3[PO_4]_2.8H_2O$) and siderite ($FeCO_3$) (Truze [1990]), and both contain iron. Vivianite only occurs in organic-rich sediments (figure 7.1k), the same intervals where the magnetite concentration is less, and indicates enhanced geochemical activity which could possibly affect the magnetite. Alternatively, the lack of sharp peaks in the detrital % record may be due to unrepresentative sampling - i.e. sampling of just the more organic layers.

The Lac du Bouchet catchment area is small, so localised events that are not directly controlled by climate, could have an appreciable effect on the sediment record; they would not be diluted so easily. Examples of such events might be a landslip altering the top-soil/sub-soil input into the lake, or turbidites within the lake itself. The coarse sediments with high susceptibilities at about 9m depth (50 kyr) might be a result of such an event. Overall, however, these effects do not have an important role in the susceptibility record,

because otherwise the match between susceptibility and tree pollen % would not be as good as it is, and the match between susceptibility in Lac St.Front and in Lac du Bouchet would not be as good either.

7.3 Comparison of the Bouchet record with other maar lake records

Other maar lakes of the Velay region, and maar lakes from Germany and Italy, have been cored as part of the Euromaars programme. Figure 7.2 shows susceptibility records from Lac du Bouchet, Lac St.Front and the dry maar at Praclaux (all from the Velay of France), and from Lago Grande di Monticchio (Italy).

Lac St.Front was cored in June 1992 as part of the Euromaars program. The cored sequence probably reaches down as far as stage 5b, about 80 kyr. The sedimentation rate is ten times that of Bouchet for the Holocene (stage 1), and twice as fast as at Bouchet for stages 2, 3 and 4, thereby giving a far more detailed record of the last glacial. These differences are partly explained by the larger catchment area of Lac St.Front providing a larger sediment source. Both the character and much of the detail of the susceptibility record corresponds closely to that of Lac du Bouchet.

The dry maar at Praclaux was cored in September 1993. Its sediments represent a time window that overlaps that of Bouchet and extends back further in time to perhaps 400 ka ($\delta^{18}O$ stage 11). A thick (some tens of cm) volcanic ash layer is present at ~24m depth, and it is likely that this is the same layer as seen at Bouchet at 42.5m depth. Evidence (scorie etc.) from the explosion that created the Bouchet maar ought to be seen in the Praclaux sequence. Praclaux, and other dry maars, offer the opportunity of extending the Velay palaeoenvironmental and palaeomagnetic records to cover much of the Brunhes chron. In comparison to the Bouchet record, the character of the susceptibility record from Praclaux is more continuous and less step-wise.

The Monticchio maar, in the Monte Vulture volcanic complex 120km east of Naples, Italy, was cored in September 1990, as part of the Euromaars program (Zolitschka and Negendank [1993], Robinson [1993], Turton [1993]). The cores (50m long) are thought to extend ~70 kyr, almost to the $\delta^{18}O$ stage 4/5 boundary. There are numerous volcanic ash layers in the sequence; these are seen as spikes in the record. The Holocene/glacial boundary is at ~8m depth, but the drop in susceptibility occurs at ~15m: clearly there is a non-climatic contribution to the control of susceptibility, possibly to do with lake in-filling or changing water levels (Robinson [1993]). As a general trend, however, the Monticchio record exhibits the Specmap $\delta^{18}O$ stage 2-3-4 sequence, with stage 3 warmer than stages 2 and 4.

The maars from the Eifel region of Germany typically have shorter sequences - Holzmaar and Meerfeldemaar only extend to 30 ka.

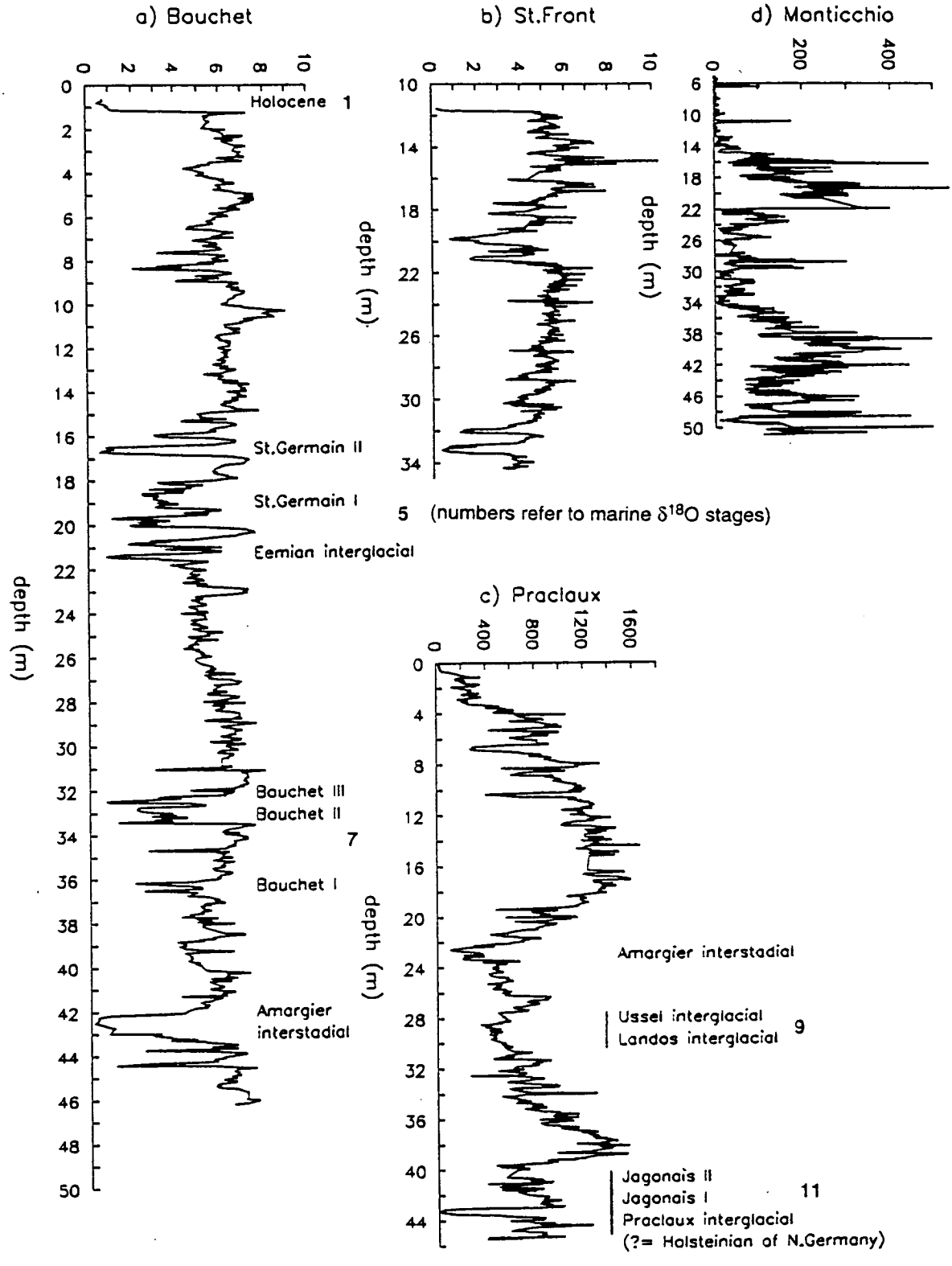

Fig. 7.2 Susceptibility records from four Maar lakes. All records are on their original depth scale, but have been stretched and positioned to give a rough idea of coincident features. The local interglacial and interstadial names, and their correspondence to the marine $\delta^{18}O$ stages is given, as interpreted by de Beaulieu and Reille. (a) the stacked record from Lac du Bouchet ($\times 10^{-6}$ m^3/kg). (b) Lac St.Front (25km east of Bouchet) core B ($\times 10^{-6}$ m^3/kg), data from Thouveny. (c) Lago Grande de Monticchio (east of Naples)(Turton [1992]). (d) Praclaux (10km SE of Bouchet), whole core measurements of core C (some spurious core section boundary effects may remain), data from Thouveny [pers. comm.].

In the European maar lakes, susceptibility is lower when climate is warmer. Close matches can be observed between nearby maars, for example Bouchet and St.Front, but the susceptibility record from each maar must be assessed on its own merits, as the exact response of the local environment to the local climate will vary in each case. In particular, the balance of detrital and organic sedimentation rates may change, and non-climatic effects may also have influence over the record.

7.4 Magnetic records as palaeoenvironmental indicators

Magnetic mineralogical records such as susceptibility have been used in many environments, for example in marine sediments (Robinson [1986], Kent [1982]), loess deposits (Maher and Thompson [1992], Heller et al. [1991]), and bogs (Ellsingen et al. [1992]). The mechanism by which susceptibility varies in response to palaeoclimate is different in each case.

In the North Atlantic marine sediments studied by Robinson [1986], susceptibility is higher during glacials, and varies inversely to the $CaCO_3$ content; this was attributed to decreased $CaCO_3$ productivity and increased detrital (aeolian / ice-rafted) inputs in the glacial. However, different mechanisms operate in different marine regions. Glacials give high susceptibilities in the North Atlantic cores of Robinson and core RC11-120 from the south Indian Ocean (Kent [1982]), whereas glacials give low susceptibilities in core RC11-209 from the equatorial pacific (Kent [1982]), and Arctic cores between Greenland and Svalbard (Nowaczyk and Baumann [in press]).

The loess deposits in China represent up to 2.4 myr of continental environmental history. The sequences are mainly loess, with palaeosols formed during warmer/wetter climatic conditions; susceptibility is higher in the palaeosols. The variation is due to the pedogenic formation of ultra-fine magnetite in the palaeosols (Maher and Thompson [1992]). Correlation of susceptibility to the marine $\delta^{18}O$ record is good.

At La Grande Pile bog in eastern France, susceptibility varies in a similar way to the maar lakes (Ellsingen et al. [1992]).

In each of the environments where susceptibility has been measured, a different mechanism has been responsible for its variation with time, and therefore the significance of the magnetic records from each locality must be assessed individually.

Generally, susceptibility measurements are quick to make, non-destructive and can be made on whole cores. It can be used not only for reconnaissance, but also as a sensitive palaeoenvironmental indicator. More detailed uses of magnetic measurements in "environmental magnetism" are given in Thompson and Oldfield [1986].

7.5 Comparison of the Bouchet record with world palaeoclimate records

Past climatic changes are recorded in marine sediment and in polar ice. The global ice volume is recorded in $\delta^{18}O$ in marine sediments (section 6.3), and very detailed temperature records of the last glacial and interglacial are recorded by $\delta^{18}O$ in ice from Greenland and Antarctica. To see how these changes are expressed in a mid-latitude continental area, I compare these records with those from Lac du Bouchet.

There have been other studies to compare continental and marine data-sets: Woillard and Mook [1982] correlated the pollen profiles from La Grande Pile to the Specmap $\delta^{18}O$ record, using ^{14}C dates. The correlation between the French pollen sequences of La Grande Pile, Les Echets, and Lac du Bouchet is reviewed in Pons et al. [1992]. Broecker et al. [1988] posed the question "can the Greenland climatic jumps [seen in the Camp Century and Dye 3 ice cores between 60 and 20 ka] be identified in records from ocean and land?", and concluded that although rapid fluctuations are seen in both north Atlantic cores and la Grande Pile pollen record, dating uncertainties meant it was "not yet possible to say whether or not the events are genetically related." Guiot et al. [1992] found that they were not significantly recorded at la Grande Pile. Most recently, Bond et al. [1993] were able to correlate the Dansgaard-Oeschger events from the Summit ice core to three north Atlantic sediment records.

When comparing different records from around the globe, it is important to know the accuracy of the dating of the records. I estimate that the error-bars on the Lac du Bouchet dating models (chapter 6) should be on order of about ±3 kyr, assuming $\delta^{18}O$ stage 7 has been correctly identified. There is greater uncertainty around the slumped interval between 10.7 and 14m depth. The uncertainties inherent in the dating of all of the records presented here should be taken into account when looking at the figures.

In this section, the tree pollen % has generally been plotted beside the susceptibility record, to give two measures of the Bouchet palaeoenvironment.

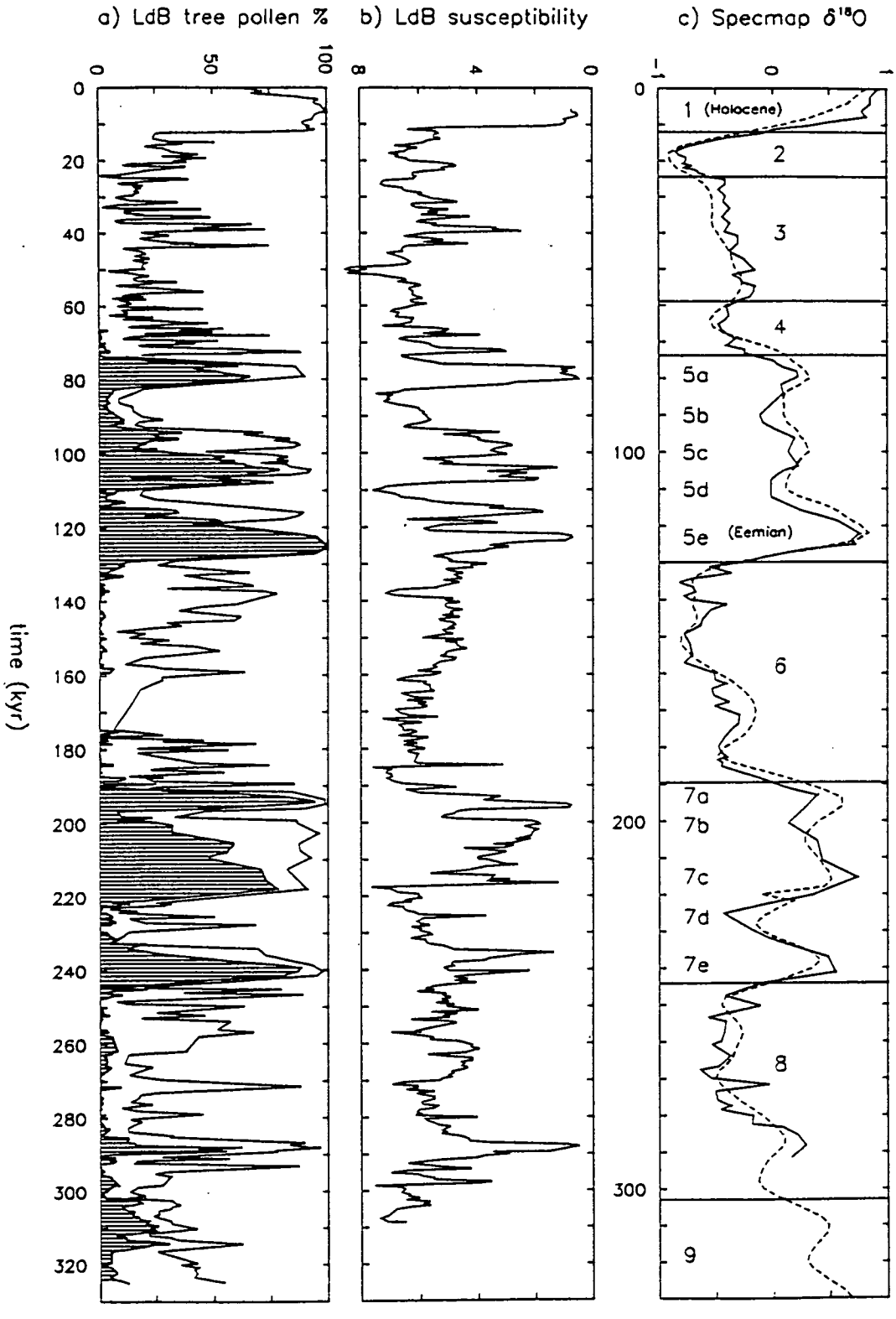

Fig. 7.3 Comparison of the marine $\delta^{18}O$ record of Martinson et al. [1987] with the Lac du Bouchet records of tree pollen %, tree pollen % (without pine) (shaded) (below 70 kyr ago only) (Reille and de Beaulieu), and susceptibility. The Bouchet records have been converted to a time-scale using model 1 (figure 6.6).

The Specmap $\delta^{18}O$ record and Lac du Bouchet.

The Specmap $\delta^{18}O$ record (for example, Martinson et al. [1987]) primarily represents the global ice volume, and therefore has a close relationship to global temperature (see section 6.3 for a summary of $\delta^{18}O$ and Specmap).

Figure 7.3 shows the Bouchet susceptibility and the Specmap $\delta^{18}O$ records to be broadly similar in form, with peaks in the $\delta^{18}O$ record corresponding to low susceptibility values (note the susceptibility scale inversion). The $\delta^{18}O$ record is smoother than the Bouchet records, because the global ice volume cannot change as quickly as the environment around a small lake, because of bioturbation in the marine sediment, and because the $\delta^{18}O$ record is a stack of records from around the world. Therefore only a broad comparison can be made, and little knowledge can be gained on the nature of the short period changes seen at Bouchet. The glacial stages 2, 3 and 4 are difficult to differentiate in the Lac du Bouchet records (as in other sediment records); there is a general lowering of susceptibility values around 40 ka, but the duration is shorter than stage 3, so it is difficult to say there is a match. Little detail can be seen within the glacial stage 6 either at Lac du Bouchet or in the $\delta^{18}O$ record, and the trend of this part of the susceptibility record is opposite to that expected. The relative magnitudes of the warm climatic conditions at Bouchet (for example stages 5a, 5c and 5e), as given by the tree pollen % (without pine) record, correspond well with the magnitudes of the ice volume record.

The palaeoclimate at Bouchet has generally followed the worldwide trend, but some differences are apparent, especially during the glacial periods.

The Summit ice core records and Lac du Bouchet

Results have recently become available from a 3km ice core (GRIP, Greenland Ice-core Project) taken at the Summit of the Greenland ice cap that are of great significance for Quaternary palaeoclimatic studies. The record has a fine resolution to 115 ka, and has been independently confirmed from a sister core from 27km away (GISP2, Greenland Ice-Sheet Project) (Grootes et al. [1993]). Older than 115 ka, the results are less certain because the ice is closer to bedrock, and thus more likely to be folded; the $\delta^{18}O$ records from the GRIP and the GISP2 cores do not correlate as well here. The GRIP results are presented in two papers: Dansgaard et al. [1993] discuss the climate instability over the whole record and the relationship to other $\delta^{18}O$ records. The GRIP members [1993] concentrate on climatic instability in the Eemian interglacial, and conclude that the present (Holocene) interglacial is unusually stable. Bond et al. [1993] correlated the last 80 kyr of the Summit ice record with three north Atlantic cores. They proposed that the fluctuations were organised into cycles composed of a steady cooling for 5 - 15 kyr, followed by a large discharge of icebergs into the north Atlantic, recorded as "Heinrich events" (Bond, Heinrich et al. [1992])

in the sediments, and then an abrupt shift to a warmer climate, thus giving a saw-tooth effect to the records. The question of what mechanism was driving these proposed cycles was left open.

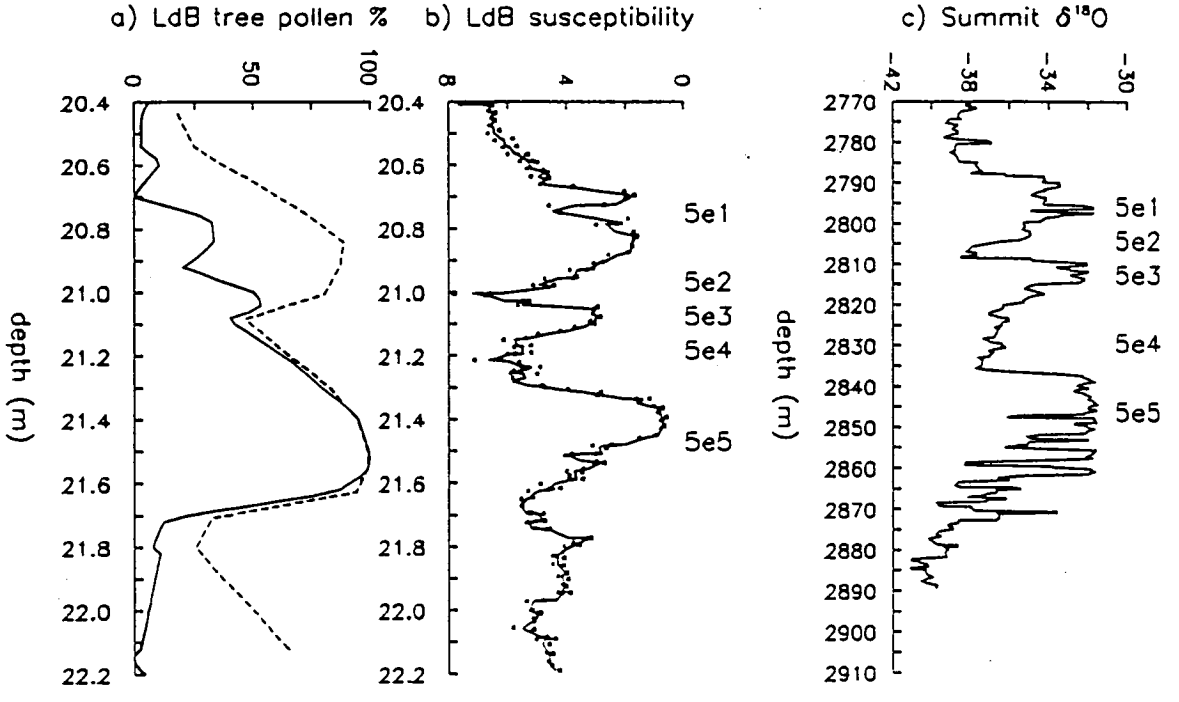

Fig. 7.4 Comparison of the Eemian interglacial ($\delta^{18}O$ stage 5) as expressed in the $\delta^{18}O$ (per mil.) record from the Summit ice core (GRIP members [1993]), the tree pollen % record (dashed) and tree pollen % (without pine) record (solid) (de Beaulieu and Reille), and the susceptibility ($\times 10^{-6}$ m^3/kg) records from Lac du Bouchet. The GRIP member's sub-divisions of stage 5 are given to the left of the ice record, and my interpretation of their possible equivalent at Lac du Bouchet is marked next to the susceptibility plot.

The Eemian interglacial ($\delta^{18}O$ stage 5e) at Summit (GRIP) and Lac du Bouchet.

The Eemian records from Lac du Bouchet and Summit (GRIP) are compared in figure 7.4. The similarity between the Bouchet susceptibility record and the Summit $\delta^{18}O$ record is clear: both have three warm peaks and the middle warm peak (5e3) has the shortest duration in both; the first cooling (5e4) is longer than the second (5e2) in both. The pollen record is not as yet resolved in enough detail here, partly because the middle warm peak falls between sections in core H (the main core sampled for pollen) (figure 5.2), and partly due to the wide sampling interval. Taken at face value, this evidence suggests that the same climate fluctuations were experienced both at Bouchet and on Greenland, and that this division of the Eemian is real. This would mean that these fluctuations extend over the greater north Atlantic region at least. Preliminary methane measurements of air trapped in the Eemian ice

vary in a similar way (GRIP members [1993]), suggesting that this fine structure of the Eemian might be global.

However, the other palaeoclimatic records from France do not show such a clear division of the Eemian; records from Grande Pile and les Echets show only mild fluctuations. The GISP2 sister ice-core from near to Summit displays a different Eemian signature. Marine records tend to be too smoothed to reveal sudden changes. There could be several reasons why the Eemian is expressed differently in the different records: (a) the Eemian fluctuations are only regional in extent, centred on the north Atlantic area; (b) some records don't have sufficient resolution to record the changes due to low sedimentation rate, bioturbation, too wide a sample spacing etc.; (c) the fluctuations might affect one aspect of the climate more than another - large scale ice volume and sea level changes may not have had time to occur; (d) the fluctuations might be small, but Lac du Bouchet could be at a sensitive site - for example if the tree line moved only by a small amount, but moved across the altitude of the lake, large changes in local palaeoenvironment would be recorded at Bouchet, but not at other sites; (e) the susceptibility record might not be responding directly to climate in this interval; (f) the Summit ice of Eemian age is close to the bedrock, and is disturbed by the greater stresses in this regime, making the record unreliable. To resolve this question, studies of the Eemian signature in many different records from different environments should be carried out.

The last glacial at Summit and Lac du Bouchet; Dansgaard-Oeschger events.

The short, rapid warmings recorded in Greenland ice during the last glacial have been given the name Dansgaard-Oeschger events (Dansgaard et al. [1993]). Sudden temperature fluctuations of as much as 5°C can take place, and Bond et al. [1993] have suggested that sudden warming is initiated by massive iceberg input into the north Atlantic, and thus the fluctuations extend over the north Atlantic region. If Bond et al. are correct, it is reasonable to expect that these same fluctuations may also be expressed in the Lac du Bouchet records. However, Guiot et al. [1992] are not enthusiastic about correlating increased tree pollen % with the Dansgaard-Oeschger events, and point out that as it is difficult to distinguish between $\delta^{18}O$ stages 2, 3 and 4, it might be unreasonable to try correlate these shorter warm episodes.

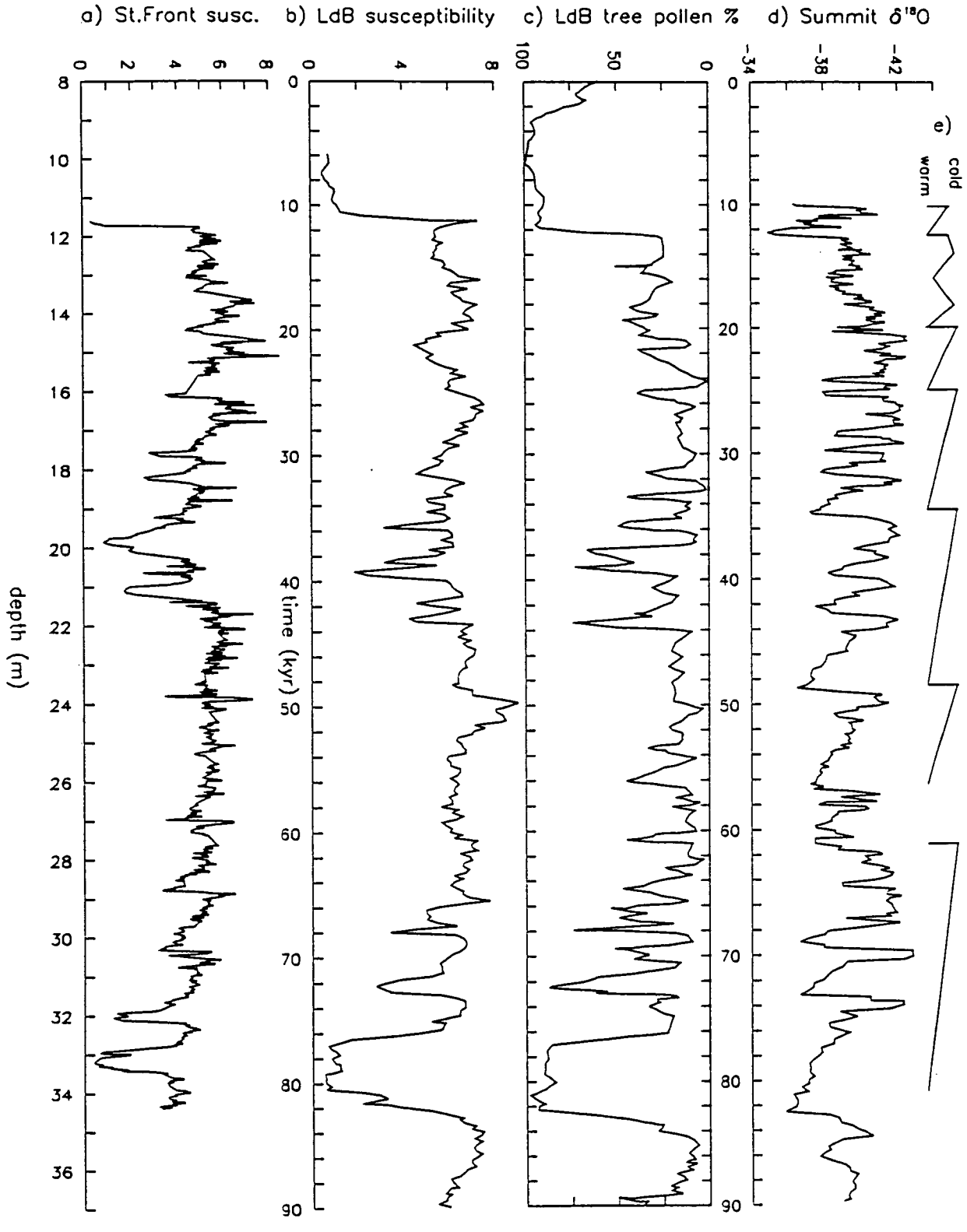

Fig. 7.5 Comparison of the last 90 kyr at Lac du Bouchet, Lac de St.Front, and Summit (Greenland). a) St. Front susceptibility ($\times 10^{-6}$ m^3/kg) (depth scale); b) Lac du Bouchet susceptibility ($\times 10^{-6}$ m^3/kg) (time scale); c) Summit (GRIP) $\delta^{18}O$ record; d) The inferred cooling cycles of Bond et al. [1993].

The Lac du Bouchet palaeoenvironmental records from the last glacial bear a greater resemblance to the Summit ice $\delta^{18}O$ record than they do to the Specmap $\delta^{18}O$ record (figure 7.5). Lac du Bouchet records short, warm events, which are of similar duration to the Dansgaard-Oeschger events. The warm event following shortly after stage 5a at about 72 ka is a feature common to many records, and can be traced on figure 7.5. There is some hint of a saw-tooth pattern in the susceptibility records from both Lac du Bouchet and Lac St.Front, and this might be similar to the steady cooling and sudden warming features proposed by Bond et al. [1993].

On the other hand, the Bouchet records have fewer short warm events, and there is very poor correspondence during the time between about 46 and 62 ka, when Bouchet displays a fairly uniform cold signature, which is also the case at Lac St.Front. This is also the part of the core which is most uncertain, both in dating and palaeoenvironmental significance, because of the slump feature seen there. The Summit record relies on an ice-flow model for its dating older than 14 ka, and this makes one-to-one correlation of the events impossible. More detailed pollen records, as will be produced from Lac St.Front, should help to clarify matters.

It is likely that the short warm events at Lac du Bouchet are related in some way to the Dansgaard-Oeschger events of Greenland and the north Atlantic, simply because of the large size of the changes and the proximity of the sites. However, there are far fewer events at Lac du Bouchet, and they fall in a shorter time interval - this too is an important result, because it means that even though significant changes are occurring on Greenland and in the north Atlantic, these sometimes may not significantly affect the nearby continent. This ties in with the conclusions of Pons et al. [1992] in that the climate at Lac du Bouchet was less oceanic than today, and the Atlantic Ocean had less of an influence there.

7.6 Spectral analysis of the Bouchet record; Milankovitch theory

Some of the major developments in the study of the Quaternary ice age - the Milankovitch theory of climate change and dating of the marine $\delta^{18}O$ stratigraphy - were made based on spectral analysis of palaeoclimatic records. The periodicities in the Lac du Bouchet palaeoenvironmental records have been examined by spectral analysis.

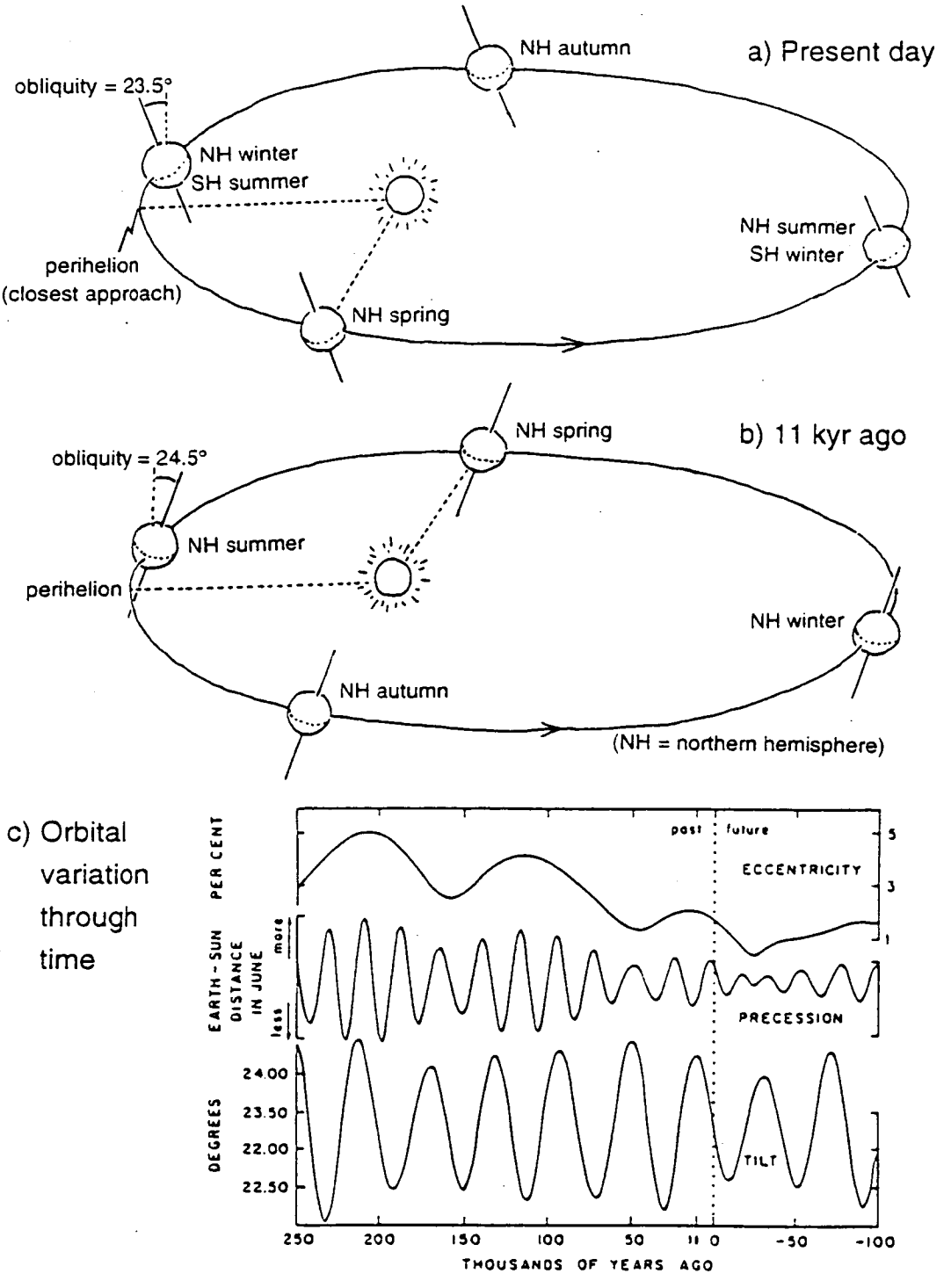

Fig. 7.6 The Earth's orbital parameters: obliquity and precession of the equinoxes. (a) Today's orbital configuration. Perihelion occurs in the northern hemisphere (NH) winter, so NH summers get less insolation than SH summers. Obliquity is at 23.5°, around the centre of its range, so the insolation contrast between the seasons is about average. (b) The orbital configuration at 11 ka. In comparison to today, the Earth's axis has precessed around 180° relative to the perihelion (which also moves, but more slowly). Perihelion occurs in the NH summer, so NH summers got more insolation than the SH summers. The obliquity is at its maximum, so summers got more insolation than today, and winters less. The deglaciation occurred around this time, and these are the insolation conditions favourable to deglaciation. (c) Variations in obliquity, precession and eccentricity through time (from Berger [1988]).

Milankovitch theory and Quaternary climate

The astronomical theory of climate change (Milankovitch theory) is summarised here, and explained in detail in Berger [1988]. Climate responds to changes in the amount of sunlight reaching the atmosphere and the Earth's surface (insolation), which in turn varies due to changes in the Earth's orbit. Two parameters of the Earth's orbit cause changes in the distribution of insolation. The *precession* of the equinoxes controls whether the northern or southern hemisphere points at the sun at closest approach (perihelion), and varies with periods of 23 and 19 kyr (the 23 kyr period is dominant over the last 300 kyr). The *obliquity* (tilt) of the Earth's axis controls the contrast in insolation between summer and winter, with a periodicity of 41 kyr. Thus insolation not only varies with time, but also with season and latitude. A third parameter, the *eccentricity* of the orbit, has a periodicity of ~100 kyr; it modulates the precession effect, but has only a tiny effect on the annual average insolation. The precessional periods dominate the insolation variation at low- to mid- latitudes, and the obliquity periodicity dominates at high latitudes. See figure 7.6.

The global ice volume, as recorded in marine $\delta^{18}O$ records, has a dominant frequency of about 100 kyr from 800 ka to the present, and 40 kyr from 2400 ka to 800 ka; the other orbital periodicities are also seen (Berger [1988]). The insolation signal for summer around 65°N most closely corresponds to the Specmap $\delta^{18}O$ record (figure 7.7). The insolation changes are amplified by positive feedbacks (for example ice-albedo), mostly in the northern hemisphere ice sheets, and the changes here are propagated to the world climate. The mechanisms that amplify and distribute the input signal involve interactions between glaciers, ocean circulation, atmospheric circulation, clouds, H_2O, CO_2, CH_4 and so on, and are therefore complex. They are studied by computer simulation (global circulation models).

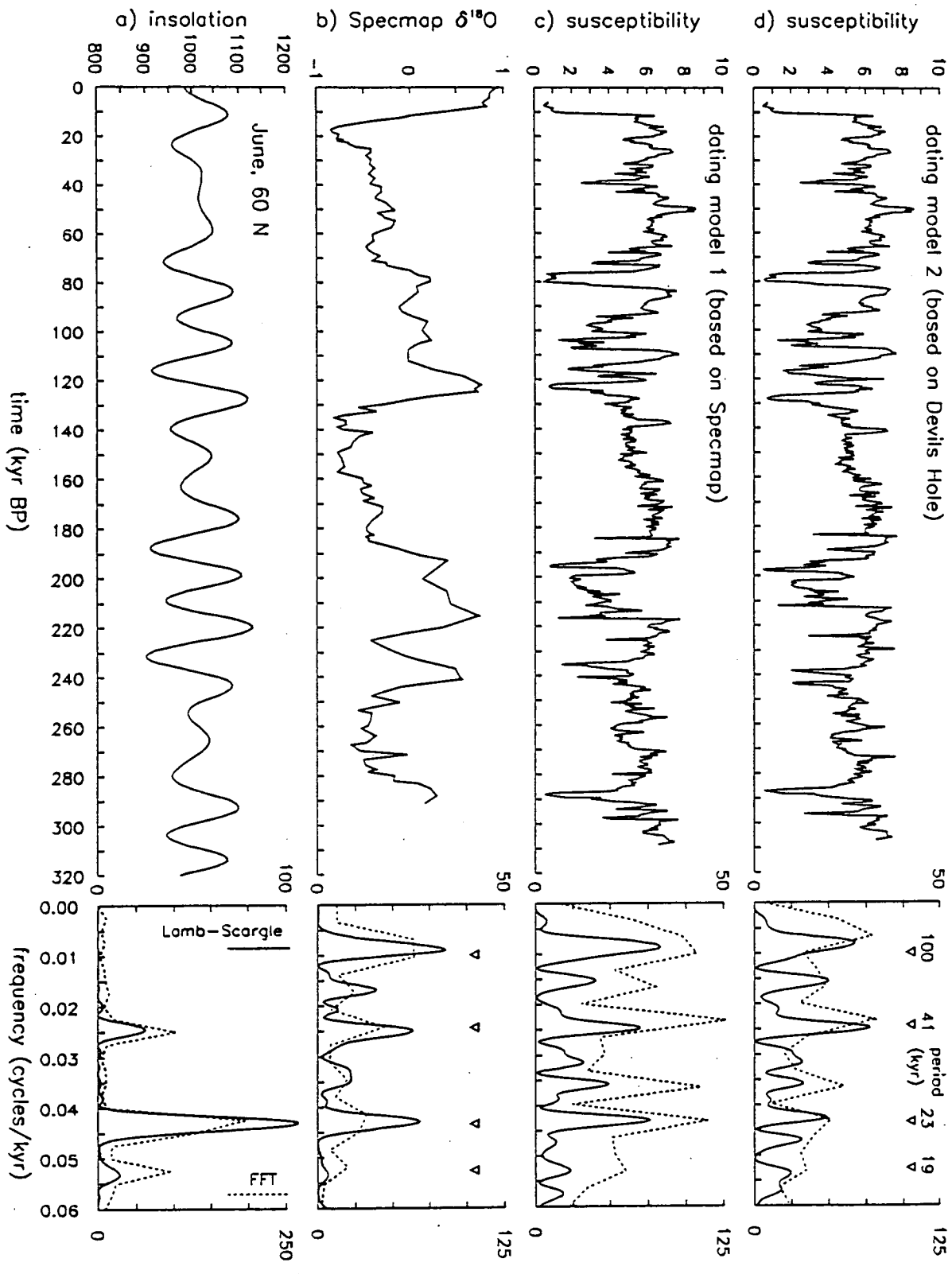

Fig. 7.7 Time series (top 4 diagrams) and spectral analysis (bottom 4 diagrams) of: (a) the summer (June) insolation at 60°N. (b) the Specmap $\delta^{18}O$ record; (c) Lac du Bouchet susceptibility, dated using model 1 (based on Specmap); (d) Lac du Bouchet susceptibility, dated using model 2 (based on Devils Hole). Spectral analysis by Fast Fourier Transform (FFT) (dotted line) and the Lomb-Scargle method (solid line).

Spectral analysis methods

Two spectral analysis methods - the fast fourier transform (FFT), and the Lomb-Scargle method - have been used in this section. Both transform the records (time-series) from the time domain to the frequency domain, so that any periodicities present can be evaluated.

The Fortran subroutine of R.C. Singleton [1968] was used to calculate the FFT. The time-series must be evenly spaced, but the number of time-domain data-points need not be a power of two, but any number that can be factorised by low primes. The ends of the series have been cosine tapered to 10% of the length of the whole series, to reduce ringing.

The Lomb-Scargle method is comparatively recent, developed by Horne and Balinaus [1986] and Scargle [1989], originally for astronomical time-series where the data were not recorded at evenly spaced intervals. The Fortran subroutine of Press and Rybicki [1989] was used. The advantages of the method are that it gives weight on a per-data-point basis rather than a per-interval basis (like the FFT), so that problematic even-spacing need not be carried out. It gives a greater resolution then the FFT at the low-frequency end of the spectrum.

For a reliable identification of a stable periodicity, there must be at least 10 wavelengths in the time-series (trad.). It is a general problem with spectral analysis of palaeoenvironmental data that the records are generally on or below this limit, and this is the case with the Bouchet data: periodicities found above about 30 kyr (a tenth of the series length) have a greater uncertainty. However, the fall-off in reliability is not sharp, and information can be gained when there are only a few wavelengths in the time-series.

Another constraint on the reliability is the depth→time model - small changes in the model can lead to differences in the frequency spectra. Therefore, two depth→time models have been analysed for comparison.

Spectral analysis of the Lac du Bouchet palaeoenvironmental records

In figure 7.7, spectral analysis has been carried out on the susceptibility record, dated using the two models of figure 6.6, the Specmap $\delta^{18}O$ record of Martinson et al. [1987], and the June insolation at 60°N curve of Berger [1978]. The records (time-series) are shown as well as their frequency spectra.

The spectral analyses of the example insolation curve (figure 7.7a) and the Specmap record (figure 7.7b) (which was dated by "tuning" to the Milankovitch periodicities) may be regarded as verifications of the two analysis methods: all the expected periodicities are found, using 300 kyr long records. There is hardly any ringing (i.e. spurious side-lobes either side of the main peaks) in the (simple) insolation spectra, where the result is already known, indicating that this is not a problem for the Lac du Bouchet spectra. The Lomb-Scargle method gives a greater resolution than the FFT. The ~100 kyr eccentricity period is

not present in the frequency spectra of the insolation because it only appears in the time-series as an envelope round the other variations, and not as an absolute wavelength in itself. That this is the dominant periodicity in the palaeoclimatic records for the last 800 kyr has been a perplexing problem for palaeoclimatologists.

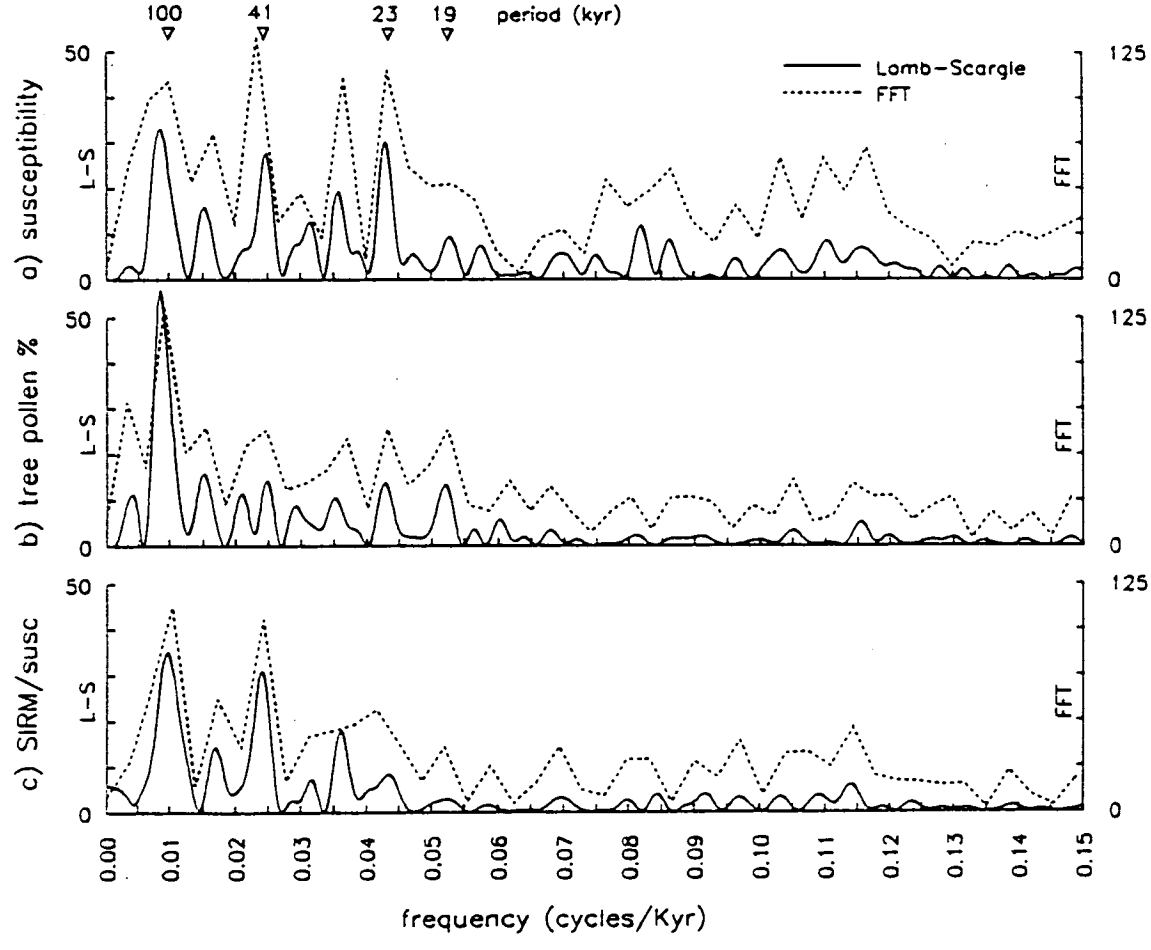

Fig. 7.8 Spectral analysis, by FFT and Lomb-Scargle methods, of: (a) susceptibility; (b) tree pollen %; (c) SIRM/susceptibility.

The main result of the spectral analysis is that periodicities of 23, 41 and ~100 kyr are found in the susceptibility records dated with both models, and using both spectral analysis methods. In all four susceptibility spectra three out of the four highest peaks correspond to the Milankovitch periodicities. Other frequencies are also found at 0.0155 and 0.036 cycles/kyr (periodicities of about 64 and 28 kyr respectively); their significance, if any, is uncertain. The Specmap-based depth→time model leads to susceptibility spectra which are very similar to that of the Specmap record - this was expected, because as the susceptibility record was dated by matching to the Specmap record in the time domain, similarity in the frequency domain follows. The Devils Hole depth→time model is quite

similar to the Specmap model, so again it is not such a surprise to find the Milankovitch periodicities in the record. However, the crucial difference here is that the Devils Hole depth →time model involves *no* prior assumptions about what periodicities should be found in the record.

On this basis, the Bouchet susceptibility records are consistent with Milankovitch theory, but the relative dating methods employed here mean that only small weight should be attached to this conclusion. Most of the spectral power in the Bouchet records is concentrated at longer periods, in the range of the astronomical periodicities.

No one periodicity seems to be dominant in the Bouchet series, and the uncertainties inherent in the dating and the analysis itself make it unwise to speculate further about the balance of power between the Milankovitch periodicities. However, the dominance of a 23 kyr period, as found by Ruddiman and McIntyre [1981] in north Atlantic sea surface temperature proxies, does not appear in the Bouchet records.

7.7 Conclusions

The magnetic susceptibility record from Lac du Bouchet is a good indicator of past environmental variations. Low susceptibility results from warm climate at Lac du Bouchet. It is a uni-variate record which principally indicates the proportion of detrital material in the sediment, and it compares very well, both in detail and trend, with the tree pollen % records and with palaeoclimate records derived from multi-variate pollen analyses.

The warm episodes at Lac du Bouchet have a lower sedimentation rate than the glacials, and have the appearance of punctuating the largely glacial 50m record. The traditional two-fold distinction of warm climatic events into "interglacials" or "interstadials" is constricting, and inadequate to describe the sliding-scale of intensity of warm events seen at Lac du Bouchet. The last glacial ($\delta^{18}O$ stages 2, 3, 4) is marked by short, warm climatic events, occurring between 30 and 45 ka and just after the end of stage 5. The warm sub-stages 5a, 5c and 5e (the Eemian) are clearly marked by low susceptibilities and the dominance of non-pine tree pollen. Large palaeoenvironmental fluctuations occur within the stage, and even within the 5 sub-stages. Stage 6 is less marked by warm episodes according to susceptibility, but the pollen records show occasions of increased tree pollen %. Stage 7 has sudden large palaeoenvironmental changes, like stage 5, but unlike the Holocene (stage 1).

Sampling for magnetic work was carried out at 2.5cm spacing, and was the only sampling to be carried out on all of the 50m cores; the magnetic records, like susceptibility, are therefore the only fully complete and detailed records from Lac du Bouchet (see figure 7.4 for an example).

In comparison with susceptibility records from other regions and other environments, it is noted that the mechanism responsible for varying the susceptibility was different in most cases, and the record from each location must be assessed individually before attaching weight to them.

The same broad features are seen at Lac du Bouchet as in the global ice volume recorded in the Specmap marine $\delta^{18}O$ records, but there are different trends in the glacial stages. The main sub-divisions of the warm $\delta^{18}O$ stages 5 and 7 are clearly marked by the tree pollen % (without pine), and also in the susceptibility records, and these formed the main dating points for the sequence (described in chapter 6).

The rate of sedimentation at Lac du Bouchet is a fast enough to allow the resolution of subtle shorter events, of the type recorded in Greenland ice. The Eemian interglacial ($\delta^{18}O$ stage 5e) recorded at Bouchet by susceptibility displays a very similar fine structure to that in the GRIP ice core at Summit, Greenland. The form of this fine structure is not seen in the pollen sequences of la Grande Pile or les Echets, or the GISP2 ice core 27km distant from the GRIP core. Finer resolution pollen analysis at Lac du Bouchet, and further Eemian records from other locations are needed before general conclusions can be drawn about the stability or instability of interglacials.

The Bouchet susceptibility and pollen records show many short duration warm events punctuating the last glacial between about 30 - 42 ka; these may well be related to the warm Dansgaard-Oeschger events also recorded in Greenland ice throughout the last glacial. However, dating uncertainties prevent a one to one correlation of the events between the two sites, and Guiot et al. [1992] have warned against simplistic interpretations of short duration increases in tree pollen %. The non-appearance of the Dansgaard-Oeschger events outside of the middle glacial is also an important result, as it means that even large climatic changes in nearby regions might not greatly affect the continental environment at Lac du Bouchet.

It is more likely that any Eemian fluctuations will be common to the Greenland and Lac du Bouchet records than the glacial Dansgaard-Oeschger events, because the climate at Lac du Bouchet was influenced more by the ocean (i.e. the north Atlantic) during the interglacial than in the glacial (Pons et al. [1992]).

Lake sediments are sometimes regarded as being of secondary importance to marine sediments for palaeoclimatic studies on the time-scale of a few 100 kyrs; magnetic measurements like susceptibility are usually regarded as being of secondary importance to pollen and geochemical analysis of sediments. The work done at Lac du Bouchet shows that susceptibility, when taken with the other available evidence, does give a very good detailed continuous proxy-palaeoenvironmental record for the last 300 kyr. The Lac du Bouchet record is older than the Summit ice cores and comparable in length to many marine cores,

and was obtained at a fraction of the cost. An international maar drilling program, as proposed by Negendank and Zolitschka [1993], would be of great value to the study of past continental environments and climates at most latitudes.

Chapter 8

Palaeomagnetic and Geomagnetic aspects

8.1 Introduction

The past geomagnetic field is known from the record in volcanic and sedimentary rocks (palaeomagnetism). Palaeomagnetism has revealed geomagnetic phenomena such as reversals and palaeosecular variations. It has proved to be a remarkably useful tool in geology and geophysics: field reversals are ideal chronostratigraphic markers; the understanding of reversals and the sea-floor spreading hypothesis developed together; and the past movement of tectonic plates is tracked by apparent polar wander.

The Lac du Bouchet sediment sequence holds a palaeomagnetic record of geomagnetic changes back to over 300 ka (the Brunhes-Matuyama reversal occurs at ~ 780 ka). The records are used here to investigate field palaeointensity variation, palaeosecular variation, the nature of excursions, and the influence (if any) of orbital variations on the field. These observations offer clues to the processes in the outer core which generate the field. Palaeomagnetic records from Lac du Bouchet can be applied to fine scale magnetostratigraphy, and calculating changes to the cosmogenic production of ^{14}C (and hence helping to calibrate ^{14}C dates) and climatically sensitive compounds such as nitric oxide (NO).

A full description of the field over the globe is not possible from just one locality, and all of the interpretations make assumptions about the relative contributions of the dipole and non-dipole field. If the field is assumed to be due to a centred dipole, its pole and relative moment can be calculated. The changes in palaeointensity are large enough to have a large dipole (global) component.

The Lac du Bouchet direction records (declination and inclination) are very detailed. However, the directions in some core sections below 25m (~150 ka) are disturbed by the coring process, especially the declinations. It is therefore the past geomagnetic intensity (palaeointensity) which forms the main interest of this chapter.

Palaeointensity

Palaeointensities recovered from sediments are not absolute values, because the DRM acquisition process cannot be reproduced in the laboratory. The main assumptions about the recording and recovery of sedimentary palaeointensity are:

- ♣ The sediment acquires a magnetisation that is linearly related to the field intensity at the time of deposition.
- ♣ The effect of varying magnetic mineralogy down the sequence can be normalised with laboratory magnetisations also dependent on the mineralogy.
- ♣ Other influences over the record such as coring disturbance, VRM and so on can be identified and removed by demagnetisation or by discarding samples.

These assumptions are probably approximately true when the magnetic mineralogy is fairly constant down the core (King et al. [1983]) and the environment of deposition is relatively free of turbidites, major currents and so on. Thus great care is needed when looking at palaeointensity records which are based on these assumptions. Only after magnetic and palaeomagnetic evaluation of the sediment has been carried out (chapter 4) can the normalised intensity records be called, with reason, records of relative geomagnetic palaeointensity.

Because of these pitfalls, many workers have tended to be over-cautious, even to the extent of believing that sediments can record no more than whether the field is of either normal or reversed polarity. At the opposite end of the caution scale, a great temptation has been to over-interpretation. For example Wollin [1977, 1978] used non-normalised NRMs to suggest that climate was directly related to the field, when in fact the NRM was dominated by the climatic signal, as pointed out by Kent [1982]. Other similar over-interpretations include the "re-enforcement syndrome" with excursions, in which excursional directions in records are linked to other reported excursions when the lithological factors are not fully considered, and when the dating control is inadequate. This under- and over-interpretation, apart from highlighting difficulties in the method, has not been constructive. Now, however, balanced views are becoming the norm, and the difficulties with sedimentary palaeointensity are addressed (see, for example, Thouveny [1993], Tauxe [1993]).

After partial demagnetisation, characterisation of the magnetic mineralogy, normalisation and stacking (chapters 4, 5), a depth→time model was used to date the record (chapter 6), and an independent palaeointensity record for Lac du Bouchet results. This is now compared to other sedimentary palaeointensity records. These are few, and none of them have as good a combination of time coverage and detail as the Bouchet

palaeointensity, and they have more or less similar uncertainties. An extra factor enters at this point: differences in the records may now also be due to the non-dipole component of the field. However, large enough variations, such as those seen at Lac du Bouchet, should be expressed globally. Some records match well, a few clear palaeointensity lows are present in all records, and some parts of some records do not match well at all.

Independent estimates of palaeointensity are compared with the Bouchet record. These are determined from TRM in volcanic rocks, and from the changing production of the cosmogenic isotopes ^{14}C and ^{10}Be (which is influenced by the geomagnetic field). Both are in general agreement with the sedimentary palaeointensity data (Mazaud [1991], Thouveny [1993]) over the narrow common interval (0 - ~30 ka), and this is strong evidence that the sedimentary palaeointensity records are valid.

8.2 The direction records

The direction records are shown in figure 8.1. Both declination and inclination have been demagnetised at 10 mT, processed to remove coring-disturbed samples and sections (section 5.6), and averaged at 0.25 kyr intervals (see section 5.5).

The inclination has an average of 60.1°, compared with the value of 63.35° expected from an axial geocentric dipole field at 44.9°N.

Declination shows short (over a few kyrs) swings of roughly 25°, but up to 50°. It is not possible to detect long term variations, if they exist, because the core sections are not azimuthally aligned and the declinations of each core section (1 to 1.5m, roughly 6 to 10 kyr) are averaged to zero. Inclination shows short period swings of up to 20°, and longer term variations are also seen.

Caution must be exercised with the direction records, as the sedimentology does have some influence at some depths. For example, the trough in inclinations between 75 and 82 kyr ago is suspicious because it corresponds to the organic-rich sediments of stage 5a, which record the palaeofield less faithfully (chapter 4). The low inclinations between 52 and 62 kyr (using depth→time model 1) correspond to the slumped layer (section 6.4, Truze and Kelts [1993]) and are not a true representation of the palaeofield. In general, the inclination tends to be lower in the palaeomagnetically unreliable sediments. There may be some errant directions due to physical disturbance of the sediments by the coring process that slipped through the direction processing (section 5.6). However, the rest of the directions show changes which do not correspond to the lithology, and these are taken to be a fair representation of the palaeofield. There are also the ever-present uncertainties surrounding the dating.

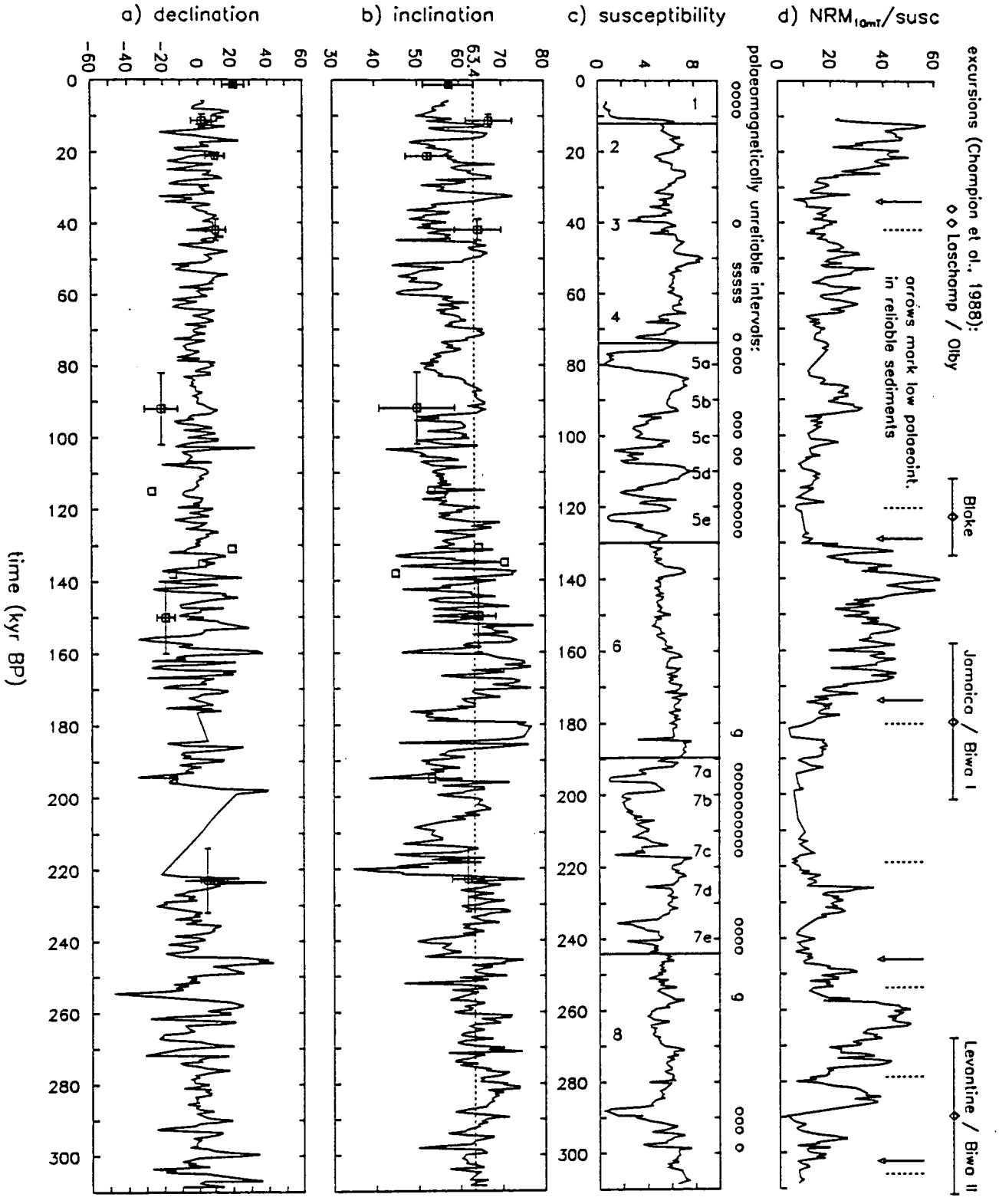

Fig. 8.1 The Lac du Bouchet palaeomagnetic records: a) declination$_{10mT}$; b) inclination$_{10mT}$. The squares in a) and b) are palaeomagnetic directions from lava flows from Lipari, north of Sicily, Italy (Lanza and Zanella [1992]), with inclinations converted from 38.5°N to 44.9°N by the relation tan(inc) = 2tan(lat). Excursions, compiled by Champion et al. [1988], are shown; c) Susceptibility from Lac du Bouchet is included as a lithological control. d) relative palaeointensity. Low intensities in reliable sediment are marked with solid arrows. "ssss" = slumps. Dating of the Lac du Bouchet records is by depth→time model 1 (based on Specmap) (figure 6.6).

There are few other direction records published for the last 300 kyr, and none has the detail of Lac du Bouchet. Therefore it is difficult to independently verify the records. Recent TRM results from volcanic lavas from the island of Lipari, southern Italy (Lanza and Zanella [1992]), extend back to 225 kyr ago, and are therefore included in figure 8.1. These TRM results are consistent with our records. Lipari (38.5°N, 5°E) is close enough to Lac du Bouchet for non-dipole spatial differences in the field to be small. The inclinations correspond quite closely, having a similar range of variation; this indicates that the Lac du Bouchet sediments are picking up real geomagnetic inclinations faithfully.

In their study of the palaeomagnetism of the Grande Pile sediments, Ellingsen et al. [1992] found palaeosecular variation in the NRM, but concluded that the sequence could not be regarded as a magnetostratigraphic standard for the last interglacial-glacial cycle.

Times of excursions or short reversals as compiled and assessed by Champion et al. [1988] are also marked on figure 8.1. No clearly excursional directions are seen in the Bouchet record. However, any outlying directions were removed during processing on the assumption that they were due to coring disturbance, necessary because of the noisy nature of the original direction record. The conclusion of Thouveny and Creer [1992], based on the top 70 kyr, that excursional directions of the field would have to have been of short (a few centuries) duration, may well be true for this longer sequence. A more detailed analysis of the 50m cores would be needed to either confirm this or to locate excursional directions.

8.3 Palaeointensity: assessing reliability

The magnetic mineralogy, the stability of the NRM, and the suitability of the sediments for palaeointensity studies were assessed in chapter 4. Partial demagnetisation at either 10 or 20mT removes VRM to leave a stable remanence. Susceptibility, ARM and SIRM are used as uni-variate estimators of magnetic mineralogy, which comprises the composition of the magnetic grains, their concentration, and their domain state (~grain-size). Since the variation of grain-size and composition down the core is small, susceptibility, ARM, and SIRM are equally good for normalising the NRM of magnetic mineralogical effects.

The more organic sediments were found to have an anomalously low NRM intensities; they are characterised by susceptibilities below 4.2×10^{-6} m^3/kg (figure 4.1). However, the magnetic mineralogy starts to differ significantly from the normal below about 1×10^{-6} m^3/kg, so I concluded that the main controls over the quality of geomagnetic recording were the physical and chemical conditions at deposition. Samples with low susceptibility and a low or high SIRM/susceptibility (a grain-size estimator) were removed from the normalised intensity records.

To verify that the choice of normalisor and demagnetisation step makes negligible difference, the six relative palaeointensity records are compared in figure 8.2. Differences are slight.

Records from the individual cores within the lake were stacked, so that local sedimentological differences are averaged, and the signal/noise ratio increased. In fact the only place where a stack of different cores makes a difference is between 52 and 62 ka, in the region of the slumped section, and even this is partly due to poor inter-core correlation (figure 5.1) in this interval.

It is probable that there is no large-scale control of climate by the field. Therefore any similarities between the susceptibility (~environmental) record and the normalised intensity (geomagnetic) record are likely to be due to inadequate recording or recovery of the field. The un-normalised NRM intensity record has both palaeoenvironmental and geomagnetic influences. Therefore the three types of record are compared in figure 8.3, in both the time and frequency domains.

In figure 8.3, the palaeointensity record shows very little similarity to the susceptibility record, indicating that the normalisation has been successful. In the case of Lac du Bouchet, the un-normalised NRM_{10mT} also shows predominantly geomagnetic control, but this result is not generally applicable to other sediments, as has been demonstrated by Kent [1982]. The data in the frequency domain also show differences.

Only after these internal tests have been done should the normalised intensity records be called records of relative geomagnetic palaeointensity, and even then it is understood that the records are not ideal due to the approximately satisfied assumptions.

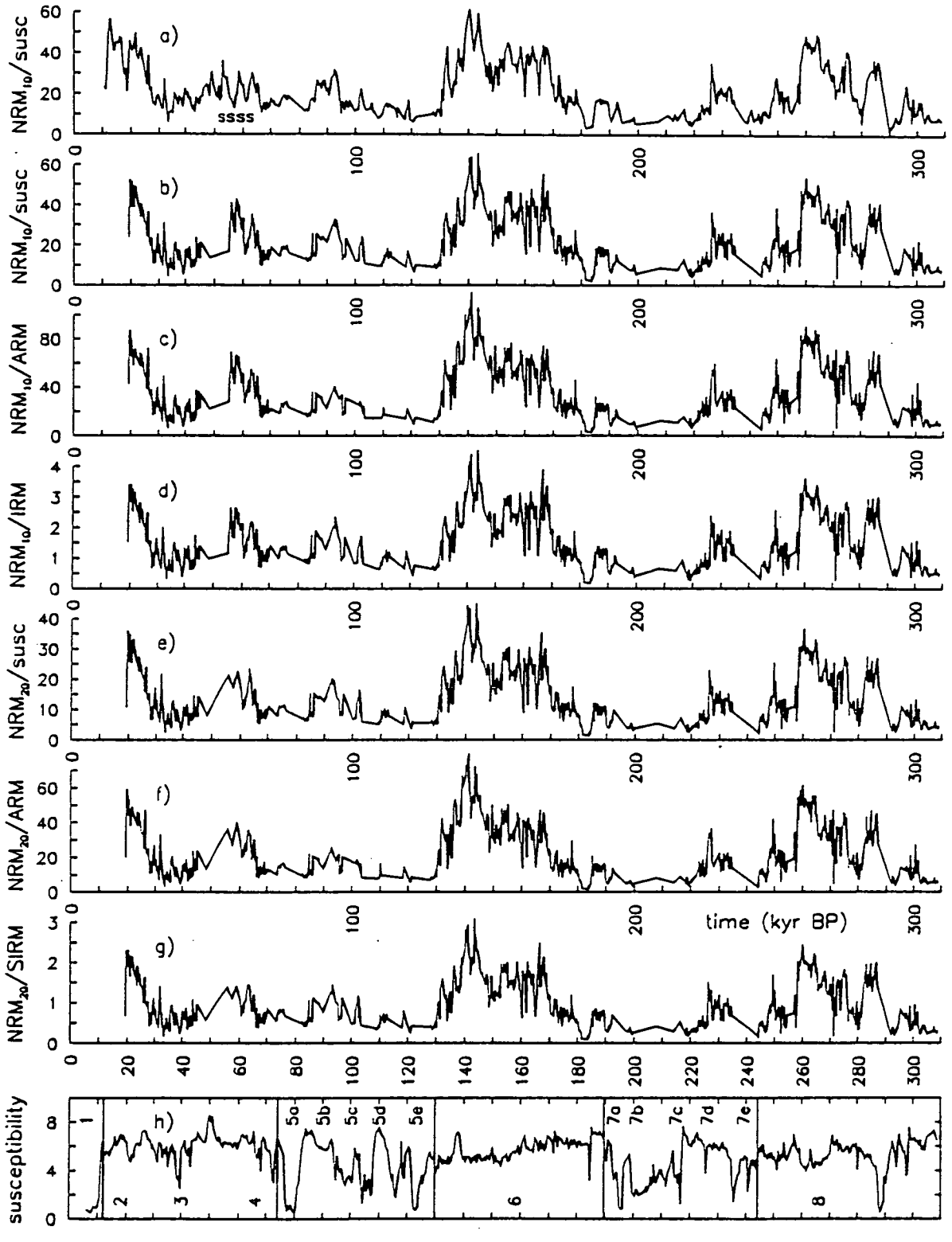

Fig. 8.2 NRM intensity demagnetised at 10 or 20mT, and normalised with susceptibility, SIRM or ARM. Dating by depth→time model 1 (based on Specmap). (a) is a stack of cores G, H, I and the previous 20m stack (Edinburgh version), and (b) to (f) are stacks of cores G, H and I only. The susceptibility record is shown as a lithological comparison. Samples with a susceptibility less than 4.2×10^{-6} m^3/kg (organic-rich samples) have been removed from the NRM records.

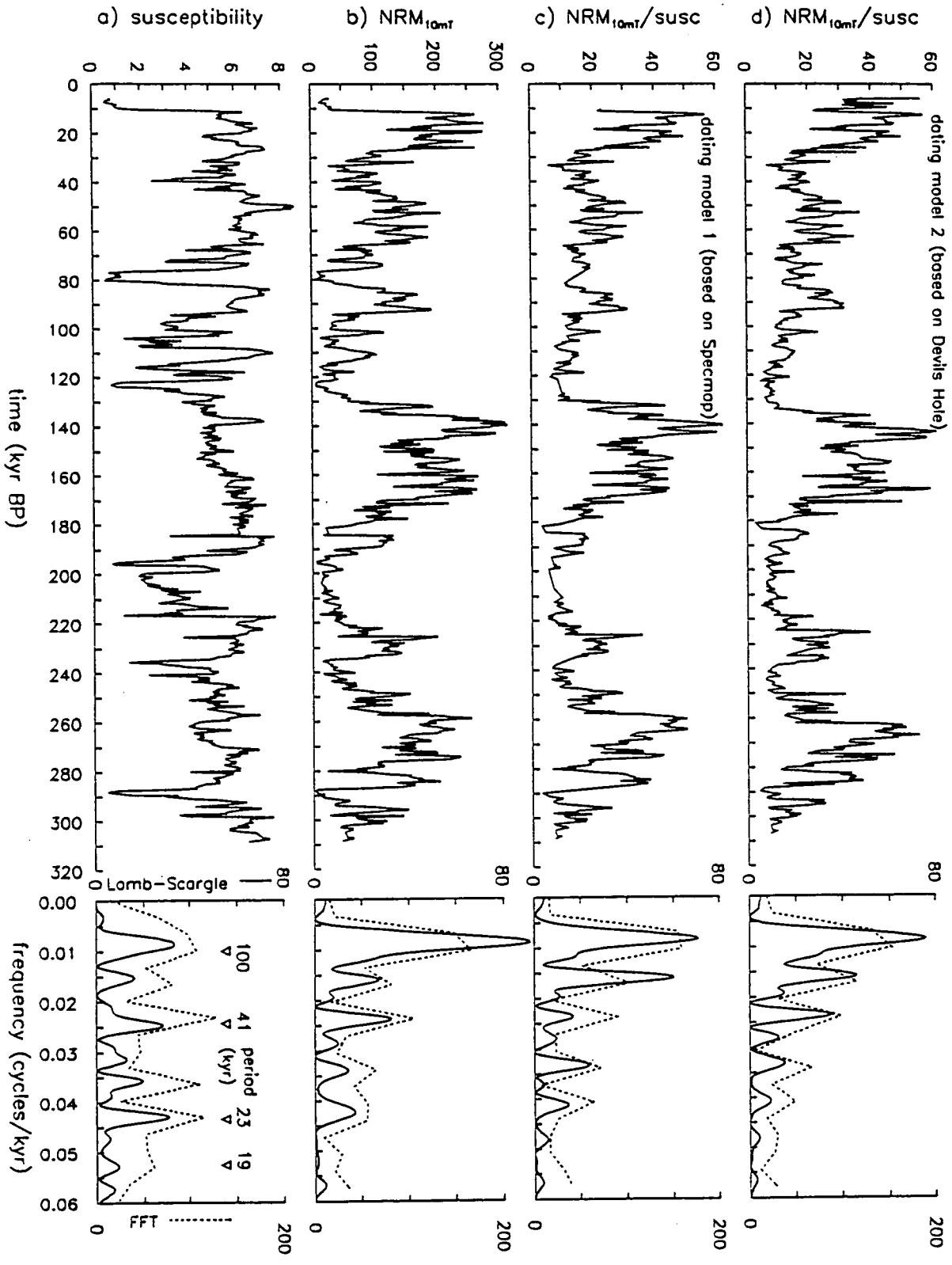

Fig. 8.3 A figure comparing: a) susceptibility - a record controlled only by lithological (and therefore palaeoenvironmental and palaeoclimatic) factors; b) NRM intensity - a record with both lithological and geomagnetic controls; c) and d) NRM intensity normalised with susceptibility - records dominantly controlled by geomagnetic palaeointensity. The records have been transformed to the frequency domain by FFT and Lomb-Scargle spectral analysis. The time-series are above, and the corresponding frequency spectra below.

8.4 The Lac du Bouchet palaeointensity record

An independent record has been produced of the relative geomagnetic palaeointensity at Lac du Bouchet. The uncertainty in the record is thought to be mainly due to: a) uncertainties in the linearity of response of the magnetisation to the palaeofield because of differing depositional/sedimentological conditions between organic and glacial sediments; and b) uncertainties in the dating model.

The Lac du Bouchet palaeointensity record is characterised by several features. The amplitude variation is large, the troughs reach 15% of the maximum value. There are long periods of low intensity between 130 and 95 ka, and between 225 and 185 ka. There are also periods when the intensity is high, between 275 and 255 ka, 170 to 135 ka, and 25 to 10 ka (and probably continuing to the present). It is these palaeointensity highs which give the long wavelength of ~125 kyr seen in the spectral analysis (figs 8.3, 8.6). Super-imposed on this background there are also less marked, but significant, highs and lows of shorter wavelength. The peak between 60 to 45 ka includes the slumped section, so the reliability of both palaeointensity and dating is not good here. Further super-imposed on top are short but large amplitude changes on the scale of kyr or less, which could well be similar secular variation to that observed directly in historical times.

8.5 Palaeointensity: Lac du Bouchet in comparison to other records

Studies of sedimentary palaeointensity are at an early stage, and only a few records have been published. A preliminary aim of these studies is to prove beyond doubt that the sedimentary palaeointensity method works. The main aim is to produce an accurate master record (reference curve) of palaeointensity variations through the last few 100 kyrs, and to have an idea of the form and extent of the non-dipole variations from this record. This knowledge can then be used to confine theories of the geodynamo, and might well be of use for fine-scale magnetostratigraphy.

A proto- master record has already been published by Meynadier et al. [1992], from a stack of three Somali Basin and four Mediterranean Sea marine sedimentary records (Tric et al. [1992]), however not all of the published records agree with it (Tauxe [1993]) (figure 8.4); more records are needed from around the world before a consensus can be reached.

Independent measures of palaeointensity are crucial to testing the validity of the relative palaeointensities from sediments. Absolute palaeointensity Thellier-Thellier experiments on TRM in volcanic lavas and the record of production of cosmogenic isotopes are studied as two alternative sources of palaeointensity information.

The locations of all these palaeointensity sites are marked on figure 1.2.

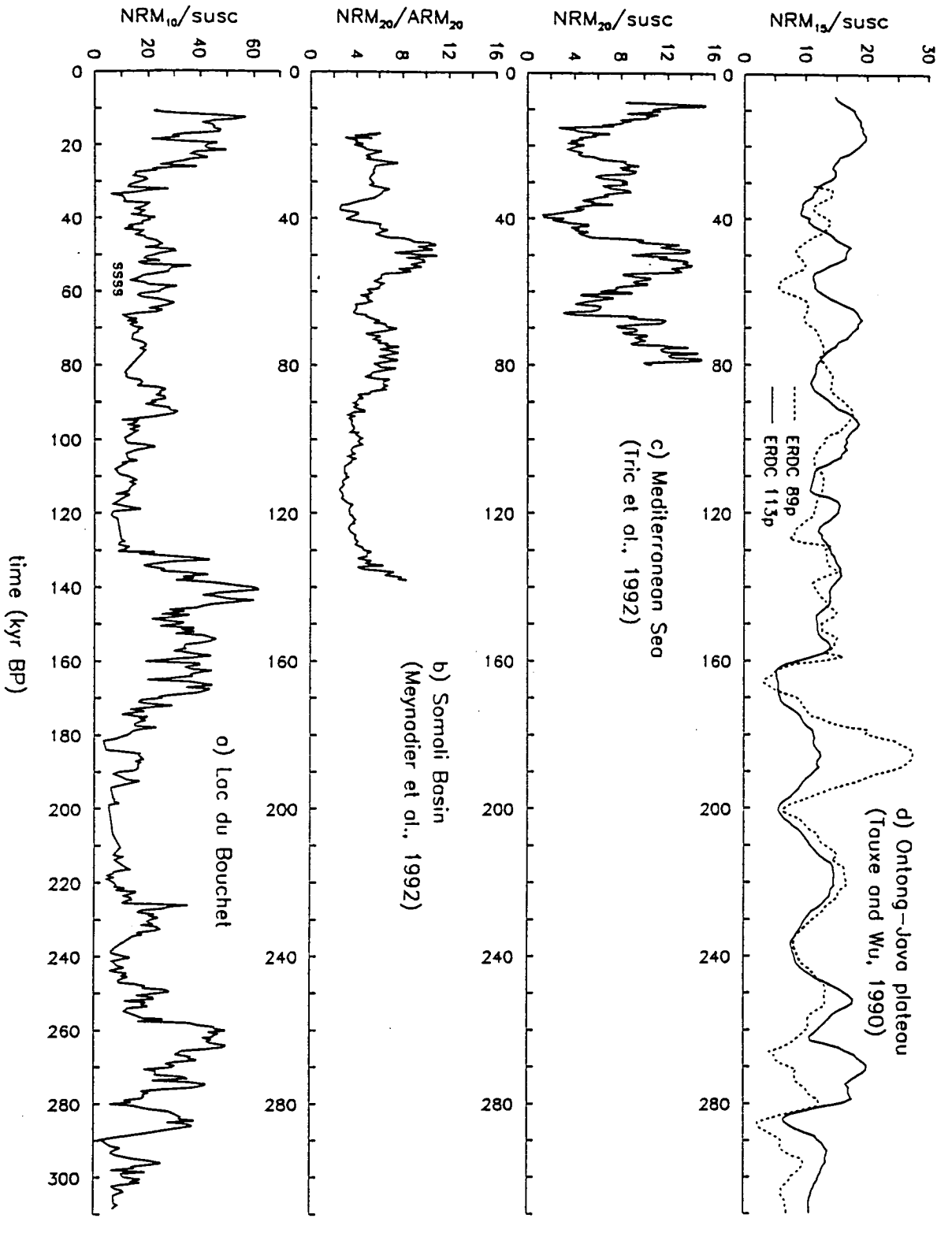

Fig. 8.4 Comparison between several records of sedimentary geomagnetic palaeointensity. a) the record from Lac du Bouchet; b) the stacked record of Meynadier et al. [1992] from three Somali Basin records; c) the stacked record of Tric et al. [1992] from four Mediterranean Sea records; d) two records from the Ontong-Java plateau (Tauxe and Wu [1990]).

Other sedimentary palaeointensity records

The large amplitude and wavelength of the palaeointensity changes seen at Bouchet mean that they are due largely to the dipole field. Therefore similar changes should be seen in other records from around the globe. Figure 8.4 shows some such marine sedimentary palaeointensity records alongside that of Lac du Bouchet.

The record of Tric et al. [1992] is itself a stack of four records from the Mediterranean Sea (35-40°N, 13-33°E), and the record of Meynadier et al. [1992] is a stack of three from the Somali Basin (0-3°N, 46-51°E). Two records from the Ontong-Java plateau (0-2°N, 156-159°E), from Tauxe and Wu [1990] are also shown. All of these authors emphasise the importance of careful magnetic mineralogical study of the sediments, to check that there is little down-core variation. Meynadier et al. also combine and include the Mediterranean records to produce a composite record - "a significant step in the establishment of a reference curve of geomagnetic field intensity for the last 140 kyr"; the two stacked records correspond very well. There are similarities between these and the Lac du Bouchet record: they have a similar range of variation, the with the lows down to roughly 15-20% of the maximum (the Bouchet lows are perhaps lower); all show lows at about 40 ka, highs around 50 ka, and another low at roughly 65 ka. A long low intensity period between 95 and 130 ka is common to the Somali Basin and the Bouchet records, but beyond the range of the Mediterranean record. On the other hand, both the dating and relative size of the palaeointensity highs and lows show some marked differences, especially between 30 and 10 ka. The records from the Ontong-Java plateau are long, but not detailed. They show a smaller amplitude range, and do not correspond closely to the other palaeointensity records of figure 8.4.

The three reasons for differences in the palaeointensity records are: a) the non-dipole field causing regional differences in the palaeofield; b) imperfect recording/recovery of the palaeointensity; and c) problems in the dating of the cores. Error-bars are left off figure 8.4 because they tend only to represent the standard deviation of the stacks, which, though important, leaves the true uncertainty under-estimated.

It is perhaps the third point which is the cause of greatest uncertainty in the records, and therefore it is crucial that the dating methods are critically assessed in all studies. The Somali Basin cores have quite a detailed $\delta^{18}O$ stratigraphy, matched to Martinson et al.'s reference record [1987], and good susceptibility matching between the cores. Only one $\delta^{18}O$ record from the Mediterranean cores is given, which does not extend into $\delta^{18}O$ stage 5, and the other cores are correlated by sapropel and volcanic ash layers common to the cores. The Ontong-Java records have smooth $\delta^{18}O$ records, and can only be poorly dated - in fact the two alternative datings of the records given in Tauxe and Wu [1990] and Tauxe [1993]

differ by about 15 kyr for all of the interval between the top and 150 ka except for $\delta^{18}O$ stage 5e (the 1990 dating is shown in figure 8.4). Errors will not be as large as this for the Mediterranean or Somali records, but large differences of anything up to about 10 kyr are not out of the question. Lac du Bouchet has the most accurate dating of the records shown, but it is not without its own problems. The pollen zones of the Holocene and the late-glacial give good control, the ^{14}C dating is good until 40 ka, and $\delta^{18}O$ stages 5 and 7 are well controlled, but the glacial sediments have poorer dating control, and the slumped section (52 - 62 ka using depth→time model 1) still poses a problem.

Further continuous records of palaeointensity are needed to clarify the situation, and some exist. Carlo Laj presented a 200 kyr stacked north Atlantic record at the E.G.S. meeting in April 1992, and Steve Lund presented another north Atlantic record at the fall 1992 A.G.U. meeting - both of these show many correspondences with the Lac du Bouchet record, but have not yet been published. The new 4 myr palaeointensity record of Valet and Meynadier [November 1993] from three equatorial Pacific cores looks, at first sight, to match less well with the Lac du Bouchet palaeointensity.

The relative size of particular highs and lows show much variation in the records at different localities. It is difficult to say whether this is due to non-dipole effects or to inaccurate recording/recovery problems without more records. The location of the Mediterranean palaeointensity record not far from Lac du Bouchet in southern France means that these two records should match better than they do; this is a problem. In fact it is this lack of detailed correspondence that, more than any other evidence, reveals the inadequacies of the dating and the sedimentary palaeointensity method. On the other hand, there is a fair correspondence between the north Atlantic records and the French records, and also between the individual records in the Somali Basin and Mediterranean Sea stacks.

Given the problems with dating, and the general nature of sedimentary palaeointensity, the correspondences that have been noted are perhaps as good as could be hoped for at this stage. More records are needed.

Two new developments in studies of sedimentary palaeointensity should expand the global data-set quickly. Long "U-channel" samples can be partially demagnetised and measured with pass-through cryogenic magnetometers, giving at a great time saving over individual samples (Weeks et al. [1993]). There is a current proposal by Clement and Constable to start to open up archive-halves of DSDP and ODP marine cores for palaeomagnetic measurement, which, if the proposal succeeds, promises to increase the global data set quickly and at small expense.

Palaeointensity estimates from TRM

The geomagnetic field is recorded in volcanic rocks when they cool below the Curie point (TRM). By re-creating the conditions of TRM acquisition in the laboratory, and checking that there is no chemical alteration, the TRM intensity can be normalised to recover an absolute palaeointensity; this is the basis of the Thellier-Thellier technique. The TRM gives a geologically instantaneous reading of the field, whereas DRM depends on the field over the period of time when the magnetic grains are "locked in". The two types of palaeointensity are complimentary: the spot TRM absolute palaeointensity is used to verify and calibrate the continuous sedimentary relative palaeointensity. Palaeointensity varies over the surface of the Earth, so to enable comparison between sites, the Lac du Bouchet palaeointensity is converted to a VDM (virtual dipole moment, the moment of a dipole at the Earth's centre that would cause the recorded intensity) using equations (1) and (2) below. For a VADM (virtual axial dipole moment) an axial geocentric dipole is assumed, and it is proportional to the relative palaeointensity. There is not much difference between the relative VDM and VADM records from Lac du Bouchet.

$$M = Fr^3 (4 - 3\cos^2\lambda)^{-½} \quad (1)$$

$$\tan I = 2\tan\lambda \quad (2)$$

where: M = dipole moment
λ = site latitude
F = site palaeointensity
I = site inclination
r = radius of Earth

Thouveny [1993], compared the Bouchet data with TRM data, and a similar analysis is presented here, using the same TRM data (tabulated in Thouveny's paper), with a slightly different stack and depth→time model for the Bouchet data (figure 8.5). In addition I include the VDMs from lavas from Reunion, in the Indian Ocean, which cover two periods from 0 to 12 ka and from 82 to 98 ka (Chauvin et al. [1991]).

Absolute palaeointensities from lavas are available for only a fraction of the time covered in the Bouchet records. They are geologically instantaneous readings of the field, and they do not sample the field densely enough to be sure of averaging out the short secular variation. Standard deviations of the TRM palaeointensity are typically ¼ of the value for all three data-sets plotted in figure 8.5, but are left off the figure for clarity. The lavas are dated by K/Ar, thermo-luminescence, ^{14}C and one U/Th.

There is general agreement for the period 10 to 40 ka: both volcanic and Bouchet palaeointensities are low from 40 to 30 ka, and then increase to 10 ka. However, there are differences in the details, but it is very difficult to ascribe a particular cause to these because of the uncertainties and assumptions in both the dating and the palaeointensities.

The TRM data from Reunion, dated at between 82 and 98 ka, disagree with the records from Lac du Bouchet and the Somali Basin. Most of this interval, though within the warm $\delta^{18}O$ stage 5, comprises palaeomagnetically reliable Bouchet sediment. There might be a problem with the dipole assumption in calculation of the VDM at Reunion, because the inclinations there (mean 50.9°) differ significantly from those expected from an axial dipole at this latitude (37.5°)

Palaeointensity estimates from cosmogenic isotopes

Cosmogenic isotopes are produced in the stratosphere in reactions involving cosmic rays. The geomagnetic field partially shields the Earth from cosmic rays, so when the field is weak, more rays will penetrate, and the production of ^{14}C and so on will go up. Thus ^{14}C varies inversely to palaeointensity through time. Past changes in ^{14}C are recorded in the carbon of coral skeletons. This completely independent palaeointensity estimate forms a valuable way of testing sedimentary palaeointensities.

Elsasser et al. [1956] developed an equation describing the relative production (Q/Q_0) in terms of the past dipole strength (M):

$$Q/Q_0 = (M/M_0)^{-½} \qquad (3)$$

The situation is complicated by the steeply inclined field at the poles guiding the cosmic rays down (to produce aurorae etc.), so production will be greater there. There is also saturation of production at times of weak field, changes in the cosmic ray flux over this time are also very poorly known, and the recording process is affected by storage of some ^{14}C in the oceans, creating a lag in the record.

The primary motivation for studying this changing production is to correct ^{14}C dates to real, calendar years. The difference is appreciable - ^{14}C dates are younger by 2 and 3 kyr at only 10 to 30 ka. Mazuad et al. [1991] took the relative palaeointensity record of Tric et al. [1992], used (3) to calculate a theoretical production rate, and compared this with the recorded changes in ^{14}C described by Bard et al. [1990]; the two compare quite well (figure 6.2 is a copy of the key figure from Mazaud et al. [1990]). It has been noted both here (section 6.2) and by Tauxe [1993] that the Lac du Bouchet palaeointensity record might well provide a better fit.

In figure 8.5, the U/Th-^{14}C age anomaly can be taken as a rough measure of ^{14}C production. It is at a minimum between 30 and 20 ka, although that interval is very poorly sampled, and then increases to the present day; the Lac du Bouchet records show a broad palaeointensity minimum between 45 and 27 ka, followed by an increase. The correspondence is not exact, but there is agreement over the general trend. More U/Th-^{14}C data would be very useful.

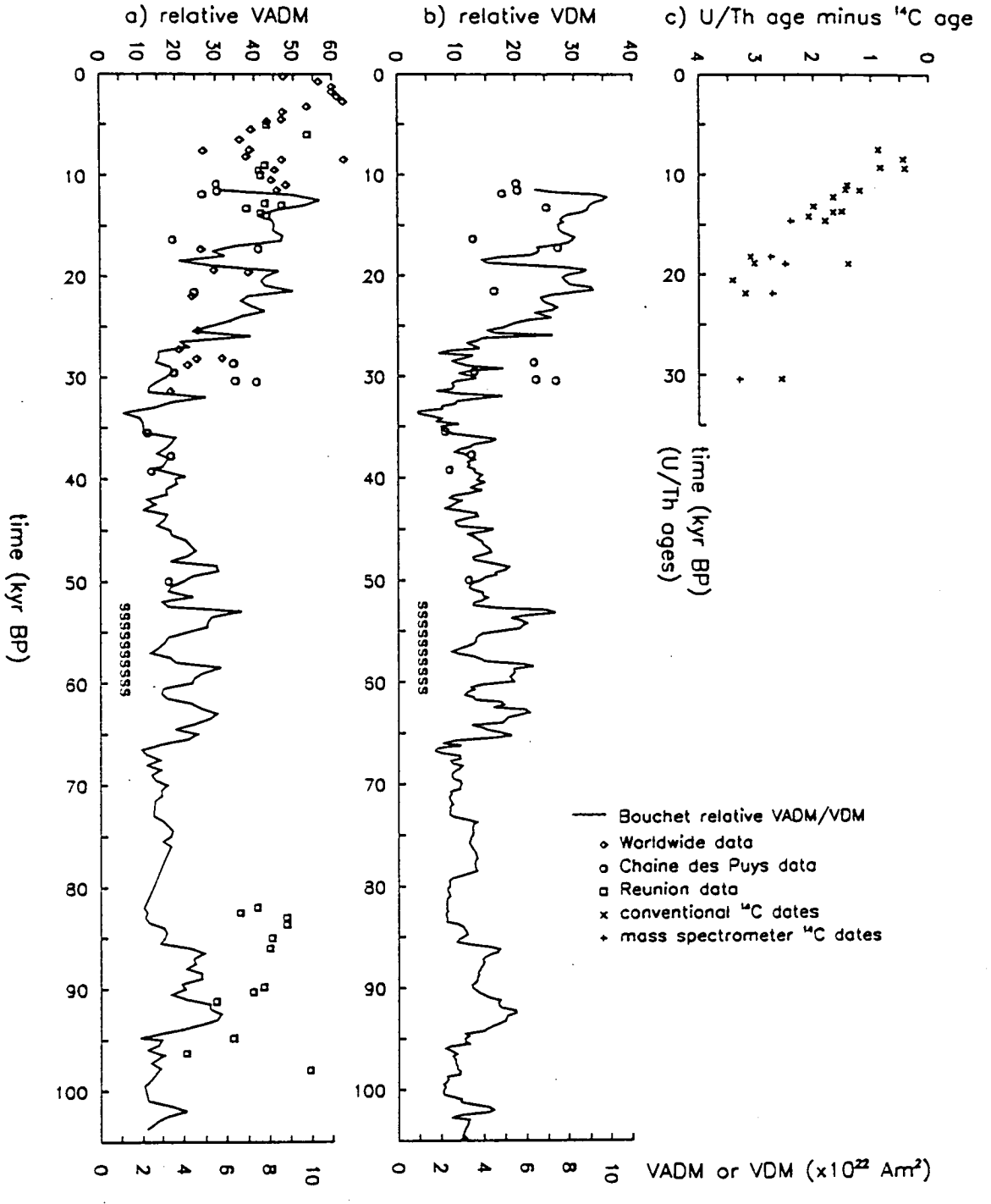

Fig. 8.5 Lac du Bouchet data in comparison with absolute palaeointensities from lavas, and the changing ^{14}C concentration: a) Chaine des Puys (Massif Central, France) and world-wide TRM data are tabulated and referenced in Thouveny et al. [1993]. Reunion (Indian Ocean) TRM data are from Chauvin et al. [1991] (I have assigned working ages by interpolating between the 4 dated lava flows), The relative VADM is NRM_{10mT}/susceptibility from Lac du Bouchet as in figure 8.1; b) Lac du Bouchet relative VDM was calculated using inclinations and NRM_{10}/susceptibility in equations (1) and (2) in the text; c) data from Bard et al. [1990], greater age difference = weaker dipole moment (see text). N.B. in (a) and (b) the Lac du Bouchet data and the TRM V(A)DMs are on different scales, and are only roughly matched to enable general comparison. "sss" = slump. Bouchet data dated using depth→time model 1, based on Specmap (figure 6.6). The present-day moment of the dipole is about 8×10^{22} Am^2.

Other reactions depend on the cosmic ray flux, and therefore on the dipole moment. For example, nitrogen (N_2) is dissociated by cosmic rays (mostly secondary electrons) at mid to high latitudes, and reacts with O_2 to form NO, which is a climatically sensitive compound because it catalyses the dissociation of ozone, O_3 (Thouveny [1993], Nicolet [1975], Johnson [1974]).

8.6 Spectral analysis

Spectral analysis was performed on the 300 kyr palaeointensity record from Lac du Bouchet, using Lomb-Scargle and FFT methods (figure 8.6). Windows of the data of length 200 kyr were analysed as a rudimentary test of stationarity.

The main power is concentrated at long periods, greater than 15 kyr, and is concentrated in two peaks, one at 105 - 130 ka, and one at 59 - 70 ka. Minor peaks are found at ~42, ~30 and ~24 kyr. These have a different form to the peaks in susceptibility (see figure 8.3), so the majority of the palaeoenviromental signal (and therefore the Milankovitch periodicities) has been successfully normalised out of the NRM intensity record.

The concentration of spectral power in periods of a few 10 kyrs is a significant result in terms of the geomagnetic processes in the Earth's core, because theoretical geomagnetists usually concentrate their efforts at analysing changes on much shorter time-scales. This result indicates that long term changes are also important.

Both of the main peaks have only a few wavelengths in the record, so it is not possible say whether or not these periodicities are significant stable features of the geomagnetic dynamo. The periodicities that result from the analysis depend very much on the dating of the sequence. They also depend on features at specific intervals in the records which can be ignored (visually) in the time domain, but which cannot in the frequency domain. In this respect, the Lomb-Scargle method has a clear advantage, because gaps where palaeomagnetically unreliable intervals have been removed are ignored, whereas the FFT requires an evenly spaced record with gaps filled by interpolation. Different-looking spectra can be produced from small changes in stacking, processing or dating, and this is borne in mind when looking at such spectral analyses.

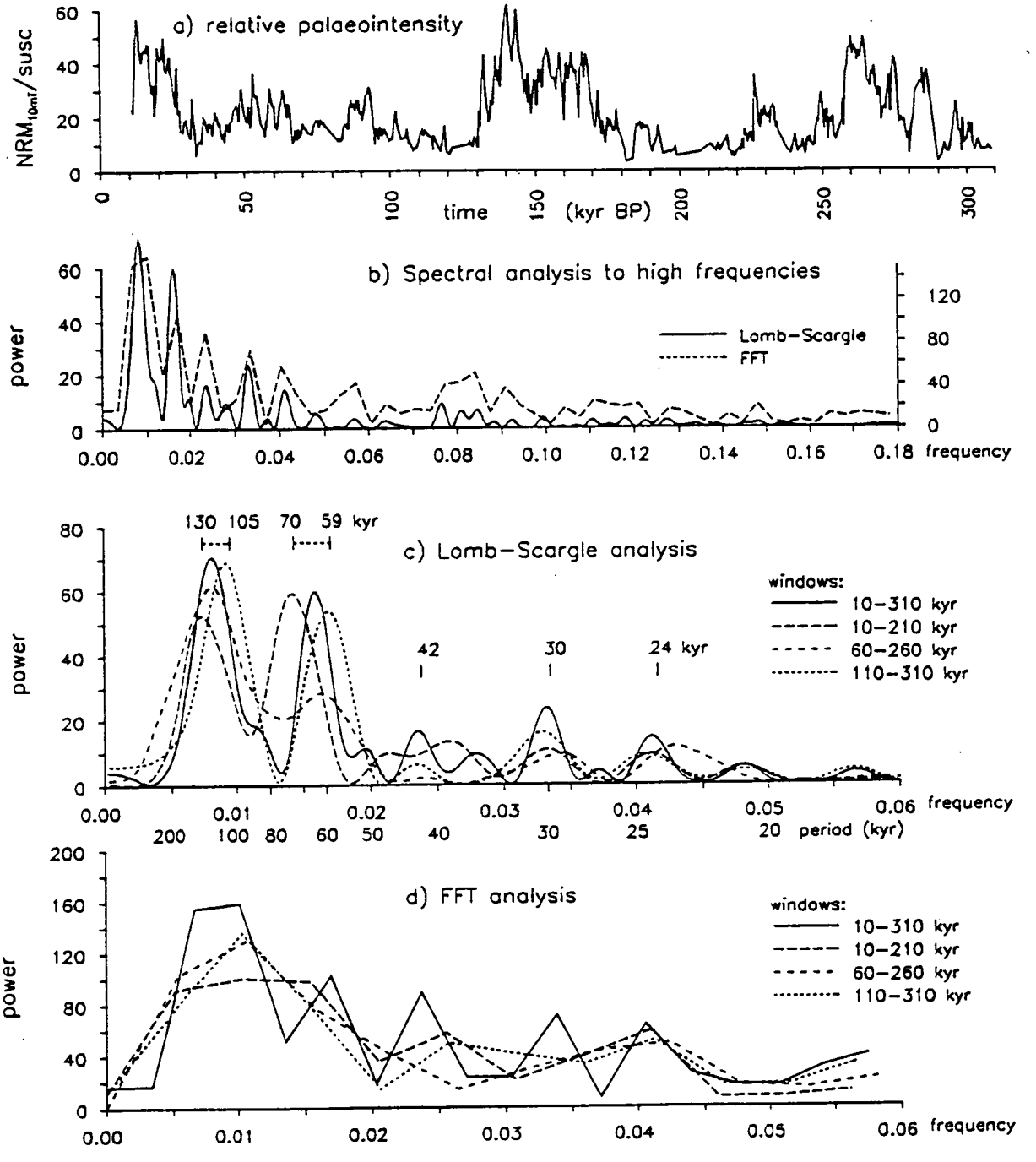

Fig. 8.6 Spectral analysis of the Lac du Bouchet palaeointensities: a) the palaeointensity time-series, (NRM_{10mT}/susceptibility), dated using depth→time model 1 (based on Specmap); b) Lomb-Scargle and FFT analysis of (a) down to short period (high frequency); c) Lomb-Scargle analysis of windows of the palaeointensity record; d) FFT analysis of windows of the palaeointensity record.

8.7 Excursions

Excursional directions are not found in the Lac du Bouchet sediments, but ages of excursions correspond to low palaeointensities at Lac du Bouchet.

Definition. Excursions have been defined as a "sequence of virtual geomagnetic poles which reach intermediate latitudes [or more] for a short interval of time before returning to the original polarity" (reported in Verosub and Banerjee's review [1977]). Champion et al. [1988] prefer the name "short polarity reversals", or subchrons, for excursions with unambiguously, multiply-reported fully reversed directions, but I will call the whole set of short events "excursions" throughout.

The problem. It is a reflection of the poor understanding of geomagnetic behaviour that excursions are defined using virtual poles, a concept which looses its meaning when the field departs significantly from its normal, predominantly dipole behaviour, as it does during excursions. Study of a detailed records of both direction and intensity, such as we have from Lac du Bouchet, gives a better understanding.

Previous work. Cox [1968] predicted that, given a stochastic reversal process and therefore Poisson polarity distribution, there ought to be many short duration (>50 kyr) polarity intervals which were yet to be found. Also, intuitively, each large departure from axial dipole behaviour will not necessarily result in a reversal, so times of excursional behaviour ought to be found within a single polarity interval. Four such excursions have been multiply-reported for the last 300 kyr: Laschamp / Olby; Blake; Jamaica / Biwa I; and Levantine / Biwa II (Champion et al. [1988], shown in figure 8.1). The relation between the Laschamp excursion and the Lac du Bouchet record has been discussed in detail in Thouveny and Creer [1992a, 1992b]. Lac du Bouchet has an ideal location to study the recording of excursions in sediments, as the Laschamp excursion was originally discovered in lava flows only 100 km away from Bouchet, so any differences due to non-dipole behaviour of the field are negligible. They concluded that excursions must be "ephemeral secular variation features", brief events of a few centuries maximum duration, by assuming they were not seen in the record because of the smoothing of the input signal during the locking-in time, when it is recorded as a DRM. An alternative explanation is that the field does have excursional directions for a longer time, but the DRM acquisition is less effective in weak fields or the locking-in time is longer than studies suggest.

In a similar fashion to relative palaeointensities, excursional directions found in sediments are open to over-interpretation. I have tried to follow the position set out by Verosub and Banerjee [1977] and Thompson and Berglund [1976] in not under-estimating the effect of on the palaeomagnetic signal of lithology and coring disturbance.

Excursions at Lac du Bouchet? Figure 8.1 shows the Lac du Bouchet palaeointensity and direction records, with the susceptibility record given as a lithological control. Excursions as compiled by Champion et al. [1988] are also given. No excursional directions are found, partly because any errant directions were discarded during the direction processing, as artefacts of the coring process (section 5.6). Times of very low palaeointensity occur in palaeomagnetically reliable sediment (i.e. not organic-rich, slumped or missing) (figure 8.1). These times are found within longer intervals of low palaeointensity. There is a good correspondence, given dating uncertainties, of the low palaeointensities and times of reported excursions, especially for the Laschamp, Blake and Jamaica excursions. Further palaeointensity lows occur at other times, especially in the lower third of the record. Palaeointensity lows are also found at the time of the Laschamp and Blake excursions in the records of Tric [1992] and Meynadier [1992].

Excursions and low palaeointensity. Excursions are more likely to occur when the dipole field is weak and the non-dipole field is relatively strong, compared with the normal (≈ present day) situation. Verosub and Banerjee [1977] report work by Harrison and Ramirez [1975] of a simple excursion model: an anti-parallel dipole at the core-mantle boundary needs to have only 11% of the moment of the main dipole to give fully reversed directions, 20% of normal field intensity, and >40° deviations over 3 to 6% of the Earth's surface. When the main dipole is reduced to the extent indicated by the palaeointensity records from Bouchet and elsewhere (figure 8.4), excursional directions would be much easier to generate. In this framework (similar to that of Verosub and Banerjee), excursions are enabled by a low dipole moment and a more dominant non-dipole field than today (at present an axial dipole accounts for 80% of the field). Excursional directions would often be regional in nature, and be of variable, possibly short, duration. Several excursions could occur in an interval of time bounded by a broad palaeointensity low (weak dipole moment). Excursional directions would imply a low dipole moment rather than an axial dipole at a large angle.

Such a view of excursions could reconcile the non-appearance of excursional directions at Lac du Bouchet, and perhaps reconcile even more difficult results, like those of Nowaczyk and Baummann [in press], who report extended intervals of reversed directions from several Arctic marine sediment cores over the last 150 kyr.

Excursions and reversals. Reversals of the magnetic field direction are often located within low palaeointensity episodes, although there is caution about taking this to be a general result (see the compilation of palaeointensity records at reversals in Tauxe [1993]). This might mean that excursions and reversals are similar phenomena, the difference being that with reversals the dipole moment reduces to such an extent that it can just as easily re-gain moment in the opposite polarity. This is not inconsistent with the "saw-tooth" theory of

Valet and Meynadier [1993], in which the palaeointensity decays over a long period of time until it reverses to a relatively high moment, then decays again until the next reversal and so on.

This study of the Lac du Bouchet palaeofield agrees with Champion et al. [1988] that excursions and reversals are due to a common underlying source, but it does not agree with their suggestion that full reversals do not take place at excursions because the excursional palaeointensity is too low.

Summary. In summary, low palaeointensities correspond to times of reported excursions. This is what would be expected if there was a weak dipole field and a relatively strong non-dipole field.

8.8 Fine-scale magnetostratigraphy

The use of the geomagnetic reversal sequence for stratigraphy is familiar, but the reversal interval is too large to be of use on the shorter scale of a kyrs or 10 kyrs. Other features of the geomagnetic field have been proposed to be of use for stratigraphy on shorter scales.

Excursions have proved problematic for magnetostratigraphy, because spurious excursional directions can easily be produced by sedimentary structures or coring effects. Their nature is poorly understood, and they may often only be regional in extent. Additionally, if the occurrence of excursions is enabled by a low dipole moment, several excursions may occur at different localities and at different times within the broad palaeointensity low.

Magnetostratigraphy by palaeosecular variation in direction has met with some success on a regional scale. A Holocene master curve from British lake sediments was set up (Turner and Thompson [1981]), and other European records matched to it, although independent dating was stressed as a necessary check.

Palaeointensity variations (those discussed in sections 8.4 and 8.5) might be used for fine scale magnetostratigraphy, because the variations are large and distinctive (figure 8.4). However, before this could be possible, a definitive illustration of the validity of sedimentary palaeointensity, a well dated reference curve, and a better understanding of the regional variations, would all have to be obtained. Probably the most realistic use would be as an independent correlation tool to supplement the marine $\delta^{18}O$ stratigraphy.

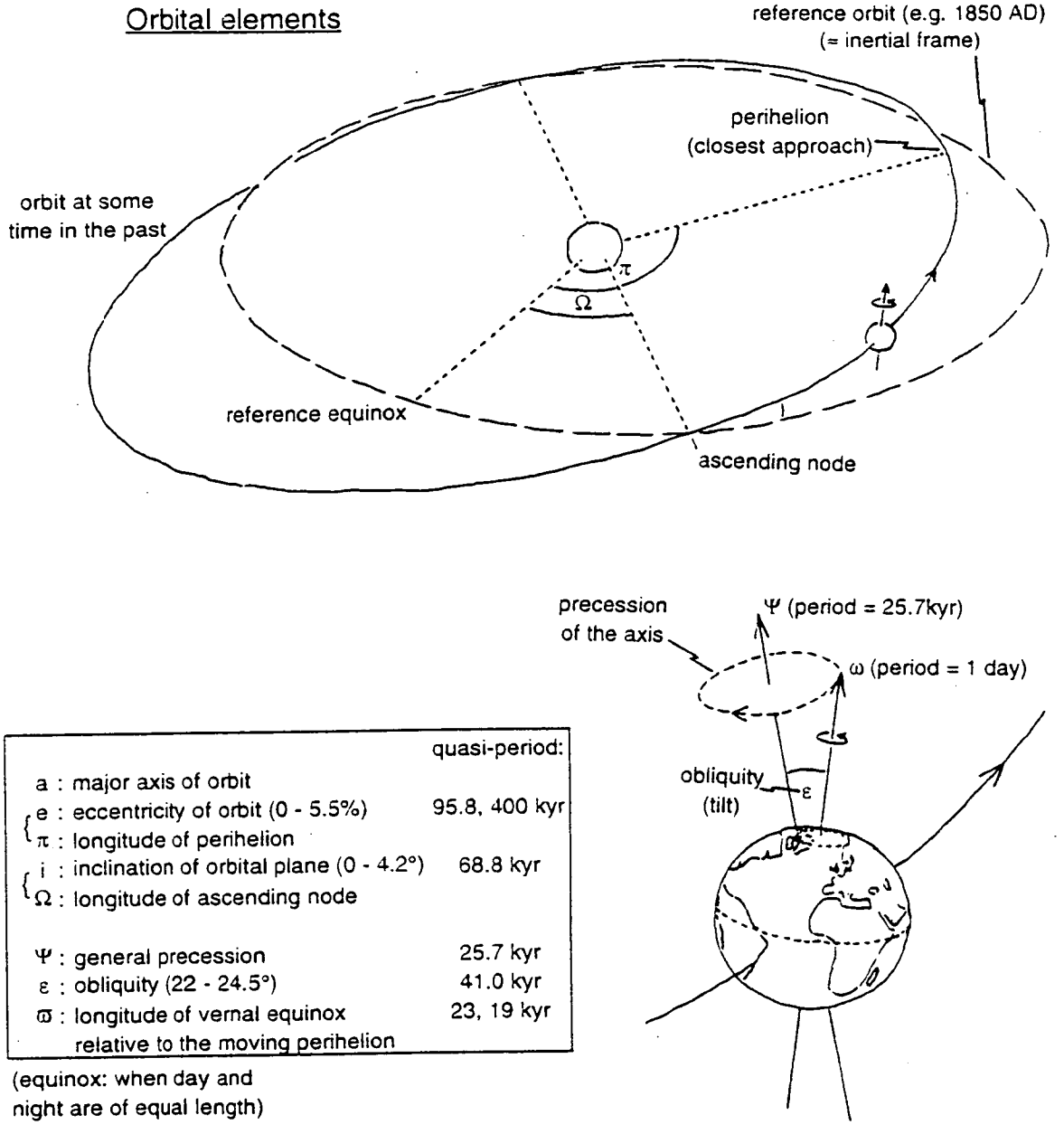

		quasi-period:
a	: major axis of orbit	
e	: eccentricity of orbit (0 - 5.5%)	95.8, 400 kyr
π	: longitude of perihelion	
i	: inclination of orbital plane (0 - 4.2°)	68.8 kyr
Ω	: longitude of ascending node	
Ψ	: general precession	25.7 kyr
ε	: obliquity (22 - 24.5°)	41.0 kyr
ϖ	: longitude of vernal equinox relative to the moving perihelion	23, 19 kyr

(equinox: when day and night are of equal length)

Fig. 8.7 Orbital elements. See Berger [1976].

8.9 Geomagnetism and the Earth's orbital variations

Periodicities have been found in palaeomagnetic records which are similar to periodicities of aspects of the Earth's orbital variation, and it was therefore suggested that the orbital variation might perturb the geomagnetic dynamo (Kent and Opdyke [1977], Creer et al. [1990]). The method of inference has been, simply, periodicity matching. The only mechanism for a link that has been studied in any depth was proposed by Malkus [1963, 1968], but was found to provide insufficient energy to drive the geodynamo (Rochester et al. [1975]).

Some aspects of the Earth's orbital variation (eccentricity, precession of the equinoxes, and axial obliquity) are familiar from the Milankovitch theory of climate change, because they affect the amount of sunlight received by the Earth (insolation). When assessing the possibility of orbital influence over the geodynamo by an unknown mechanism, it makes sense to consider all the variations of the Earth's orbit and spin axis (figure 8.7). The Earth's orbit is fully described by six elements: eccentricity (e); length of the semi-major axis (a); longitude of perihelion (π); inclination of the orbit (i); the longitude of the node (Ω); and the position of the Earth on this orbit. Two further parameters affect the Earth's spin axis: precession (Ψ, sometimes denoted by Ω, but Ψ is used here to avoid confusion); and axial obliquity (tilt) (ε). The variation of these parameters over the last 5 myr and also for the next 1 myr is given in Berger [1976].

If a periodicity was found to be common to both orbital changes and the geodynamo, this would imply some mechanism to link the two. As yet, the only such mechanism to be described is by Malkus [1968]: if left to their own devices, the core and the mantle would precess at different rates (because their dynamic ellipticities differ), but because they are constrained to move together, a force acts at the core-mantle boundary. Rochester et al. [1975] calculate the power generated by this mechanism to be in the region of 10^8 watts, as compared to the power needed to drive the geodynamo, which is between 10^9 and 10^{12} watts (the amount needed to overcome ohmic dissipation in the core). This precessional force delivers a constant power, but a dipole moment varying periodically with some aspect of the orbit would imply a varying power input. The precessional power is modulated by about 10% by the obliquity as it varies from 22° to 24.5° (Chappell [1975]). Substituting the limiting values of obliquity into equations (23) and (43) of Rochester et al. [1975], I find that the power input varies by about 20%. This power input is at least 2 orders of magnitude too small to drive the geodynamo, though it might conceivably perturb it. It is noted that no convincing evidence has been found for a stable 41 kyr periodicity in any palaeomagnetic records.

Kent and Opdyke [1977] studied core RC10-167 from the Pacific Ocean off Japan, and found a periodicity of 43 kyr in their relative palaeointensity record (NRM normalised with ARM), based on dating which assumed a constant sedimentation rate and the Brunhes-Matuyama boundary at 700 ka. This periodicity is stretched to 48 kyr when the currently accepted age for the reversal, at 780 ka (Cande and Kent [1992]), is used. They suggested that their 43 kyr periodicity corresponds to the Earth's obliquity variation, but the revised dating of the core makes this less likely.

Wollin et al. [1978] found a ~100 kyr periodicity similar to the eccentricity period, but used non-normalised intensity records, which have been discredited (Kent [1982]).

For the Lac du Bouchet 120 kyr records of inclination, declination and NRM intensity, Creer et al. [1990] found most of the spectral power in periodicities between 20 and 50 kyr. They note that the periods of precession and axial obliquity also fall in this band, and suggest that these orbital variations might have perturbed the geomagnetic dynamo.

All of this evidence for a link is weak: the inferences are based on records from a single sites; the dating control is poor for Kent and Opdyke's record; the 20m Lac du Bouchet records are too short to be meaningful; the 41 kyr periodicity might be due to an imperfect removal of the palaeoclimatic signal; and any variations in the field might well be due to processes internal to the core.

The periodicities found in the 300 kyr Lac du Bouchet relative palaeointensity record, of 105 - 130 kyr and 59 - 70 kyr, are similar to the periodicities for variations of orbital eccentricity (mean of 96 kyr) and the inclination of the orbital plane (68 kyr). The weak peak at 42 kyr is similar to the axial obliquity period of 41 kyr. Again, this is very weak evidence for a link, because some doubt remains over the dating of the sediments, the results come from a single site, and the record is still not really long enough for the periodicities to be reliable enough to be considered as stable features of the geodynamo.

Spectral analysis of the RC10-167 core palaeointensity record (new dating) by Tauxe [1993] finds a 40 kyr periodicity for the interval 300 - 780 ka. Peaks of 65 - 75 kyr and 105 - 115 kyr are also apparent in her analysis, and these are similar to the peaks found in the 300 kyr Lac du Bouchet relative palaeointensity record. However, the correspondence between the two series in the time domain is not good, so it is still difficult to claim this as evidence of orbital periodicities in the geodynamo. Unlike the 41 kyr and ~100 kyr periodicities (obliquity and eccentricity), the 69 kyr periodicity (inclination of the orbital plane) does not affect the insolation or the climate, so it cannot be said that this periodicity results from inadequate removal of a palaeoclimatic signal in the intensity normalisation.

8.10 Summary

Records of inclination, declination and intensity of the geomagnetic field over the last 310 kyr have been produced from the Lac du Bouchet sediment sequence.

The relative palaeointensity record was obtained by partially demagnetising the NRM intensity at 10mT, and normalising out the effects of the magnetic mineralogy with susceptibility. Neither the choice of normalisor nor the choice of demagnetisation step were found to be critical. Low susceptibility ($<4.2\times10^{-6}$ m^3/kg) characterises the organic samples, which are found to be poor recorders of the field (figure 4.1); they have been removed from the relative palaeointensity record. The record bears little similarity to the to the susceptibility (environmental) record, either in the time or the frequency domain, suggesting that the normalisation has been successful. Long period, large amplitude variations are shown by the relative palaeointensity record, and lows down to 10% of the maximum intensity occur.

In comparison with other relative palaeointensity records from around the globe, the Lac du Bouchet record matches well with some, but not with others. Comparison with independent measures of palaeointensity from TRM in volcanic lavas and in the changing concentration of cosmogenic ^{14}C reveals agreement in the general rising trend in palaeointensity from 30 to 10 ka, but there are differences in the details. In these comparisons, it is difficult to say whether the differences are due to the non-dipole field, imperfect recording/recovery of the geomagnetic signal, or dating errors.

On the whole, the agreement over general trends suggests that palaeointensities from sediments have some merit. This situation is perhaps as good as could be expected with the few available records; it will take more records from around the globe to clarify the picture and to reach a consensus on whether or not sedimentary palaeointensity actually "works", and to find what a global average palaeointensity curve looks like for the past few 100 kyrs.

Low palaeointensities at Lac du Bouchet correspond to times of reported excursions. This is what would be expected if there was a weak dipole field and a relatively strong non-dipole field.

Spectral analysis of the Lac du Bouchet relative palaeointensity record reveals that spectral power is concentrated at long periods. Peaks are found at periodicities of ~115 kyr and ~65 kyr, with minor peaks at ~42, ~30 and ~24 kyr. The 65 kyr periodicity is similar to the periodicity in variation of the inclination of the Earth's orbital plane (68.8 kyr), and is also found in a palaeointensity record from the west Pacific. The significance of periodicities found by spectral analysis is uncertain, mainly because of uncertainties in the dating and the short length of the Lac du Bouchet record relative to the periodicities found. A periodic variation of the geodynamo might still be due to processes internal to the core.

Chapter 9

Conclusions

A 300 kyr record of geomagnetic palaeointensity has been recovered from the sediment sequence of Lac du Bouchet which displays large amplitude, long period variation. A 300 kyr magnetic susceptibility record from the same sequence reflects changes in the local palaeoenvironment, itself related to the global Quaternary palaeoclimatic changes.

The present study in relation to previous studies of the Lac du Bouchet sediments

The results obtained from previous studies have formed a sound base for the present work, and many of the results are confirmations of previous results, but for the new sediment available from the new cores. The principal advance has been the acquisition of records representing a much longer time-span: 300 kyr with the present 50m cores compared with 120 kyr from the previous 20m cores (table 1.2). This was enabled by heavier duty coring equipment, and limited by the base of fine sediments at 50m depth. The study has been split into palaeoenvironmental and palaeomagnetic aspects, in contrast to previous studies, which concentrated on the latter. Dating by correlation to the marine $\delta^{18}O$ stratigraphy has played a greater role, because only the top of the sequence is directly dated. The study of palaeointensities has built on the work of Thouveny, Smith and Creer on the upper Lac du Bouchet sediments, and has also been able to incorporate the new wave of studies of long records of relative palaeointensity from sediments.

Summaries of conclusions from the chapters

Dating. The dating of the sediment sequence is a critical part of the study, because it enables comparison to other records from around the globe, and also allows time spectral analysis. The upper 45 kyr of the sequence was already well dated by ^{14}C, and the bulk of the sequence is dated by matching the warm episodes at Lac du Bouchet (clearly identified by palynology) to the warm stages of the marine $\delta^{18}O$ stratigraphy. The base reaches down to stage 9, and the sequence covers three full glacial-interglacial cycles.

Palaeoenvironmental aspects. At Lac du Bouchet, susceptibility reflects the concentration of magnetite, and is low in the organic-rich sediment deposited under warm climatic conditions. There is an excellent inverse correlation between the susceptibility record and the arboreal / non-arboreal pollen ratio (tree pollen %) record, which is high under warm climatic conditions. Therefore susceptibility may be used as an indicator of palaeoenvironment in the case of Lac du Bouchet. The mechanism by which it is lowered in organic-rich sediments involves a decreased detrital sedimentation rate (due to decreased

erosion of the magnetite-rich crater walls), with dilution due to an increased organic sedimentation rate; diagenesis of the magnetite might also play a part.

The sediments record environmental changes with a high resolution: a sample of width 2cm represents between 200 years (in glacial sediments) and 400 years (in organic-rich sediments). Sample spacing averages out at about 1.2cm when all 4 cores are taken into account.

The broad sequence of warm and cold climates at Lac du Bouchet corresponds closely to the global climate revealed by the marine $\delta^{18}O$ ice volume record. The correlation during warm $\delta^{18}O$ stages 5 and 7 is closer than the correlation during glacial stages 2, 3, 4 and 6. Spectral analysis of the susceptibility record reveals the insolation (Milankovitch) periodicities of ~100, 41 and 23 kyr.

Fast environmental changes are evident from both magnetic and palynological records, and in both warm and cold stages. The short intervals of increased tree pollen and low susceptibility between 30 and 45 ka may well be related to the Dansgaard-Oeschger events seen in Greenland ice and north Atlantic sediments, but dating uncertainty prevents any one-to-one correlation. However, the Dansgaard-Oeschger events cover a longer time-span than the short warm events at Bouchet, and perhaps the more important result is that the environment in southern France under glacial conditions often shows some independence from the large changes going on both in the neighbouring Greenland / north Atlantic region (up to 5° temperature swings), and world-wide. Short warm events are also seen in $\delta^{18}O$ stages 6 and 8 at Lac du Bouchet.

Rapid fluctuations are found in the organic-rich sediments corresponding to the warm $\delta^{18}O$ stages 5 and 7. The rapid changes in $\delta^{18}O$ stage 5e found in the GRIP ice core from Summit, Greenland, match well to the susceptibility record at Lac du Bouchet. The potentially very important result that previous interglacials have been unstable in at least two regions awaits more detailed palynological work on the Lac du Bouchet cores, and it is noted that this fine structure of stage 5e is not reproduced in the sister ice core GISP2 or at the other French long-core pollen sites. Marine sediments typically do not have the resolution to detail such fine structure.

Palaeomagnetic and geomagnetic aspects. The direction and relative intensity of the geomagnetic field at Lac du Bouchet over the last 300 kyr have been recovered. The resolution is slightly less good than for palaeoenvironmental work, because the geomagnetic signal is smoothed due to the acquisition of the remanence over a small depth range below the sediment-water interface. The glacial sediments are very good recorders of the field, because the composition of the magnetic mineral (low Ti titanomagnetite) and its grain-size (~4 - 8μm) are consistent down-core, and the concentration varies only modestly. The

organic-rich sediments are less good at recording the field - inclination is generally shallowed and only low intensities are recovered. Older than 160 ka, the declinations are disturbed by Mazier corer (used to collect the deeper parts of the sequence).

The palaeomagnetic study has concentrated on the relative palaeointensity record. Sediments deposited under warm conditions, characterised by low susceptibilities, were removed from the intensity records. Secondary magnetisations have been removed from the NRM intensity by demagnetisation in a 10mT alternating field. The effects of the magnetic mineralogy could be removed by normalisation with any of susceptibility, ARM or SIRM, because of the consistent down-core magnetic mineralogy; susceptibility was preferred because all samples had had this property measured.

Different physical and chemical conditions (e.g. lock-in depth, diagenesis of the magnetite) in organic-rich and non-organic sediment affect the fidelity of DRM recording. The (very) low susceptibilities in organic-rich sediment are not totally explained by the changes in detrital mineral %, so diagenesis may remove some, and at the same time cause the observed degradation of the geomagnetic signal. However, as the organic-rich sediments have been removed from the analysis, the remaining records should not be significantly affected.

The palaeointensity record obtained in this way displays large amplitude variation, with spectral power concentrated at long wavelengths. These changes are not an intuitively expected result. The size of the changes implies that the dipole field is changing, and the changes should therefore be seen globally. The implication is that time-scales of a few 10 kyrs are important in the geomagnetic processes of the Earth's core.

Times of reported excursions fall during times of low relative palaeointensity. This is to be expected if the dipole field is low and the non-dipole field is more dominant. Excursions would then be often regional in extent, possibly short (a few centuries), and their occurrence bounded in time by the low dipole moment. No clear excursional directions are observed at Lac du Bouchet.

The data-set of comparable sedimentary relative palaeointensity records of similar rock-magnetic reliability and time-span from around the globe is still rather small. The whole set shows similar ranges of variation, and there is some agreement over general trends, but there are differences in the details and in the timing of some peaks and troughs. The differences are due to the non-dipole field (between geographically separated sites), poor dating of some records, and poor recording of the field; in order to gauge the contributions of these alternatives, more well dated independent records are needed. There is a similar agreement over general trends when the Lac du Bouchet record is compared with palaeointensities derived from entirely independent recording methods: from TRM in lavas and ^{14}C variations.

More sedimentary palaeointensity records are needed before a consensus can be reached over a global standard record of relative palaeointensity over the last few 100 kyr. Some doubt remains over the method of sedimentary palaeointensity, due to the only qualitative understanding of the acquisition process under geological conditions. However, the general agreement between independent records (to which this study contributes) indicates that the method has some merit.

Spectral analysis of the Lac du Bouchet palaeointensity record confirms that spectral power is concentrated at long periodicities. Two major peaks in the spectra are found at ~ 125 and ~65 kyr, and the quality of this result depends on correct dating of the sediments.

Investigation of any astronomical influence over the geodynamo is one of the stated aims of both the Euromaars project and this Ph.D. The ~65 kyr periodicity is similar to the periodicity for the inclination of the orbital plane (68 kyr). It is certain that this periodicity is not due to inadequate normalisation of the environmental component in the NRM intensity, because it is not one of the Milankovitch periodicities that affect palaeoclimate (although a small ~65 kyr peak also occurs in the susceptibility spectra). There is a minor 40 kyr peak in the Lac du Bouchet relative palaeointensity spectra. Periodicities of 40 kyr and around 65 kyr are also found in a new analysis of the relative palaeointensity from marine sediment core RC10-167 (Tauxe [1993]). The only mechanism that has been proposed for a link between orbital variation and geomagnetism is that of precessional torques. Substituting the limiting values for obliquity into Rochester et al.'s [1975] equations, this small energy input into the core is modulated by ±10% by obliquity (periodicity 41 kyr). Speculation that the observed palaeointensity periodicities are due to changes in the Earth's orbital motion is perhaps unwise, given the early stage of studies of relative palaeointensity from sediments, the (short) length of the Bouchet record, the unsound dating of marine records, and the lack of a described mechanism by which the orbit and the core are linked.

Further work

Further work is already being carried out in Marseille on the sediment sequences of Lac St.Front and Praclaux (both within a few miles of Lac du Bouchet), and these will go far to confirm and support the palaeoenvironmental and palaeomagnetic records from Lac du Bouchet. Lac St.Front contains records twice as detailed as those of Lac du Bouchet for the last 75 kyr, and the sediments from the dry maar Praclaux will extend the maar records from the region to 400 ka.

Palaeomagnetic sampling and analysis of the interval between 46 and 50m depth in the Lac du Bouchet cores (unsampled due to the hardness of the sediment) needs to be carried out to complete the palaeomagnetic records for the whole of the available sequence.

Good dating of sedimentary records is of paramount importance for the comparison of different records, and for spectral analysis. The argon-argon dates for the tephra at 42.5m depth are of immediate concern.

Further independent records of relative palaeointensity from sediments are needed to improve the global data-set, with the aim of creating a standard record of dipole moment changes over the past few 100 kyrs. Indeed, for both palaeoenvironmental and palaeomagnetic studies, other long, well-dated, continuous records, of the quality of those from Lac du Bouchet, from different regions of the globe, will contribute to both spatial and temporal understanding of geomagnetic and climatic changes back in time.

Epilogue

Finally, Edinburgh's James Clerk Maxwell on the scientific method [1874]. (A lesson to all scientists to be wary of the temptations of poetry):

Hail, Nonsense! dry nurse of Red Lions,
  From thee the wise their wisdom learn,
From thee they cull those truths of science,
  Which into thee again they turn.
What combinations of ideas,
  Nonsense alone can wisely form!
What sage has half the power that she has,
  To take the towers of Truth by storm?

References

Bard, E., Hamelin, B., Fairbanks, R.G. & Zindler, A. (1990a). Calibration of the ^{14}C timescale over the past 30,000 years using mass spectrometric U-Th ages from Barbados corals. Nature, 345, 405-410.

Bard, E., Hamelin, B., & Fairbanks, R.G. (1990b). U-Th ages obtained by mass spectrometry in corals from Barbados: sea level during the past 130,000 years. Nature, 346, 456-458.

de Beaulieu, J.L. & Reille, M. (1992). The last climatic cycle at la Grande Pile (Vosges, France): a new pollen profile. Quaternary Science Reviews, 11, 431-438.

Berger, A.L. (1976). Obliquity and precession for the last 5000000 years. Astronomy and Astrophysics, 51, 127-135.

Berger, A.L. (1988). Milankovitch theory and climate. Reviews of Geophysics, 26, 624-657.

Bertrand, P., Brocero, S., Lallier-Verges, E., Tribovillard, N. & Bonifay, E. (1992). Sédimentation organique lacustre et paléoclimats du Pléistocène aux moyenes latitudes: exemple du Lac du Bouchet, Haute Loire, France (résultats préliminaires). Bull. Soc. géol. France, 163, 427-433.

Bond, G., Broecker, W., Johnsen, S., McM anus, J., Labeyrie, L., Jouzel, J. & Bonani, G. (1993) Correlations between climate records from North Atlantic sediments and Greenland ice. Nature, 365, 143-147.

Bonifay, E., Creer, K.M., de Beaulieu, J.L., Casta, L., Delibrias, G., Perinet, G., Pons, a., Reille, M., Servant, S., Smith, G., Thouveny, N., Truze, E. & Tucholka, P. (1987). Study of the Holocene and late Würmian sediments of Lac Du Bouchet (Haute-Loire, France): first results. In: "Climate - History, Periodicity and Predictability," eds. Rampino, Sanders, Newman & Königsson, Van Nostrand Reinhold Co., New York, pp588.

Blunk, I. (1989). Magnetic susceptibility anisotropy and deformation in Quaternary lake sediments. Z. dt. geol. Ges., 140, 393-403.

Broecker, W.S., Andree, M., Bonani, G., Wolfli, W., Oeschger, H., & Klas, M. (1988). Can the Greenland climatic jumps be identified in records from ocean and land? Quaternary Research, 30, 1-6.

Broecker, W.S. & Denton, G.H. (1989). The role of ocean-atmosphere reorganisations in glacial cycles. Geochimica et Cosmochimica Acta, 53, 2465-2501.

Cande, S.C. & Kent, D.V. (1992a). A new geomagnetic polarity time scale for the late Cretaceous and Cenozoic. Journal of Geophysical Research, 97 (B10), 13917-13951.

Cande, S.C. & Kent, D.V. (1992b). Ultrahigh resolution marine magnetic anomaly profiles: a record of continuous palaeointensity variations? Journal of Geophysical Research, 97 (B11), 15075-15083.

Champion, D.E., Lanphere, M.A. & Kuntz, M.A. (1988). Evidence for a new geomagnetic reversal from lava flows in Idaho: Discussion of short polarity reversals in the Brunhes and late Matuyama polarity chrons. Journal of Geophysical Research, 93 (B10), 11667-11680.

Chappel, J. (1975). On possible relationships between upper Quaternary glaciations, geomagnetism, and vulcanism. Earth and Planetary Science Letters, 26, 370-376.

Chauvin, A., Gillot, P-Y. & Bonhommet, N. (1991). Palaeointensity of the Earth's magnetic field recorded by two late Quaternary volcanic sequences at the island of La Réunion (Indian Ocean). Journal of Geophysical Research, 96 (B2), 1981-2006.

Constable, C.G. & Tauxe, L. (1987). Palaeointensity in the pelagic realm: marine sediment data compared with archaeomagnetic and lake sediment records. Geophysical Journal of the Royal Astronomical Society, 90, 43-59.

Creer, K.M. (1991). Dating of a maar lake sediment sequence covering the last glacial cycle. Quaternary Proceedings, 1, 75-87.

Creer, K.M., Thouveny, N. & Blunk, I. (1990). Climatic and geomagnetic influences on the Lac du Bouchet palaeomagnetic SV record through the last 110000 years. Physics of the Earth and Planetary Interiors, 64, 314-341.

Dansgaard, W., Johnsen, S.J., Clausen, H.B., Dahl-Jensen, D., Gundestrup, N.S., Hammer, C.U., Hvidberg, C.S., Steffensen, J.P., Sveinbjörnsdottir, A.E., Jouzel, J., & Bond, G. (1993). Evidence for general instability of past climate from a 250-kyr ice-core record. Nature, 364, 218-220.

Day, R., Fuller, M. & Schmidt, V.A. (1977). Hysteresis properties of titanomagnetites: grain-size and compositional dependance. Physics of the Earth and Planetary Interiors, 13, 260-267.

Ellingsen, K.L., Løvlie, R. & Seret, G. (1992). Magnetomineralogy and revised excursions for the last interglacial-glacial cycle in the Grande Pile lacustrine sequence, France. Quaternary Research, 37, 16-28.

Emiliani, C. (1955). Pleistocene temperatures. Journal of Geology, 63, 539-578.

Gilbert, W. (1600). De magnete. 1958 Dover edition of 1893 translation by P. Fluery Mottelay, Dover Publications Inc.

Grootes, P.M., Stuiver, M., White, J.W.C., Johnson, S. & Jouzel, J. (1993). Comparison of oxygen isotope records from the GISP2 and GRIP Greenland ice cores. Nature, 366, 552-554.

Guiot, J. (1990). Methodology of the last climatic cycle reconstruction in France from pollen data. Palaeogeography, Palaeoclimatology, Palaeoecology, 80, 46-69.

Guiot, J., Pons, A., de Beaulieu, J.L. & Reille, M. (1989). A 140,000 year continental climate reconstruction from two European pollen records. Nature, 338, 309-313.

Guiot, J., Reille, M., de Beaulieu, J.L. & Pons, A. (1992). Calibration of the climatic signal in a new pollen seqeunce from La Grande Pile. Climate Dynamics, 6, 259-264.

Halley, E. (~1702). A theory of the variation of the magnetical compass.

Hays, J.D. (1971). Faunal extinctions and reversals of the Earth's magnetic field. Bull. geol. Soc. Am., 82, 2433-2447.

Hollerbach, R. & Jones, C.A. (1993). Influence of the Earth's inner core on geomagnetic fluctuations and reversals. Nature, 365, 541-543.

Horne, J.H. & Baliunas, S.L. (1986). A prescription for period analysis of unevenly sampled time series. Astrophysical Journal, 302, 757-763.

Huntley, B. (1990). European post-glacial forests: compositional changes in response to climatic change. Journal of Vegetation Science, 1, 507-518.

Imbrie, J., Hays, J.D., Martinson, D.G., McIntyre, A., Mix, A.C., Morley, J.J., Pisias, N.G., Prell, W.L. & Shackleton N.J. (1884). The orbital theory of Pleistocene climate: support from a revised chronology of the marine $\delta^{18}O$ record. In: "Milankovitch and Climate", part 1, 269-305, eds. A.L. Berger et al.

Johnston, H.S. (1974). Photochemistry in the stratosphere - with applications to supersonic transports. Acta Astronautica, 1, 135-156.

Jouzel, J., Lorius, C., Petit, J.R., Genthon, C., Barkov, N.I., Kotlyakov, V.M. & Petrov, V.M. (1987). Vostok ice core: a continuous isotope temperature record over the last climatic cycle (160,000 years). Nature, 329, 403-407.

Kent, D.V. (1982). Apparent correlation of palaeomagnetic intensity and climatic records in deep-sea sediments. Nature, 299, 538-539.

Kent, D.V. & Opdyke, N.D. (1977). Palaeomagnetic field intensity variation recorded in a Brunhes epoch deep-sea sediment core. Nature, 266, 156-159.

King, J.W., Banerjee, S.K., Marvin, J. & Özdemir, Ö. (1982). A comparison of different magnetic methods for determining the relative grain size of magnetite in natural materials: some results from lake sediments. Earth and Planetary Science Letters, 59, 404-419.

King, J.W., Banerjee, S.K. & Marvin, J. (1983). A new rock magnetic approach to selecting sediments for geomagnetic palaeointensity studies: application to palaeointensity for the last 4000 years. Journal of Geophysical Research, 88 (B7), 5911-5921.

Kukla, G. (1989). Long continental records of climate - an introduction. Palaeogeography, Palaeoclimatology, Palaeoecology, 72, 1-9.

Lanza, R. & Zanella, E. (1991). Palaeomagnetic directions (223-1.4 ka) recorded in the volcanites of Lipari, Aeolian Islands. Geophysical Journal International, 107, 191-196.

Laskar, J. & Robutel, P. (1993). The chaotic obliquity of the planets. Nature, 361, 608-615.

Le Goff, M. (1985). Description d'un appareil à désaimanter par champs alternatifs; élimination de l'aimantation rémanente anhystérétique parasite. Can. J. Earth Sci., 22, 1740-1747.

Maher, B.A., & Thompson, R., (1992). Palaeoclimatic significance of the mineral magnetic record of the Chinese loess and palaeosols. Quaternary Research, 37, 155-170.

Malkus, W.V.R. (1963). Precessional torques as the cause of geomagnetism. Journal of Geophysical Research, 68, 2871-2886.

Malkus, W.V.R. (1968). Precession of the Earth as the cause of geomagnetism. Science, 160, 259-264.

Martinson, D.G., Pisias, N.G., Hays, J.D., Imbrie, J., Moore, T.C., & Shackelton, N.J. (1987). Age dating and the orbital theory of the ice ages: development of a high-resolution 0 to 300,000-year chronostratigraphy. Quaternary Research, 27, 1-29.

Mazaud, A., Laj, C., Bard, E., Arnold, M. & Tric, E. (1991). Geomagnetic field control of ^{14}C production over the last 80 ky: implications for the radiocarbon timescale. Geophysical Research Letters, 18, 1885-1888.

McHargue, L.R. & Damon, P.E. (1991). The global beryllium 10 cycle. Reviews of Geophysics, 29, 141-158.

Merril, R.T. & McFadden, P.L. (1990). Paleomagnetism and the nature of the geodynamo. Science, 248, 345-350.

Meynadier, L., Valet, J-P., Weeks, R., Shackleton, N.J. & Hagee, V.L. (1992). Relative geomagnetic intensity of the field during the last 140 ka. Earth and Planetary Science Letters, 114, 39-57.

Morley, J.J. & Hays, J.D. (1981). Towards a high-resolution, global, deep-sea chronology for the last 750,000 years. Earth and Planetary Science Letters, 53, 279-295.

Negendank, J.F.W. & Zolitschka, B. (1993). International maar deep drilling project (MDDP) - a challenge for earth sciences? In: Lecture Notes in Earth Sciences, 49, "Palaeolimnology of European Maar Lakes", eds. J.F.W. Negendank & B. Zolitschka.

Nowaczyk, N.R. & Baumann, M. (in press). Combined high resolution magnetostratigraphy and nannofossil biostratigraphy for late Quaternary Arctic Ocean sediments. Deep Sea Research, in press, manuscript no. M1214.

Nicolet, M. (1975). On the production of nitric oxide by cosmic rays in the mesosphere and stratosphere. Planet. Space Sci., 23, 637-649.

Oldfield, F. (1992). The source of fine-grained 'magnetite' in sediments. The Holocene, 2, 180-182.

Parkinson, W.D. (1983). Introduction to geomagnetism. Scottish Academic Press.

Pons, A., Guiot, J., de Beaulieu, J.L. & Reille, M. (1992). Recent contributions to the climatology of the last glacial-interglacial cycle based on French pollen sequences. Quaternary Science Reviews, 11, 439-448.

Prell, W.L., Imbrie, J., Martinson, D.G., Morley, J.J., Pisias, N.G., Shackleton, N.J. & Streeter, H.F. (1986). Graphic correlation of oxygen isotope stratigraphy application to the late Quaternary. Paleooceanography, 1, no.2, 137-162.

Press, W.H. & Rybicki, G.B. (1989). Fast algorithm for spectral analysis of unevenly sampled data. Astrophysical Journal, 338, 277-280.

Rampino, M.R. (1981). Revised age estimates of Brunhes palaeomagnetic events: support for a link between geomagnetism and eccentricity. Geophysical Research Letters, 8, 1047-1050.

Raynaud, D., Barnola, J.M., Chappellaz, J., Zardini, D., Jouzel, J. & Lorius, C. (1992). Glacial-interglacial evolution of greenhouse gases as inferred from ice core analysis: a review of recent results. Quaternary Science Reviews, 11, 381-386.

Robinson, C. (1993). Lago Grande di Monticchio: a palaeoenvironmental reconstruction from sediment geochemistry. Ph.D. thesis, University of Edinburgh.

Robinson, S.G. (1986). The late Pleistocene palaeoclimatic record of North Atlantic deep-sea sediments revealed by mineral magnetic measurements. Physics of the Earth and Planetary Interiors, 42, 22-47.

Rochester, M.G., Jacobs, J.A., Smylie, D.E. & Chong, K.F. (1975). Can precession power the geomagnetic dynamo? Geophysical Journal of the Royal Astronomical Society, 43, 661-678.

Ruddiman, W.F. & McIntyre, A. (1981). Oceanic mechanisms for amplification of the 23,000-year ice-volume cycle. Science, 212, 617-627.

Scargle, J.D. (1989). Studies in astronomical time series analysis. III. Fourier transforms, autocorrelation functions, and cross-correlation functions of unevenly spaced data. Astrophysical Journal, 343, 874-887.

Smith, G. (1985). Late glacial palaeomagnetic secular variations from France. Ph.D. thesis, University of Edinburgh.

Smith, G. & Creer, K.M. (1986). Analysis of geomagnetic secular variations 10000 to 30000 years bp, Lac du Bouchet, France. Physics of the Earth and Planetary Interiors, 44, 1-14.

Stacey, F.D. (1972). On the role of Brownian motion in the control of detrital remanent magnetization of sediments. Pure and Applied Geophysics, 98, 139-145.

Stuiver, M., Pearson, G.W. & Braziunas, T. (1986). Radiocarbon age calibration of marine samples back to 9000 cal yr B.P. Radiocarbon, 28, 980-1021.

Tauxe, L. (1993). Sedimentary records of relative palaeointensity of the geomagnetic field: theory and practice. Reviews of Geophysics, 31, 319-354.

Tauxe, L. & Valet, J-P. (1989). Relative paleointensity of the Earth's magnetic field from marine sedimentary records: a global perspective. Physics of the Earth and Planetary Interiors, 56, 59-68.

Tauxe, L. & Wu, G. (1990). Normalised remanence in sediments of the western equatorial Pacific: relative palaeointensity of the geomagnetic field? Journal of Geophysical Research, 95 (B8), 12337-12350.

Thompson, R. & Berglund, B. (1976). Late Weichselian geomagnetic 'reversal' as a possible example of the reinforcement syndrome. Nature, 263, 490-491.

Thompson, R., & Oldfield, F. (1986). Environmental magnetism. Allen and Unwin.

Thouveny, N. (1987). Variations of the relative palaeointensity of the geomagnetic field in western Europe in the interval 25-10 kyr BP as deduced from analyses of lake sediments. Geophysical Journal of the Royal Astronomical Society, 91, 123-142.

Thouveny, N. (1991). Les variations du champ magnétique terrestre dans le dernier cycle climatique (0 120000 ans BP). Documents du CERLAT, Mém. 3, Lac du Bouchet (II), 350p.

Thouveny, N., Creer, K.M. & Blunk, I. (1990). Extension of the Lac du Bouchet palaeomagnetic record over the last 120,000 years. Earth and Planetary Science Letters, 97, 140-161.

Thouveny, N. & Williamson, D. Palaeomagnetic secular variation as a chronological tool for the Holocene. In: Evaluation of climate proxy data in relation to the European Holocene. Special issue of the ESF project, European palaeoclimate and man 1.

Thouveny, N. & Creer, K.M. (1992a). On the brevity of the Laschamp excursion. Bull. Soc. géol. France, 163, 771-780.

Thouveny, N. & Creer, K.M. (1992b). Geomagnetic excursions in the past 60 ka: ephemeral secular variation features. Geology, 20, 399-402.

Thouveny, N., Creer, K.M. & Williamson, D. (1993). Geomagnetic moment variations in the last 70,000 years, impact on production of cosmogenic isotopes. Global Planet. Change, 7, 157-172.

Tric, E., Valet, J-P., Tucholka, P., Paterne, M., Labeyrie, L., Guichard F., Tauxe L. & Fontugne, M. (1992). Palaeointensity of the geomagnetic field during the last 80,000 years. Journal of Geophysical Research, 97 (B6), 9337-9351.

Truze, E. (1990). Etude sedimentologique et geochemique des depôts du maar du Bouchet (Massif Central, France). Evolution d'un systeme lacustre au cours du dernier cycle climatique (0 - 120,000 ans). Doctorat thesis, Université d'Aix Marseille II, Faculté de Luminy

Truze, E. & Kelts, K. (1993). Sedimentology and palaeoenvironment from the maar Lac du Bouchet for the last climatic cycle, 0-120,000 years (Massif Central, France). In: Lecture Notes in Earth Sciences, 49, "Palaeolimnology of European Maar Lakes", eds. J.F.W. Negendank & B. Zolitschka.

Tucker, P. (1980). A grain mobility model of post-depositional realignment. Geophysical Journal of the Royal Astronomical Society, 63, 149-163.

Tucker, P. (1981). Palaeointensities from sediments: normalization by laboratory redepositions. Earth and Planetary Science Letters, 56, 398-404.

Tucker, P. (1983). Magnetization of unconsolidated sediments and theories of DRM. In: "Geomagnetism of baked clays and recent sediments", eds. K.M. Creer, P. Tucholka, C.E. Barton, Elsevier, Amsterdam, 9-19.

Turton, I. (1993). Palaeomagnetic investigations of Lago Grande di Monticchio (southern Italy). In: Lecture Notes in Earth Sciences, 49, "Palaeolimnology of European Maar Lakes", eds. J.F.W. Negendank & B. Zolitschka.

Valet, J-P. & Meynadier, L. (1993). Geomagnetic field intensity and reversals during the past four million years. Nature, 366, 234-238.

Verosub, K.L. (1977). Depositional and postdepositional processes in the magnetisation of sediments. Reviews of Geophysics and Space Physics, 15, 129-143.

Verosub, K.L. & Banerjee, S.K. (1977). Geomagnetic excursions and their palaeomagnetic record. Reviews of Geophysics and Space Physics, 15, 145-155.

Weeks, R., Laj, C., Endignoux, L., Fuller, M., Roberts, A., Manganne, R., Blanchard, E. & Goree, W. (1993). Improvements in long-core measurement techniques: applications in palaeomagnetism and palaeoceanography. Geophysical Journal International, 114, 651-662.

Williams, T., Creer, K.M. & Thouveny, N. (1993). Preliminary 50m palaeomagnetic records from Lac du Bouchet, Haute-Loire, France. In: Lecture Notes in Earth Sciences, 49, "Palaeolimnology of European Maar Lakes", eds. J.F.W. Negendank & B. Zolitschka.

Williams, W. & Dunlop, D.J. (1989). 3-dimensional magnetic modelling of ferromagnetic domain structure. Nature, 337, 634-637.

Winograd, I.J., Coplen, T.B., Landwehr, J.M., Riggs, A.C., Ludwig, K.R., Szabo, B.J., Kolesar, P.T. & Revesz, K.M. (1992). Continuous 500,000-year climate record from vien calcite in Devils Hole, Nevada. Science, 258, 255-260.

Woillard, G.M., & Mook, W.G. (1982). Carbon-14 dates at Grande Pile: correlation of land and sea chronologies. Science, 215, 159-161.

Wollin, G., Ryan, W.B.F., Ericson, D.B. & Foster, J.H. (1977). Palaeoclimate, palaeomagnetism and the eccentricity of the Earth's orbit. Geophysical Research Letters, 4, 267-270.

Wollin, G., Ryan, W.B.F. & Ericson, D.B. (1978). Climatic changes, magnetic intensity variations and fluctuations of the eccentricity of the Earth's orbit during the past 2000000 years and a mechanism which may be responsible for the relationship. Earth and Planetary Science Letters, 41, 395-397.

Yukutake, T. (1972). The effect of change in the geomagnetic dipole moment on the rate of the Earth's rotation. Jounal of Geomagnetism and Geoelectricity, 24, 16-47.